Bulletin

of

The Geological Society of America

VOLUME 60 May 1949 NUMBER 5

CONTENTS

Subsurface constitution of Bikini Atoll as indicated by a seismic refraction survey. By M. B. Dobrin, Beauregard Perkins, and B. L. Snavely.. 807–828

Upper Pliocene vertebrates from Keefe Canyon, Meade County, Kansas. By C. W. Hibbard and Elmer S. Riggs..... 829–860

Observations on some Yellowstone geysers. By F. Donald Bloss and Tom F. W. Barth..... 861–886

Stratigraphy and origin of bauxite deposits. By E. C. Harder..... 887–908

Structure at Kirkland Lake, Ontario, Canada. By Harold Hopkins..... 909–922

Structure of the Northern Muddy Mountain area, Nevada. By Chester R. Longwell..... 923–968

Subscription $10 per year.

Publication Office: Mt. Royal & Guilford Aves., Baltimore 2, Md.

Communications for publication should be addressed to The Geological Society of America, Dr. H. R. Aldrich, Secretary, 419 West 117th Street, New York 27, N. Y.

NOTICE.—Four weeks notice of change of address is necessary. In accordance with the rules established by the Council, claims for non-receipt of the preceding number of the Bulletin must be sent to the Secretary of the Society within three months of the date of the receipt of this number in order to be filled gratis.

Entered as second-class matter in the Post-Office at Baltimore, Md., under the Act of Congress of July 16, 1894.

Accepted for mailing at special rate of postage provided for in Section 1103 Act of October 3, 1917, authorized on July 8, 1918.

PAPERS IN PRESS FOR FORTHCOMING ISSUES

Intrusives of Central Minnesota. By Margaret S. Woyski

Volcanic Rocks of Northeastern New Mexico. By R. F. Collins

Petrology of Volcanic Rocks of Northeastern New Mexico. By Helen Stobbe

Geologic and Geographic Reconnaissance of Eastern Markagunt Plateau, Utah. By Herbert E. Gregory

Geology of the Manzanita and North Manzano Mountains, New Mexico. By Parry Reiche

Stratigraphy and Petrology of the Buck Hill Quadrangle, Texas. By S. S. Goldich and M. A. Elms

Geology of the Monadnock Region of New Hampshire. By Katharine Fowler-Billings

BULLETIN OF THE GEOLOGICAL SOCIETY OF AMERICA
VOL. 60, PP. 807-828, 10 FIGS., 2 PLS. MAY 1949

SUBSURFACE CONSTITUTION OF BIKINI ATOLL AS INDICATED BY A SEISMIC-REFRACTION SURVEY*

BY MILTON B. DOBRIN, BEAUREGARD PERKINS, JR., AND BENJ. L. SNAVELY

CONTENTS

	Page
Abstract	808
Introduction	808
Acknowledgments	809
Historical background	810
Theory of seismic refraction interpretation	811
Field procedure	813
General	813
Shooting technique	813
Seismic records	813
Surveying	814
Location and sequence of shots	814
Results	815
Time-distance curves	815
Determination of depths	817
Structure	819
Geologic interpretation	823
Possible constitutions of the velocity zones	823
Indications of subsidence	826
Inferences regarding geologic history of Bikini	826
Proposed additional investigation	827
References cited	828

ILLUSTRATIONS

Figure	Page
1.—Relation of time-distance curve to wave trajectory for 3-layer case	812
2.—Time-distance curve for Enyu-Namu profile	814
3.—Time-distance curves for Enyu-Yuro profile	816
4.—Time-distance curve for Yuro-Cherry profile	816
5.—Time-distance curves for Enyu-Cherry profile	817
6.—Cross sections showing subsurface structure indicated by seismic survey along Enyu-Cherry and Enyu-Namu profiles	819
7.—Cross sections showing subsurface structure indicated by seismic survey along Yuro-Cherry, Enyu-Yuro, and "AB" profiles	820
8.—Contour map of depths to top surface of 17,000 ft/sec zone	821
9.—Contour map of depths to top surface of 11,000 ft/sec zone	821
10.—Three alternative interpretations of anomaly in arrival times at eastern end of Enyu-Cherry profile	822
Plate	**Facing page**
1.—Sample records	812
2.—Chart showing shot and hydrophone locations in Bikini lagoon	814

* This work was supported by the Bureau of Ordnance and the Bureau of Ships and was done by personnel of the Naval Ordnance Laboratory and the Oceanographic Section of Joint Task Force One.

ABSTRACT

As a part of the fundamental scientific investigation carried out in connection with the atomic bomb tests of 1946, a seismic refraction survey was made by Joint Task Force One to obtain information on the subsurface structure of Bikini Atoll. Naval depth charges were fired on the lagoon bottom along four lines extending across the atoll and the resulting seismic waves were picked up by water-coupled microphones near shore. A total of 126 charges were exploded in the survey.

The time-distance curves indicate the existence of three zones with different sound velocity beneath the lagoon floor. For the uppermost layer, averaging about 2500 feet thick, the speed is 7000 ft/sec. Below this is a layer ranging from approximately 5000 to 10,000 feet in thickness with a seismic velocity of 11,000 ft/sec. Underlying the latter is a zone of undetermined thickness having a speed of 17,000 ft/sec. The recent boring, 2556 feet deep, on Bikini Island appears to confirm the conclusion reached from the seismic data alone that the uppermost zone consists of diverse calcareous materials such as are encountered on the sea floor within and around atolls at shallow depths,—*i.e.*, a few hundred feet at the most. Results of a vertical velocity survey to 1800 feet in the same hole show a continuous transition from a velocity of 7000–11,000 ft/sec. It appears probable, therefore, that no essentially different rock materials enter into the composition of the atoll down to the top of the 17,000 ft/sec zone, and that the change in velocity is due mainly to progressive compaction and cementation of the calcareous sediments. In this case the 11,000 ft/sec layer indicated by the refraction data might consist of such sediments in a state of maximum cementation or of finer calcareous material, deposited in deeper water, that might have undergone greater compaction than the overlying coarser sediments. Parts of it, or even most of it, may be dolomitized; it might possibly consist mainly of pyroclastic sediments, although this seems less likely. Only a boring can provide a positive identification.

The zone with a velocity of 17,000 ft/sec appears to represent the igneous basement. Its surface has considerable relief, the highest portion being near the center of the atoll about 7000 feet below sea level. From this summit a sharp nose plunges southeastward to the atoll's edge, the greatest observed depth being about 13,000 feet.

The seismic data suggest several possible histories of Bikini Atoll, but all require relative subsidence in the thousands of feet. If the material down to the 17,000 ft/sec zone is calcareous sand, the seismic evidence calls for a minimum of 7000 feet of subsidence. If a terrace on the surface of this zone at 13,000 feet is attributed to subaerial erosion, a minimum of 13,000 feet of subsidence is then required. If, on the other hand, the intermediate zone is identified as volcanic or pelagic material, it is still necessary to assume that there was at least 2000 feet of subsidence. Thus, for Bikini at least, the seismic results tend to favor the conception, first advanced in its simplest form by Darwin, that atolls are formed by long-continued subsidence of initial noncalcareous islands or shallow banks.

INTRODUCTION

It has long been an aphorism among geologists that atolls are the most uncommunicative of geologic forms. The recent algal and coral deposits which cover the accessible portions of their reefs, islands, and lagoon bottoms give few clues as to their origin, structure, or internal constitution. Ever since the pioneering investigations of Darwin more than a century ago, the geologic history of atolls has been the subject of widespread controversy.

The atomic bomb tests carried on during 1946 at Bikini, in the Marshall Islands,

provided an opportunity to explore the interior of a typical atoll by a powerful geophysical technique, the seismic refraction method. The survey was a part of the fundamental scientific investigations conducted prior to the actual bomb detonations and standard rather than atomic explosives were employed. It was undertaken jointly by the Naval Ordnance Laboratory and the Oceanographic Section of Joint Task Force One with instruments and personnel assembled primarily for measuring the underwater effects of the atomic bombs.

Because of limited time and equipment, the refraction survey was undertaken as a reconnaissance with no expectation of obtaining more than a general picture of the atoll's subsurface constitution. The investigation has nevertheless demonstrated the existence of two layers of different elastic characteristics above the basement rock and determined the speed of sound in these layers, as well as their approximate thickness. It has also indicated the approximate amount of relief in the surface of the second layer and in that of the basement.

ACKNOWLEDGMENTS

The survey required the participation of a large number of individuals, and it is regretted that credit cannot be given here to all who contributed. The instrumentation and its applications to this project have been described in another publication (Snavely *et al.*, 1947) by those primarily responsible for its design and development.

Dr. J. V. Atanasoff, leader of the Low Frequency Group from the Naval Ordnance Laboratory, was responsible for the overall planning of the project in co-operation with Commander Roger Revelle, Head of the Oceanographic Section of the Task Force. The Low Frequency Group was a division of the Bureau of Ordnance Instrumentation Section of Joint Task Force One under Captain A. E. Uehlinger. As supervisors of the participating groups, Captain Uehlinger and Commander Revelle performed a vital function in securing proper authorization for the project, in making necessary arrangements, and in obtaining facilities.

H. N. Clarkson and K. W. Erickson supervised the installation and maintenance of the underwater gear used by the Naval Ordnance Laboratory Low Frequency Group and, assisted by the late Chief Gunner J. C. Orr, U. S. Navy, also supervised all the explosive shots and the navigation of the shooting boat. Mr. Gale White's background of experience with the shooting and receiving technique was invaluable to the entire operation. With Mr. R. Beresford, Dobrin, and Snavely, he also manned the Naval Ordnance Laboratory receiving station at Enyu Island, which formed one end of three profiles. The recording equipment used by the Oceanographic Section was operated by Lt. Coleman Sklaw, Lt. (jg) T. C. Atchison, and Ensign A. S. Fulton, under the supervision of Perkins. During the shooting of the first profile (Enyu-Namu), a group from the Geotechnical Corporation under R. Maurice Tripp received shots with land geophones on Namu Island and obtained results which will be published separately. Jay P. Leary of the Naval Ordnance Laboratory assisted in working up the records.

The co-operation of Prof. Maurice Ewing, of Columbia University, in the initial planning of the project and the interpretation of the results is gratefully acknowledged. The shooting and receiving technique employed was originally used by him

during the course of his wartime research and its adoption on this project was the result of his suggestion. The authors have discussed the geologic interpretation of the seismic data with Prof. R. A. Daly, Prof. Chester R. Longwell, Prof. Carl Dunbar, Dr. W. M. Bradley, Mr. W. W. Rubey, Dr. Harry Ladd, Dr. E. S. Larson, Jr., Dr. N. A. Bowen, Prof. J Harlen Bretz, the late Prof. R. T. Chamberlin, Prof. W. H. Bucher, Dr. T. Wayland Vaughan, Prof. H. H. Hess, and Dr. Roger R. Revelle, all of whom have generously contributed their time and made valuable suggestions. Except where specifically acknowledged, however, they are not to be considered responsibie for any of the conclusions presented.

HISTORICAL BACKGROUND

The scarcity of factual evidence which atolls have provided to geologists has led to a multiplicity of conflicting theories (Davis, 1928) as to their origin ever since Darwin (1842) and Dana (1852) first called attention to the problem when describing the atolls of the Pacific and Indian oceans. The most serious controversies have generally taken place between those who maintain that relative subsidence is necessary for reef and atoll formation and those who postulate upgrowth of the structures from stable foundations.

The first concept, which Darwin originated, presupposes an initial volcanic island fringed along its shore line with living corals and other lime-secreting organisms. As the level of the sea rose with respect to the island, the organisms grew upward on the limestone remains of previous generations. When the original volcanic summit disappeared beneath the central lagoon, the barrier reef encircling it became an atoll.

The earliest theories requiring stable noncalcareous foundations were the closely related ones of Rein and Murray, both discussed by Davis (1928), which proposed the building up of shallow banks upon stationary submerged volcanic cones by deposition of pelagic limestone. When the tops of the banks approached sea level, shallow water organisms built the present reefs over them. The most widely accepted of these hypotheses is the glacial control theory of Daly (1915), which states that a 300-foot eustatic lowering of sea level during the glacial periods of the Pleistocene resulted in the planing off, through wave cutting, of pre-existing volcanic banks or islands to the lowest level of the ocean. With the melting of the glaciers and the consequent rise of sea level, new coral and algal formations grew up from the wave-cut platforms, resulting in present day reefs and atolls. The most recent theory postulating still-standing foundations is the antecedent platform theory of Ladd and Hoffmeister (1936), which calls for the growth of coral on the top of preexisting structures, such as pyroclastic banks cut to the lower limit of wave action.

Stearns (1946) and Kuenen (1947) have recently proposed mechanisms for reef and atoll formation which involve subsidence as the dominant factor but call upon glacial control to explain certain features observed in present-day structures.

During the course of the earlier studies on reefs and atolls, it became evident that the best experimental test of subsidence would be to measure the thickness of the reef limestone deposits on a typical atoll. In 1899, the Royal Society of London (1904) sponsored a 1114-foot boring on Funafuti Atoll, in the Ellice Islands, bringing

up from this depth core samples which consisted only of limestone from shallow water organisms. These results were unfortunately inconclusive because the experts who examined the cores could not agree whether the limestone below the first few hundred feet was originally laid down where it was found or whether it had fallen as talus down the sides of a volcanic cone. In addition to this hole, drilled from one of the islands of the atoll, two much shallower holes were drilled from the bottom of the lagoon. The first geophysical investigation of an atoll was an Eötvös torsion balance survey of Jaluit, in the Marshalls, carried on by Matsuyama (1918) of Kyoto University. He compared the gradients and curvatures measured on the various islands of the atoll with theoretical values that would be expected from a number of assumed basement depths and densities. It was concluded that the limestone was between 750- and 2200 feet thick. Davis (1928) cited these results as virtual confirmation of the Darwin theory. Matsuyama's pioneer work failed to carry full conviction, however, on account of the considerable ambiguity inherent in measurements of this type.

From this time until the end of World War II there was no opportunity for any further geophysical investigations that might cast light upon the coral reef problem. Operation Crossroads in 1946 made possible the refraction survey of Bikini Atoll reported here. The following summer a resurvey of Bikini conducted by the Navy Department primarily to evaluate the effect of the atomic bomb explosions (Revelle, 1947), gave opportunity to drill five holes on Bikini Island, the deepest on the lagoon side penetrating 2556 feet (Ladd, Tracey, and Lill, 1948). In this hole, engineers of the Geotechnical Corporation (Beers and Shugart, 1948) ascertained the vertical seismic speed distribution to 1800 feet by lowering a detector into the hole and shooting at the surface. In 1947, an aerial magnetometer survey was run over Bikini Atoll and also over a neighboring sea-mount by the Navy and the U. S. Geological Survey, and results are now in the open files of the Survey's Geophysics Section of its Geologic Branch. The 1947 boring did not penetrate beneath a zone of loose calcareous sand. Attempts are now being made to arrange for a 8500-foot boring at Bikini in the near future.

THEORY OF SEISMIC REFRACTION INTERPRETATION

The present survey employed the seismic refraction technique to investigate the atoll's interior. In this, data on the transmission time of explosion waves through the ground are converted into information on subsurface structure by standard interpretation methods discussed at length in the literature of prospecting geophysics. (*See*, for example, Nettleton, 1940). For convenience, however, the fundamental principles are reviewed here.

Figure 1 shows the paths of the seismic waves from an explosion at A on a horizontal surface below which there are three zones of respective velocities—V_0, V_1, and V_2, separated by horizontal interfaces. It is assumed that the deeper the bed, the higher the speed. The time-distance curve in the upper part of the figure shows the time required for the shock wave traveling through the ground to arrive at any point a distance x along the surface from A. Near the explosion point the arrivals

take a direct path through the V_0 zone and will fall along a line through the origin with a slope of $1/V_0$. At point D, the waves that have taken the path ABCD will, because of the higher speed of the second layer, overtake those traveling along the direct path; the slope of the time-distance curve changes at this point to $1/V_1$, the

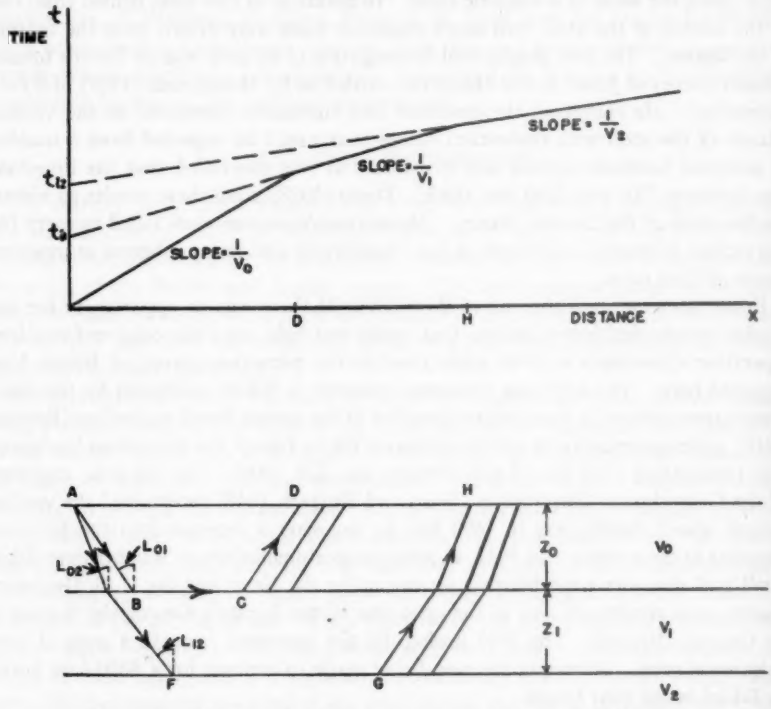

FIGURE 1.—*Relation of time-distance curve to wave trajectory for 3-layer case*

The lower diagram shows the geometry of the wave paths from shot to detector. The upper is the corresponding plot of first arrival times vs. shot-detector distances. $V_0 < V_1 < V_2$. t_{i1} and t_{i2} are respective intercept times associated with waves that have taken paths of type ABCD and AFGH. From the intercept times one can compute thicknesses Z_0 and Z_1.

energy now having penetrated to the V_1 zone. At point H, the waves that have traveled down to the top of the V_2 zone begin to overtake the others, and the time-distance curve from here on has a slope of $1/V_2$. The depth Z_0 to the V_1 zone can readily be computed from the intercept time T_{i1} of the $1/V_1$ curve and the thickness Z_1 can similarly be determined from the intercept obtained by projecting the $1/V_2$ line back to the origin.

The formulae for thicknesses (derived by Nettleton, 1940, p. 251–254) assuming horizontal interfaces and uniform velocity in each layer, are as follows:

$$Z_0 = T_{i1}V_1V_0/2(V_1^2 - V_0^2)^{\frac{1}{2}}$$

$$Z_1 = [T_{i2} - 2Z_0(V_2^2 - V_0^2)^{\frac{1}{2}}/V_0V_2][V_1V_2/2(V_2^2 - V_1^2)^{\frac{1}{2}}]$$

The total depth Z to the V_2 surface is the sum of Z_0 and Z_1.

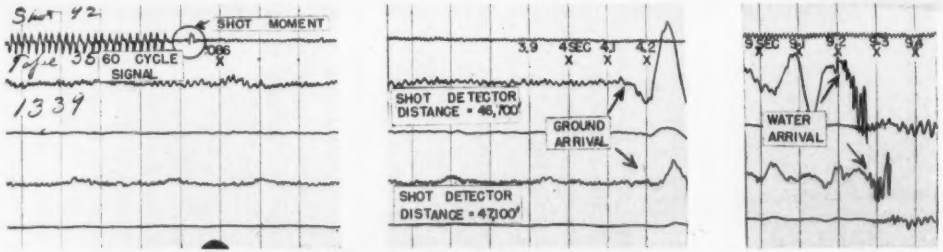

RECORD OF SHOT 92 MADE BY SHELL
OSCILLOGRAPH ON USS GILLIS ANCHORED OFF YURO Is.

The two high-sensitivity traces appear to break shortly after the water-wave arrivals. The water waves on the record were weak and were intensified by pencil as far as they could be followed.

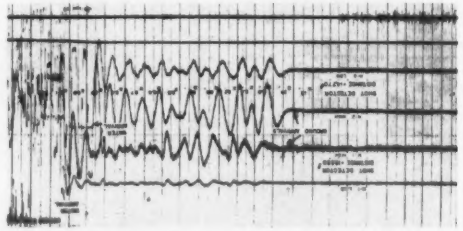

RECORD OF SHOT 120 MADE BY
HATHAWAY OSCILLOGRAPH ON ENYU Is.
(TIME BREAK NOT SHOWN)

SAMPLE RECORDS

TYPICAL GROUND-WAVE AND WATER-WAVE ARRIVALS RECORDED AT STATION IN LAGOON AND AT LAND STATION. SHOT-DETECTOR DISTANCE IS DETERMINED FROM WATER-WAVE ARRIVAL TIME.

The depth to a marker, calculated from the refraction data, is not that under the detector but is actually the depth to a point offset in the direction of the shot an amount determined by the geometry of the refracted wave path. The formula for this offset distance is, for the upper interface:

$$L_0 = Z_0 V_0/(V_1^2 - V_0^2)^{\frac{1}{2}}$$

while for the lower interface it is:

$$L_1 = Z_0 V_0/(V_2^2 - V_0^2)^{\frac{1}{2}} + Z_1 V_1/(V_1^2 - V_0^2)^{\frac{1}{2}}$$

FIELD PROCEDURE

GENERAL

In the Bikini survey both shots and detectors were under water, the shots being fired along profiles extending across the lagoon between fixed detectors near shore. Standard naval depth charges were dropped to the lagoon bottom at intervals along the profiles and fired by demolition cable. The details of the instrumentation have been described by Snavely *et al.* (1947). It is sufficient to note here that the hydrophone and its associated recording system respond both to the low-frequency pressure changes induced in the water by ground waves and to the much higher-frequency vibrations transmitted directly through the water. The pressure variations were recorded photographically by a Hathaway oscillograph at one station and by a Shell Oil Company oscillograph at the other.

SHOOTING TECHNIQUE

Both Mark 6 (300 pounds) and Mark 10 (25 pounds) depth charges were used as explosives. They were dropped from the stern of an LCT (Landing Craft, Tanks). An electric detonator was inserted in the booster instead of the usual hydrostatic firing device. A special radio time-break transmitter made possible accurate recording of the shot moment on the oscillograph records.

SEISMIC RECORDS

The records (Pl. 1), as previously noted, show ground-wave and water-wave arrivals at hydrophones located at distances of 2000–98,000 feet from the shots. The water-wave arrival could usually be read to the nearest .001 second, the ground-wave to the nearest .002 second for the shorter shots and to the nearest .010 second for the longer ones. The moment of explosion was transmitted by radio and was indicated on a special trace of the record. In general, energy from the shots was received at each detector station by a pair of hydrophones operating at frequencies from 1 to 200 cycles per second situated from several hundred to a thousand feet apart along the profiles. At one station (Enyu Island, Pl. 2) there was, in addition, a sonic-frequency hydrophone responsive to frequencies from 50 to 10,000 cps. The latter was most useful in locating the water-wave arrivals from the more distant shots. Figure 2 shows two sample records and demonstrates the nature of the signals from the low frequency hydrophones.

SURVEYING

Shot and hydrophone locations in the lagoon were determined by means of sextant bearings taken on beacons, buoys, and tangents to islands. Two angles were measured about a common point and the location was plotted on a chart with a 3-arm protractor. The accuracy of the survey was greater on the eastern side of the lagoon

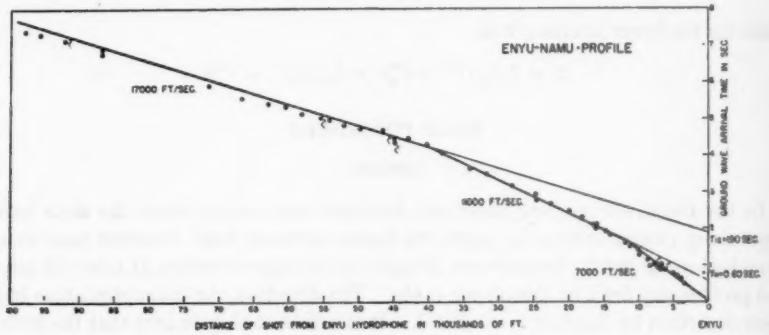

FIGURE 2.—*Time-distance curve for Enyu-Namu profile*
Detectors off Enyu Island.

where numerous beacons and markers were readily visible than in the western portion where few beacons could be observed and it was necessary to rely on tangents to islands.

Shot-detector distances were determined not from the plotted shot and hydrophone positions but from the travel times of the water-borne shock wave from explosion to receiver. Tables by Kuwahara (1939) were used to ascertain the theoretical speed of sound in sea water as a function of temperature and salinity. In addition, the speed was determined experimentally by timing the water wave along the eastern portion of the Enyu-Namu profile (Pl. 2) where the shot and detector locations were ascertained with a high degree of accuracy by sextant bearings on beacons whose co-ordinates were known to within a few feet. The theoretical speed for the temperature of 83° ± 0.5°F and salinity of 34.45 ± 0.35 ppm is 5047 ft/sec. The measured speed was 4980 ft/sec. The 1½ per cent discrepancy may indicate that Kuwahara's tables are not correct or at least are not applicable for shallow water. There is a remote possibility, however, that the tuning fork may have been fast by this percentage, so that the measured speed cannot be considered definitive. For computation of distances, a sound velocity of 5000 ft/sec was assumed. This was exceedingly convenient for purposes of calculation, and if the true speed is between the theoretical and measured values, it could not introduce an error greater than 1 per cent in the seismic velocities or in the calculated depth of the observed velocity interfaces.

LOCATION AND SEQUENCE OF SHOTS

The four profiles shot across Bikini Lagoon (Pl. 2) are designated by the Operation Crossroads code names of the islands at each end. On the first profile from Enyu

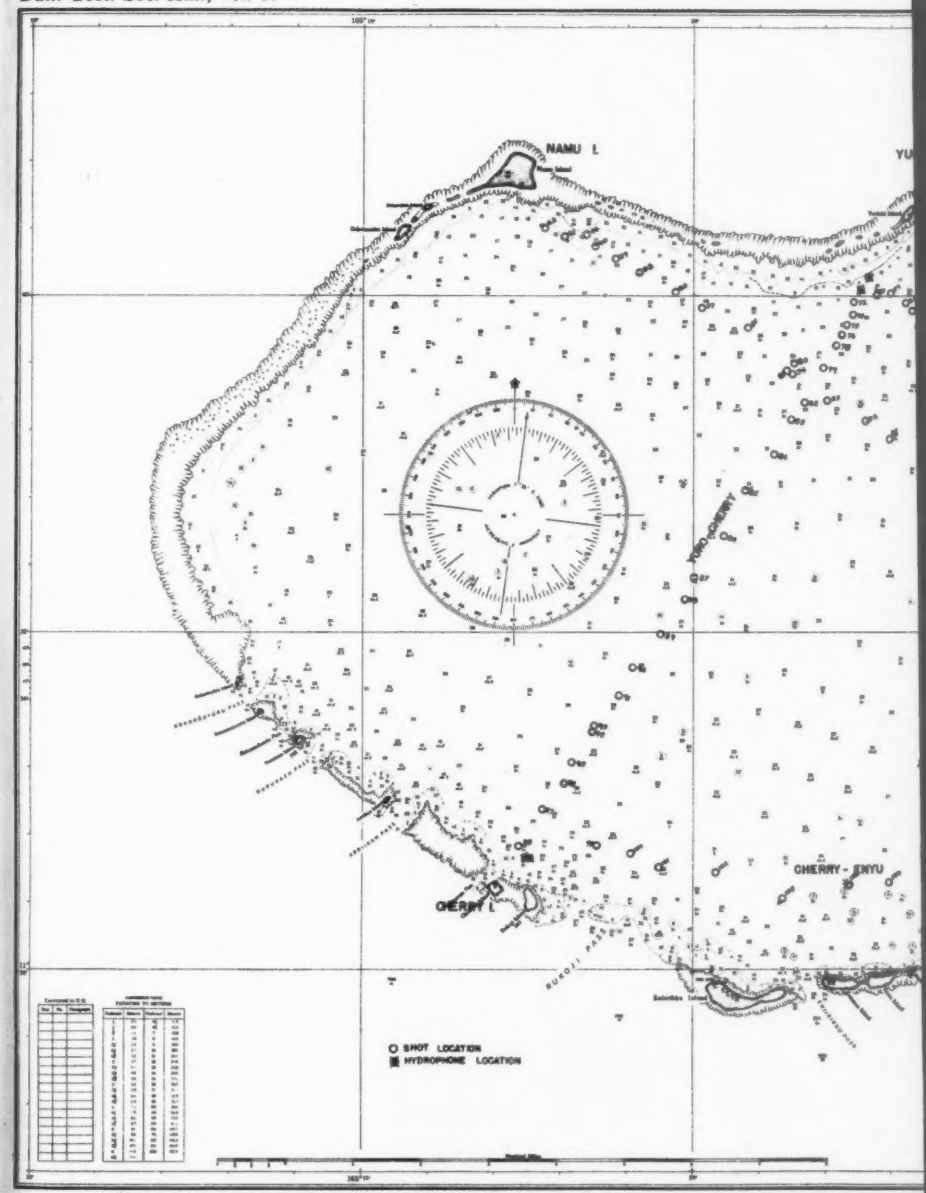

CHART SHOWING SHOT AND HYDROPH

Profiles designated by code names

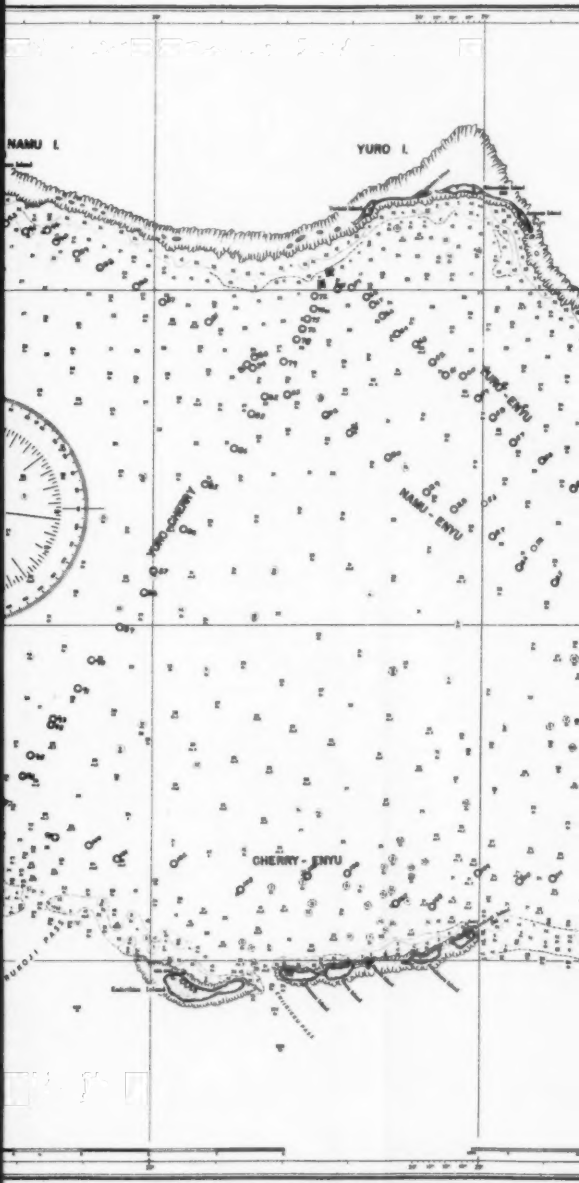

SHOT AND HYDROPHONE LOCAT

Profiles designated by code names of islands at respec

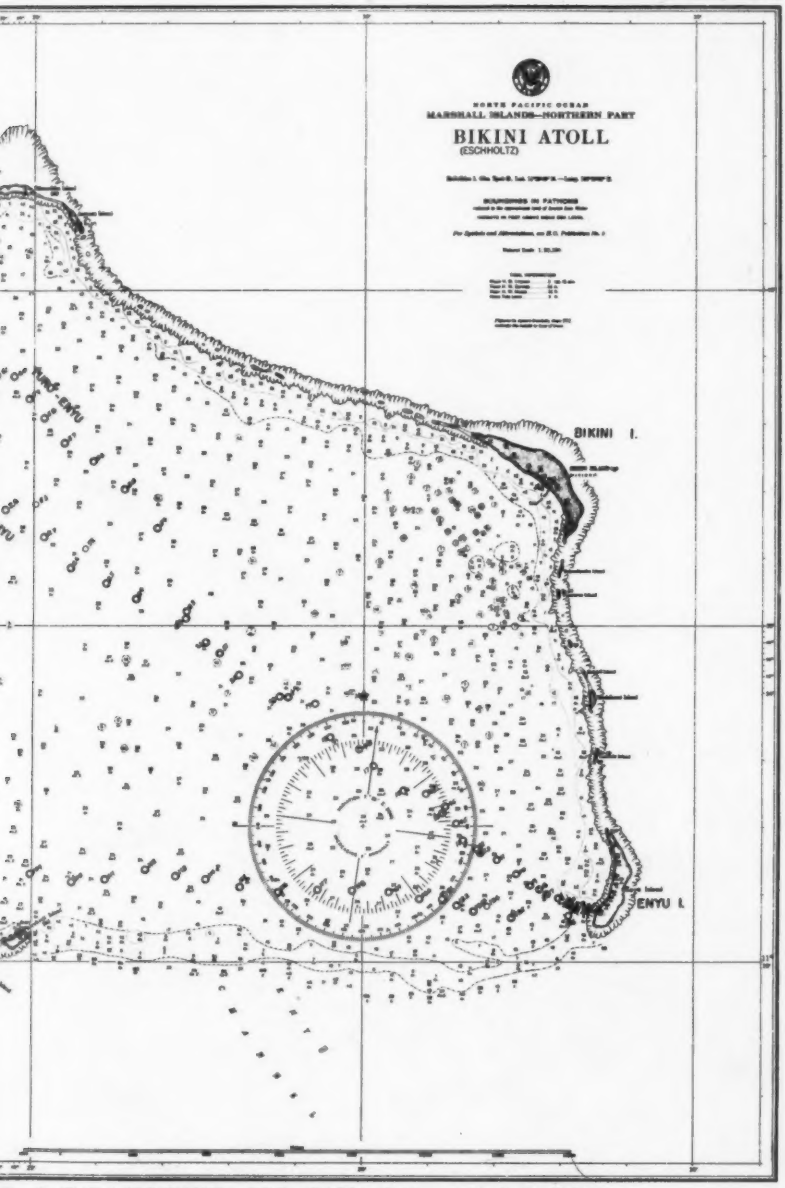

E LOCATIONS IN BIKINI LAGOON

nds at respective ends.

to Nam
were pic
to surfa
phones
the line
were pi
Geotech
are to b

The h
a pair o
anchore
hydroph
The sho
phones
were re
At the
Cherry
at Eny

The t
profiles,
the limi
detailed
work, it
ration b
same in
varied c
zones w

When
ing shot
reasonal
discrete
arrivals
question
accompa
the ave
speeds i
The sec
Cherry
ft/sec (

[1] This p
cable to sh

to Namu, shot before Test Able, the shots out to a distance of 98,000 feet from Enyu were picked up at the south end of Enyu Island by hydrophones which were connected to surface equipment in the BuOrd hut, near the center of the island. Three hydrophones were laid off Enyu at distances of 1000, 2000, and 3000 feet from shore along the line of the Enyu-Namu profile. Those shots within 40,000 feet of Namu Island were picked up by geophones placed on that island and operated by engineers of the Geotechnical Corporation. The results obtained with the land instruments on Namu are to be published separately.

The hydrophones at Enyu were used for the last three profiles also, but in addition, a pair of similar hydrophones was operated from the *USS Gillis* (AGS 13) which was anchored off Yuro Island and then off Cherry Island as indicated in Plate 2. Two hydrophones, several hundred feet apart, were laid on the bottom at each location. The shots fired along the Enyu-Yuro profile[1] were picked up by the Enyu hydrophones and also by those recording on the *Gillis* near Yuro. The Yuro-Cherry shots were received at the Yuro end of the profile and also by the Enyu hydrophones. At the completion of this profile, the *Gillis* hydrophones were moved to a point off Cherry Island and all shots after number 110 were received by the *Gillis* as well as at Enyu.

The technique of shooting here employed, with fixed detectors at the ends of long profiles, was the most expeditious method of surveying that could be devised for the limited time available for the work. If the objective of the survey had been the detailed mapping of one marker, as is generally the case in commercial refraction work, it would have been desirable to move the detectors so as to maintain such separation between shot and detector that all first arrivals would have come from the same interface. In the present reconnaissance, the shot-detector distance was varied on each profile so that refracted waves from each of the subsurface velocity zones were picked up along different portions of the profile.

RESULTS

TIME-DISTANCE CURVES

When the arrival times of the ground waves were plotted against the corresponding shot-detector distances on the four profiles (Figs. 2–5), the points fell, within reasonable limits of error, along linear segments which indicated three zones of discrete speed in the first few miles below the lagoon floor. Some of the ground wave arrivals at more distant stations are quite weak and the precise time of arrival is questionable. Points plotted on the time-distance curves from such traces are accompanied by question marks. At successively greater shot-detector distances the average inverse slopes are 7000, 11,000, and 17,000 ft/sec. The first of these speeds is very consistent over all four profiles, the deviation not exceeding 200 ft/sec. The second apparent speed was also consistent except for a portion of the Enyu-Cherry profile near the southeastern edge of the lagoon where it changes to 9000 ft/sec (Fig. 5). The interpretation of this anomaly will be discussed subsequently.

[1] This profile covered only the northwest half of the line between Enyu and Yuro. Target vessels made it impracticable to shoot along its southeast portion.

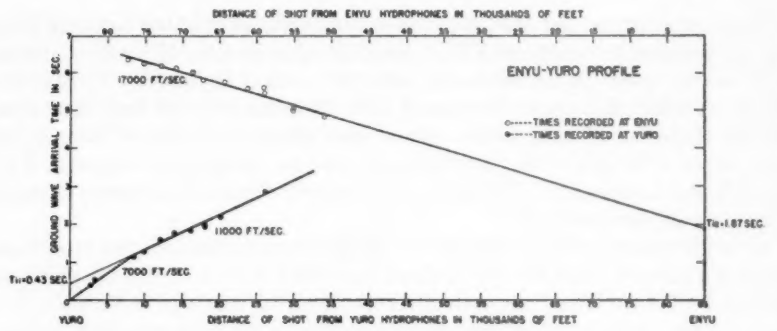

FIGURE 3.—*Time-distance curves for Enyu-Yuro profile*
Detectors off Enyu and Yuro Islands. No shooting allowed along east side of profile because of target vessels.

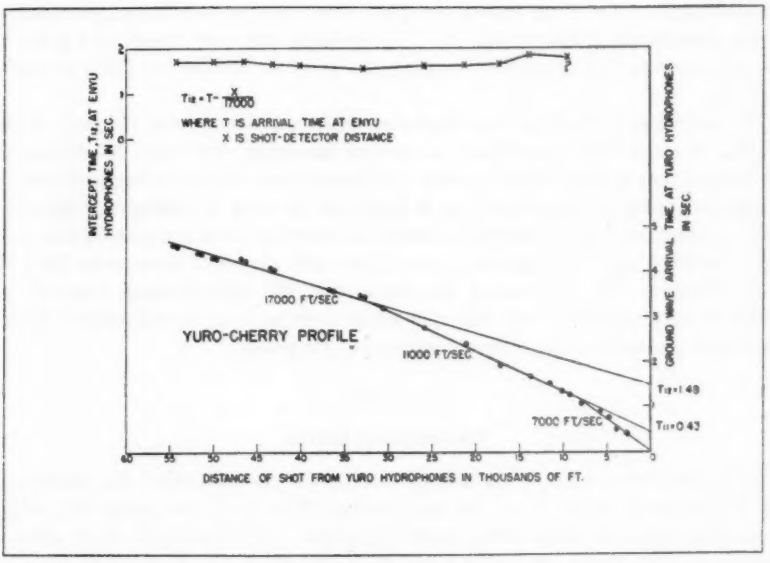
Tu = T - X/17000
WHERE T IS ARRIVAL TIME AT ENYU
X IS SHOT-DETECTOR DISTANCE
INTERCEPT TIME, Tu, AT ENYU HYDROPHONES IN SEC
17000 FT/SEC
YURO-CHERRY PROFILE
11000 FT/SEC
7000 FT/SEC
Tu=1.48
Tu=0.43
GROUND WAVE ARRIVAL TIME AT YURO HYDROPHONES IN SEC
DISTANCE OF SHOT FROM YURO HYDROPHONES IN THOUSANDS OF FT.

FIGURE 4.—*Time-distance curve for Yuro-Cherry profile*
Detectors off Enyu and Yuro Islands. Intercept plot for arrival times at Enyu of shots along the profile.

The apparent speed of the third linear segment ranges from 16,500 to 18,000 ft/sec, but reverse control in the Enyu-Cherry profile indicates a speed of 17,000 ft/sec and this is assumed in the calculation of depths to be the actual speed of the third layer everywhere beneath the atoll.

Most of the shots along the Yuro-Cherry profile were also received by the Enyu hydrophones along lines which were approximately at right angles to the profile. The results of this are indicated by the intercept times plotted on the upper portion of Figure 4.

The apparent decrease in slope at the west end of the Enyu-Cherry time-distance curve suggested the possibility of a fourth and higher speed zone below the 17,000 ft/sec layer. Such a zone, with its apparent speed of 25,000 ft/sec, would have a depth of 25,000 feet. It was decided, however, that the bend in the curve could more reasonably be explained as a rise to the west, since the difference between inter-

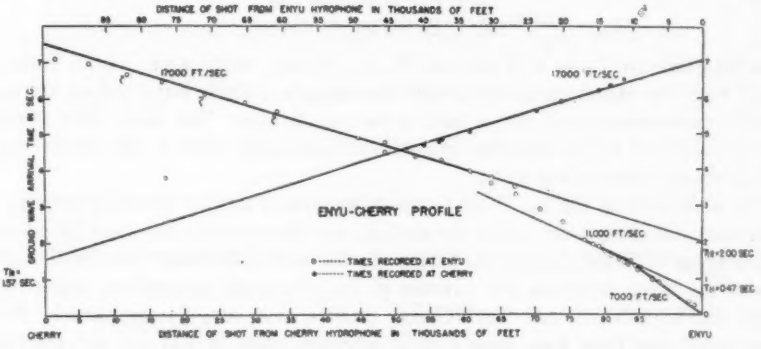

FIGURE 5.—*Time-distance curves for Enyu-Cherry profile*

Detectors off Cherry and Enyu Islands. Note anomalous arrival times recorded at Enyu from shots 20,000–35,000 ft. away. Possible explanations for this indicated in Figure 10.

cept times observed at the two ends of the profiles from shots in the region of reverse control indicated a high at the west end; moreover, the same bend was not observed at the corresponding distance in the time-distance curves for the other profiles.

DETERMINATION OF DEPTHS

In computing depths from the observed time-distance data, the intercept times were separated into delay times corresponding to the two ends of the least-time trajectory for each shot. The method employed was based on one described by Gardner (1939). Three of the four shooting profiles were laid out as sides of triangles at the vertices of which were detectors receiving impulses from each of the adjacent sides. These detector stations were at Enyu (E), Yuro (Y) and Cherry (C).

In the case of arrivals from the top of the 17,000 ft/sec marker, we can solve for the delay times at the three detector stations by setting up equations for each of the sides. If T_E, T_C, and T_Y are the delay times at the respective vertices and T_{iEC}, for example, is the intercept time on a shot fired at E and received at C, then:

$$T_E + T_C = T_{iEC} = 1.64$$
$$T_C + T_Y = T_{iCY} = 1.46$$
$$T_E + T_Y = T_{iEY} = 1.90$$

the numerical values being readily obtained from the time-distance curves. Solving, we obtain:

$$T_E = 1.04$$
$$T_C = 0.60$$
$$T_Y = 0.86$$

As a check on two of these delay times, let us calculate T_E and T_C from data recorded on the Enyu-Cherry profile alone. This profile has reverse control on arrivals from the deeper interface, so that taking the intercept times for the shots at station 114 received at the respective ends we obtain:

$$T_E + T_{114}^* = T_{iE114} = 2.00$$
$$T_C + T_{114}^* = T_{iC114} = 1.54$$
$$T_C + T_E = T_{iCE} = 1.64$$

The solutions are $T_E = 1.06$ sec. and $T_C = 0.58$ sec., which agree within limits of error with the values computed around the triangle. These latter values are considered more reliable and will be used in the calculations. The delay times at each shot position are now ascertained by subtracting the delay times at the receiver from the intercept times at the shots.

For arrivals from the top of the 11,000 ft/sec zone it was not generally possible to determine the delay times under the shots in any more precise way than by halving the average intercept time for each line. In the case of the delay time for this zone under the Enyu receivers, the average of the two times determined respectively from the Enyu-Namu and Enyu-Cherry profiles, 0.26 sec., was employed. Both lines emanating from Yuro gave average intercept times of 0.44 sec. and therefore the delay time under this station has been assumed to be 0.22 sec. Since no sufficiently close shots were received at Cherry, no delay time for the shallow interface could be computed under this station. A value of 0.25 sec. was assumed here in computing the depth to the deeper interface at Cherry.

Substituting the velocities in the expressions for depth previously given, and using delay times instead of intercept times, we obtain for the thicknesses of the two upper layers:

$$Z_0 = 9080\, T_{d1}$$
$$Z_1 = 14400\, T_{d2} - 17200\, T_{d1}$$

Offset positions were calculated from the following formulae, obtained by substituting the proper velocities in the expressions previously presented for offset:

$$L_1 = 0.83\, Z_0$$
$$L_2 = 0.45\, Z_0 + 0.85 Z_1$$

To compute the thickness, Z_1, of the second layer beneath any surface location, one must know the thickness, Z_0, of the uppermost layer. In general, there will be no arrivals from the first interface along the portions of the profile where there are arrivals from the second one. The calculation of Z_1 requires, however, that some value of Z_0 be assumed where it cannot be measured directly. This is a source of considerable uncertainty, since any error in the depth assumed to the first interface will be carried over as an approximately equal error of reverse sign in the total depth to the second.

A more serious source of error lies in the incomplete control over the speed of any given layer within the area of the survey. Any local variation of speed in the deepest

* This should be considered as the average of the two delay times obtained after station 114 is offset in opposite directions.

marker anywhere along the wave trajectory should affect the apparent depth. With reverse control on this bed available along only a limited portion of a single profile and with numerous gaps even in the one-way control, there is no assurance that such variations do not occur.

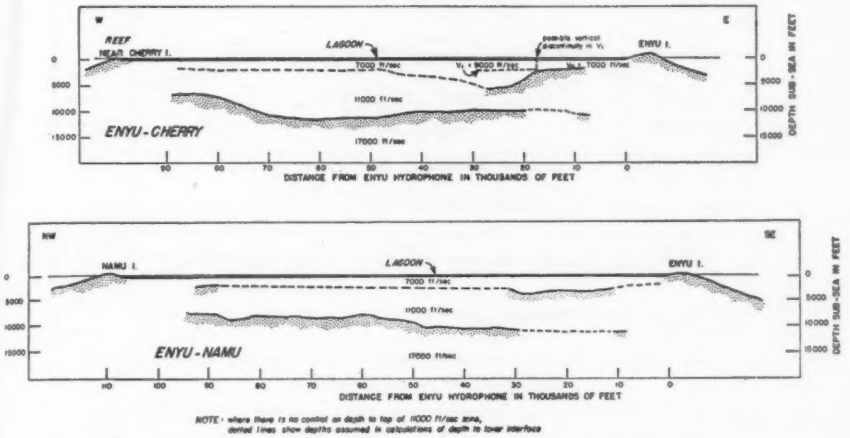

FIGURE 6.—*Cross sections showing subsurface structure indicated by seismic survey along Enyu-Cherry and Enyu-Namu profiles*

Horizontal and vertical scales equal. Interfaces are between the media having seismic velocities as indicated.

Because of these uncertainties, as well as those inherent in the seismic refraction technique even under optimum conditions of control (Nettleton, 1940, p. 255), the depths indicated in the cross section and contours given below are not exact but represent what is thought to be the most reasonable of several possible ways in which one can account for the observed time data. The depths to the upper interface are probably reliable to the nearest 200 feet (except along the anomalous zone of the Enyu-Cherry profile) while those to the lower interface may be in error by 1000 to 1500 feet. Fortunately, these uncertainties are not sufficient to affect the fundamental conclusions one can draw from the results regarding the internal constitution and geologic history of the atoll.

STRUCTURE

Figures 6 and 7 show vertical cross sections of the sub-surface below the four shooting profiles and also along a "synthetic" profile AB which extends almost directly south from Romuk Island (Fig. 8). The last profile was chosen mainly as a mode of representing the depth data afforded by two shots (107 and 108), displaced somewhat southward from the Enyu-Cherry line, which indicate a sharp fall-off in the depth to the 17,000 ft/sec zone as the edge of the reef is approached.

It is observed from the sections that the depth to the first interface averages about 2500 feet whereas that to the second is in the neighborhood of 10,000 feet.

The top surface of the 17,000 ft/sec zone is characterized (Fig. 8) by a prominent nose plunging to the southeast through the center of the atoll. The highest observed portion of this surface is under the southwestern portion of the atoll although there is insufficient control to be certain that the depth does not continue to decrease as

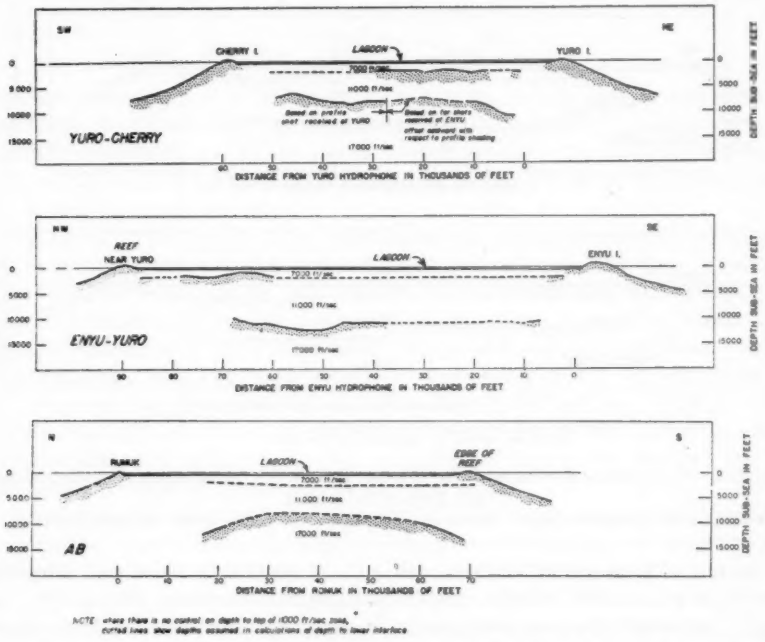

FIGURE 7.—*Cross sections showing subsurface structure indicated by seismic survey along Yuro-Cherry, Enyu-Yuro and "AB" profiles*

Horizontal and vertical scales equal. Interfaces are between the media having seismic velocities as indicated.

the western edge of the atoll is approached. Low regions are observed under the northeast and south central parts of the atoll. It should be borne in mind, however, that the greatest depth observed on this interface is about a mile higher than the ocean floor in the areas between the atolls of the Marshall group.

The top of the 11,000 ft/sec layer (Fig. 9) has a more uniform depth, except for the anomalous plunge observed near the southern border of the lagoon beginning about 3 miles west of Enyu. The cross section of the Enyu-Cherry profile and the contour map (Fig. 9) show a rapid 3000-foot drop to the west and an assumed rise of similar magnitude on the other side of the low point. The drop must represent a sharply cut valley wall or a fault if it is assumed that the speed of the second zone is everywhere 11,000 ft/sec. If a different assumption were made, the data would yield a different picture. Two other possible assumptions are:

1) V_1 changes from 11,000 to 9000 ft/sec at the point along the profile corresponding to the apparent break in slope on the time-distance curve. Farther west, at an undetermined distance, the speed changes back to 11,000 ft/sec.

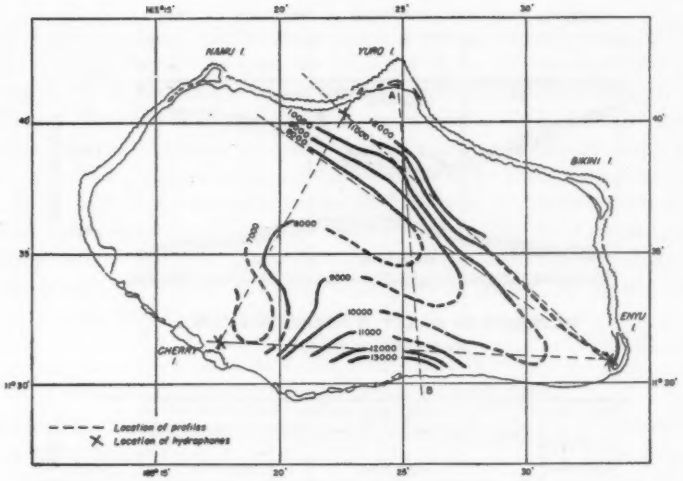

BIKINI ATOLL

CONTOURS ON TOP OF 17000 ft/sec ZONE

DATUM - SEA LEVEL DEPTHS IN FEET

FIGURE 8.—*Contour map of depths to top surface of 17,000 ft/sec zone*

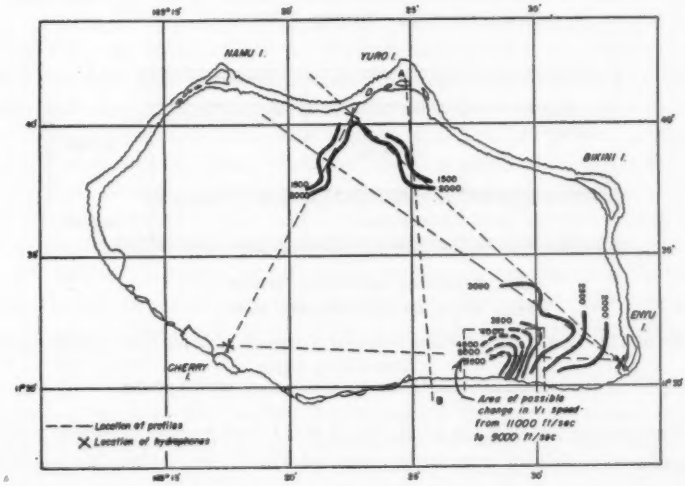

BIKINI ATOLL

CONTOURS ON TOP OF 11000 ft/sec ZONE

DATUM - SEA LEVEL DEPTHS IN FEET

FIGURE 9.—*Contour map of depths to top surface of 11,000 ft/sec zone*

These contours are based on the assumption that speed of second zone is uniformly 11,000 ft/sec everywhere under the lagoon. Figure 10 shows alternative possibilities.

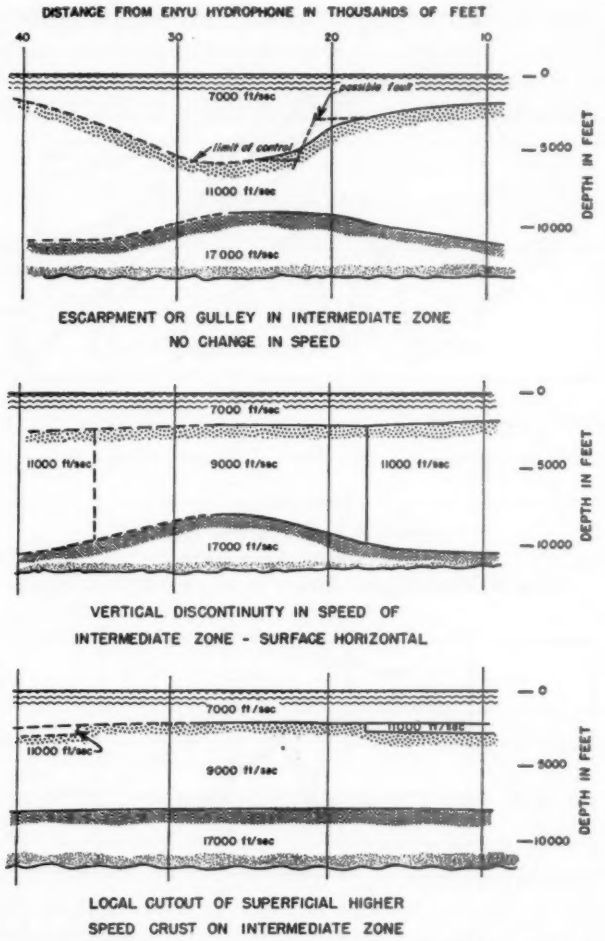

FIGURE 10.—*Three alternative interpretations of anomaly in arrival times at eastern end of Enyu-Cherry profile*

Dotted lines show postulated configurations where control is missing.

2) Everywhere beneath the atoll, the 11,000 ft/sec marker is merely a thin crust on top of a much thicker layer with a speed of 9000 ft/sec. Along the southern edge of the atoll, this crust has been eroded back so that below a portion of the Enyu-Cherry profile there is direct contact between the 7000 ft/sec zone and the 9000 ft/sec zone, with an apparent slope in the time-distance curve of 9000 ft/sec.

The sections resulting from all three assumptions are shown schematically in Figure 10. The Enyu-Cherry time-distance curves show that there is no anomaly in the arrival times from the deepest interface which corresponds to that in the inter-

mediate speed zone above. If the lower interface were horizontal, one would expect that any change either in the speed or thickness of the intermediate zone should, according to the depth-intercept time relations, give rise to some anomaly in the arrival times observed from the 17,000 ft/sec marker. Since there is none, one must postulate that a rise in the lower interface just compensates either for the depression in the top surface of the intermediate zone or for the change in its velocity which might explain the anomaly in the arrivals from the upper interface. The upper and middle diagrams of Figure 10 illustrate this. The third assumption does not require such a conveniently coincidental rise in the surface of the 17,000 ft/sec zone, but positive evidence for a thin high-speed refracting bed is not believed sufficient to make this the most likely explanation.

GEOLOGIC INTERPRETATION

POSSIBLE CONSTITUTIONS OF THE VELOCITY ZONES

Thus far there has been no attempt to identify or postulate the compositions of the three zones indicated by the seismic refraction data. The 1947 borings have not made definite identification possible because of their limited depths and their location on Bikini Island, at the atoll's edge instead of under the lagoon, where the refraction data apply. The well logs give evidence, however, which, combined with other indications, virtually specifies the nature of the uppermost zone and also provides us with a strong clue to the identity of the intermediate layer. Until a deeper or more ideally located hole is drilled, therefore, the internal constitution of the atoll can only be inferred from the best available geological and geophysical evidence.

Cuttings from the 2556-foot hole on Bikini Island (Ladd *et al.*, 1948) show only calcareous material from the surface to the bottom. The first 600 feet contains occasional hard streaks of limestone with loose calcareous sand in between. From 600 feet to the bottom, only loose sand (nearly all of Tertiary age) is encountered. Vertical seismic velocities measured in this hole to a depth of 1800 feet fluctuated irregularly but showed definite trends when smoothed. In the first 1000-foot interval velocities averaged about 7500 ft/sec although local values between successive detector positions were as high as 11,000 ft/sec. Actually, velocities over intervals of 100 feet or so cannot be determined accurately and the local fluctuations may indicate only the normal uncertainty in reading arrival times. In the remaining 800 feet the speeds were observed to increase more or less regularly from about 7000 ft/sec to 10,000 ft/sec.

The refraction data indicate that the zone with a horizontal speed of 7000 ft/sec extends from a depth of 2000 or 3000 feet upward to the lagoon bottom, since the time-distance segments representing it intercept the origin at zero time. Core samples several feet long (Emery, 1946) taken from the lagoon floor show that the bottom sediments over much of the lagoon consist largely of fragments of the calcareous alga *Halimeda*. Shallow water sediments of the same lithologic type would be expected to continue downward from the lagoon bottom to the first seismic discontinuity.

The 140-foot boring in the lagoon bottom at Funafuti (Skeats, 1918) showed the upper 70 feet to consist almost entirely of *Halimeda*. The second 70 feet contain

mostly coral and foraminiferal limestone cemented by calcite. The investigation of the materials obtained from drill cores and cuttings at Bikini Island has not been completed. *Halimeda* does not seem to extend an appreciable distance below the surface. But all calcareous materials brought to the surface in the drilling are of kinds that would not have been laid down in water deeper than a few hundred feet. In this sense all are "shallow water" sediments as opposed to those ordinarily at the bottom of the deep sea. Small irregularities in the refraction arrival times from the uppermost zone as well as fluctuations in the vertical velocities observed in the well shooting suggest that some inhomogeneities exist in the elastic properties of these sediments.

The only observations in the literature on the speed of sound in recent calcareous material were made by Ewing *et al.* (1948) off Barbados and by Woollard and Ewing (1939) at Bermuda. Off Barbados they obtained a speed of 5620 ft/sec in the uppermost layer and at Bermuda, 8800 ft/sec. The Barbados, Bermuda, and Bikini speeds all lie within the range of 5600 to 13,800 ft/sec quoted by Birch (1942) for "soft" limestone.

The second zone, with an apparent horizontal seismic velocity of 11,000 ft/sec, is the most difficult to identify. Its constitution, when established, will very probably provide the key to the atoll's origin and geologic history. If one extrapolates the observed interval velocities in the lower half of the 1800-foot velocity log in the Bikini Island boring, one would predict a speed of 11,000 ft/sec at a depth of 2000 feet. This is the speed which, according to the refraction data, extends downward without increase (although it may decrease) for a considerable depth below an interface at 2000–3000 feet sub sea. The most direct implication to be drawn from all the data taken together is that the calcareous deposits continue to the top of the 17,000 ft/sec zone and that the 11,000 ft/sec marker is the top of a zone in which the speed of seismic waves no longer increases with depth. Such a seismic speed distribution would suggest that the calcareous sand becomes increasingly compacted, cemented, and possibly replaced by dolomite down to a depth below which no further change is possible. The increase in compaction and cementation appears to begin at 1000 feet and the limiting depth would be 2000 to 3000 feet.

Upon receipt of the data from the vertical velocity survey, some question arose as to whether the seismic refraction data, indicating discrete zones of constant speed separated by surfaces of discontinuity, were compatible with the vertical velocity log, which shows an increase of speed with depth below 1000 feet. A calculation was accordingly made to determine the time-distance curve that would be observed if the horizontal velocity varied with depth in the same way as the vertical speeds registered in the up-hole shooting. On the basis of the smoothed log, it was assumed that the horizontal speed is 7000 ft/sec from the surface to 1000 feet and that it increases downward for the next 1000 feet at a uniform rate of 4 ft/sec for each foot, so that at 2000 feet it would be 11,000 ft/sec, the value indicated by refraction for the first interface. Below this a uniform speed of 11,000 ft/sec was assumed. A calculation based on curved-path theory showed that all arrivals from the zone of increasing speed would be masked by earlier direct-path arrivals through the 7000 ft/sec zone and also by arrivals along the top of the 11,000 ft/sec zone. Hence the

observed refraction data would not be contradicted by an increase of speed with depth from 1000 feet to the top of the intermediate layer. Such an assumption would require an increase of about 20 per cent in the computed depth to the first interface and about 10 per cent to the second, but it would not change the significant features of the refraction picture.

Since the suggested interpretation of the 11,000 ft/sec zone as "shallow water" calcareous material in a limiting condition of compaction or cementation cannot be established as correct until a deep boring is put down, some alternative possibilities might be suggested. All such interpretations are necessarily speculative at this stage and they are proposed mainly to point out the range of possibilities allowed by the geophysical observations.

In the Funafuti boring, dolomite was encountered at 600 feet, continuing to the bottom of the 1114-foot hole. No dolomite, on the other hand, was found at Bikini down to 2556 feet. It is not inconceivable that there is a thick dolomite zone under Bikini so deep that it was not reached by the drill.[2] If its top surface were 2000 or 3000 feet under the lagoon bottom it might well constitute the first seismic interface. Available literature (Birch, 1942) on the speed of sound in dolomite indicates that it ranges from 16,000 to 19,600 ft/sec. This is, to be sure, higher than the observed speed of 11,000 ft/sec, and it may indicate that any dolomite constitutes a relatively small proportion of the calcareous material at this depth. The previously suggested encrustation of higher speed material at the top surface of the intermediate zone might represent a layer of greater dolomitization.

Professor Daly has suggested that the second zone might consist of volcanic materials such as pyroclastics. No data are available on seismic velocities in materials of this kind, but when evidence from the 1946 aerial magnetic survey makes it possible to estimate the depth to igneous material under Bikini, the plausibility of this hypothesis can be assessed more definitely. Finally, there is the possibility that the zone consists of pelagic or other organic limestone deposited on an elevated igneous platform or an undersea peak under such conditions that it would not dissolve or be swept off by ocean currents. The 11,000 ft/sec speed is well within the range of previous measurements on limestone of such origin (Birch, 1942).

Identification of the 17,000 ft/sec zone must also be based on circumstantial considerations. This seismic speed lies within the range that has been observed both in igneous rocks, such as granites and basalts, and in compact limestones. While it is conceivable that there might be a hard limestone layer at the base of the atoll, it would be very difficult to explain the considerable thickness that would be indicated for it by the 8-mile long segments representing it on the time-distance curves unless its speed were greater than or identical to that of the basement. The 6000-foot relief of its top surface would also be peculiar. It is more likely that the zone represents the igneous basement, which under the part of the Pacific that lies east of the andesite line is predominantly basaltic. This identification is essentially supported by the seismic measurements of Brockamp and Wölcken (1929) who obtained a speed of 18,300 ft/sec for some known basalt formations in Germany.

---

[2]We are indebted to Professor Bucher for calling attention to this possibility.

INDICATIONS OF SUBSIDENCE

If it is assumed that calcareous material deposited in water not more than a few hundred feet deep extends from the surface to the top of the 17,000 ft/sec zone, one must conclude that there has been 7000–13,000 feet of subsidence, or relative change in sea level, in the atoll's geological history. The broad terrace in the northeast portion of the 17,000 ft/sec surface suggests that the topographic relief of this surface is due to sub-aerial erosion. If this could be proved, we would know that the total subsidence must have been at least 13,000 feet. But no such proof is possible at present.

If, on the other hand, the intermediate zone has some other constitution than compacted coral or algal sand, the almost certain identification of the uppermost zone as calcareous establishes a minimum subsidence of 2000–3000 feet. Moreover, the anomalous arrival times suggesting a greater depth to the intermediate zone under Enyu Channel may require the assumption of a substantially larger minimum subsidence.

The existence of a broad and probably igneous summit under the atoll about 6500 feet below sea level is especially interesting in view of the announcement by Hess (1946) that fathometer surveys over a wide belt of the Central Pacific have revealed the existence of 160 flat-topped truncated and beveled cones, which he calls "guyots", ranging in depth from 3000–6000 feet. Additional seamounts, or "guyots", have subsequently been charted by Emery (1946). One of these adjoins Bikini on the northwest. Hess explained these as volcanic islands that sank too early in geological time or too rapidly for reef-building organisms to grow substantial accumulations during subsidence.

There is a possibility that the buried igneous mountain under Bikini coincides in geological origin with the near-by submerged truncated cones. Unfortunately the seismic survey could not give as precise data on the depth and shape of the former as the fathometer has given on the contours of the latter, and comparisons are difficult. However, the basement surface under Bikini apparently has considerably more relief than the almost flat tops of Hess's "guyots".

INFERENCES REGARDING GEOLOGIC HISTORY OF BIKINI

The geophysical data suggest several lines of speculation relative to the origin and geologic history of Bikini. Vaughan (1923) and Hobbs (1923) have pointed out the fallacy of assuming that a single theory can explain the origin of all coral reefs and atolls everywhere in the world, and it would certainly not be warranted to assume that all atolls have the composition indicated for Bikini.

In the present state of our knowledge, all theories regarding Bikini's geologic history must depend on the identity assumed for the 11,000 ft/sec layer indicated by the refraction data. If, as seems logical, this layer consists of calcareous material, like that now being deposited, which has been compacted into a state of maximum consolidation, the atoll must have formed somewhat in the manner Darwin proposed, with a total subsidence of more than 2 miles. If the layer is presumed to be dolomitic, one can postulate essentially the same mechanism with the additional stipulation that conditions favored dolomitization of the reef limestone from the time of its

initial deposition until a thickness was reached 2000–3000 feet less than the present thickness.

If one assumes that the intermediate zone is volcanic and consists of tuffs or pillow lavas, it is logical to propose an eruption from a submerged volcano of igneous products that emerged above sea level, forming a volcanic island something like Falcon Island today (Hoffmeister and Ladd, 1944). An island of such soft material would offer small resistance to wave cutting and, like Falcon, would soon be scalped to sea level. At this stage, shallow-water organisms would affix themselves to the platform's surface and upon subsidence would build up a calcareous layer several thousand feet thick.

If the intermediate layer should consist of pelagic or other deep-sea limestone, the mechanism becomes essentially a combination of that called for by the old Rein-Murray theory and of Darwinian subsidence. Organic matter deposited on the surface of a deeply buried igneous platform builds up an increasing thickness of pelagic lime until its top is shallow enough for calcareous organisms such as corals and algae to take over. Subsidence would become the controlling factor at this point and the present structure would be the result of a several thousand foot relative rise in sea level. Banks, ridges, and other isolated topographic highs at depths as great as 400 fathoms off the California coast have been shown by Revelle and Shepard (1939) to have only a sparse and discontinuous veneer over rocky bottom. They ascribe this fact to the action of turbulence associated with intermittent bottom currents which suspends the sedimentary particles momentarily and allows the component of gravity downslope eventually to remove the particles from the topographic high. If this process exists on mid-ocean banks, it is not likely that any appreciable amount of pelagic material could have accumulated on the initial platforms and this theory would thus not be tenable.

PROPOSED ADDITIONAL INVESTIGATION

Further progress toward solving the complex problems presented by atolls might be made through several types of investigation. The deep boring now being contemplated would be of utmost value, but further geophysical studies would be desirable to get maximum return from the investment the boring will require. A vertical velocity survey in the proposed hole should give valuable data which would facilitate further interpretation of the refraction results. With the boring to provide precise tie points at various interfaces, a much more detailed refraction survey of the atoll than was possible in 1946, with more profiles and complete reverse control, could detail the atoll's structure much more precisely and reliably than was then possible. It would extend the information obtained by the drill over a wide area at low expense and make it possible to draw from the results of seismic surveys on other atolls more general conclusions concerning the similarity in structure and history of the various atolls without numerous expensive borings.

Finally, absolute gravity measurements—particularly with a Vening Meinesz pendulum operated on a submarine in the ocean outside an atoll and also inside its lagoon—should give valuable information on the degree of isostatic compensation under atolls and furnish additional evidence as to their nature and origin.

REFERENCES CITED

Beers, Roland F., and Shugart, T. R. (1948) *Seismic velocities at Bikini* [Abstr.], Geophysics, vol. 13, p. 498.

Birch, Francis (Editor) (1942) *Handbook of physical constants*, Geol. Soc. Am., Spec. Papers, no. 36, 325 p.

Brockamp, B., and Wolcken, K. (1929) *Zeits. für Geophysik*, vol. 5, p. 482.

Daly, R. A. (1915) *The glacial control theory of coral reefs*, Am. Acad. Arts Sci., Pr., vol. 51, p. 155–251.

Dana, J. D. (1852) *On coral reefs and islands*, New York.

Darwin, Charles L. (1842) *The structure and distribution of coral reefs*, London.

Davis, William M. (1928) *The coral reef problem*, Am. Geog. Soc., Spec. Pub., no. 9.

Emery, K. O. (1946) *Submarine geology of Bikini Atoll*, [Abstr.], Geol. Soc. Am., Bull., vol. 57, p. 1191.

Ewing, Maurice, Pekeris, C. L., and Worzel, J. L. (1948) *Propagation of sound in the ocean*, Geol. Soc. Am., Mem. 27, 205 p.

Gardner, L. W. (1939) *An areal plan of mapping subsurface structure by refraction shooting*, Geophys., vol. 4, p. 247–259.

Hess, H. H. (1946) *Drowned ancient islands of the Pacific Basin*, Am. Jour. Sci., vol. 244, p. 772–791.

Hobbs, W. H. (1923) *Reef formations as an index of mountain building processes*, Pan-Pac. Sci. Cong., Pr., Australia, vol. 2, p. 1128–1131.

Hoffmeister, J. E., and Ladd, H. S. (1944), *The antecedent platform theory*, Jour. Geol., vol. 6, p. 388–401.

Kuenen, Ph. H. (1947) *Two problems of marine geology: atolls and canyons*, Koninkl. Nederl. Akad. Wet. Verh. (Tweede Sectie) Dl. XLIII, p. 1–69.

Kuwahara, S. (1939) *Velocity of sound in sea water and calculation of the velocity in sonic sounding*, Hydrographic Rev. (Monaco), vol. 16, p. 123–140.

Ladd, H. S., and Hoffmeister, J. E. (1936) *A criticism of the glacial-control theory*, Jour. Geol., vol. 44, p. 74–92.

———, Tracey, J. I., and Lill, C. G. (1948) *Drilling on Bikini Atoll, Marshall Islands*, Science, vol. 107, p. 51–55.

Matsuyama, Motonori (1918) *Determination of the second derivatives of the gravitational potential on the Jaluit Atoll*, College of Science, Mem, Kyoto, vol. 3, p. 17–68.

Nettleton, L. L. (1940) *Geophysical prospecting for oil*, New York.

Revelle, R. (1947) *Bikini revisited*, [Abstr.], Science, vol. 106, p. 512–513.

———, and Shepard, F. P. (1939) *Recent marine sediments*, Am. Assoc. Petrol. Geol., Symp., Edited by P. D. Trask, p. 245–280.

Royal Society of London (1904) *The Atoll of Funafuti*.

Skeats, E. W. (1918) *The coral reef problem and the evidence of the Funafuti boring*, Am. Jour. Sci., 4th ser., vol. 45, p. 81–90.

Snavely, B. L., Beresford, R., Clarkson, H. N., Erickson, K. W., White, G., and Atanasoff, J. V. (1947) *Use of a water coupled microphone system for seismic surveying*, [Abstr.], Geophys. vol. 12, p. 500.

Stearns, Harold (1946) *An integration of coral reef hypotheses*, Am. Jour. Sci., vol. 244, p. 245–262.

Vaughan, T. Wayland (1923) *Coral reefs and submerged platforms*, Pan-Pacific Sci. Cong., Pr., Australia, vol. 2, p. 1128–1131.

Woollard, G. P., and Ewing, Maurice (1939) *Structural geology of the Bermuda Islands*, Nature, vol. 143, p. 898.

NAVAL ORDNANCE LABORATORY, WASHINGTON, D. C., AND COLUMBIA UNIVERSITY, NEW YORK, N. Y.; OFFICE OF NAVAL RESEARCH, WASHINGTON, D. C.; NAVAL ORDNANCE LABORATORY, WASHINGTON, D. C.

MANUSCRIPT RECEIVED BY THE SECRETARY OF THE SOCIETY, APRIL 30, 1948.

BULLETIN OF THE GEOLOGICAL SOCIETY OF AMERICA
VOL. 60, PP. 829-860, 11 FIGS., 5 PLS. MAY 1949

UPPER PLIOCENE VERTEBRATES FROM KEEFE CANYON, MEADE COUNTY, KANSAS

BY CLAUDE W. HIBBARD AND ELMER S. RIGGS

CONTENTS

	Page
Abstract	829
Introduction and acknowledgments	830
Rexroad formation	832
General considerations	832
Measured section	832
Drilled section	833
Vertebrate fossils from the Keefe Canyon deposits	834
Reptilia	834
Mammalia	835
Summary	859
References cited	859

ILLUSTRATIONS

Figure	Page
1. Small mammals. Occlusal views of teeth	837
2. Teeth of mole, marten, pack-rat, peccary and horse	839
3. Parts of peccary, giant camel, and Pliocene llama	842
4. Skulls of giant camel, *Gigantocamelus spatulus* (Cope)	848
5. Jaws of giant camel, *Gigantocamelus spatulus* (Cope)	849
6. Teeth of giant camel, *Gigantocamelus spatulus* (Cope)	850
7. Limb bones and vertebra of giant camel	851
8. Jaws of giant camel and Pliocene llama	852
9. Lower jaw and dentition of giant camel	853
10. Lower jaws of *Pliauchenia cochrani* sp. nov., holotype	856
11. Dentition of Pliocene llama, *Tanupolama blancoensis* Meade	857

Plate	Page
1. Keefe Canyon, Meade County, Kansas	830
2. Keefe Canyon quarry, Meade County, Kansas	831
3. Skull of *Gigantocamelus spatulus* (Cope)	844
4. Teeth of mastodon and skeletal elements of camels	845
5. Skeletal parts of camels and ground sloth	858

ABSTRACT

A late Pliocene artesian spring basin in Meade County, Kansas, was a trap for animals that came to the spring for water. They were either trapped by quicksand or became mired in the bog area around the edge of the spring. Some of the larger mammals that inhabited the region at the time the Rexroad fauna lived were recovered from this deposit. The following forms new to the Rexroad fauna were recovered from the Keefe Canyon deposit: ?*Megalonyx* sp.; *Dipoides rexroadensis* sp. nov.; *Martes foxi* sp. nov.; *Platygonus bicalcaratus* Cope; *Gigantocamelus spatulus* (Cope); *Pliauchenia cochrani* sp. nov.; and *Tanupolama blancoensis* Meade.

INTRODUCTION AND ACKNOWLEDGMENTS

The Rexroad fauna of Meade County, Kansas, is one of the better known late Cenozoic faunas of the High Plains region. To date, most of the forms recovered have been smaller animals. Previously only fragmentary evidence was at hand to indicate the presence of some of the larger mammals that were associated with the smaller forms.

In the fall of 1943, while Thad McLaughlin, Henry Firner, Elmer S. Riggs, and Claude W. Hibbard were searching the Guy Fox pasture for possible vertebrate remains, Riggs discovered a bone deposit which consisted chiefly of the remains of large mammals. The fossil deposit was found in Keefe Canyon, SW¼ SW¼ sec. 34, T.34 S., R. 30 W., Meade County, Kansas. The deposit was opened and worked during September and October. It was worked in 1944 from July 21 to September 20 by Hibbard, Riggs, and Dick Rinker. In 1945 the deposit was worked from July 23 to August 25 by Hibbard, Riggs, Rinker, Russell Camp, Manuel Maldonado, Dr. W. J. Baumgartner, and Dr. G. C. Rinker.

The specimens recovered were prepared for study by E. S. Riggs. The larger specimens were figured and checked under his direction and drawings were made by John Conard Hansen and Virginia L. Cassell. Drawings of the small forms were made by Frances Neidig and W. C. Sherman.

The deposit containing the fossils in Keefe Canyon was an old artesian spring basin. The present stream dissected the deposit and at least one-half of it and the overflow area of the basin had been removed by erosion (Pl. 1, fig. 1). At the time the spring was active, the area was apparently rather flat. Whether the underlying sands and gravels of the Rexroad formation formed the aquifer is not known.

At the Keefe Canyon quarry the vertical tube allowing the escape of the artesian water was approximately 30 inches in diameter and was developed in the underlying silt beds. The tube contained very fine sand, dominantly flour sand. The opening of the tube expanded broadly into the basin created by the flow. Concavities occurred in the walls of the silt near the mouth of the tube. Coarse sands, many small bone fragments, and horse teeth were lodged in these. This material had been churned by the artesian waters to become highly polished, and some were badly broken. Sometimes as much as half a gallon of fine bone fragments, mixed with highly polished enamel fragments of teeth, were encountered with some coarse sand. When a pocket like the one described above was encountered there was certain to be one or two horse teeth in it that had acted as millstones in breaking down the more fragile material. It was from the pockets of coarse sand and ground bone that the jaws and teeth of the small vertebrates were recovered.

The floor of the basin consisted of fine white flour sand overlying reddish silt. The maximum thickness of the sand was approximately 3 feet, rapidly thinning laterally to the edge of the basin. The part excavated was approximately a half circle with a 16-foot diameter. The sand tube of the spring was only 2 feet from the present stream bank. It may be estimated that about one-half of the deposit had been destroyed by erosion. The bone deposit was a conglomeration of disassociated, churned, broken, polished, and ground fragments matted with the complete material recovered (Pl. 2, figs. 1, 2). Parts of at least 2 mastodons, 21 giant camels, 15 smaller camels, numerous peccaries, a number of zebras, a giant dog, and a sloth were

FIGURE 1. QUARRY TO THE EXTREME LEFT
Meade Gravels near top of canyon wall.

FIGURE 2. BONE DEPOSIT AT BASE OF QUARRY
Note thickening of caliche to the left.

KEEFE CANYON, MEADE COUNTY, KANSAS

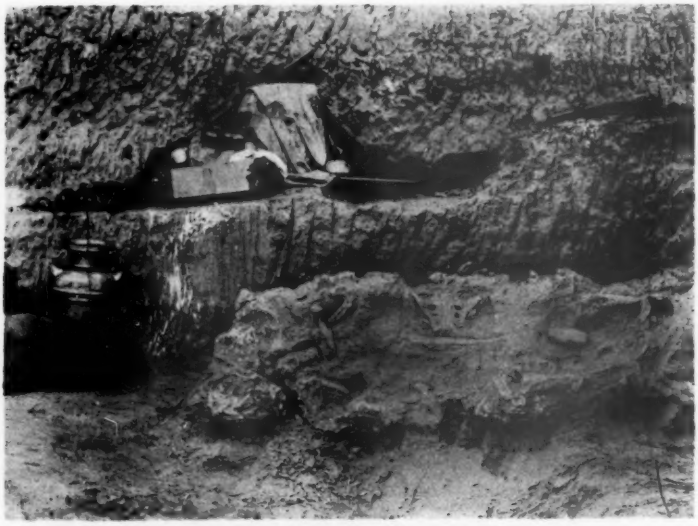

FIGURE 1. FLOUR SAND FROM ARTESIAN SPRING CONTAINING FOSSILS

FIGURE 2. CLOSE-UP VIEW OF A CHURNED MASS OF BONES

KEEFE CANYON QUARRY, MEADE COUNTY, KANSAS

found besides the fragmentary remains of birds and smaller mammals. Only 2 large pebbles were found in the deposit. The bones and the large teeth acted as grinding agents in the churning sand and water. The flour sand was covered by a layer of clay from 1 to 3 inches in thickness, blue gray to green gray. The clay thinned laterally into the sandy silt. Above the band of nearly pure clay was a zone of silty clay grading upward into a reddish sandy silt containing caliche. At the edge of the basin, reworked silty clay was mixed with many bone fragments and some plant material. The area around the artesian spring appears to have been a great deal like the bog areas around the present artesian springs along Crooked Creek Valley. Obviously the animals were mired in the bog or quicksand when they came to the pool for water. Around the edge of the spring skeletons were trampled and broken over a long period of time by animals which either watered there or became mired themselves. There was evidence that the bones along the edge of the basin were exposed to weathering, which probably helped to fracture them since they were not deeply buried. The bones recovered from the flour sand are white; all material in the silt and clay proper are reddish brown to dark brown as though they were stained under bog conditions. No lignite seams occurred in the deposit.

The spring was apparently destroyed by the deposition of silt and fine sand which occurs above it throughout the general region. The massive caliche horizon in the Rexroad occurs approximately 6 feet above the top of the quicksand. Above the spring proper only caliche nodules were found, to a depth of 1 foot, but 50 yards upstream the caliche forms a massive bed slightly more than 2 feet thick. A distinctive caliche zone occurs in the region above the fossil-bearing horizon (Pl. 1, fig. 2). The widespread massive hard white caliche of bed 5 apparently developed under rather stable conditions. The climate was probably semi-arid and the caliche was deposited near the surface, as a primary deposit which may have later been altered, added to, or removed by solution; at least its origin is different from that of the caliche nodules and vertical stringers observed in the silt deposits.

The top of another old artesian spring had been removed by erosion in sec. 22, T. 33 S., R. 29 W., Meade County, and the sand tube which allowed the exit of water was excavated in 1936 and followed to the depth of 10 feet. Many fossil teeth were recovered from the sand. A more recently abandoned artesian spring is the Cragin quarry of late Pleistocene age, SW¼ sec. 17, T. 32 S., R. 28 W., on the Big Springs ranch, Meade County. A few yards northeast of the Cragin quarry and in the bottom of the valley is an artesian spring which flows approximately 800 gallons a minute. The evidence indicates that this spring flowed during part of the late Pleistocene at the level and locality of Cragin quarry but has later shifted because of the down-cutting of Crooked Creek and its tributaries.

Acknowledgment is made to the Geological Society of America for a grant from the Penrose Bequest, used to help defray the expense of the drawings; also, to E. Raymond Hall of the University of Kansas Museum of Natural History for permission to Hibbard to finish the report of the study after leaving the University of Kansas. We are indebted to Thad McLaughlin for his generous and untiring help and to the members of our field parties who contributed greatly in the removal of the fossil vertebrates from the Keefe Canyon quarry. Through the generosity and kindness of the following, who co-operated in every way possible during the war years we were able to complete the excavation in Keefe Canyon: the Kansas State Fish and Game

Commission, who permitted us to use their dwelling quarters; Mr. Guy Fox, owner of the land in Keefe Canyon, and numerous friends in Meade County. We are further indebted to Bryan Patterson, Chicago Natural History Museum; G. G. Simpson, American Museum of Natural History; and W. H. Burt, University of Michigan, Museum of Zoology, for permission to use specimens under their care for comparative study.

REXROAD FORMATION

GENERAL CONSIDERATIONS

H. T. U. Smith (1940, p. 95) named the Rexroad formation from exposures along tributaries of Crooked Creek on the Rexroad ranch, sec. 22, T. 33 S., R. 29 W., Meade County, Kansas. The beds at the type locality consist of gray to reddish silt containing stringers of caliche, buff sandy silt, and a few thin seams of lignite. Due to Hibbard's error in considering that *Equus* (*Plesippus*) *simplicidens* Cope and *Nannippus phlegon* (Hay) were confined only to deposits of Upper Pliocene, and to the fact that the Meade gravels as described by Cragin (1896, p. 53) were not restudied, the Meade gravels were included at the type locality of the Rexroad formation as the uppermost bed of the formation.

Frye and Hibbard (1941, p. 407) removed by definition the overlying basal Meade gravels from the Rexroad formation and assigned the upper Pliocene beds named by Smith the "Rexroad formation" to the Rexroad member of the Ogallala formation of Kansas. This was done chiefly to expedite the mapping and the report on the ground water of the region. Frye and Hibbard were unable to recognize the base of the formation at that time. The summers of 1942 to 1945 inclusive and a part of 1947 have been spent in that region studying deposits of the Rexroad formation. In the summer of 1943, McLaughlin and Hibbard recognized the base of the Rexroad formation in Meade and Seward counties.

For a review of the Rexroad problem and the recognition of the Rexroad as a distinct formation one is referred to McLaughlin (1946, p. 33, 113) and Byrne and McLaughlin (1948, p. 31, 34, 73).

Except for the flat-lying Rexroad beds in Wolf Canyon, the exposed beds have been involved in secondary regional sinking and dip either toward the Cimarron Valley or Crooked Creek Valley. The beds in Keefe Canyon dip toward the Cimarron Valley and disappear beneath the valley floor.

MEASURED SECTION

Section of the Rexroad and Meade formations, Keefe Canyon, Sec. 3, T. 35 S., R. 30 W., and SW ¼ Sec. 34, T. 34 S., R. 30 W.

(Measured by McLaughlin and Hibbard)

Bed No.	Description	Thickness (feet)
13.	Topsoil	
	Pleistocene	
	Meade formation	
12.	Silt, fine sandy, reddish	3.0
11.	Silt, fine sandy, tan to pinkish, with stringers of caliche near top	24.5
10.	Clay, reddish brown	3.0
9.	Silt, fine sandy, brownish buff	5.75
8.	Sand and gravel, coarse, locally cemented with calcium carbonate	33.0
	Disconformity	

Bed No.	Description	Thickness (feet)
Pliocene		
	Rexroad formation	
7.	Silt, fine sandy, reddish buff, grading upward into buff; contains stringers of caliche near the top	24.5
6.	Silt, fine sandy, reddish buff to tan grading to gray near top with zones of caliche.	13.0
5.	Caliche, thin zone, in places massive	2.0
4.	(Local within bed 3) Clay, blue-gray, containing white flour sand pockets (Keefe Canyon quarry, Locality 22)	3.0
3.	Silt, fine sandy, reddish buff, lenses of clay, bog-stained, light brown to blue gray, 12.5 feet above the base is a 3-foot zone with gastropods	23.5
2.	Interval covered.	
1.	Sand, fine to medium, micaceous, light yellow to rusty, cemented, alternating with clay and silt. Base not exposed	25.0

DRILLED SECTION

Because of the good exposure of beds in Keefe Canyon and the fact that these beds could be correlated with test hole samples, a drilling rig was set at the head of the canyon on the flat upland and test hole no. 17 was drilled (Byrne and McLaughlin, 1948, p. 117–118).

Log of test hole 17 in the SE¼ NE¼ Sec. 33, T. 34 S., R. 30 W., Meade County, Kansas

Drilled by the State Geological Survey, 1944. Surface altitude, 2655 feet. (Authority, Samples studied by Oscar S. Fent and Thad G. McLaughlin.)

Description	Thickness (feet)	Depth (feet)
Soil, silty, tan	4.5	4.5
Pleistocene		
Meade formation		
Silt, light gray to light brown, contains caliche and fine to coarse sand	23.5	28
Silt, light buff, and caliche, buff; sandy	5	33
Silt, clayey, light brown	4	37
Sand, coarse to fine, and gravel, medium to fine	3	40
Gravel, coarse, to sand, fine	15	55
Silt, light gray, contains caliche	3	58
Sand, coarse, to gravel, coarse, contains caliche	12	70
Pliocene		
Rexroad formation		
Silt, white and light buff, contains caliche and fine to coarse sand	25	95
Silt, clayey, light brown and white	15	110
Silt, clayey, gray brown to light brown, contains sand and fine gravel	10	120
Gravel, fine to medium, sand, and silt, light brown and white; contains caliche	7	127
Silt, clayey, dull yellow and light blue-gray	12	139
Sand, coarse to fine, and gravel, medium to fine; contains a little silt, greenish-gray and buff	61	200
Sand, coarse to fine, and gravel, fine	30	230
Sand, coarse to fine, and silt, light greenish-gray	22	252

Description	Thickness (feet)	Depth (feet)
Laverne formation		
Silt, soft, light gray to light tan, contains fine to medium sand	8	260
Silt, clayey, light gray, light buff, and light blue gray	20	280
Clay, thin-bedded, blue gray, contains fine sand	20	300
Clay, light blue gray	20	320
Clay, silty, blocky, dull greenish-gray	6	326
Silt and clay, brittle, gray	4	330
Silt and clay; gray and blue gray; contains very fine sand	23	353
Silt, green, contains fine to very fine sand	7	360
Clay, silty, light green gray and blue gray	10	370
Clay, soft, light gray	50	420
Clay, soft, light gray, contains thin beds of caliche and a little sand	25	445
Sand, coarse to fine, and gravel, fine	47	492
Clay, silty, white to pink buff	5	497
Sand, coarse to fine, contains white and buff silt	23	520
Sand, coarse to fine, and gravel, fine	80	600
Sand, coarse to fine, and gravel, fine; in part cemented; contains light buff and pink silt in lower part	14	614
Permian (red beds)		
Shale, silty, dull red	11	625

VERTEBRATE FOSSILS FROM THE KEEFE CANYON DEPOSIT

The Keefe Canyon deposit, SW¼ SW¼ sec. 34, T. 34 S., R. 30 W., Meade County, Kansas, is known as University of Kansas Museum of Natural History, Locality 22. The fossil remains included in this study are chiefly those of mammals and represent a part of the Rexroad fauna of Meade County, equivalent in age to the Blanco fauna of Texas.

Class REPTILIA
Order TESTUDINATA
Family TESTUDINIDAE
Testudo riggsi Hibbard

Testudo riggsi HIBBARD, 1944, Univ. Kans. Sci. Bull., vol. 30, pt. 1, no. 7, p. 72, Fig. 1.

This small land turtle was reported by Hibbard in 1944, as having been taken from deposits of middle Pliocene age. Later studies in 1944, 1945, and 1947, proved that the upper part of the Saw Rock Canyon section, from which the turtle remains were taken, belongs in the Rexroad formation. The beds of the Rexroad formation were traced northwestward on the north side of the Cimarron Valley from Locality 22, sec. 34, T. 34 S., R. 30 W., to SW¼ sec. 20, T. 34 S., R. 30 W. At this locality, an exposure of part of the Rexroad formation is overlain by the basal Meade sands and gravels. Three specimens of *Testudo riggsi*, nos. 7404, 7405, and 7406, taken from this bed of red sandy silt agree with the holotype and paratype, as well as with fragments recovered in Keefe Canyon quarry.

The sandy silt exposure from which the 3 specimens of *Testudo* were taken is the same horizon as the one just southwest across the Cimarron River from which the type was taken.

Class MAMMALIA
Order INSECTIVORA
Family SORICIDAE
?Sorex sp.
(Fig. 1J)

Two rami, nos. 7011 and 7012, of a shrew slightly larger than *Sorex taylori* Hibbard were recovered from the Keefe Canyon quarry.

Family TALPIDAE
Hesperoscalops rexroadi Hibbard
(Fig. 2B)

Hesperoscalops rexroadi HIBBARD, 1941, Am. Mid. Nat., vol. 26, no. 2, p. 337.

This mole has been known only from rather fragmentary skeletal elements from the Rexroad deposits. A single tooth, no. 7691, a left M_1 or M_2 was recovered from the spring deposit in Keefe Canyon. The tooth has an overall anteroposterior diameter of 2.8 mm. The characters of the tooth are the same as those of the type specimen from Loc. 2a, Meade County, Kansas.

Order EDENTATA
Family MEGALONYCHIDAE
?Megalonyx sp.
(Pl. 5, fig. 7)

A rather small sloth phalanx, no. 7547, was recovered from the mass of camel bones, the first remains of a sloth taken from the Rexroad formation. Sloth remains reported from deposits of Blancan age are not too numerous and at present are known only from fragmentary material. The unity of the Blanco fauna of Texas and the Rexroad fauna of Kansas indicates that the above toe bone probably belonged to *Megalonyx* described by Cope from the Blanco beds.

Measurements (mm.) of phalanx, no. 7547

Greatest overall length	59.3
Depth of distal end	31.5
Width of distal end	23.0
Depth of proximal end	36.0

Order RODENTIA
Family GEOMYIDAE
Geomys quinni McGrew

Geomys quinni MCGREW, 1944, Field Mus. Nat. Hist., geol. ser., vol. 9, no. 2, p. 49–52.

A part of a left ramus, no. 6996, bearing P_4, and the anterior part of a skull, no. 6995, with incisors, right and left P^4 and M^1, of this gopher were recovered. The diastema between the incisors and P^4 in specimen no. 6995 is 11.4 mm long. For a discussion of this gopher in other Rexroad deposits *see* Franzen (1947).

Family CASTORIDAE
Dipoides rexroadensis sp. nov.
(Fig. 1G)

HOLOTYPE: No. 7693, Kans. Univ. Mus. Nat. Hist. left upper molar, $?M^1$. Collected by Hibbard and party, 1944.

HORIZON AND TYPE LOCALITY: Upper Pliocene, Rexroad formation, Keefe Canyon, SW¼ SW¼ sec. 34, T. 34 S., R. 30 W., Meade County, Kansas, Loc. 22, Rexroad fauna.

DESCRIPTION OF TYPE: Left upper molar apparently an M^1. Hypsodont tooth with an S-pattern and the base of the tooth entirely open. Anteroposterior length of the occlusal surface is 6.5 mm. Greatest width of the occlusal surface is 5.5 mm, which is the posterior part of the tooth. Tooth narrows anteriorly. Mesostria and hypostria (see Stirton, 1935, for terminology) extend to base of tooth and are open. They are filled with cement. Tooth is not enlarged at base and is

that of an adult animal. Overall length is 12.3 mm. *Dipoides rexroadensis* is considerably larger than *Dipoides stirtoni* Wilson known from Pliocene lake beds of Malheur County, Oregon, and *Dipoides williamsi* Stirton from middle Pliocene, taken at White Cone, Hopi County, Arizona. *D. rexroadensis* approaches the size of *Procastoroides lanei* (Hibbard), specimen no. 4577, more nearly than *Dipoides*. It is distinguished from *Procastoroides lanei* with which it was found by its smaller size and the more triangular shape of the occlusal surface of the tooth (Hibbard, 1941, p. 280, 309, Pl. 2, fig. 1).

Procastoroides lanei (Hibbard)

Procastoroides sweeti BARBOUR AND SCHULTZ, 1937, Am. Mus. Novitates, no. 942, p. 6.
Eocastoroides lanei HIBBARD, 1938, Kans. Acad. Sci., Tr., vol. 40, p. 244.

Seven larger isolated beaver teeth referred to the above form were found associated with the tooth of *Dipoides rexroadensis*. Tooth no. 6847, a LM_2, has an anteroposterior occlusal length of 10.0 mm, and the greatest width of the occlusal surface is 7.0 mm. Hibbard (1941, p. 279–281) discusses the large amount of variation observed in the beavers from this region. It should be pointed out again that the type of *Eocastoroides lanei* Hibbard and the right maxillary, no. 4577, from Meade County, Loc. 1, NW¼ SE¼ sec. 15, T. 33 S., R. 29 W., Meade County, Kansas, were not taken from the Rexroad formation as was first thought, but from the Meade formation just above the basal Meade sands and gravels overlying the Rexroad formation in this area.

Family CRICETIDAE

Symmetrodontomys simplicidens Hibbard

Symmetrodontomys simplicidens HIBBARD, 1941, Am. Mid. Nat., vol. 26, no. 2, p. 354.

Five lower jaws of this mouse were recovered by sifting the sand removed from the quarry. Nos. 7003, 7007, and 7008 are left rami, each possessing M_1–M_2. Nos. 7005 and 7006 are right rami, each with M_1–M_2. The characters of the jaws and teeth are the same as those of the type from Meade County, Kansas, Loc. 3, sec. 22, T. 33 S., R. 29 W.

Parahodomys quadriplicatus Hibbard
(Fig. 2C)

Parahodomys quadriplicatus HIBBARD, 1941, Am. Mid. Nat., vol. 26, no. 2, p. 356.

Only isolated teeth of this pack rat were recovered. Figure 2C is that of a left M^1.

Ogmodontomys poaphagus Hibbard
(Fig. 1K)

Ogmodontomys poaphagus HIBBARD, 1941, Am. Mid. Nat., vol. 26, no. 2, p. 352.

A number of isolated teeth, 4 rami, and parts of 2 maxillaries of this vole were taken. A right ramus, no. 6988, contains M_1–M_3. Crown length of tooth row is 8.2 mm. A left ramus, no. 6987, Fig. 1K, is that of an old adult. A left maxillary, no. 6992, contains M^1 and M^2. Anteroposterior length of the 2 teeth along the occlusal surface is 5.0 mm. Specimens agree with type and paratypes from Loc. 3, Meade County, Kansas.

Order CARNIVORA
Family MUSTELIDAE
Martes foxi sp. nov.
(Fig. 2D)

HOLOTYPE: No. 7001, Kans. Univ. Mus. Nat. Hist. fragment of right ramus, bearing M_2, collected summer of 1944, by Dick Rinker.

HORIZON AND TYPE LOCALITY: Upper Pliocene, Rexroad formation, Keefe Canyon, Meade County, Kansas, SW¼ SW¼ sec. 34, T. 34 S., R. 30 W.; Loc. 22.

DIAGNOSIS: Smallest of the known fossil *Martes*, approximately the size of a female "Western Marten", *Martes caurina caurina* (Merriam), but distinguished by more pronounced angle of jaw and more oblong M_2 in contrast to the more circular M_2 in recent forms of *Martes*.

DESCRIPTION OF HOLOTYPE: Smallest known fossil species of *Martes*. Tooth is that of an adult animal. Greatest diameter of M_2 is 3.15 mm, least diameter is 2.4 mm.

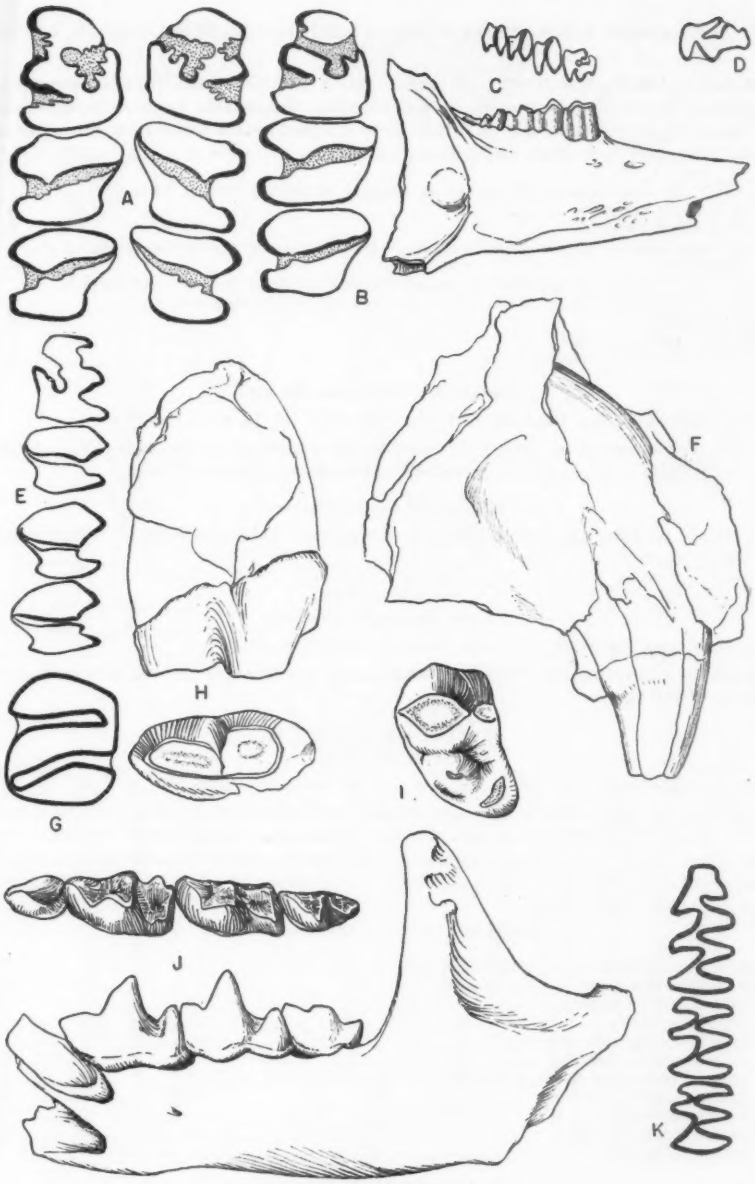

FIGURE 1.—*Upper Pliocene mammals*

(A) *Notolagus velox* Wilson. Paratype, CIT2134, left and right $P_3 - M_1$. Occlusal view. ×6. (B) *Notolagus velox*. Paratype, CIT2135, left $P_3 - M_1$. Occlusal view. ×6. (C) *Notolagus lepusculus* (Hibbard). KU6998, right ramus, $P_3 - M_2$. Labial and occlusal views. ×2. (D) *Notolagus lepusculus*. KU7000, RP_3, immature. Occlusal view. ×6. (E) *Notolagus lepusculus*. KU6999, $RP_3 - M_2$. Occlusal view. ×6. (F) *Borophagus diversidens* Cope. KU7266, part of right maxillary with canine and P^2. Lateral view. ×1. (G) *Dipoides rexroadensis* sp. nov. Holotype, KU7693, $?LM^1$. Occlusal view. ×2. (H) *Borophagus diversidens* Cope. KU7266, RP^4. Labial and occlusal views. ×1. (I) *Borophagus diversidens*. KU7266, LM^1. Occlusal view. ×1. (J) *Sorex*? sp. KU7012, left ramus, $P_4 - M_2$. Labial and occlusal views. ×10. (K) *Ogmodontomys poaphagus* Hibbard. KU6987, left $M_1 - M_2$. Occlusal view. ×6.

Ramus typical of genus *Martes*. Masseteric crest is more pronounced than in Recent forms. Angle has a well-developed groove on its dorsal surface. Subcondylar notch corresponds in size and shape to notch in *Martes caurina*. This species is named for Mr. Guy Fox on whose land was located the quarry from which this specimen was taken.

Measurements (mm.) of holotype of *Martes foxi* sp. nov.

Width of ramus below M_2	3.0
Depth of ramus below M_2	8.5
Length from posterior edge of alveolus of M_2 to posterior border of condyle, measured on lingual side	14.8
Distance from anterior border of inferior dental foramen to posterior border of alveolus of M_2	5.7
Distance from anterior border of inferior dental foramen to anterior edge of condyle	5.8
Width of condyle	9.0
Maximum depth of condyle	2.65
Height of subcondylar notch	3.2

Brachyprotoma breviramus Hibbard

Brachyprotoma breviramus HIBBARD, 1941, Am. Mid. Nat., vol. 26, no. 2, p. 340.

A left lower carnassial, no. 7015, of this mustelid was recovered from fine sand. Anteroposterior diameter of tooth is 6.0 mm; width across posterior border of talonid is 2.5 mm.

Taxidea cf. *taxus* (Schreber)

A left M_1, no. 7694, well worn, of a badger was recovered, and is referred to the badger living in the region.

Family CANIDAE

Canis lepophagus Johnston

Canis lepophagus JOHNSTON, 1938, Am. Jour. Sci., vol. 35, p. 385.

A left lower carnassial, no. 7692, of this small coyote was recovered that has an anteroposterior diameter of 18.0 mm.

Borophagus diversidens Cope

(Fig. 1F, H, I)

Borophagus diversidens COPE, 1892, Am. Nat., vol. 26, no. 312, p. 1028.

A part of the skull of this large bone-eating dog was recovered from among the mass of camel bones. The material consists of the right maxillary, in part, and a left M^1 and M^2, no. 7266. There is no evidence of P^1. P^2 is reduced, apparently single rooted, crowded lingually and anteriorly by P^3 so that it is situated along lingual side of canine. P^3 is two rooted. Lingual root of P^4 is missing. M^2 is reduced and single rooted.

Measurements (mm.) of specimen no. 7266.

Upper canine, anteroposterior length at alveolus	17.5
Upper canine, transverse width at alveolus	13.6
P^2, anteroposterior length	7.5
P^3, transverse width	5.6
P^3, (tooth missing)—alveolar length	17.0
P^4, anteroposterior length of crown	21.4
P^4, greatest anteroposterior length of tooth	30.0
M^1, anteroposterior length	16.2
M^1, transverse width	25.4
M^2, anteroposterior length	18.0
M^2, transverse width	7.8

Order PROBOSCIDEA

Family GOMPHOTHERIIDAE

Stegomastodon successor (Cope)

Mastodon successor COPE, 1892, Acad. Nat. Sci. Philadelphia, Pr., vol. 44, p. 227.
Stegomastodon successor COPE, OSBORN, 1936, Proboscidea, vol. 1, p. 671.

From the bog deposit at Loc. 3, sec. 22, T. 33 S., R. 29 W., Meade County, Kansas, 4 of the upper and lower teeth, in occlusion, of a young short-jawed mastodon, no. 4640 were recovered.

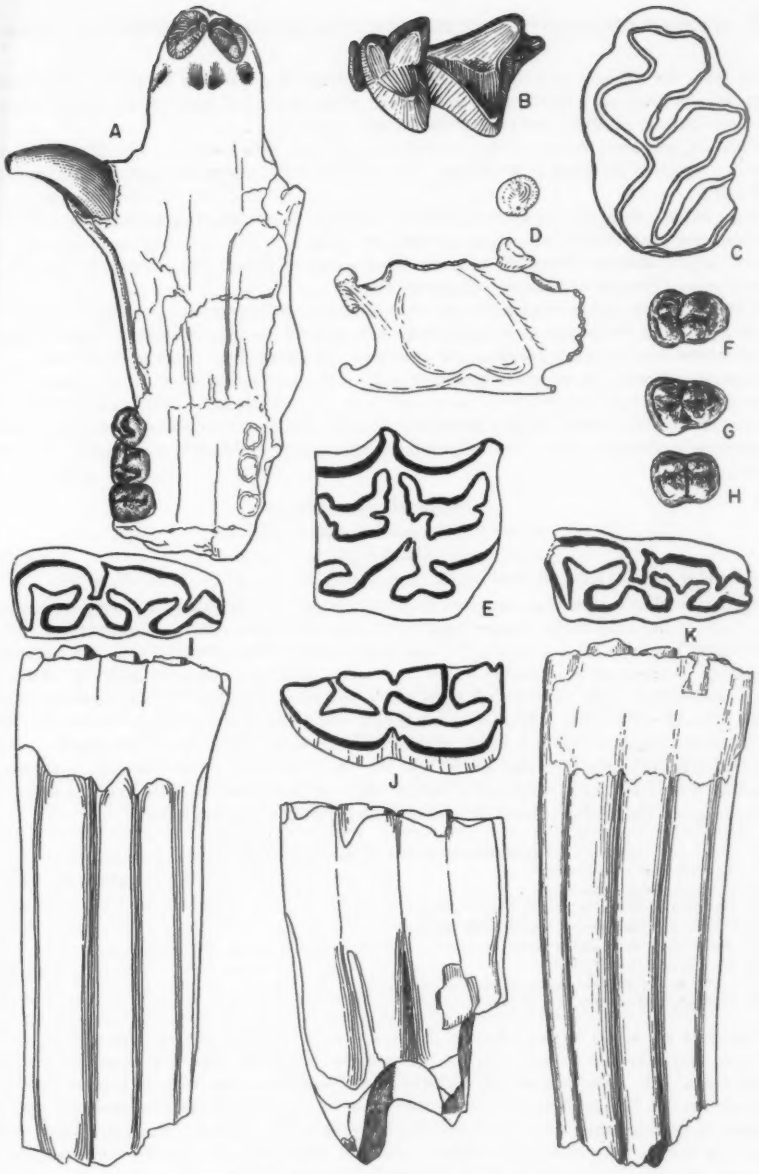

FIGURE 2.—*Upper Pliocene mammals*

(A) *Platygonus bicalcaratus* Cope. KU7274, part of premaxillary and maxillary region of skull. Anteropalatal view. ×½. (B) *Hesperoscalops rexroadi* Hibbard. KU7691, LM_1 or M_2. Occlusal view. ×10. (C) *Parahodomys quadriplicatus* Hibbard. KU7695, LM^1. Occlusal view. ×10. (D) *Martes foxi*, sp. nov. Holotype, KU7001, part of right ramus with M_2. Labial and occlusal views. ×2. (E) *Equus* (*Hippotigris*) *simplicidens* Cope. KU6819, right upper molar. Occlusal view. ×1. (F) *Platygonus bicalcaratus* Cope. KU7696, RM^3. Occlusal view. ×½. (G) *Platygonus bicalcaratus*. KU7697, LM^3. Occlusal view. ×½. (H) *Platygonus bicalcaratus*. KU6972, LM^3. Occlusal view. ×½. (I) *Equus* (*Hippotigris*) *simplicidens* Cope. KU7045, right lower molar. Labial and occlusal views. ×1. (J) *Equus* (*H.*) *simplicidens*. KU7044, LP_2. Labial and occlusal views. ×1. (K) *Equus* (*H.*) *simplicidens*. KU7045a, right lower molar. Labial and occlusal views. ×1.

These teeth are different from the short-jawed mastodon, *Stegomastodon mirificus* (Leidy) taken from the overlying basal Meade sands and gravels. The teeth of *S. successor* are shorter, consist of a fewer number of ridges, and the trefoils are less complicated.

Right M_3, no. 4640, consists of the anterior cingulum and 5½ ridge-crests. The greatest anteroposterior length of the tooth is 209.0 mm. The greatest width, across the second (anterior) loph, is 80.0 mm.

Right M^3, no. 4640, has the anterior cingulum missing. It consists of 5½ ridge-crests. Greatest width of this tooth is 85.0 mm., across the anterior loph.

Left M^3, no. 4640, consists of the anterior cingulum and 5½ ridge-crests. Anteroposterior length is 193.0 mm. The side of the first loph is broken.

The lower third molars of an adult specimen of *Stegomastodon mirificus*, no. 24314, University of Michigan, from the Meade sands and gravels possess the following characters. Anterior cingulum has been worn from both teeth. RM_3 consists of 7½ ridge-crests. Greatest width, 93.0 mm., is across fourth loph. Anteroposterior length is 221.0 mm. LM_3 consists of 7 ridge crests. The posterior one-half crest is united with the seventh loph. Overall length of tooth is 215.0 mm. Its greatest width is 91.0 mm, which is across fourth loph. Teeth of *S. mirificus* have a rectangular appearance in contrast to the elongated triangular appearance of the lower third molars of *S. successor*.

Family MAMMUTIDAE

Mammut (*Pliomastodon*) *adamsi* (Hibbard)

(Pl. 4, fig. 4)

Pliomastodon adamsi HIBBARD, 1944, Kans. Univ., Sci. Bull., vol. 30. pt. 1, no. 10, p. 109.

Specimens of this mastodon recovered from the spring basin are those of young individuals. The material had been badly churned and was broken and disassociated. Specimen no. 7267 is part of right ramus containing M_1–M_2. M_3 has not erupted. M_1 consists of 3 lophs and a posterior cingulum. Greatest anteroposterior length of tooth is 80.0 mm. Greatest width is 54.0 mm, across middle loph. M_2 consists of 3 lophs and a posterior cingulum. Greatest anteroposterior length of tooth is 113.0 mm. Greatest width is 68.0 mm, across posterior loph. A LM_1, no. 7268, has an overall length of 76.8 mm, and a width of 55.0 mm, across middle loph. A palate, no. 6983, was recovered with both right and left M^1 and M^2. It is not certain that it belongs to the above described lower teeth since fragmentary remains indicated that there was more than one individual in the deposit. Both molars consist of 3 lophs, teeth are those of a young animal.

Measurements (mm.) of specimen no. 6983

LM^1, anteroposterior diameter	81.0
RM^1, anteroposterior diameter	81.5
LM^1, transverse diameter across second loph	56.8
RM^1, transverse diameter across second loph	55.0
LM^2, anteroposterior diameter	110.0
RM^2, anteroposterior diameter	112.0
LM^2, transverse diameter across posterior loph	68.0
RM^2, transverse diameter across posterior loph	68.5

The teeth are not as large as those of the type, though the type was an older individual with M^2 worn nearly to base. Also, from the tusk associated with the type it appears that the individual was a male. The type of *Pliomastodon adamsi* was taken from near the head of Saw Rock Canyon, Seward County, Kansas. Since description of the type, it has been observed that the remains of the mastodon were taken from typical beds of the Rexroad formation, which occurs above the horizon where the invertebrates, *Osteoborus progressus* and *Dipoides* were recovered in the same exposure.

Tusks encountered with the above specimens were all very small. If they belonged with the maxillaries they would indicate that the maxillaries were those of a female. The difference in the size of M^2 between the young individual and the type is considered to be due to age, or to both age and sex.

Presence of the mastodons in these deposits is further evidence of a much more wooded condition along the streams during Rexroad time than now.

Order LAGOMORPHA
Family LEPORIDAE
Notolagus lepusculus (Hibbard)
(Figs. 1C, D, E)

Notolagus velox WILSON, 1937, S. Calif. Acad. Sci., Bull., vol. 36, pt. 3, p. 98.
Dicea lepuscula HIBBARD, 1938, Am. Mid. Nat., vol. 21, no. 2, p. 509.

Three lower jaws of this small rabbit were recovered from the spring deposit. Pattern and size of teeth correspond with those of the type of *Notolagus lepusculus*. No. 6998 is a right ramus of a young adult rabbit bearing P_3–M_3. Crown length of teeth is 8.8 mm. Depth of ramus below M_3 is 9.8 mm. No. 6999 is part of a right ramus bearing P_3–M_3, of a younger individual. The teeth have a crown length of 7.9 mm. No. 7000, another right ramus bearing only P_3–P_4, is that of an immature individual (Fig. 1D). The crown of P_3 is rather elongated. The internal re-entrant angle of P_3 is not bifurcated as in the type or as in specimens of *Notolagus velox* Wilson (Figs. 1A, B). Size and the uncrenulated internal re-entrant angles of the lower molariform teeth distinguish *N. lepusculus* from *N. velox*.

We are greatly indebted to Chester Stock of the California Institute of Technology for the opportunity to study the specimens of *Notolagus velox* and for permission to figure the drawings of them for comparison.

Order PERISSODACTYLA
Family EQUIDAE
Equus (*Hippotigris*) *simplicidens* Cope
(Figs. 2E, I, J, K)

Equus simplicidens COPE, 1892, Am. Philos. Soc., Pr., vol. 30, p. 124.
Plesippus simplicidens (COPE) MATTHEW, 1924, Am. Mus. Novitates, no. 131, p. 2.
Hippotigris simplicidens (COPE) MCGREW, 1944, Field Mus. Nat. Hist., geol. ser., vol. 9, no. 2, p. 55.

Forty isolated teeth of the above horse were recovered. Most were taken from the vertical sand tube which allowed the upward escape of the water. Many of them were badly abraded. Two upper teeth, nos. 7540 and 7541, greatly resemble those teeth of *Pliohippus* and do not appear as advanced as the teeth of *E. simplicidens* which were recovered from the overlying basal Meade sands and gravels. M^3, no. 7540, is 46.4 mm long; anteroposterior length of crown is 25.7 mm, and transverse width is 23.4 mm. Protocone has an anteroposterior length of 10.7 mm.

The other molar, no. 7541, is a LM^1 or LM^2. Hypocone of this tooth is as large as protocone.

The only associated series of teeth, DP_3–DP_4, was recovered in part of a ramus, no. 6980. Anteroposterior crown length of the series is 99.8 mm.

On the lower teeth, especially in the younger specimens, the metaconid and metastylid are round and internally convex, separated by a sharp V-shaped valley as in other specimens of *E. simplicidens*. The above characters were stressed by McGrew (1944) as characters of the African zebra (*Hippotigris*).

No remains of the little horse *Nannippus phlegon* (Hay) were found. It is interesting to note that the remains of this horse are more abundant in the base of the overlying Meade formation than in the Rexroad formation.

Order ARTIODACTYLA
Family TAYASSUIDAE
Platygonus bicalcaratus Cope
(Figs. 2A, F, G, H; 3A)

Platygonus bicalcaratus COPE, 1893, Texas Geol. Survey, 4th Ann. Rept., 1892, p. 68.
Platygonus texanus GIDLEY, 1903, Am. Mus. Nat. Hist., Bull., vol. 19, art. 16, p. 478.

Isolated teeth of *Platygonus* have not been uncommon in the Rexroad deposits. Complete dentitions have not been found that would allow a determination of the species present. At Locality 22, numerous remains of *Platygonus* were recovered. They varied from the premaxillaries of either embryonic or very young peccaries containing the unerupted tooth buds to the dentition of old individuals. One can group the teeth into 3 lots: those with the characters of *Platygonus bicalcaratus*

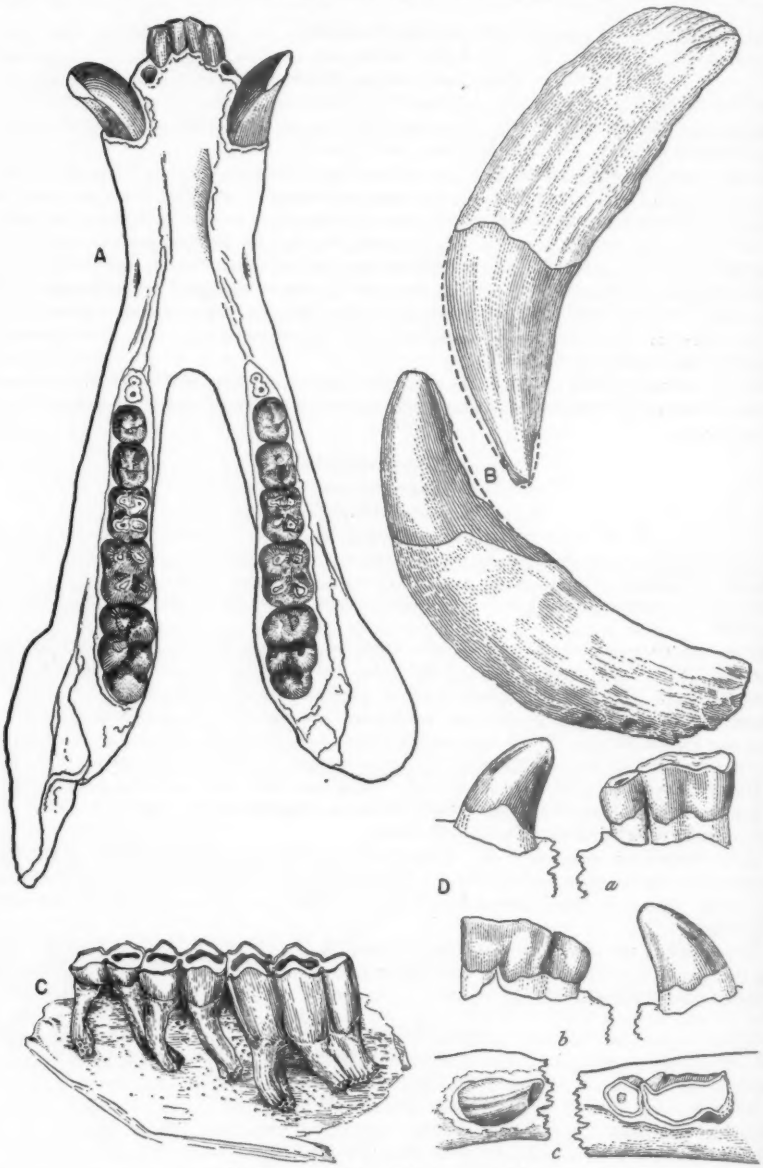

FIGURE 3.—*Upper Pliocene mammals*

(A) *Platygonus bicalcaratus* Cope. KU7273, rami with dentition. Dorsal views. ×½. (B) *Gigantocamelus spatulus* (Cope). KU7209, upper and lower canines of male. Labial view. ×½. (C) *Tanupolama blancoensis* Meade. KU7143, left $M_1 - M_3$. Labial view. ×½. (D) *Gigantocamelus spatulus* (Cope). KU7160, P_1, P_2 and P_4. a, labial view. b, lingual view. c, occlusal view. All ×½.

Cope, those with characters of *Platygonus texanus* Gidley, and those with characters intermediate between these two species. Cope, in his description of *P. bicalcaratus* had only a part of a superior canine, a lower canine, and what he considered to be part of the last inferior molar. All will agree that Cope had before him a part of a peccary premolar or molar. Gazin (1938) points out that the fragment of the tooth studied by Cope is probably an incomplete P_3 or P_4 rather than M_3. Gidley (1903) had 2 palates of a peccary from the Blanco which varied slightly in size and character of teeth. Because of the complete lack of a posterior heel on M^3, he referred this specimen to *P. bicalcaratus* and described the other specimen, a palate with upper dentition in which M^3 possessed a posterior heel as *P. texanus*. Meade (1945) has referred lower dentitions to both *P. bicalcaratus* and *texanus*. The lower dentitions referred to *P. texanus* were so disposed of in general because M_3 possessed a rather well-developed heel. The lower teeth referred by Meade to *P. bicalcaratus* do not include any last molars. He definitely states that M_3 is unknown and that the tooth should have a less well-developed posterior heel than M_3 in *P. texanus*, since the heel of M^3 is lacking in *P. bicalcaratus*.

TABLE 1.—*Measurements of upper dentitions of* Platygonus bicalcaratus *Cope*

	Specimens no.			
	7274	7535	6972	7536
	millimeters			
Diastema, I to C	25.4	—	—	—
C, anteroposterior length	21.0	—	—	—
C, transverse width	11.5	—	—	—
Diastema, C to P^2	58.3	—	—	—
Alveolar length P^2–P^4	36.4	33.7	—	—
P^2, anteroposterior length	11.8	9.5	—	10.2
P^2, transverse width	11.0	7.5	—	9.9
P^3, anteroposterior length	11.8	11.8	—	10.8
P^3, transverse width	12.3	9.8	—	12.4
P^4, anteroposterior length	14.0	14.0	—	11.6
P^4, transverse width	13.7	11.8	—	13.2
M^1, anteroposterior length	—	16.1	—	14.1
M^1, transverse width	—	12.5	—	12.6
M^2, anteroposterior length	—	—	18.0	18.4
M^2, transverse width	—	—	15.0	16.5
M^3, anteroposterior length	—	—	21.0	21.5
M^3, transverse width	—	—	17.4	16.5

The characters used by Gidley to separate the 2 species of *Platygonus* from the Blanco beds of Texas and the supposedly valid characters discussed by Meade to disinguish the 2 species, are here considered, after the study of our material, to be only differences of individual variation. One would not expect to find 2 forms of peccaries occupying the same region without diverse habitats. With diverse habitats one form would be more apt to be fossilized than the other, or at least there would be more fossils of one form in a given deposit than the other. At present the specimens are about equally divided numerically in the deposits from which they have been taken.

In the material recovered are: a right maxillary, no. 7535, with P^2 and M^3; posterior part of a palate, no. 6972, with RM^2—M^3, and LM^2; another right maxillary, no. 7563, with P^2—M^3; anterior part of skull, no. 7274, with 2 incisors, right canine, and RP^2—P^4; palate , no. 7536, with RP^2—M^3, and LM^2—M^3; complete right and left rami, no. 7273, lacking I_3 and P_2; right ramus, no. 7272, with P_3—M_3; nos. 6976, 7531, 7532, and 7533, rami of immature individuals, 3 of which contain DP_4.

Palate, no. 6972, with RM^2—M^3, and LM^2, possesses teeth typical in pattern to the upper teeth referred by Gidley to *P. bicalcaratus*. In contrast, is palate no. 7536, with RP^2—M^3, and LM^2—

M^3 in which RM^1 has a typical tapir pattern, a character Gidley assigns to *P. bicalcaratus*, though M^3 possesses a well-developed heel. The extreme development of the groad heel on RM^2 is seen in specimen, no. 7696, Fig. 2F. An intermediate tooth is seen in Fig. 2G, a LM^3, in which the heel is reduced and the oblique ridge from the inner cusp is less prominent and is intermediate between the connection with the heel and the cingulum which approaches the condition in palate no. 6972. The upper premolar and molar series are variable in tooth characters. In regard to the lower jaws where M_3 was present there was no reduced heel. All of the unworn teeth possessed high anterior and posterior crests which were completely divided by cross valleys.

TABLE 2.—*Measurements of lower dentitons of* Platygonus bicalcaratus *Cope*

	Specimens no.			
	7273	7272	6976	7532
	millimeters			
Distance from tip of I to posterior border of M_3	215.0	—	—	—
Diastema between C–P_2	70.0	—	—	—
Alveolar length of P_2–P_4	35.0	33.0	—	—
Alveolar length of P_2–M_3	101.0	95.0	—	—
Alveolar length of M_1–M_3	65.0	60.0	—	58.8
P_2, anteroposterior length	—	—	—	—
P_2, transverse width	—	—	—	—
P_3, anteroposterior length	11.6	11.0	D 10.5	—
P_3, transverse width	10.0	8.7	5.7	—
P_4, anteroposterior length	13.0	12.2	D 19.5	13.0
P_4, transverse width	12.2	10.6	9.5	12.5
M_1, anteroposterior length	16.0	15.4	—	14.8
M_1, transverse width	12.2	—	—	11.5
M_2, anteroposterior length	19.5	18.7	—	18.2
M_2, transverse width	15.5	14.0	—	15.4
M_3, anteroposterior length	27.5	25.8	—	26.5
M_3, transverse width	17.8	14.9	—	17.0

D, milk tooth.

Gigantocamelus spatulus (Cope)

(Pl. 3; Pl. 4, figs. 1, 5, 6; Pl. 5, fig. 6; Figs. 3B, D; 4;5; 6; 7; 8A, B, C; 9)

Pliauchenia spatula COPE, 1893, Texas Geol. Survey, 4th Ann. Rept., 1892, p. 70, Pl. 21, figs. 1 and 2.

Pliauchenia (*Megatylopus*) *spatula* COPE, MATTHEW AND COOK, 1909, Am. Mus. Nat. Hist., Bull., vol. 26, p. 396.

Gigantocamelus fricki BARBOUR AND SCHULTZ, 1939, Univ. Nebr. St. Mus., Bull., vol. 2, no. 2, p. 20, Figs. 5–10.

Gigantocamelus spatula (COPE), MEADE, 1945, Univ. Texas, Pub. 4401, p. 531, pls. 53 and 54.

A large male skull, no. 6943, (Table 3, Pl. 3), is slightly crushed and distorted to the right ventral side. The skull has a narrow sagittal crest, an occipital crest that projects well over the condyles, a small brain cavity, and lacks the depression between the orbits which is present on the skull of *Camelus*. Dorsal surface of orbital region is more convex than that surface observed in *Lama*. The infraorbital foramen, situated above P^4 is small in comparison to that of *Camelus*. Temporal fossa has an anteroposterior length of 140.0 mm. Anterior border of posterior narial aperture is situated at posterior edge of M^3. Maxillary is excluded from nasal opening. Premaxillary broadly joins the nasal. From posterior border of external nares to tip of supraoccipital crest is 702.0 mm. There is no evidence of a facial fossa between the maxillary and frontal as observed in *Lama* and *Camelus*. P^1 is more caniform than P_1 and not as recurved.

SKULL OF GIGANTOCAMELUS SPATULUS (COPE)
Skull of old male, KU6943, slightly crushed anteriorly. Dorsal view. X¼.

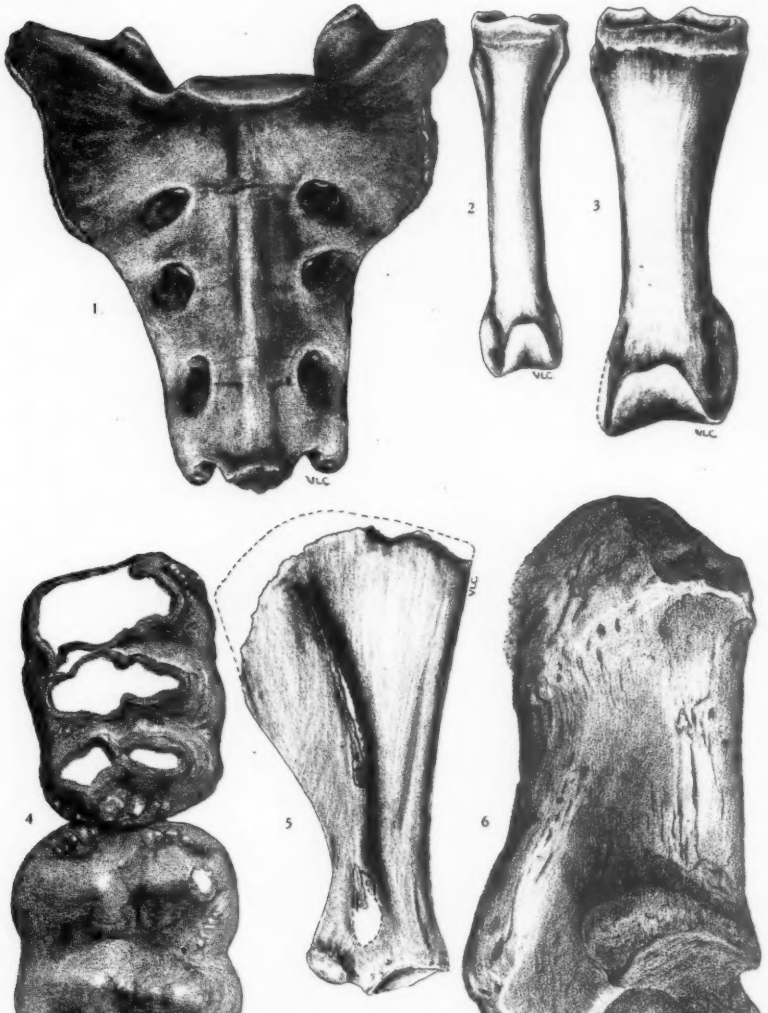

TEETH OF MASTODON AND SKELETAL ELEMENTS OF CAMELS

The skull, no. 6944, (Fig. 4A) is that of a young male. P^3 is well-developed with ends of the crescent turned inwardly toward center of tooth. On lingual side of M^1 and M^2, at the re-entrant angle, there is a very slender cylindrical-shaped style which arises from base of tooth and extends along side of tooth as far as triturating surface and is worn away to that level. It is not attached to

TABLE 3.—*Skull measurements of* Gigantocamelus spatulus *(Cope)*

	No. 6943 ♂	No. 4644 ♂	No. 7167 ♀
	millimeters		
Length, maximum (including supraoccipital crest and premaxillae)	870.0	—	—
Condylo-basal length (condyles to anterior of premaxillae)	795.0	—	—
Width maximum, at orbits	355.0	—	—
Length, tip of premaxillary to anterior base of P^3	287.0	—	245.0
Length of dental series (C–M^3 inclusive, alveolar)	421.0	—	359.0
Length, P^4–M^3 inclusive, alveolar	194.0	214.0	167.0
Length of P^4–P^4 inclusive, alveolar	92.0	57.0	54.0
Length of M^1–M^3 inclusive, alveolar	140.0	152.0	125.0
Diastema, P^1–P^3	130.0	—	102.0
Diastema between C–P^1	38.0	—	61.0
Greatest anteroposterior length of canine at alveolus	39.0	40.0	19.0
Height of canine from alveolus	37.0	—	35.0
Height of P^1 from alveolar border	—	23.0	13.0
P^1 greatest anteroposterior length	23.0	21.0	11.0
greatest transverse width	18.0	—	8.0
P^3 greatest anteroposterior length	—	31.0	27.0
greatest transverse width	—	20.0	17.0
P^4 greatest anteroposterior length	—	36.0	32.0
greatest transverse width	—	25.0	25.0
M^1 greatest anteroposterior length	—	45.0	32.0
greatest transverse width	—	34.0	36.0
M^2 greatest anteroposterior length	49.0	63.0	46.0
greatest transverse width	46.0	39.0	40.0
M^3 greatest anteroposterior length	60.0	65.0	38.0
greatest transverse width	42.0	35.0	40.0

lobe of tooth. (Fig. 4B). A few of these cylindrical-shaped stlyes were recovered from the matrix; they had become detached from the parent molars. This style is therefore to be considered only as a sporadic development.

Skull, no. 7167, (Fig. 4C) is that of a female. Skull is crushed laterally and part posterior to M^3 is missing. It is much lighter than that of the males (Table 3), measures 240.0 mm from tip of premaxillary to anterior borders of P^3; while the same part measures 290.0 mm on the skull of the old male, no. 6943. Anterior border of posterior narial aperture ends, as in no. 6943, just posterior to

PLATE 4.—TEETH OF MASTODON AND SKELETAL ELEMENTS OF CAMELS

Figure

1. *Gigantocamelus spatulus* (Cope). KU7647, sacrum. Ventral view. ×¼.
2. *Tanupolama blancoensis* Meade. KU7149, phalange. Anterior view. ×½.
3. *Pliauchenia cochrani* sp. nov. KU7184, anterior phalange. Anterior view. ×½.
4. *Mammut* (*Pliomastodon*) *adamsi* (Hibbard). KU6983, LM^1 and M^2. Occlusal view. ×¼.
5. *Gigantocamelus spatulus* (Cope). KU7166, scapula. Lateral view. ×¼.
6. *Gigantocamelus spatulus*. KU7165, calcaneum. Medial view. ×½.

M^3. I^3 is known only from the alveolus. Canines and P^1 are greatly reduced in comparison to those of the males.

Skull, no. 7159, (Fig. 6A) female, lacks anterior part of skull in front of P^3, and left zygomatic arch. The basisphenoid is not damaged and presents a noticeable contrast to that of *Camelus*. It is high and its ventral surface ends in a decidedly sharp ridge which extends forward beyond the pterygoid processes. Anterior border of posterior narial aperture ends at midline of first lobe of M^3. The palate is not crushed. Distance between RM^3 and LM^3 taken between the centers of the posterior lobes is 92.0 mm; distance between RP^3 and LP^3 is 55.0 mm. Narrowest constriction of rostrum of skull is 46.5 mm, in comparison to 66.0 mm in the male, no. 6943. Infraorbital foramen is situated above P^4. Greatest vertical diameter of foramen is 21.0 mm, compared to 20.0 mm in a

TABLE 4.—*Jaw measurements of* Gigantocamelus spatulus (*Cope*)

	No. 6945 ♂	No. 6947 ♂	No. 7160 ♂	No. 6946 ♂	No. 7161 ♀	No. 7200 ♂
	millimeters					
Length, maximum, including incisors	—	—	—	673.0	—	—
Length from posterior of condyle to anterior of canine	646.0	—	—	632.0	—	—
Depth of ramus below anterior edge of M_3	103.0	104.0	97.0	84.0	91.0[a]	85.0
Depth of ramus, midway, between C and P_3	68.0	71.0	63.0	52.0	59.0	—
Length of dental series (C-M_3 inclusive, alveolar)	447.0	—	418.0	448.0	401.0	—
Length, alveolar, of premolar series including P_1	368.0	—	350.0	358.0	—	—
Length, alveolar, P_3–M_3	217.0	—	205.0	213.0	198.0	212.0
Length, alveolar, P_3–P_4	58.0	50.0	39.0	51.0	51.0	50.0
Length, alveolar, M_1–M_3	161.0	—	163.0	163.0	161.0	163.0
Diastema, C–P_1	54.0	58.0	30.0	60.0	—	—
Distance from C to P_3	205.0	175.0	172.0	195.0	176.0	—
Distance, P_1–P_3	139.0	105.0	121.0	121.0	—	104.0
Height of ascending ramus	360.0[a]	—	317.0[a]	300.0[a]	—	—
Depth of ramus below anterior end of M_1	108.0	98.0	87.0	75.0	78.0	79.0
Height of canine above alveolar border	45.0	51.0	—	64.0	30.0	—
Anteroposterior length of canine at alveolar border	34.0	37.0	—	33.0	20.0	—
Trans. width of canine at alveolar bortder	25.0	26.0	—	24.0	13.0	—
Distance from P_3 to anterior edge of I_3	—	249.0	—	284.0	—	—
Width of incisor series	—	112.0	—	110.0	—	—
Width between canines at alveolar border	—	82.0	—	61.0	—	—
Width across tips of canines (outside)	134.0	170.0	—	—	—	—

[a] Approximate.

recent skull of *Camelus*, no. 13513KU. In *Camelus*, the foramen is situated above anterior edge of M^1. The orbit of skull No. 7159, is round with a vertical height of 74.0 mm, and transverse diameter of 73.0 mm. Dorsal process of jugal extends posteriorly onto surface of squamosal for 32.0 mm. Ventral extension of jugal extends 87.0 mm, along ventral surface of squamosal. Characters of the dentition are the same as in the male, no. 6943. There is a small supraorbital notch in both the males and females, not as deep as in *Camelus* nor constricted at the anterior border as in *Camelus*. Meade (1945, p. 531) reports, "a large vacuity located just above and anterior to the orbit." No vacuity occurs, in this region, in the skulls here described. The bone is thinner in this area and the reported vacuity may be due to the breaking of the bone, or, if ever present in these skulls, it was very small and closed due to slight lateral crushing.

A number of isolated upper canines were recovered (Fig. 3B). The type of wear on these teeth differs with each tooth. No. 7525, a left upper canine with an overall length of 135.0 mm, the greatest anteroposterior width, 43.0 mm, and a transverse width of 36.0 mm, has all of the enamel

removed on the anterointernal surface where it came in contact with the lower canine. Upper canine, no. 7209, with an overall length of 124.0 mm, greatest anteroposterior width of 45.0 mm, and a transverse width of 34.0 mm, still possesses a 14.0 mm enamel band at its narrowest point.

TABLE 5.—*Skeletal measurements of* Gigantocamelus spatulus *(Cope)*

Radia-ulnae	No. 6951	No. 7203	No. 7168	No. 7510
	millimeters			
Length, maximum	825.0	760.0[a]	—	—
Greatest width at sigmoid notch	137.0	135.0	134.0	—
Greatest width at distal end	129.0	—	133.0	134.0
Length, articular, proximal end to sigmoid crest	705.0	—	713.0	646.0
Greatest articular width, distal end	114.0	—	115.0	117.0
Metacarpals	**No. 7518**	**No. 7682**		
Length, maximum	448.0	455.0		
Width, proximal end	103.0	106.0		
Width, distal end	136.0	140.0		
Metatarsals	**No. 6952**	**No. 7162**	**No. 7683**	**No. 7206**
Length, maximum	—	435.0	—	431.0[a]
Length of front side	420.0	415.0	375.0	420.0
Proximal width, maximum	95.0	88.0	91.0	89.0
Distal width, maximum	122.0	120.0	114.0	—
Tibia	**No. 6953**			
Greatest overall length	634.0			
Proximal width, maximum	187.0			
Distal width, maximum	120.0			
Calcanei	**No. 7199**	**No. 7515**	**No. 7165**	
Greatest overall length	213.0	203.0	210.0	

[a] Approximate.

LOWER JAWS: a pair of lower jaws, no. 6945, (Fig. 5B) of a male without the incisors, RP_1, RP_2, and LP_2; male , no. 6947, (Fig. 8A) lower jaws without posterior part, broken just posterior to second lobe of RM_2, and just anterior to LP_2; male, no. 7160, lower jaws lacking incisors and canines, and the right ramus missing posterior to RP_2; no. 7200, complete right ramus of male; no. 6946, (Fig. 9C) complete lower jaws of a male, with tip of right canine missing; right and left rami of female, no. 7161, (Fig. 5A) lacking posterior part back of M_3, were found with skulls of Nos. 6943, 6944, 7159 and 7167.

Tips of the lower incisors in young animals are broad, thin, and spatulate. Crowns wear down rather rapidly. Occlusal surface wears to an elongated oval, becoming nearly circular with further wear. Many times the tooth is worn down below the enamel surface.

In all specimens except one, lower canines were worn on their posterior face where they came in contact with upper canines. In specimen no. 6945, lower canines are worn on their anterior face. Canines of males flare outward while those of females are greatly reduced and remain in line with incisors. Symphysis of lower jaws of males extends posteriorly to alveolus of P_1. In specimen no. 6947, symphysis extends 52.0 mm, posterior to P_1

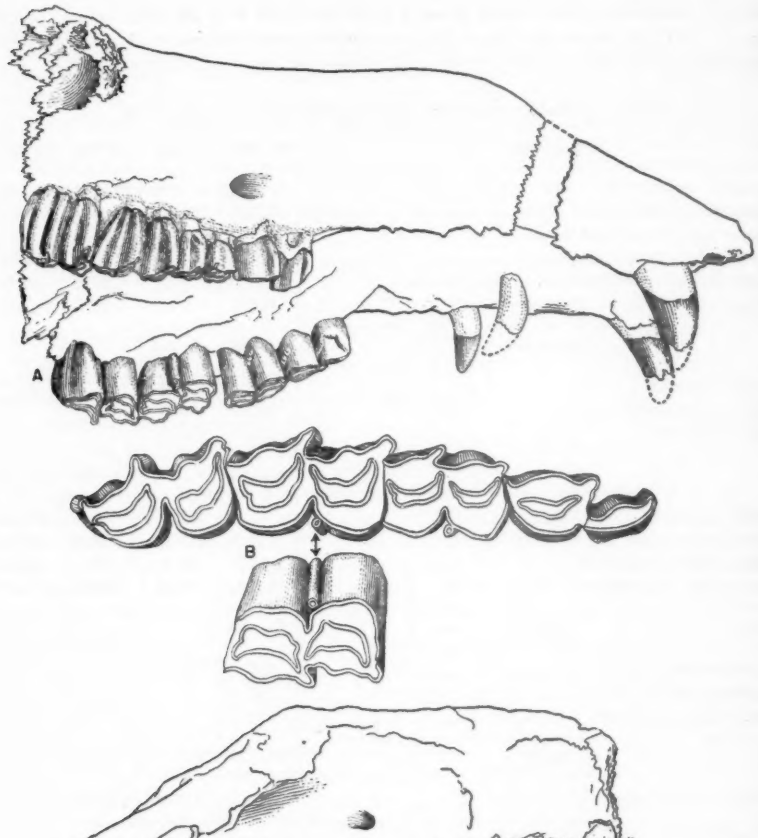

FIGURE 4.—Gigantocamelus spatulus (*Cope*)

(A) Anterior part of skull, male, KU6944. Lateral view. Approximate ×⅓. (B) RP^3 — M^3 showing styles, of the above skull, KU6944. Occlusal view. Approximately ×⅓. (C) Anterior part of skull, female, KU7167. Lateral view. Approximately ×⅓.

P_1, lacking in females, in the males is recurved with anterior and posterior enamel ridges.

P_2 is absent in both males and females.

P_3 is noticeably variable. In specimen no. 7160, a male, (Fig. 3D) it is single rooted and peg-shaped. An isolated single-rooted, peg-shaped P_3, no. 7233, was found which has an anteroposterior

crown length of 11.9 mm. This tooth is flattened on its posterior surface where it rested against P_4. Transverse width of its crown is 9.5 mm.

P_4 is molariform.

Anterior parts of M_1 and M_2 resemble anterior parts of M_1 and M_2 of *Tanupolama*.

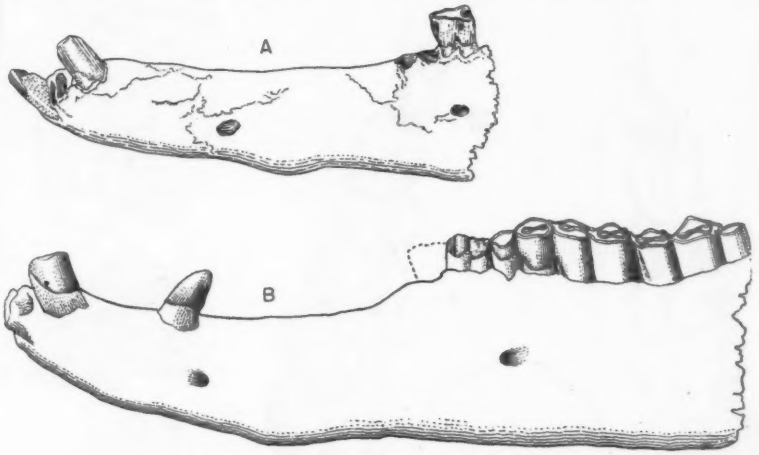

FIGURE 5.—Gigantocamelus spatulus *Cope*

(A) Female, KU7161, anterior part of left ramus. Note reduced canine and lack of P_1. Labial view. ×½. (B) Male, KU6945, anterior part of left ramus. Note well-developed P_1. Labial view. ×½

M_3 consists of 3 lobes (Figs. 6D, E; 9A, B). Posterior lobe of M_3 resembles that of *Tanupolama* since it is deflected labially and is not in line with first and second lobes along lingual side of tooth. The third, or posterior lobe, is set off from second lobe by re-entrant angles on both lingual and labial sides. Re-entrant angles are still present in old, worn, short-crowned teeth. In young teeth, third lobe approaches the condition observed in *Camelops* in that it is deflected lingually and is nearly in line with lingual edge of first and second lobes of M_3.

LIMB BONES: Massive, although for size of skull and vertebrae they are short compared to the limb bones of *Tanupolama*, (Table 5). No femurs and only fragmentary parts of pelvis and scapula were recovered.

Only a few complete vertebrae were recovered. The sacrum consists of 4 vertebrae (Pl. 4, fig. 1). Greatest overall length of sacrum, no. 7647, measured along centra is 222.0 mm; sacrum, no. 7681, 235.0 mm; sacrum, no. 7519, 221.0 mm.

A number of long thoracic vertebrae were encountered in the quarry. Whether these belong with *Gigantocamelus* or *Pliauchenia* is unknown. Centra and dorsal spines appear heavy enough for the large camel. Thoracic vertebra, no. 7169, (Fig. 7B) has an overall height of 785.0 mm; greatest anteroposterior width of dorsal spine, 68.0 mm; depth of centrum from neural canal, 78.0 mm. No measurements were given by Barbour and Schultz (1939) in regard to the vertebrae of their composite mount or other associated material. If these thoracic vertebrae belong to *Gigantocamelus*, as it appears, the camel was decidedly hump-backed and stood higher at the shoulders than has been shown in reconstructions of *Gigantocamelus*.

The astragalus is known from 10 or more specimens and the calcaneum from 6 or more specimens (Pl. 4, fig. 6). These are uniform and do not show individual variation.

Phalanges numerous in deposit and show considerable variation in size. A few second phalanges were found and these are rather broad, which may indicate development of a greater pad than in *Camelops*.

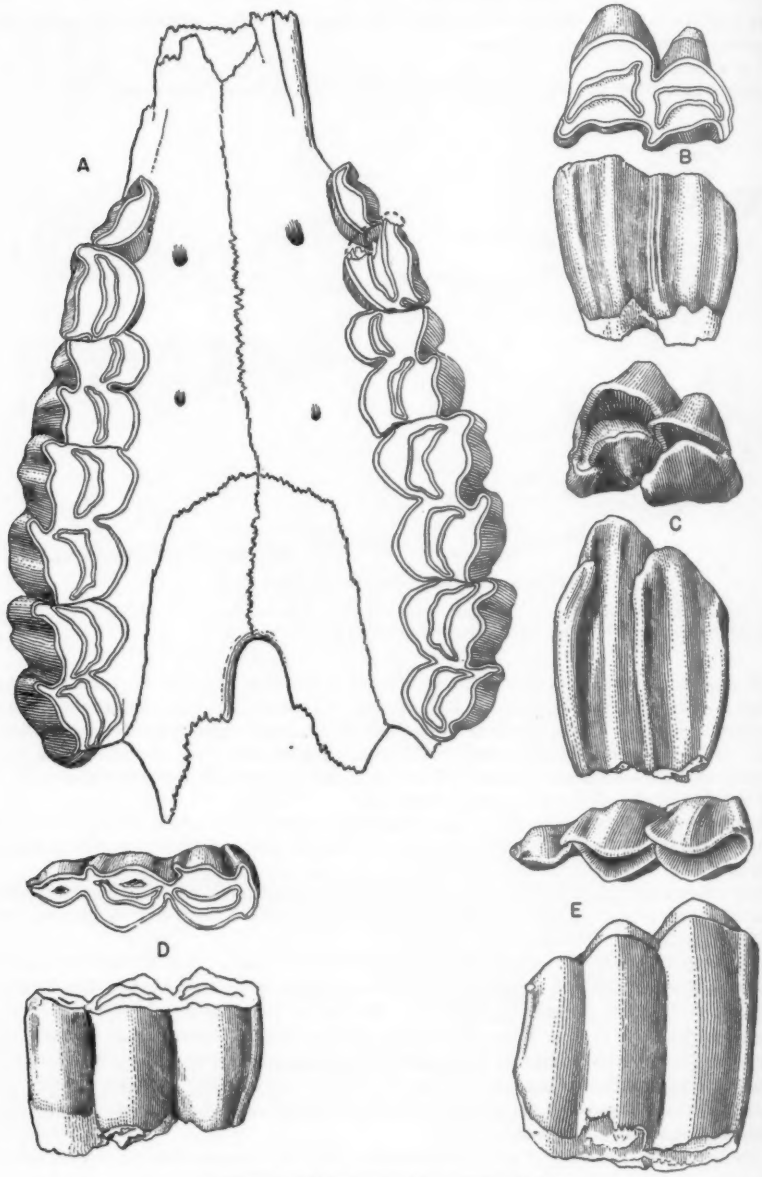

FIGURE 6.—Gigantocamelus spatulus (*Cope*)

(A) Anterior part of skull, female, KU7167. Ventral view. ×⅓. (B) RM^3, KU7171, worn. Occlusal and labial views. ×⅓. (C) RM^3, KU6938, unworn. Occlusal and labial views. ×⅓. (D) RM_3 KU7687, worn. Occlusal and labial views. ×⅓. (E) RM_3, KU7684, unworn. Occlusal and labial views. ×⅓.

FIGURE 7.—Gigantocamelus spatulus (*Cope*)

(A) Ulna-radius, KU6951. Front view. ×¼. (B) Dorsal vertebra, KU7169. Lateral view. ×¼. (C) Metatarsal, KU7162. Front view. ×¼.

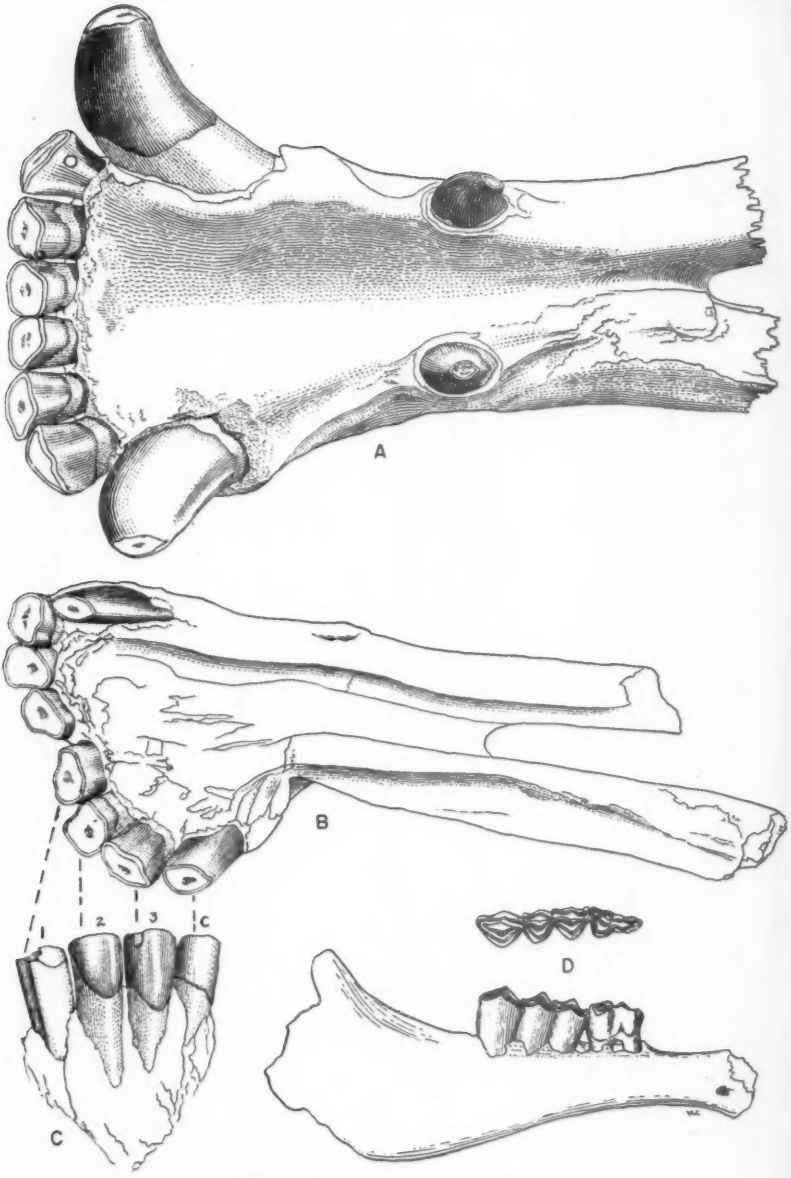

FIGURE 8.—Gigantocamelus *and* Tanupolama

(A) *Gigantocamelus spatulus* (Cope). KU6947, anterior part of lower jaws, male. Dorsal view. Approximately X½. (B) *Gigantocamelus spatulus*. KU7201, anterior part of lower jaws, female. Dorsal view. Approximately X½. (C) *Gigantocamelus spatulus*. KU7201, left $I_1 - C$. Anterolateral view. Approximately X½. (D) *Tanupolama blancoensis* Meade. KU7500, right ramus, DP_3, DP_4. Labial and occlusal views. Approximately X½.

FIGURE 9.—Gigantocamelus spatulus (*Cope*)

(A) A composite series of unworn teeth, $RP_3 - M_3$. Lingual view. ×½. (B) $RP_3 - M_3$, KU6946. Labial view. ×½. (C) Left ramus, KU6946. Labial view. ×½.

DISCUSSION: Parts of at least 21 individuals of *Gigantocamelus spatulus* were recovered, based on the count of right M_3. Many individual skeletal elements are lacking. In most cases the material confirms the findings of Cope, Barbour and Schultz, and Meade. The following information has been acquired from the study of the material in regard to the great camel; (1) in the deposit studied, the remains of males outnumber females 2 to 1; (2) there is considerable sexual dimorphism—the males are larger, with more heavily developed skulls and teeth, especially the canines. The upper canines have only a slight outward flare and the lower canines have a decided outward flare. P^1 and P^2 are well-developed in the male and caniform, while in the female P^1 and P^2 are caniform but reduced. The dental formula as given by Barbour and Schultz for the genus is that of the male, $I\frac{0-1}{3}$, $C\frac{1}{1}$, $P\frac{3}{3}$, $M\frac{3}{3}$. The female definitely lacks P_1, at least in the specimens examined, and has greatly reduced canines (Figs. 5A, 8B). The anterior parts of the lower jaws, no. 7201, a female, have canines with an anteroposterior width of 18.0 mm; and a transverse width of 10.0 mm. The spatulate-shape of the incisors is of short duration in both sexes. They soon wear to an oval grinding surface becoming nearly round in old age.

If the thoracic vertebrae which were recovered with the long dorsal spines are those of *Gigantocamelus*, the camel was decidedly hump-backed.

Gigantocamelus is considered distinct from *Megatylopus* Matthew and Cook because of the absence of the lachrymal vacuities and because the anterior border of the posterior narial aperture does not extend forward as in *Megatylopus gigas* Matthew and Cook.

Pliauchenia cochrani sp. nov.

(Figs. 10A, B, C)

HOLOTYPE: No. 7643, left ramus bearing vestigial P_1, alveolus of P_2, and P_4 — M_2; no. 7644, right ramus bearing vestigial P_1, P_3 — M_2; and M_3, no. 7180. All 3 specimens belong to the same individual, an adult animal.

HORIZON AND TYPE LOCALITY: Upper Pliocene, Rexroad formation, Keefe Canyon, SW¼ SW¼ sec. 34, T. 34 S., R. 30 W., Meade County, Kansas, Locality 22, Rexroad fauna.

DESCRIPTION OF TYPE: A camel the size of *Camelops sulcatus* Cope having a well-developed P_3, which is two rooted, and a vestigial P_1. Distinguished from *Tanupolama* by absence of anterior stylar processes on M_1, M_2, and M_3. M_3 is typical of *Camelops* in structure.

Measurements (mm) of holotype

	Left	Right
P_3, occlusal length	—	18.5
P_3, greatest width	—	10.0
P_4, occlusal length	23.1	21.8
P_4, greatest width	15.5	15.0
M_1, occlusal length	32.7	32.6
M_1, greatest width	23.8	24.0
M_2, occlusal length	39.2	39.8
M_2, greatest width	25.2	26.3
M_3, occlusal length	52.3	52.0
M_3, greatest width	24.3	21.7
Alveolar length, M_1–M_3, left ramus		119.5
Occlusal length P_3–M_3, right ramus		159.6
Alveolar length P_3–M_3, right ramus		166.2
Diastema from anterior edge P_1 to P_3, right ramus		66.2
Depth of right ramus (inside) below P_4		62.2
Depth of right ramus (inside) below M_1		73.2
Depth of left ramus (inside) below M_3		80.7
Distance from posterior edge of the mental foramen to the anterior edge of P_3, right ramus		62.5
Distance from posterior edge of the mental foramen to the anterior edge of P_4, left ramus		89.2

In the type, M_1 is deeply worn. M_2 has 2 roots, a well-developed root under first lobe with a large fused tripartite root supporting second and third lobes. Internal ridges on M_2 and M_3 are more strongly developed than in any specimens of *Camelops* examined. If jaws were not broken at posterior border of the symphysis, there would be no indication that P_1 exists. It is a well-developed tooth, but lacks at least 7.0 mm of penetrating surface of ramus. In right ramus, P_1 is well exposed, and situated at anterior border of mental foramen. It has an overall height of 31.2 mm, height of enamel crown is 15.8 mm, with an anteroposterior width of 14.5 mm. It is caniform and curves posteriorly. The specimen may be that of a female and the tooth may be found to be well-developed in the males.

Four isolated lower third molars, nos. 6967a and b, 7179, and 7181, are those of immature or young adult animals since the third lobe is set off at the occlusal surface from the inner surface of the other 2 lobes; also the third lobe at the occlusal surface appears oblique to the long axis of the tooth. In these specimens, with wear, the third lobe of these teeth would not appear set off from the second lobe, or oblique to the axis of the tooth, but would be flush and continuous with the inner surface of the 2 anterior lobes of M_3, as in the type.

This species is named for Mr. Henry Cochran of Meade, Kansas, who has contributed to the success of our work in that region during the past 12 years.

This species has been assigned to *Pliauchenia* because of well-developed P_3, and absence of P_2. The absence of P_1 is a sexual character in some forms of camels. This species definitely possesses characters of *Camelops* and may be intermediate between *Pliauchenia* and *Camelops*. Length of the tooth row indicates that this species is not large enough to belong to the form from the Blanco referred to *Camelops* cf. *kansanus* by Meade. When these camels are better known they may be found to be conspecific and the differences to be only sexual and individual. It appears without doubt that the specimens from the Blanco referred by Meade to the American Museum specimen, no. 20085, are limb bones of the same animal as the dentitions he referred to *Camelops* cf. *kansanus* Leidy.

Tanupolama blancoensis Meade

(Figs. 3C; 8D; 11A, B; Pl. 4, fig 2; Pl. 5, figs. 2, 3, 4, 5)

Tanupolama blancoensis MEADE, 1945, Univ. Texas, Pub. no. 4401, p. 535–536, Pl. 55.
Leptotylopus percelsus MEADE, *nomen nudum*, 1945, Univ. Texas, Pub. no. 4401, p. 538.

Associated with the remains of *Gigantocamelus spatulus* and *Pliauchenia cochrani* in the Keefe Canyon quarry, a few jaws, teeth, and bones of the skeleton of a smaller, llama-like camel were found.

Tanupolama blancoensis is distinguished from *Tanupolama stevensi* (Merriam and Stock); *Tanupolama mirifica* Simpson; and *Tanupolama americana* Wortman by its larger size, slightly stronger mandible, and two-rooted P_3, which is reduced to a narrow blade-like crown. *Tanupolama longurio* Hay is a larger animal if the anterior first phalange measured and figured by Hay (1921) belongs to the type of *T. longurio*. Previously described forms of *Tanupolama* were taken from younger deposits. Scattered remains of *Tanupolama* are common in Pleistocene deposits of this area of the High Plains, though the material is not sufficient to make an adequate comparison with *T. blancoensis*.

It was unfortunate that Meade (1945) was not familiar with Matthew's use of the name *Leptotylopus* (Elias, 1931, p. 161, after Matthew, *Leptotylopus* sp. *nomen nudum*) and was unable to see the specimen to which he assigned the name *Leptotylopus percelsus*.

We are greatly indebted to G. G. Simpson for having the specimen A.M. no. 20085, prepared, and for making it available for our examination. The specimen is a large young male of *Tanupolama blancoensis* Meade. It was a surface find and badly weathered and broken. Anteroexternal style is developed on $M_1 - M_3$. Diastema between C and P_1 is 17.0 mm. Diastema between P_1 and P_2 is 45.0 mm. P_2 is strongly developed. Overall length of $P_2 - M_3$ is 123.0 mm. Restored length of left metacarpal is 465.0 mm, and of right metacarpal, 457.0 mm. Length of a right proximal phalange is 127.0 mm, and of a left proximal phalange, 130.0 mm. Right metatarsal length is 428.0 mm, and length of a posterior proximal phalange is 113.0 mm. Restored overall length of right

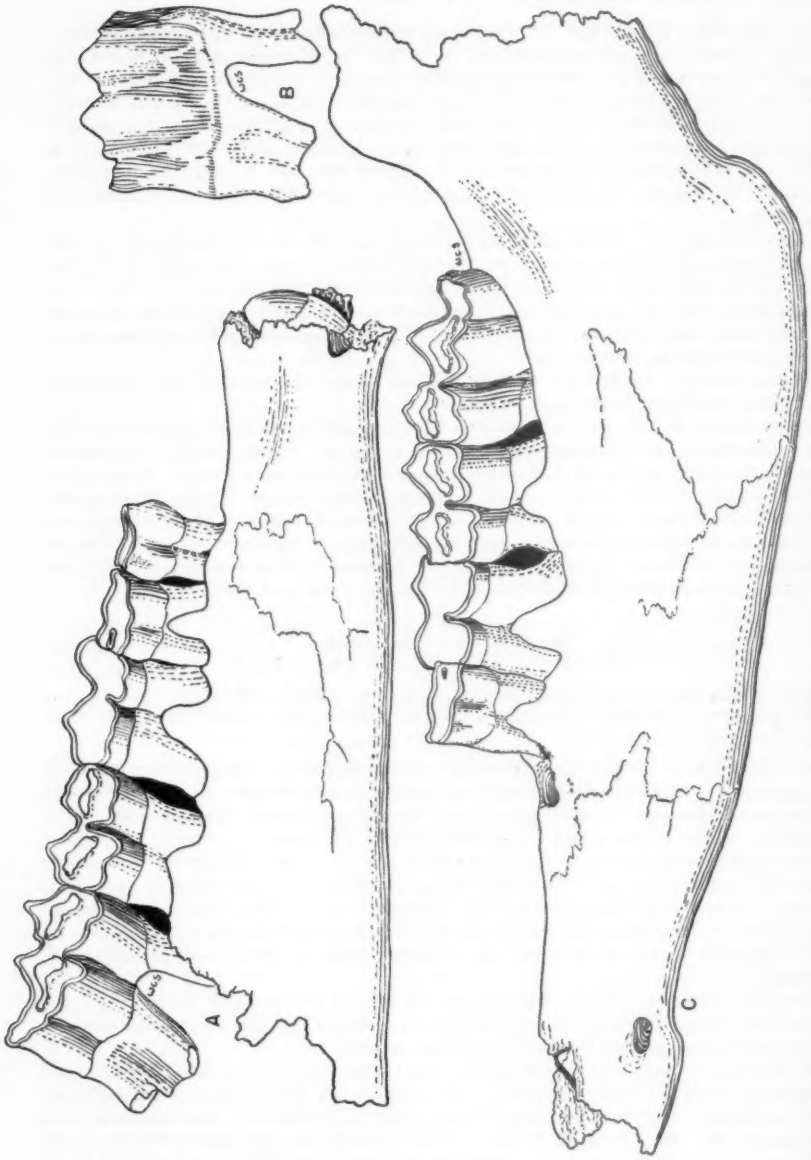

FIGURE 10.—*Pliauchenia cochrani sp. nov.*

(A) Right ramus, P_3, P_4 — M_3, holotype KU7644. Labial view. ×½. (B) Left M_3, KU7181. Lingual view. ×½. (C) Left ramus, P_3, P_4 — M_3, holotype, KU7643. Labial view. ×½.

tibia fibula is 530.0 mm; left is 505.0 mm long. Skeletal elements referred by Meade (1945, p. 538) to this form do not belong to *Tanupolama blancoensis* but are considered as belonging to *Camelops* or *Pliauchenia*.

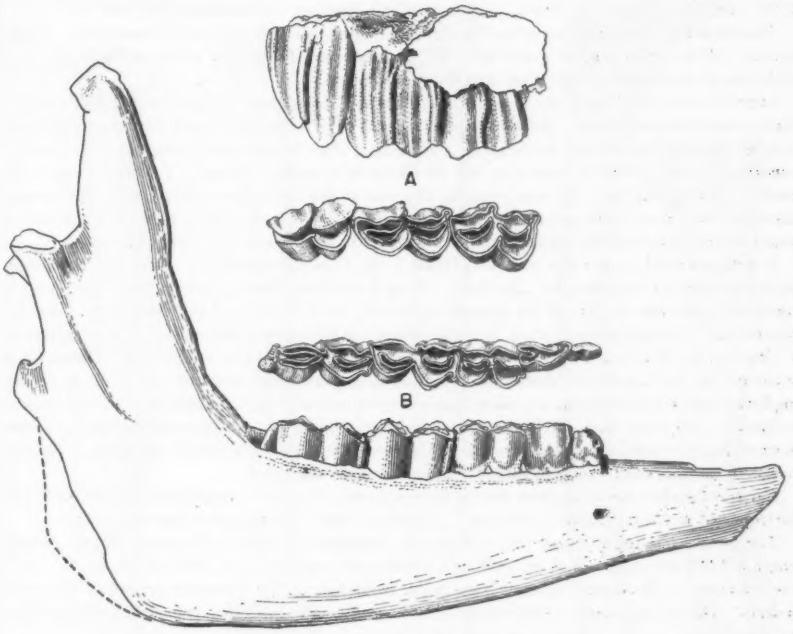

FIGURE 11.—Tanupolama blancoensis *Meade*

(A) $RM^1 - M^3$, KU7141. Labial and occlusal views. ×½. (B) Right ramus, $P_3 - M_3$, KU6962. Labial and occlusal views. ×½.

The specimens of *Tanupolama* recovered in Keefe Canyon possess the following characters:

P_4 has a narrow crown, and a deep cleft in posterior margin in young specimens. With wear, cleft is reduced to a rounded pit.

M_1 in early stage of wear possesses an anteroexternal style which disappears with wear.

M_2 has a well-developed anteroexternal and anterointernal style.

M_3 has a more strongly developed anterior style than M_2. Third lobe of M_3, in an unworn tooth (Fig. 11B), has form of an elongated cone with its apex closely applied to posterior surface of second lobe and its base extending downward and supported by a distinct third root. As this lobe is worn down at triturating surface, crown of lobe becomes more and more conspicuously a part of the tooth (Fig. 3C). This increase in prominence of the third lobe increases anteroposterior diameter of that tooth as well as molar series. Meade (1945, p. 535) states that the , "anterior lobes of M_1 and M_2 are but slightly wider basally than the posterior lobes"; width of anterior and posterior lobes of M_1 and M_2 depend upon stage of wear. In specimen no. 6962, posterior lobe of M_1 is wider than anterior lobe of M_1 while anterior lobe of M_2 is wider than posterior lobe of M_2. In specimen no. 7183, lobes of M_1 are equal, though anterior lobe of M_2 is wider than posterior lobes of M_2. Specimen no. 7493 has well-worn teeth; and posterior lobe of M_1 is wider than anterior lobe; this condition also exists in M_2.

All of the molars develop long roots. There is no trace of a second premolar in any of the 3 man-

dibles preserved. The mandibular condyle is saddle-shaped at articular surface; the angle is not inflected as is common in Recent *Lama*.

Specimen no. 7500 is the ramus of an immature animal (Fig. 8D) with DP_3 and DP_4. DP_3 has an anteroposterior length of 16.5 mm, its greatest width is 7.0 mm . DP_4 has an anteroposterior length of 33.7 mm, and a width of 11.8 mm. Distance of DP_3 from mental foramen is 28.0 mm.

Three maxillaries were recovered with molar series, all of young animals with unworn M^3. Specimen no. 7141 is a right maxillary with $M^1 - M^3$, anteroposterior length of molar series is 80.0 mm, while that of specimen no. 7144, a left maxillary, is 83.0 mm.

STRUCTURE OF THE FORE LEG: Length of humerus of *T. blancoensis* is nearer to length of *Camelus* than to that of Recent *Lama*. Humerus of *T. blancoensis* (Pl. 5, fig. 5) is approximately nine-tenths as long by axial measurement as humerus of *Camelus*. Shaft is somewhat straighter than in either *Camelus* or *Lama*. Deltoid crest does not terminate in a definite process. Pronator ridge is not marked by a rugose line. External condyle, like that in the llama, has a deep pit for ligamentary insertion, but has no tuberosity. Proximal end of bone has been modified slightly by abrasion of mesial surface, but does not appear essentially different in porportions from that of *Lama*.

A well-preserved ulna-radius, no. 7491, (Plate 5, fig. 4) as well as several incomplete specimens, gives the essential characters of that bone. Length of radial element between articular facets is practically the same as that of the museum specimen, no. 13513KU, of the dromedary. By this measurement, the radius is one-tenth longer in proportion to length of humerus than in the specimen of *Camelus*, but it is much more slender. Greatest width at distal end is 63.0 mm. Olecranon is broad and flat and apparently shorter in proportion to length of shaft than that of the llama; though epiphysial portion of olecranon is missing from specimen, overall length is 550.0 mm. Ulnar element is almost as completely co-ossified at distal end as that of the llama. Interosseous foramen has a more elevated position, and foramen at proximal end has a similar position to that of the llama. Superior margin of the olecranon is straight rather than concave as in the llama.

Carpus offers few variations from that of Recent *Lama*. Unciform presents an angular surface to the trapezoid and is notched into the latter. Lunar has a more elongate posteroproximal facet.

The metacarpal has a length and slenderness comparable to that of the ulna-radius. Overall length is 422.0 mm in specimen no. 7498, and 430.0 mm in specimen no. 7497 (Pl. 5, fig. 3). It is more than one-sixth longer than same bone in the dromedary. The 2 elements are firmly co-ossified in shaft. Distal end is narrow and is deeply cleft at median line. The leg as mounted stands 1422.0 mm high.

Of the phalanges, 10 entire specimens are preserved. The first phalanges are long and slender and are consistent with length of leg bones and great stature of animal indicated by assembled fore leg. First phalanges preserved vary from 84.0 to 108.0 mm long. Shafts are straight and slender, ligamentary and muscular attachments are lightly but clearly marked. Distinction between phalanges of fore and hind foot rests chiefly upon length of muscular attachments at proximal end, those of hind foot are larger. Only 2 second phalanges are preserved. One of these measures 42.0 mm in its axial length.

A single metatarsal, no. 7499, (Pl. 5, fig. 2) was recovered which has an overall length of 371.0 mm, a width of 45.0 mm at proximal end, and 55.0 mm greatest width at distal end.

PLATE 5.—SKELETAL PARTS OF CAMELS AND GROUND SLOTH

Figure

1. *Pliauchenia cochrani* sp. nov. KU7646, left metatarsal. Anterior view. ×½.
2. *Tanupolama blancoensis* Meade. KU7499, metatarsal. Anterior view. ×½.
3. *Tanupolama blancoensis*. KU7497, left metacarpal. Anterior view. ×½.
4. *Tanupolama blancoensis*. KU7491, left ulna-radius. Lateral view. ×½.
5. *Tanupolama blancoensis*. KU7645, left humerus. Anterior view. ×½.
6. *Gigantocamelus spatulus* (Cope). KU7648, right side of pelvis. Lateral view. ×⅛.
7. *?Megalonyx* sp. KU7547, phalanx. Lateral view, ×½.

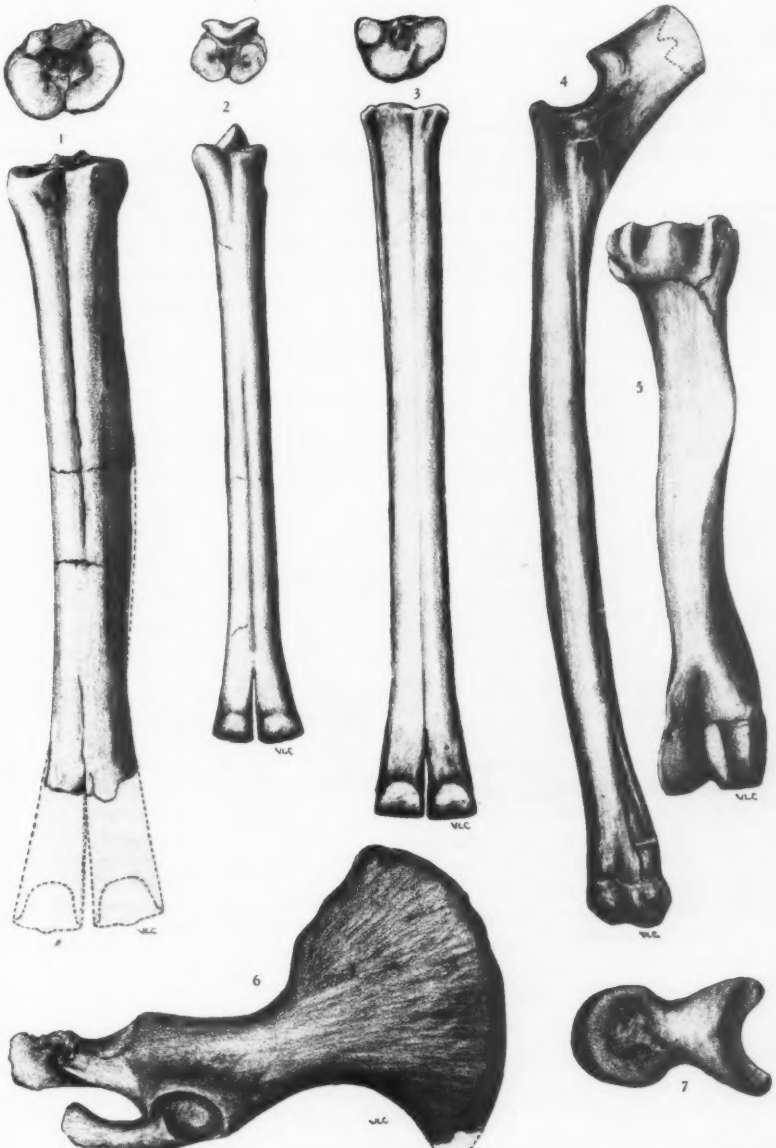

SKELETAL PARTS OF CAMELS AND GROUND SLOTH

SUMMARY

The vertebrates recovered from the Keefe Canyon quarry in many cases duplicated forms previously known from the Rexroad fauna. From this study 10 species have been added to the mammalian fauna of the Rexroad. Eight of the species have been taken from the Keefe Canyon quarry. The Rexroad fauna is now the most completely known fauna from a given horizon of the High Plains. Among the known mammals, 10 genera and 31 species are confined to the upper Pliocene. For reference to the invertebrates see Baker (1938), Hibbard (1941) and Franzen and Leonard (1947). Taylor (1941; 1942) described the reptiles and the frogs and toads. Wetmore (1944) reported upon the bird remains from the Rexroad formation. The following mammals are now known:

Mammalia
- Insectivora
  - *Sorex taylori* Hibbard
  - *Sorex?* sp.
  - *Hesperoscalops rexroadi* Hibbard
- Chiroptera
  - genus?
- Edentata
  - *Megalonyx?* sp.
- Rodentia
  - *Paenemarmota barbouri* Hibbard and Schultz
  - *Citellus howelli* Hibbard
  - *Citellus rexroadensis* Hibbard
  - *Geomys quinni McGrew*
  - *Liomys centralis* Hibbard
  - *Perognathus gidleyi* Hibbard
  - *Dipoides rexroadensis* Hibbard and Riggs
  - *Procastoroides lanei* (Hibbard)
  - *Onychomys gidleyi* Hibbard
  - *Symmetrodontomys simplicidens* Hibbard
  - *Bensonomys arizonae* (Gidley)
  - *Peromyscus kansasensis* Hibbard
  - *Baiomys rexroadi* Hibbard
  - *Sigmodon intermedius* Hibbard
  - *Parahodomys quadriplicatus* Hibbard
  - *Ogmodontomys poaphagus* Hibbard
- Carnivora
  - *Canis lepophagus* Johnston
  - *Canis* sp.
  - *Borophagus diversidens* Cope
  - *Procyon rexroadens* Hibbard
  - *Trigonictis kansasensis* Hibbard
  - *Martes foxi* Hibbard aed Riggs
  - *Spilogale rexroadi* Hibbard
  - *Brachyprotoma breviramus* Hibbard
  - *Taxidea taxus* (Schreber)
  - *Felis lacustris* Gazin
  - *Panthera* sp.
  - *Machairodus* or *Ailuraena* sp.
- Proboscidea
  - *Stegomastodon successor* (Cope)
  - *Mammut* (*Pliomastodon*) *adamsi* (Hibbard)
- Lagomorpha
  - *Pratilepus kansasensis* Hibbard
  - *Notolagus lepusculus* (Hibbard)
  - *Hypolagus regalis* Hibbard
  - *Nekrolagus progressus* (Hibbard)
- Perissodactyla
  - *Equus* (*Hippotigris*) *simplicidens* Cope
  - *Nannippus phlegon* (Hay)
- Artiodactyla
  - *Platygonus bicalcaratus* Cope
  - *Gigantocamelus spatulus* (Cope)
  - *Pliauchenia cochrani* Hibbard and Riggs
  - *Tanupolama blancoensis* Meade
  - Cervid (genus?)
  - Antilocaprid (genus?)

REFERENCES CITED

Baker, Frank C. (1938) *New Land and Freshwater Mollusca from the upper Pliocene of Kansas and a new species of Gyraulus from early Pleistocene strata*, The Nautilus, vol. 51, p. 126–131.

Barbour, Erwin Hinckley, and Schultz, C. Bertrand (1939) *A New Giant Camel*, Nebr. State Mus., Bull., vol. 2, no. 2, p. 17–27.

Byrne, Frank, and McLaughlin, Thad G. (1948) *Geology and Groundwater Resources of Seward County, Kansas*, Kans. State Geol. Survey, Bull. 69, p. 1–138.

Cragin, F. W. (1896) *Preliminary notice of three late neocene terranes of Kansas*, Colo. State College, Stud., vol. 6, p. 53–54.

Elias, Maxim K. (1931) *The Geology of Wallace County, Kansas*, Kans. State Geol. Survey, Bull. 18, p. 1–254.

Franzen, Dorothea S. (1947) *The pocket Gopher*, Geomys quinni *McGrew, in the Rexroad fauna, Blancan age, of southwestern Kansas*, Kans. Acad. Sci., Tr., vol. 50, no. 1, p. 55–59.

——— and Leonard, A. B. (1947) *Fossil and Living Pupillidae (Gastropoda = Pulmonata) in Kansas*, Kans. Univ., Sci. Bull., vol. 31, pt. 2, no. 15, p. 311–411.

Frye, John C., and Hibbard, Claude W. (1941) *Pliocene and Pleistocene Stratigraphy and Paleontology of the Meade Basin, southwestern Kansas*, Kans. State Geol. Survey, Bull. 38, pt. 13, p. 389–424.

Gazin, C. Lewis (1938) *Fossil peccary remains from the upper Pliocene of Idaho*, Washington Acad. Sci., Jour., vol. 28, no. 2, p. 41–49.

Gidley, J. W. (1903) *On two species of* Platygonus *from the Pliocene of Texas*, Amer. Mus. Nat. Hist., Bull., vol. 19, art. 14, p. 477–481.

Hibbard, Claude W. (1941) *Mammals of the Rexroad fauna from the upper Pliocene of southwestern Kansas*, Kans. Acad. Sci., Tr., vol. 44, p. 265–313.

McGrew, Paul O. (1944) *An early Pleistocene (Blancan) fauna from Nebraska*, Field Mus. Nat. Hist., Geol. Ser., vol. 9, no. 2, p. 33–66.

McLaughlin, Thad G. (1946) *Geology and Ground-water Resources of Grant, Haskell and Stevens Counties, Kansas*, Kans. State Geol. Survey, Bull. 61, p. 1–221.

Meade, Grayson E. (1945) *The Blanco Fauna*, Univ. Texas, Publ. 4401, p. 509–556.

Smith, H. T. U. (1940) *Geological studies in southwestern Kansas*, Kans. Geol. Survey, Bull. 34, p. 1–212.

Stirton, R. A. (1935) *A Review of the Tertiary Beavers*, Univ. Calif. Publ., Bull., Dept. Geol. Sci., vol. 23, no. 13, p. 391–458.

Taylor, Edward H. (1941) *Extinct Lizards from upper Pliocene deposits of Kansas*, Kans. State Geol. Survey, Bull. 38, pt. 5, p. 165–176.

——— (1942) *Extinct Toads and Frogs from the upper Pliocene deposits of Meade County, Kansas*, Univ. Kans., Sci. Bull., vol. 28, pt. 2, p. 199–235.

Wetmore, Alexander (1944) *Remains of Birds from the Rexroad Fauna of the upper Pliocene of Kansas*, Univ. Kans., Sci. Bull., vol. 30, pt. 1, p. 89–105.

UNIVERSITY MICHIGAN, DEPT. GEOL. AND MUS. PALEO., ANN ARBOR, MICH.; SILOAM SPRINGS, ARK.
MANUSCRIPT RECEIVED BY THE SECRETARY OF THE SOCIETY, JUNE 11, 1948.
PROJECT GRANT 451/45.

BULLETIN OF THE GEOLOGICAL SOCIETY OF AMERICA
VOL. 60, PP. 861-886, 14 FIGS. MAY 1949

OBSERVATIONS ON SOME YELLOWSTONE GEYSERS

BY F. DONALD BLOSS AND TOM. F. W. BARTH

CONTENTS

	Page
Abstract	862
Introduction	862
Existing geyser theories	863
Observed eruption patterns	866
Procedure	866
Spring gases in geysers	866
Discussion	866
Crater Hills Geyser	866
Sawmill and Tardy geysers	867
Connections between geysers	868
General statement	868
Sawmill and Tardy geysers	869
Grand and Turban geysers (and the Bernoulli effect)	869
Regular increase vs. fluctuation of temperature	873
Discussion	873
Jewel Geyser	873
Possible causes of termination of eruptions	875
Discussion	875
Spasm Geyser	875
Grotto and Castle geysers	875
Small, unnamed geyser	876
Temperature-depth curves	877
Criticism of usual methods of compilation	877
Improved methods of compilation	879
Principles illustrated by observed curves	880
General statement	880
Role of convection currents	880
Attainment of boiling conditions at depth	882
Superheated waters	883
Conclusions	883
References cited	886

ILLUSTRATIONS

Figure	Page
1.—Time-temperature curve at 3.5 meter depth in Sawmill Geyser	868
2.—Sketch of areal relationships between Grand and Turban geysers	870
3.—Chronologic relationships of eruptions of Grand, Turban, and satellitic vent	871
4.—Relation between discharge from Grand and eruptions of Turban	872
5.—Hypothetical cross section along traverse, abc, of Figure 2	872
6.—Time-temperature curves for several depths of Jewel Geyser	874
7.—Time-temperature curve for 2-meter depth in Spasm Geyser	876
8.—Time-temperature curve at approximately the 2.5 meter depth in geyser 80 feet west of Anemone	878

9.—Time-temperature curves for Comet Geyser 879
10.—Temperature-depth curve for Comet Geyser derived from Figure 9 880
11.—Temperature-depth curves for Chinaman Spring 881
12.—Temperature-depth curves for Beehive Geyser, Limekiln Spring, Big Cub, Catfish, and Mastiff geysers 882
13.—Temperature-depth curves for unnamed geyser 40 feet SE of Beach Spring and for Sponge Geyser 883
14.—Temperature-depth curves for Lioness Geyser, Scalloped Spring, and its neighboring spring 50 feet south 884

ABSTRACT

In addition to brief discussions of the older theories of geyser action, a more extensive résumé of the modern but lesser known theory of Thorkelsson is presented.

Eruption patterns (i.e., the observed changes with respect to time during several periods) of Crater Hills Geyser, Sawmill Geyser, and Tardy Geyser, are cited as indicative of the presence, in these geysers, of the spring gases so important to Thorkelsson's theory. On the basis of the eruption patterns, subterranean connections are concluded to exist between Sawmill and Tardy geysers and between Grand and Turban geysers. An interesting Bernoulli effect, previously undescribed in the literature, was concluded to cause Grand's surface level to lower during the early portion of Turban's eruptions. Continuous time-temperature curves for several cycles of Jewel Geyser indicated, for the depths observed, that temperatures were often higher during quiescent periods than at the beginning of the eruption. Spasm Geyser possibly illustrates an influx of relatively cool water which terminates the eruption. Grotto and Castle geysers indicate that a cause of termination of the eruption, other than a rapid influx of cooler water, probably exists.

The usual methods of securing temperature-depth data are found unsatisfactory; some new methods are suggested. Temperature-depth curves of Chinaman Spring are taken to indicate not only the importance of convection currents in the upper parts of geyser wells but also the efficacy of constrictions and narrow tubes in inhibiting convectional cooling. Numerous temperature-depth curves of active and inactive geysers indicate that boiling conditions were rarely existent in the lower depths examined. Superheated waters were often located at the surface of the pools of the numerous geysers and hot springs examined.

INTRODUCTION

The field work on which this paper is based was carried out in Yellowstone Park, Wyoming during July and August, 1947. The Upper Geyser Basin, chiefly because of the accessibility and diversity of its geysers, was the site of most of the observations. Brief side trips were made to the Biscuit Basin and Norris Geyser Basin. The ultimate goal of the work was to enable the authors to confirm, modify, substitute for, or deny any or all of the existing geyser theories. Since the earlier theories were based on surficial observations coupled with maximum thermometer readings, it was hoped that new observations plus a different approach, that of continuously recording temperatures deep in the geyser tube before, during, and after an eruption, would throw new light on geyser mechanisms. Field observations were principally confined to those phenomena which, it was believed, would give clues as to physical and thermal conditions which are essential to the mechanics of geyser action.

In addition to the usual maximum thermometers, a remote-reading resistance ther-

mometer consisting of a coil of fine nickel wire encased in a water-tight brass jacket was used. This irregularly cylindrical thermal element was 22 cm long and 5 cm in diameter at its greatest width. The temperature of the water was evinced by the resistance of the immersed, brass-enclosed, nickel coil. A 60-foot length of insulated wire connected the nickel element to a Wheatstone bridge which could be adjusted to read the resistance of the coil and thereby, when calibrated, the temperature of the water. The thermometer was of sufficient weight to remain in the geyser tube during eruptions up to 40 feet high. A smaller thermal element, however, would have allowed a deeper depth of penetration in some of the geysers.

The co-operation of Superintendent Edmund B. Rogers, Dr. C. Max Bauer, Chief Park Naturalist David Condon, District Ranger Scotty Bauman, Senior Ranger Naturalist George Marler, all of the National Park Service, and of Messrs. Earl Kelly and Howard Armstrong, is gratefully acknowledged. The authors sincerely thank the Geological Society of America for material support given in the form of a Penrose research grant.

EXISTING GEYSER THEORIES

Several plausible theories have been developed to explain geyser mechanisms. Krug von Nidda (1837) postulated upwardly ramifying cavities in which rising masses of steam were trapped to eventually fill the cavities and escape into the geyser tube proper. Masses of steam rising up the tube agitated the water column so that water was ejected from the orifice by splashing. The resultant decrease in hydrostatic pressure allowed steam in the caverns to further expand and thus caused increasingly greater amounts of water to be ejected from the orifice. The eruption proceeded, von Nidda believed, until sufficient steam had escaped from the chamber to make the hydrostatic pressure of the mixture of water and steam in the tube equal to the pressure of the steam in the chamber. A justifiable objection is that steam at reduced pressure would, at this stage, occupy the entirety of each cavity and therfore the rising masses of steam would bypass these chambers and escape directly through the tube to form a constantly boiling spring. Allen and Day (1935, p. 215) follow Lang in considering the influx of relatively cool water a necessary follow-up of an eruption in a periodic geyser. This would cause condensation of the steam in the chambers so that they would once more be filled with water and the cycle could begin anew.

Bunsen's (1847) theory, conceived to fit only "Great Geysir" in Iceland, was universally accepted and its application, unfortunately, extended to all geysers. Bunsen believed that the temperature at all points in "Geysir" steadily rose from one eruption to the next, but that, since the temperature at the midpoint of the column was closest to its corresponding boiling point, an overflow of 1 or 2 meters of water caused boiling to begin there and to proceed down the column in response to the increased overflow resulting from the boiling. Thus increasingly greater amounts of water attained boiling conditions and caused greater amounts of water to be ejected as the eruption progressed. He did not consider the cause of the termination of the eruption. Lang (Allen and Day, 1935, p. 211) in addition to postulating an influx of

cool water as terminating the eruption, concluded that convectional cooling would prevent boiling from beginning in the tube and therefore boiling would have to begin in a side chamber. Lang's modification in 1880 was thus a synthesis of the earlier theories of von Nidda and Bunsen.

Allen and Day (1935, p. 214–220) stress underground chambers as serving two main purposes in geyser action. Some must contain and, during eruption, contribute much water. Others of a sinter-lined, steam-tight nature must act as steam chambers wherein the expansion and contractions of steam may cause the fluctuation in surface level noted in geysers. In Figure 5, the caverns shown connected or associated with the tube of Grand Geyser are patterned after Allen and Day's conception of the essential parts of a geyser.

Thorkelsson's (1940) theory hinges on the assumption that hot spring waters, whether juvenile, vadose, or a combination of both, must of necessity occlude a certain amount of gases (nitrogen, argon, methane, etc.). These spring gases are carried upward with the water to reach a depth, l_1, where the pressure is such that small bubbles of gas form simultaneously throughout the liquid (like the bubbles when a bottle of soda water is uncorked). These small gas bubbles become saturated with water vapor until they are many times their original size. For example, if the temperature is 2°C below the boiling point, then spring gases compose 6.9 per cent of the volume of the bubble; the 93.1 per cent of bubble volume remaining is occupied by steam. The water column below l_1 loses little or no heat since bubbles cannot form there and, in addition, thermal equilibrium with the rock walls of the geyser tube probably exists. Above l_1, however, bubbles do form and heat is thereby subtracted from the water column. As the bubbles rise the decreased pressure of shallower depths permits them to continuously expand and thus increase their heat content at the expense of the surrounding water. Thus Thorkelsson believes the temperature in a geyser will gradually increase with increased depth below surface until l_1 is reached; below l_1 the water is at a constant temperature, T_1, which is termed the critical temperature by Thorkelsson. The actual value of l_1 is proportional to the amount of spring gases, other than steam, occluded in the water.

Thus bubbles of considerable size can arise in a geyser system although the temperatures are much below the several boiling points for those depths. Preceding an eruption these mixtures of gas and water vapor first fill the cavities to capacity, then escape into the connected geyser tube. Subjected to the cooler water of the geyser tube, these bubbles may at first collapse and their gas will once more be occluded by the water. Their collapse liberates considerable heat; thus water in the geyser tube becomes increasingly hotter, especially in the lower portions, and the ensuing bubbles may more closely approach the surface prior to collapse. As this phenomenon continues (strong convection currents will modify the process) more and more of the water in the tube will be displaced by the bubbles and, if overflow occurs into a basin of wider diameter than the tube, reduction of the hydrostatic pressure will result. This reduction in hydrostatic pressure causes ebullition to proceed rapidly downward from level l_1 to a new depth, $l_1 + \lambda_1$, and an eruption results. That the value of λ_1 is considerable and thus involves great amounts of water may be seen from Table 1, calculated (to avoid complexity) under the assumption that no gases are dissolved

in the spring water. When gases are assumed to be present, the values for l_1 and λ_1 increase greatly.

When ebullition proceeds downward from l_1 to $l_1 + \lambda_1$, it naturally does so at a certain rate of speed. Its tendency to move downward is counterbalanced, in part, by the continuous upward flow of the water of temperature T_1 which supplies the

TABLE 1.—*Relation between the temperature and depths of boiling of pure water*
Modified from Thorkelsson (1940, p. 91)

TEMP. OF THE SPRING WATER	l_1	$l_1 + \lambda_1$
degrees C	*meters*	*meters*
101	0.4	1.0
110	4.3	61.2
120	9.8	235.8
130	17.1	522.1

l_1 = lowest depth of initial boiling.
$l_1 + \lambda_1$ = maximum depth to which boiling extends (after overflow due to bubble formation).

geyser. Usually the rate at which ebullition moves downward from l_1 to $l_1 + \lambda_1$ far exceeds the upward rate of flow of the hot water. Thus when the ebullition reaches the depth $l_1 + \lambda_1$ a new equilibrium is attained and the eruption is terminated for lack of hot water supply.

Thorkelsson accounts for perpetually spouting springs by assuming that the supply of hot water proceeds upward along the tube at the same rate as the ebullition tends to move downward. So although boiling tends to continue downward, the depth $l_1 + \lambda_1$ is never attained by the ebullition and the process is not terminated.

Reasoning more quantitatively, Thorkelsson (1940, p. 62–64) derived the following equation:

$$P = p - p_0 + \frac{bpr\rho_0}{c(T_1 - T)}$$

where P is the hydrostatic pressure at any specified depth; T, the temperature at this depth; p and r, respectively, the vapor tension of water and the latent heat of steam at temperature T; ρ_0, the density of steam at S.C.; p_0, atmospheric pressure; b and c, are, respectively, the volume of spring gases at S.C. and the mass of water plus steam passing thru a square cm of channel in one second; and T_1 is the critical temperature which exists at and below the depth, l_1. Thus, since P is directly proportional to the depth in the geyser prior to boiling, a temperature-depth profile, if determined to below l_1, will give an idea of the b/c ratio for that geyser by the method of assigning various b/c ratios to the Thorkelsson equation and plotting its curve using the value of P, T, p_0, and T_1 derived from the temperature-depth curve of the geyser. With one of the assigned b/c ratios, the plotted temperature-depth curve will closely approximate the actual temperature-depth curve. This b/c ratio, if the theory holds for the tested geyser, will be the one that actually exists. Barth (1947) does this for several Icelandic geysers. A more extensive treatment of Thorkelsson's theory will be given by Barth (in press, Carnegie Inst. Washington).

OBSERVED ERUPTION PATTERNS

PROCEDURE

In this section the general sequence of events preceding, during, and following an eruption is described for several geysers. These eruption patterns are grouped under the principles which the authors believe they most clearly illustrate. The principles chosen often concern salient points of an existing geyser theory. For example, the action of spring gases (other than steam) is the central thought of Thorkelsson's theory; demonstrable connections between geysers foreshadow the possibility of adjoining subterranean caverns being integral parts of geyser systems, as well as the possiblity that a geyser's activity may be affected by that of its neighbor; disproof of the necessity of continuous rise in temperature along the entire water column deals Bunsen's theory a heavy blow; possible cause of termination of an eruption is a phase which all geyser theories must consider.

SPRING GASES IN GEYSERS

Discussion.—The presence of spring gases, other than water vapor, could considerably affect the actions of a geyser in the manner Thorkelsson has pointed out. The Crater Hills Geyser erupts at temperatures far below boiling, probably as a result of their presence. Their role in the case of Sawmill and Tardy geysers is less obvious but their presence in all three geysers is undeniable, as the observations below indicate.

Crater Hills Geyser.—This geyser, 8 miles NNW of Fishing Bridge, is in many respects rather different from the usual type of geyser. The basin is roughly elliptical, 5 by 7 meters across, and rather deep (Allen and Day, 1935, p. 432–435). The eruption pattern observes a regular rhythm. At the end of the quiet interval the water level lies tranquil 0.5 meter below the rim of the basin. Suddenly violent boiling starts at a point not far from the center of the basin, and fountains 1–2 meters high are incessantly thrown up into the air. However, all water falls back into the basin; there is no overflow. This activity is kept up for about 30 minutes, during which time the water level slowly rises until the rim of the basin is reached. At this point, the boiling abruptly ends. The water level again becomes tranquil and, during the quiet interval of about 2 minutes, drops back half a meter into the basin. Then a new eruption starts. Thus, this geyser has no visible discharge; all water is returned to the basin. The water surface oscillates regularly: during incessant boiling it rises 0.5 meter in 30 minutes; during the quiet intervals it drops 0.5 meter in 2 minutes (each rise or drop corresponds to a change in volume of approximately 15,000 liters).

The low temperature (73°C maximum) proves that spring gases other than steam are responsible for the geyser phenomena. The mechanism might perhaps be explained as follows: the geyser vent serves as an avenue of egress for gases which, according to the air lift pump principle, are periodically released. With great violence the gases are forced through the water-filled geyser system, the result being ebullition and, because of the intermittency, geyser action. The oscillation of the water surface may be explained if we assume that some of the subterranean reservoirs are alternately filled with water and with gas. To summarize:

1. An eruption lasts for about 30 minutes followed by a quiet interval of only 2 minutes. In most geysers the eruption period is shorter than the quiet period.
2. There is no discharge, not even during an eruption.
3. The eruptions start when the water is low in the basin. Most geysers erupt only when the basin is full.
4. The maximum temperature during the eruptions on August 12, 1947 was 73°C (measured in the middle of violently boiling water). Consequently spring gases, and not "ordinary" boiling must be responsible for the geyser activity.
5. The hydrogen ion concentration is pH = 3.9. Most geysers have alkaline waters.

Sawmill and Tardy geysers.—These two geysers are located in the Upper Geyser Basin approximately 60 feet from each other. Both possess symmetrical, conical basins. Sawmill's basin is 160 cm in diameter near its lip but only 20 cm in diameter at a depth of 100 cm where it connects with its tube. A crook or constriction in the tube at the 4-meter depth prevents deeper penetration with the thermometer. Tardy's basin is a diminutive edition of Sawmill's, 70 cm diameter near its rim tapering to 10 at the 70 cm depth where it joins its rather circular tube. A sharp bend or constriction exists in Tardy's tube at a depth of 2.2 meters.

Sawmill's eruptions are very irregular in many respects. They last from 40 minutes to almost 4 hours; several were about $1\frac{3}{4}$ hours long. Although duration and interval of eruption were very irregular during August of 1947, Sawmill appeared to be in eruption an average of 50 per cent of the time. No discharge occurred between eruptions, but during eruptions the discharge was computed to be 21 liters per second on the basis of measurements of the velocity of the runoff in channeled streams of a known, constant cross section. On the basis of these figures Sawmill discharges 907,200 liters or 32,000 cubic feet per day, closely approaching the estimated daily output of Old Faithful. The rate of influx of water into Sawmill's subterranean system must also be approximated by the above figure. A maximum discharge of 11,000 cubic feet was observed during a 4-hour eruption of Sawmill. Since a simultaneous influx of 5000 cubic feet of water into the system may be postulated for those 4 hours, the minimal volume of Sawmill's subterranean system is estimated to be 6000 cubic feet. During 3 hours and 53 minutes of a 3 hour and 55 minute eruption, the temperature at the 4-meter depth in Sawmill remained within 0.5° of 103.1°C (Fig. 1). This possibly indicates the existence of a large cavern or series of caverns so openly connected with each other that convection is free to equalize the temperature throughout. It could also indicate Thorkelsson's alternative hypothesis that all the water below a certain critical depth is at the same temperature.

Sawmill's surface level fluctuates; an upward fluctuation was, as a rule, the immediate precursor of an eruption. Small bubbles about one eighth of an inch in diameter could often be seen rising from the depths; their frequency increased just prior to eruptions. Sometimes for as much as 14 minutes before an eruption, large, white, vaporous bubbles left the orifice only to collapse in the waters of the surface pool. In one instance the large white vaporous bubbles were observed to pinch off and collapse at a definite level estimated to be about 3 feet below the surface of the pool. At this depth, bubbles 1 inch in diameter collapsed to one-eighth inch diameter bub-

bles which completed the rise to the surface. The surface temperature of Sawmill's pool was 87°C at this time; since convection was free to operate in the pool, the 3-foot depth was probably near the same temperature. Immediately before eruptions, large white bubbles came out of the orifice, the pool surface having in the meanwhile risen quite rapidly, and an eruption to heights of 20–30 feet would occur.

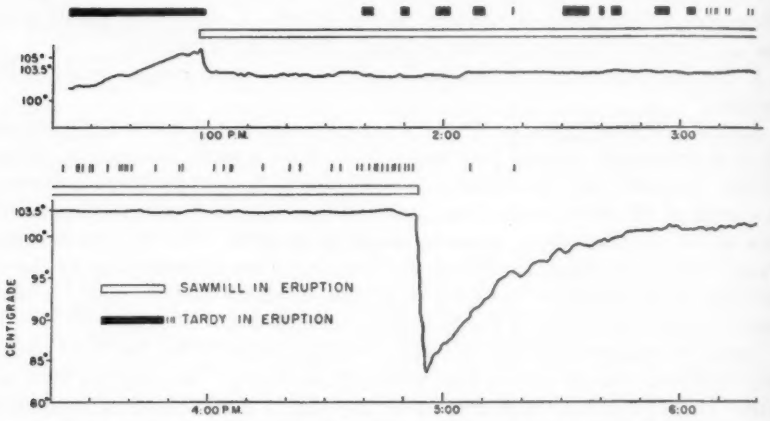

FIGURE 1.—*Time-temperature curve at the 3.5 meter depth in Sawmill Geyser*

Before, during, and after eruption. Tardy's eruptions during this period are shown by the solid black, the sustained eruption of Sawmill, by the hollow rectangles.

One-eighth-inch diameter bubbles also rose from the depths of Tardy (60 feet southeast of Sawmill). Since they were noted to rise through the surface pool which was at a temperature of 70°C, they evidently indicate the presence of spring gases as Thorkelsson (1940) suggested. The collapse of the large white bubbles to much smaller ones upon their contact with the cooler waters of Sawmill's surface pool, appears to be an almost graphic illustration of Thorkelsson's idea that the spring gases form a small but essential constitutent enabling the steam bubbles to exist in waters below the boiling point (for those conditions of temperature and pressure). During the instance cited in Sawmill, the temperature of the waters was evidently so cool that almost all the steam vapor in the bubbles condensed and only the nucleus of spring gases survived. In Tardy, condensation may occur deep in the tube so that only the gas nuclei of the steam bubbles are observable.

CONNECTIONS BETWEEN GEYSERS

General statement.—Field data indicated that Sawmill and Tardy are probably connected and that Grand and Turban geysers are certainly connected. The effect of their relationship was not readily apparent from the activity of Sawmill or Tardy. For Grand and Turban, however, the connection produced an interesting Bernoulli effect which was possibly the trigger governing Grand's eruptions.

Sawmill and Tardy geysers.—Again considering the behavior of Sawmill and Tardy (Fig. 1), one sees that Tardy erupts almost constantly to heights of 5 feet prior to an eruption of Sawmill but during eruptions of Sawmill, the interval and duration of Tardy's eruptions become erratic and the spurts from Tardy are more forceful and reach 15–20 feet in height. During quiescent periods of Sawmill, when Tardy is erupting only to heights of 3–5 feet, all its erupted water usually falls back into its pool. The rare occasions when the water level in Tardy was high enough to spill over its rim and discharge to the Firehole River coincided with a longer interval between Sawmill's eruptions. The existence of a subterranean connection between the two geysers thus appears very likely.

Grand and Turban geysers (and the Bernoulli effect).—Areal relationships of the two geysers are approximately shown by Figure 2. Grand's pool is poorly defined, irregular in shape, and relatively shallow. Preceding an eruption it attains a maximum diameter of roughly 65 feet. Grand's tube is 2 by 4 feet in cross section and 22 feet deep: the sides of the tube are near vertical except at the top where the tube rapidly flares out, trumpetlike, to merge into its shallow basin above. Turban's pool, on the other hand, is very definitely confined by an elevated rim of geyserite. Its basin is shallow at its southern end but deepens to the north to a maximum depth of 9 feet at the point of junction with its tube. A massive, rounded bridge of geyserite spans the orifice dividing it into two sections, both glutted by rhyolite boulders derived from the neighboring bluff and thrown into Turban by the tourists.

During July and August of 1947, Turban erupted to heights of 5 or 6 feet on an average of 4 times per hour. The eruptions lasted from $3\frac{1}{4}$ to 5 minutes and were presaged by the rise of large, white, vaporous bubbles from the orifice, accompanied by a rise in the surface of the pool. At its high-water mark, the rise of the surface of its pool resulted in a discharge of water over the elevated geyserite rim precedent to the actual eruption. Otherwise, discharge over the geyserite rim did not occur until the actual eruption had proceeded for 15 seconds up to 2 minutes. The time lag between the beginning of eruption and that of overflow appeared to be proportional to the distance below the high-water mark of the pool's surface at the beginning of the eruption. Turban's discharge during eruption was estimated at 20 liters or 0.7 cubic feet per second. During an average 4-minute eruption 168 cubic feet of water passed out of the orifice.

Grand geyser erupted on an average of twice a day during this same period. Maximum height of eruption was estimated to be about 140 feet, duration 18–50 minutes. Every eruption observed was distinctly divisible into spurts between which the water level of Grand receded into its orifice; then the water being discharged from Turban as well as that discharged during Grand's preceding spurt drained backward into the orifice. On July 28, 1947, an 18-minute eruption divided into 11 spurts was observed; on August 15 a 50-minute eruption of 23 spurts was noted. Most eruptions fall between these two extremes both as to number of spurts and as to duration. During eruptions the discharge from Grand was estimated to be 11.0 cubic feet or 310.0 liters per second. Thus during a 30-minute eruption of Grand, 50 per cent of which consists of active spurts, 9900 cubic feet of water is discharged. At the conclusion of Grand's eruption, the water remaining in it drains downward out of sight.

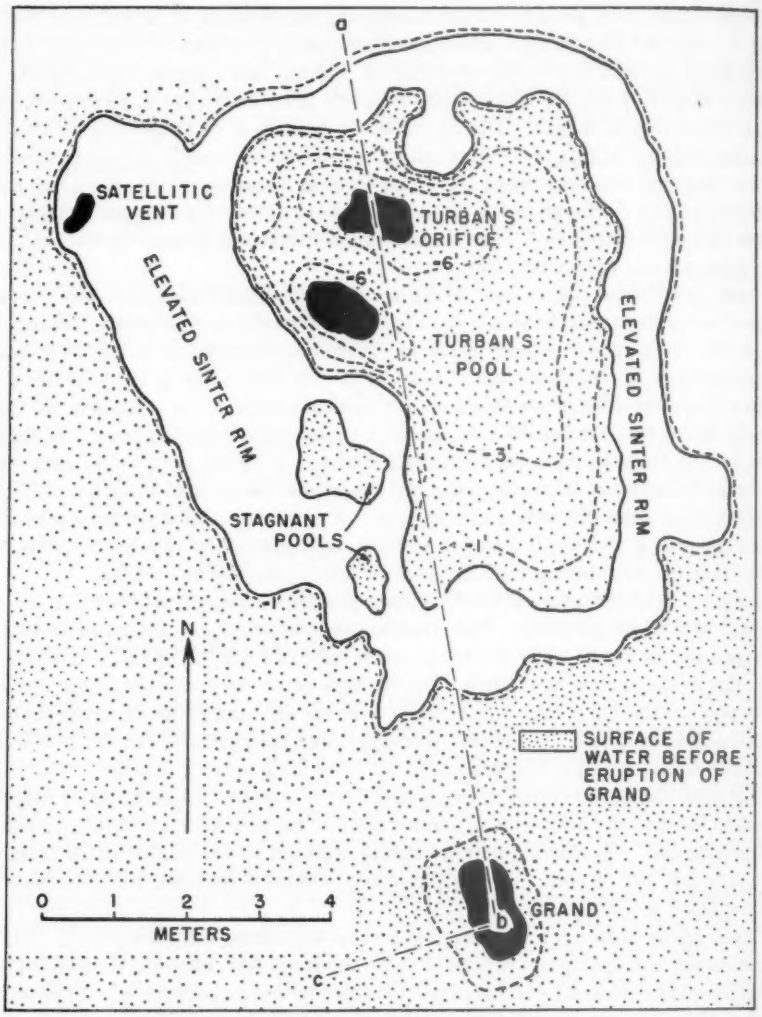

FIGURE 2.—*Sketch of areal relationships between Grand and Turban geysers*

The traverse, abc, is that of thehypothetical cross section of Figure 5. Curved, dashed lines indicate contour depths below the water surface prior to eruption of Grand.

Turban may continue the constant eruption with which it accompanies Grand for several minutes past the cessation of Grand's eruption, but when it ceases, its water also drains downward out of sight, leaving its basin dry. This draining of Turban's basin only followed its eruptions during the period of time when Grand's water level had dropped out of sight.

Eruptions of Grand were invariably preceded from 15 to 90 seconds by an eruption

of Turban. When co-ordinated with an eruption of Grand, Turban's height of eruption was 15 or 20 feet instead of its usual 5 or 6 feet; its duration of eruption increased from the 4-minute average to as much as an hour and a half (Fig. 3).

Hallock in 1883 (Allen and Day, 1935, p. 182) noted that (1) the level of Turban fell 7 inches when that of Grand rose about 1¾ inches and (2) the surface area of Tur-

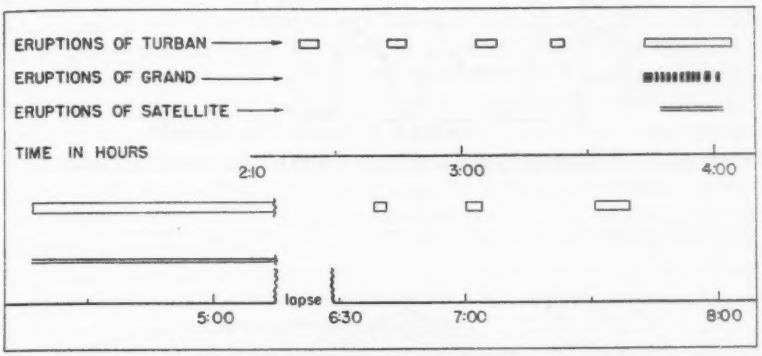

FIGURE 3.—*Chronologic relationships of the eruptions of Grand Geyser (solid black rectangles), Turban (hollow rectangles), and their satellitic vent (close-spaced double line), July 28, 1947*

Change in duration of Turban's eruption during and after activity of Grand is illustrated.

ban's pool was roughly one-quarter of that of Grand. He thereby concluded that equal volumes were involved and that the two geysers possessed a subterranean connection. Allen and Day rightly protested that the areas involved are so irregular as to escape accurate estimate. They also observed that the surface of Grand's pool is normally 2½–3 feet lower than that of Turban. Principally because they regarded this difference in level as hydrostatic, Allen and Day rejected the thesis of a subterranean connection.

During July and August of 1947, new observations were made which appear to decide the question. The surface of Grand was noted to be no more than 6–9 inches lower than that of Turban and at such times a discharge of 20 liters per second escaped over a low point of Grand's sinter rim to flow into the Firehole River. Thus the difference in level is not a hydrostatic one; it involves only the principle that a vessel cannot be filled above its rim. Therefore no hydrostatic anomaly is involved if the two geysers have an underground connection. As previously observed by Allen and Day, the level of Grand was noted to fall whenever Turban erupted. These changes in its surface level are reflected in the variable rate of discharge from Grand (Fig. 4) In all 1947 observations, the drop in the surface level of Grand always occurred just as the eruption of Turban began but an appreciable time before the stream of discharge water from Turban had reached the pool of Grand. This renders untenable Allen and Day's explanation that the lowering of Grand's surface during an eruption of Turban is due to a condensation in one of Grand's steam chambers (caused by the influx of air-cooled discharge water from Turban).

It has been noted that: (1) the duration, height, and interval of Turban's erup-

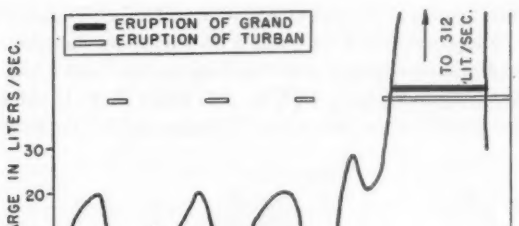

FIGURE 4.—*Relationship between discharge from Grand and eruptions of Turban* August 13, 1947.

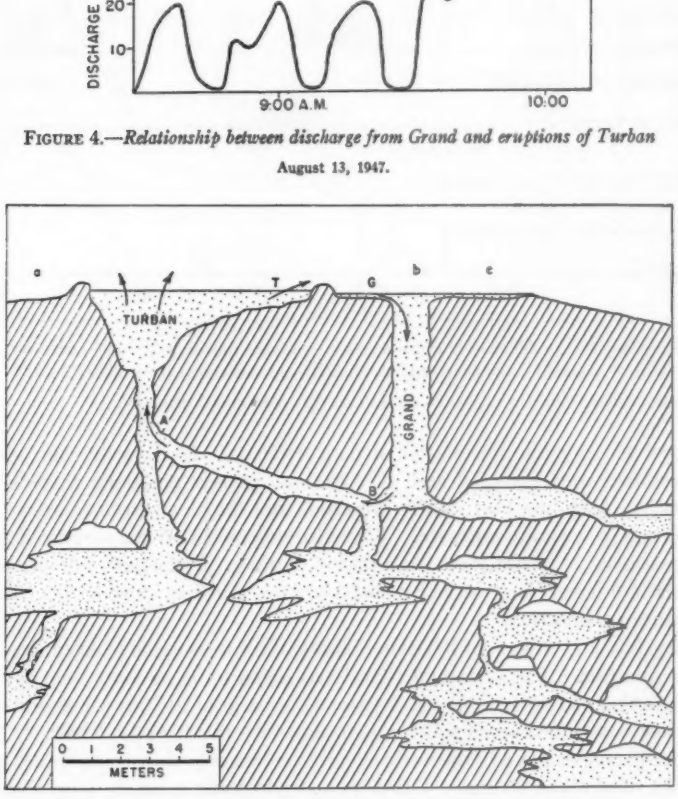

FIGURE 5.—*Hypothetical cross section along traverse, abc, of Figure 2*

Arrows indicate water currents during an eruption of Turban. Caverns after Allen and Day (1935, p. 217).

tions change greatly during an eruption of Grand; (2) Grand's rate of discharge and surface level appear to be considerably affected by eruptions of Turban; and (3) no hydrostatic difference in level between the surfaces of the two pools can be demonstrated; but that (4) a hydrostatic sympathy between the two is evident since Turban's pool drains following its eruptions only when Grand's water level is deep in its tube. These points indicate the existence of a rather direct subterranean connection (Fig. 5). The fall in the surface level of Grand's pool when Turban erupts but Grand

does not may be considered caused by the water in Turban rushing past junction A to create a Bernoulli effect, which causes a withdrawal of water from the passage AB; thereby a lowering of Grand's surface results just as soon as the water in Turban's tube possesses an upward motion, and Grand's surface would lower, as it actually does, well before discharge water from Turban enters Grand's pool. That the tube AB is relatively unobstructed appears to be indicated by the prompt response of Grand's level to an incipient eruption of Turban. During an eruption of Turban much of the water it discharges into Grand must be returned to it by means of this underground passage, thus it travels in the cycle TGBAT. During one eruption Turban discharged 0.7 cubic foot per second into Grand for fully 15 minutes, yet Grand's water level remained constant at 4 feet below its orifice. After the eruption the surface of Grand raised these 4 feet in less than 30 seconds merely in response to the remaining water which flowed into it from the terminated eruption. That the water discharged from Turban became cooler and cooler as the eruption progressed further suggests the existence of this TGBAT cycle. Senior Ranger Naturalist George Marler (personal communication) cites 300 eruptions of Grand which were in every instance synchronized with one of Turban's. This evidence appears to assure an underground connection between the two geysers.

Acceptance of this connection brings up a new problem. Grand erupts only twice a day; Turban, about 4 times per hour. How can such a difference in interval exist if the two are connected? Possible answers to this question are: (1) Grand discharges between eruptions—Turban only discharges during its eruptions; (2) Turban may have a more direct connection with the source of heat; (3) Grand's system contains more water than that of Turban and thereby takes longer to heat; (4) Grand's upper stratum of water is periodically cooled by discharge from Turban whereas Turban draws off relatively hot water from Grand by the underground connection. A combination of any or all of these four factors may be responsible for the marked difference in period between the two geysers.

REGULAR INCREASE VS. FLUCTUATION OF TEMPERATURE

Discussion.—Contrary to Bunsen's idea, the temperatures at all points in a geyser column do not steadily increase until the eruption is effected. In numerous geysers the temperature was found to fluctuate greatly at all depths in the accessible geyser tube. In fact temperature curves plotted against time for Jewel Geyser indicate a pattern antithetic to any which would uphold Bunsen's theory since the temperature in Jewel dropped just prior to eruption rather than climaxing a steady rise. Thus during the quiet period temperatures higher than those which coincided with the beginning of the eruption were attained (Fig. 6).

Jewel Geyser.—This geyser is a small one located 150 feet from Sapphire Pool in the Biscuit Basin. During various observations Jewel's period varied from 5 to almost 10 minutes; intervals between eruptions, from 4½ to 7 minutes; duration of eruption, from 15 seconds to 4 minutes. A typical eruption is immediately preceded by an upwelling of the water and a discharge from its pool. After eruption, the small portion of the discharged water trapped in connected surface pools runs back into the orifice.

At none of the depths investigated (Fig. 6) does the temperature of the water ever attain the boiling point for that depth. An exception occurred at the 3.1 meter depth where a temperature of 103.5°C, corresponding to 2°C above boiling for that

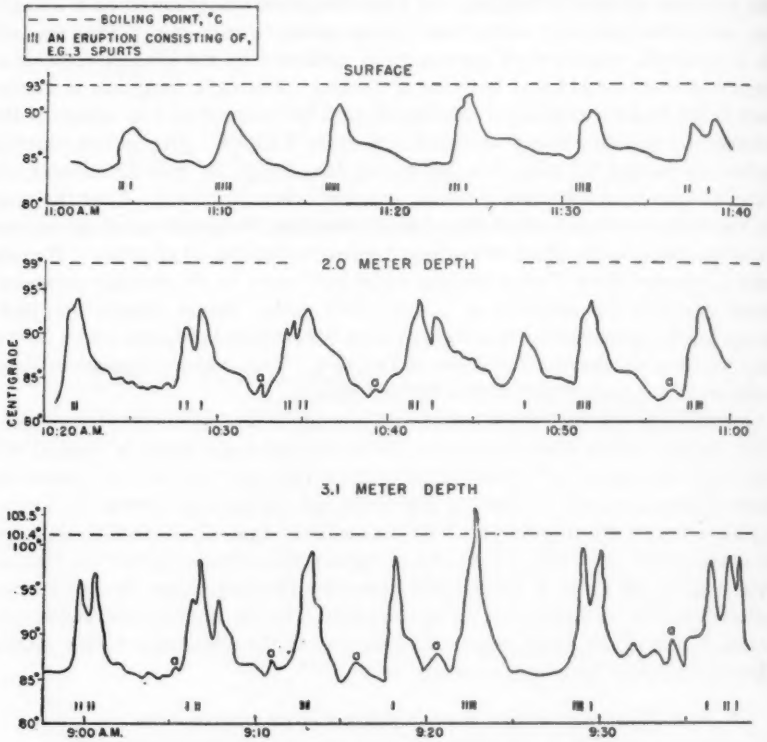

FIGURE 6.—*Time-temperature curves for several depths of Jewel Geyser*

The eruptions, divisible into distinct spurts usually of 10-seconds duration, are indicated below curve. Secondary temperature maxima which often precede an eruption are marked *a*.

depth, was recorded. It should be stated that the peak temperature was attained and succeeded by lower ones in 5 seconds or less, possibly too quickly to be recorded by the Wheatstone-bridge balancing method used. It is believed, however, that the peak temperatures recorded are no more than 1°C below the acutal peak temperatures existent; the consistency of the peak temperature readings appears to bear this out. Thus the temperature peaks were 93° and 98.3° for the 2.0- and 3.1-meter depths respectively. The water at the 2.0-meter depth does not attain the same high temperatures as at the 3.1-meter depth due, it is believed, to the growing importance of the admixture of surface-cooled water with increased proximity to the surface.

A similar effect, increased accessibility of surface-cooled water to the position of the thermometer, is believed responsible for the bimodal and trimodal temperature-

time curves delineated during eruptions of Jewel. These may occur when sufficient time elapses between the spurts of an eruption so that air-cooled water drains back into the orifice and causes appreciable cooling in the accessible portions of the tube. During the intervals between eruptions the water at the 2-meter depth became cooler than that at the surface. Temperature-depth profiles of numerous geysers indicate that this is the normal situation, namely, that water of a greater temperature than that a meter or two below, floats on top in the basin of the pool. Figure 6 also indicates that, contrary to Bunsen's theory, factors besides steadily increasing temperature may be instrumental in geyser action; in fact decreases in temperature often preceded eruptions.

POSSIBLE CAUSES OF TERMINATION OF ERUPTIONS

Discussion.—A rapid influx of relatively cool water has been postulated as instrumental in terminating a geyser eruption. Spasm Geyser may be illustrative of this phenomenon. Grotto and Castle geysers, however, indicate that their eruptions terminate without a rapid influx of cool water. The absence of this influx is indicated by the long steam periods which follow their eruptions. In the small unnamed geyser near Anemone Geyser, the steam phase often occurred after the re-entrance of its discharged water into its tube. In these cases the steaming was sporadic, yet it indicates that short periods of steaming are not necessarily incompatible with an influx of relatively cooler water. Still considering this unnamed geyser, the rapid temperature drop, possibly indicative of an influx of cool water, always occurred well after the eruption was terminated. Alternative interpretations of this temperature drop are given in the appropriate section below.

Spasm Geyser.—Spasm Geyser, in the Lower Geyser Basin, showed a remarkable cooling (Fig. 7); in the last 25 seconds of its eruption the temperature dropped about 7.5°C at the 2-meter depth. This rapid cooling indicates that an influx of comparatively cool water may, as in the hypothesis of Lang, terminate Spasm's eruption. The authors believe that a rapid influx of comparatively cooler water is not a necessity to the termination of an eruption although, as in the case of Spasm, such a mechanism may exist. A cavern, less directly connected to the source of heat and thus possessed of cooler water of a greater meteoric percentage than the rest of the geyser's tubes and reservoirs, would be drained of its waters by the geyser tube once the energy of the eruption had been spent and the tube had been emptied of water to below the point of its junction with this cavern.

The two leveling-off points visible in Figure 7 at the 100.2° and 99.2° temperatures may indicate the discharge of water from small caverns during the eruption. Aside from these two plateaus, the general trend is a steady decrease in temperature following the peak temperature which occurred early in the eruption. Yet, if a geyser system consisted of a single tube, we should expect the water to become hotter and hotter as the water from the deeper and hotter depths was expelled.

Grotto and Castle geysers.—Grotto and Castle geysers in the Upper Geyser Basin possess steam periods lasting up to 2 hours after the termination of the eruption; in them, water sources of varying heat content may exist. The comparatively cooler

water probably seeps into the system at a slightly accelerated rate following an eruption, but the mass influx per unit time is not at first sufficient to cap the steam. Thus this water is probably heated by the steam condensing upon it to the boiling temperature of 93°C. It thus boils to mingle its steam with the superheated steam

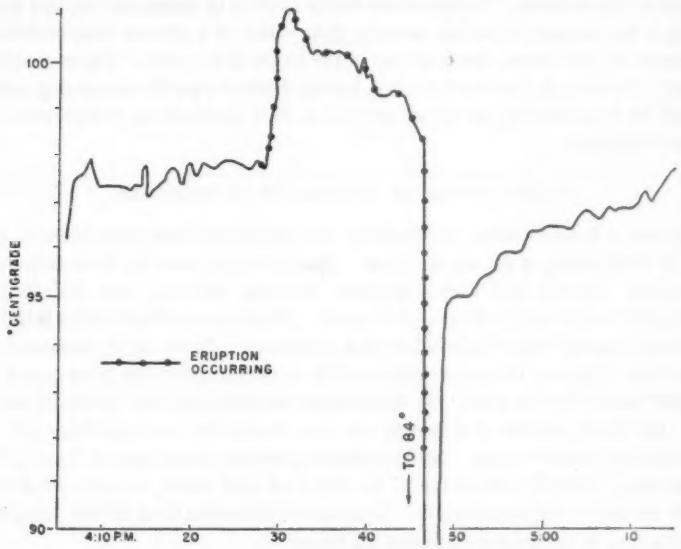

FIGURE 7.—*Time-temperature curve at 2-meter depth in Spasm Geyser August 11, 1947.*

from greater depths; both varieties billow forth from the orifice during the steam period. The cooler water seeping in gradually cools the walls of the geyser system. In addition, the boiling at great depths, while supplying the superheated steam, also causes a cooling. Heat entering the system is thus gradually diminishing while the cooler water continues to seep in at a fairly constant rate. Finally a point is reached when the calories supplied are not sufficient to heat the in-seeping water to boiling. Thus water will collect in the cooler locales and at length cap the steam to terminate the steam period.

Small unnamed geyser.—A small unnamed geyser located close to the tourist walk about 80 feet west of Anemone Geyser was noted to erupt to heights of 15 feet every 50–60 minutes. The duration of the eruptions varied from 4 to 5 minutes. Since the geyser is located on a westward-dipping sinter slope, an appreciable fraction of its erupted water was re-collected and channeled into the geyser tube during those times when a westerly wind prevailed. Occasionally discharge from Anemone also entered this geyser's orifice. The surface level of the water in the geyser tube was difficult to ascertain since a lip of rock projected over the orifice and confined visual inspection to its upper portions. The thermometer was able to test to a depth of only

8.5 feet. Eruptions are succeeded by a short-lived steam phase, in the early portions of which the steam issues forth in gusts as though alternately under greater pressures.

The temperature-time curves, compiled 6 days apart, agree very closely (Fig. 8). It is interesting to note that the peak temperatures, attained during eruptions, were much the same for each day. The average peak temperature of August 5, 1947, is about 2°C lower than that of August 11, 1947. The peak temperature was attained early in the eruption, the remainder and major part of the eruption being accompanied by a more or less steadily decreasing temperature. This cooling effect accompanying eruptions is possibly caused by the boiling and consequent loss of heat that occurs during the eruption. The leveling off of the temperature following the eruption appears to occur shortly after the discharged water begins to re-enter the orifice. The steam phase often continued after the entrance of the discharged water, sometimes sporadically. If steaming occurred during a leveling off of temperature, a slight rise in the temperature often occurred.

The rapid drop in temperature that usually followed its leveling off might be due in part to the influx of air-cooled discharge water and in part to a lowering of the surface level of the water so that the cooler liquid of shallower depths was lowered into contact with the thermometer. The minimum was rapidly attained and then, just as rapidly, the temperature rose once more. An alternative but related explanation might be that the water surface was lower than the thermometer so that it was not immersed for a few minutes before and after the attainment of the minimum temperature; the lower temperatures indicated at the right side of the minimum curve (Fig. 8) as compared with those which existed immediately to its left may be due to the fact that the water did not rise to its former level and thus the upper and cooler water was in contact with the thermometer. A future study of this geyser with a device to determine the depth to the water surface while measuring the temperatures is contemplated.

The leveling off of the temperature following eruption is difficult to interpret. It might represent just a period during which there were no upward or downward movements of the water in the tube so that water of the same temperature remained in contact with the thermometer.

TEMPERATURE-DEPTH CURVES

CRITICISM OF USUAL METHODS OF COMPILATION

These are curves secured by plotting the temperatures in a geyser versus the depths at which they were encountered. Most of the existing temperature-depth data were secured by the agency of a maximum thermometer which was lowered to one depth, pulled up and read, then lowered again to a new depth. Time necessarily elapsed between the taking of readings at two different depths. The variation with time of the temperature at a constant depth is shown by the time–temperature curve for Comet Geyser (Fig. 9). These variations, probably caused by convection currents, amounted to as much as a 1°C change within 20–30 seconds. Thus a temperature-depth profile may, to within 1° or 2°, represent a fortuitous combination of temperatures. A further disadvantage of the maximum thermometer is that a stratum of

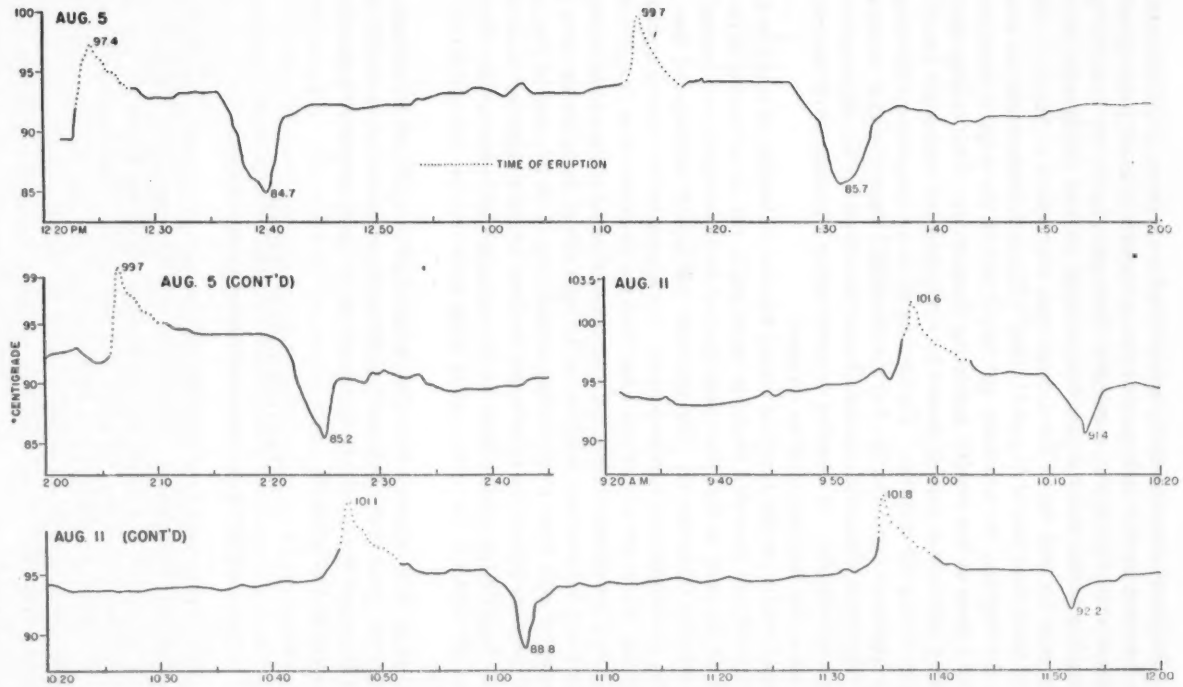

FIGURE 8.—*Time-temperature curves at approximately the 2.5 meter depth in geyser 80 feet west of Anemone* (Near tourist walk), August 5 and 11, 1947.

high temperature water at relatively shallow depths effectively prevents the thermometer from recording any cooler temperatures in the water below this zone. Thus a maximum thermometer is poorly suited for temperature-depth work.

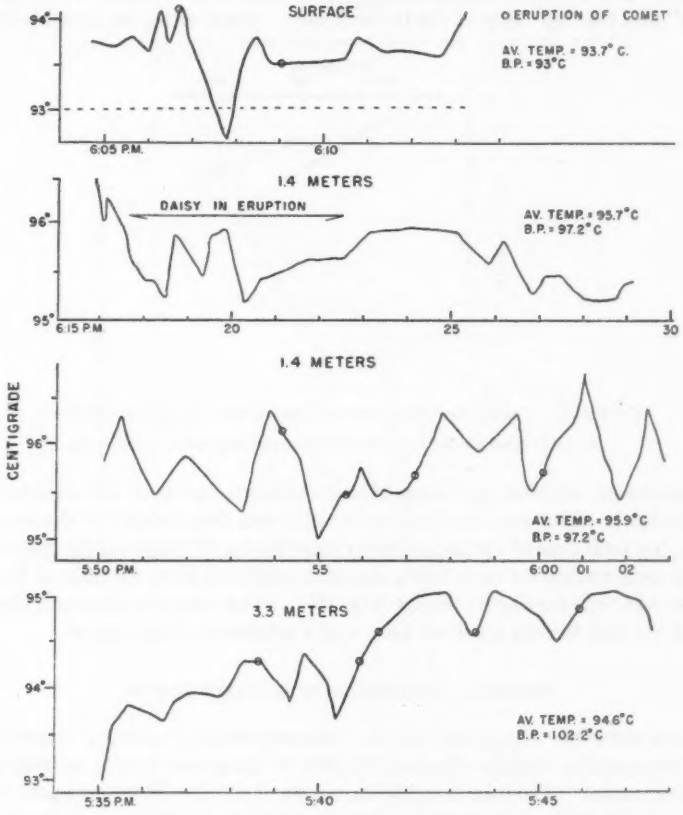

FIGURE 9.—*Time-temperature curves for Comet Geyser*

Vertical scale exaggerated to better show minor temperature variations.

IMPROVED METHODS OF COMPILATION

Possession of several remote-reading thermometers giving readings simultaneously at different depths is, of course, the ideal way to obtain temperature-depth data. Possessed of only one such thermometer, the authors were freed of just one of the disadvantages of the maximum thermometer. The time lapse between readings at different depths was still to be considered. To cope with this problem, readings were progressively made from the shallower to the deeper depths and, as the thermometer was pulled up, readings were again taken at these same depths, this time in reverse order. The average of the "down" and the "up" temperatures for each depth

was then used as the temperature of the respective depth being considered. Actually, instead of a momentary stop at each depth, the resistance thermometer was kept at each depth for approximately 10 minutes, both going down and coming up. Then for each depth examined a temperature versus time graph was plotted for both the "down" and the "up" stop of the thermometer. Then, either by visual estimation

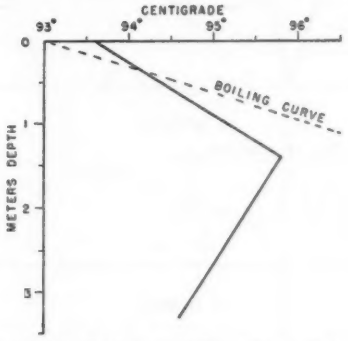

FIGURE 10.—*Temperature-depth curve of Comet Geyser derived from Figure 9*
By applying the area method to secure the average temperature for each depth.

or a planimeter, the total area below these two time-temperature curves was secured for that depth. This area (in time-degree units) was then divided by the area representing the total time of the thermometer stop times a 1° height on the graph. The average temperature for each depth was thus computed from the ratio of these two areas as was done for Comet Geyser (Fig. 10). Other temperature-depth data were secured through the less sensitive agency of a maximum thermometer.

PRINCIPLES ILLUSTRATED BY OBSERVED CURVES

General statement.—Granting that the temperature-depth curve is correctly compiled, the question remains whether this part of the geyser tube is instrumental in the geyser action. The tube bringing the hot water vital to the geyser's activity may be inaccessible to the thermometer. The temperature-depth curve of the accessible portion, on the other hand, may have little significance with respect to the geyser mechanism because of a remote connection with the mechanism of action. Actual temperature-depth curves may therefore cast little light on the geyser mechanism except where they illustrate principles of importance in testing the theories.

Role of convection currents.—Chinaman Spring in the Upper Geyser Basin constantly discharges at an estimated rate of 0.08 liter per second. At times a change of 2°C in the temperature of the geyser (Fig. 11) was encountered when the depth of immersion was increased from 1.38 to 1.6 meters. Plumbing with the thermometer revealed that, at approximately the 1.38-meter depth, either a constriction exists or else the tube itself narrows from about .61 meter to approximately .15 meter in diameter. In either case convectional cooling between the surface and water above the

1.38-meter depth is important whereas its role below the 1.38-meter depth becomes minimal. Thus Figure 11 illustrates the efficacy of constrictions or narrow diameter tubes in reducing circulation and the consequent effect on the temperature gradient.

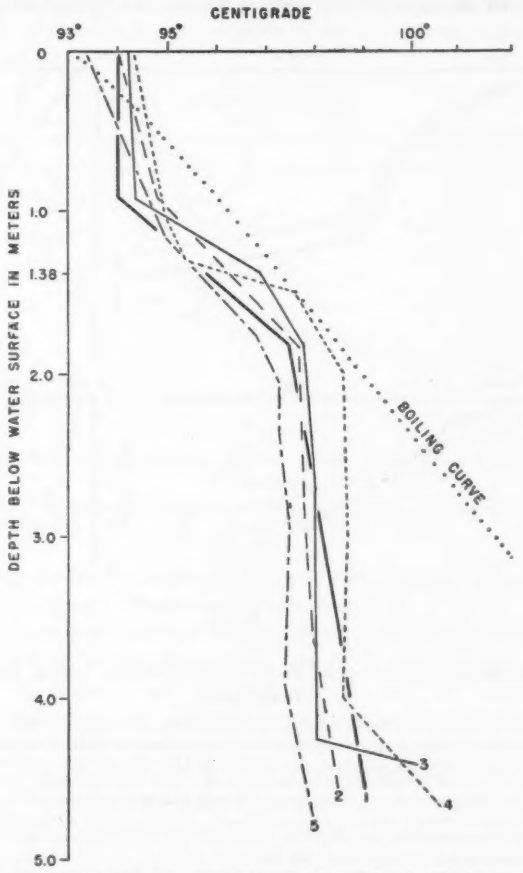

FIGURE 11.—*Temperature-depth curve for Chinaman Spring*

A constriction at the 1.38-meter depth inhibits convectional cooling below this depth. (1), (2), (3) from maximum thermometer data, July 29, 1947. (4) from average temperatures for 15-minute periods at each depth on August 5, 1947. (5) from Allen and Day (1935, p. 194) data of August 4, 1927.

In Big Cub, a dormant member of the Lion group, heat losses through convection are probably at a minimum since its water surface is located within its tube, usually 3 or 4 feet below its rather constricted orifice, and is thus partly insulated from air currents by the pocket of heated water vapor trapped above it by the narrowness of the orifice. Possibly as a result, Big Cub's temperature-depth curve adheres closely to the boiling curve until its lowest 2 meters of depth (Fig. 12C), in spite of the fact that it is dormant.

Attainment of boiling conditions at depth.—The close approximation of Big Cub's temperature-depth curve to the boiling curve was unusual. In most geysers and hot springs the existing temperatures tended to increase less rapidly than did those of the boiling curve with increased depth, perhaps because the thermometer was limited to

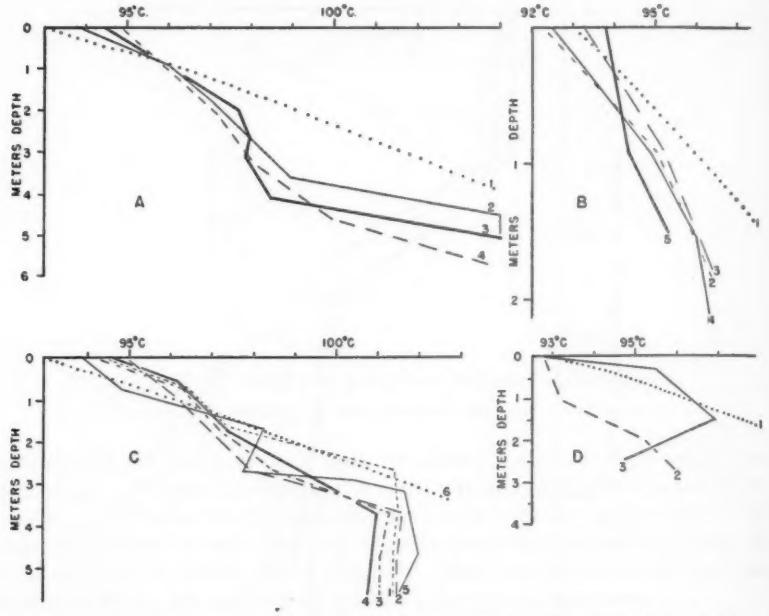

FIGURE 12.—*Temperature-depth curves for Beehive Geyser, Limekiln Spring, Big Cub, Catfish, and Mastiff Geysers*

A.—Temperature-depth curves for Beehive Geyser, (1) Boiling curve. (2), (3), (4), Temperature-depth curves for July 30, August 7 and 8, 1447, respectively. (2) From average temperatures for 10 minute periods at each depth

B.—Temperature-depth curves by maximum thermometer for Limekiln Spring, a constantly boiling hot spring. (1) Boiling curve. (2), (3), and (4) are temperature-depth curves. (5) Is that for a small, constantly boiling and discharging spring on the opposite side of the Grand Loop road from Spanker Geyser, July 29, 1947.

C.—Temperature-depth curves for Big Cub, a dormant geyser. (1), (2), (3), and (4) compiled from spot temperatures secured by resistance thermometer on August 6, 1947. (5) From the average temperatures existent during 5-minute periods at each depth on August 7, 1947. (6) Boiling curve.

D.—Temperature-depth curves for Catfish and Mastiff Geysers. (1) Boiling curve. (2), (3) Temperature depth curves for Catfish and Mastiff Geysers, respectively, derived from average of temperatures existent during 15-minute periods at each depth on August 4, 1947.

the upper portions of the tube where convectional cooling was important. As a general rule, boiling conditions were seldom encountered below a 1-meter depth.

Chinaman Spring, possibly because of the constriction limiting convection, was unique in that, in one instance (Fig. 11), boiling conditions were attained at the 1.4-meter depth. Although it discharged continuously and the conditions were just what Bunsen's theory presupposed, it did not erupt. In fact, it is known to erupt only when stimulated by addition of soap or, according to one instance described by District Ranger Scotty Bauman (personal communication), by vigorous stirring.

Beehive Geyser, which erupts just a few times a season, was not observed to erupt during July and August of 1947. Its curve was unusual in that below 3.5 meters it began to approach more closely with depth the boiling curve temperatures (Fig. 12A). An unnamed geyser 40 feet SE of Beach Spring was also exceptional in this respect; in this case, however, convergence of the two curves began below the 1.5 meter mark (Fig. 13).

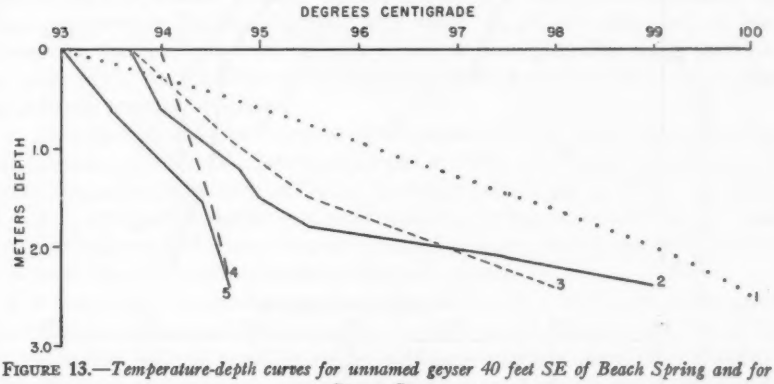

FIGURE 13.—*Temperature-depth curves for unnamed geyser 40 feet SE of Beach Spring and for Sponge Geyser*

(1) Boiling curve. (2), (3) Temperature-depth curves from maximum thermometer readings. (4), (5) similar curves for Sponge Geyser, July 25, 1947.

The constantly discharging springs, Scalloped and Limekiln springs, the dormant geyser of the Lion group, Lioness Geyser, the constantly erupting Sponge Geyser, and the almost constantly erupting Catfish Geyser possess temperatures along their water columns which become increasingly less than those required for boiling as greater depths are probed (Figs. 14B, 12B, 14A, 13, and 12D, respectively). The curve for Mastiff Geyser (Fig. 12D) indicates the possibility of an inlet of heated water at the 1.5 meter depth in its tube. In these springs and geysers the possibility is always present that increased penetration by the thermometer might have reached depths in which the boiling and temperature depth curves began to converge.

Superheated waters.—The majority of the temperature-depth curves indicate that a layer of superheated water is often located at the surface of a geyser or hot spring. This layer is usually less than a meter deep and its quiescence in the face of its metastable condition is difficult to explain.

CONCLUSIONS

1. Spring gases are present in Sawmill and Tardy geysers; careful observations might also indicate their presence in other geysers in that area. It is undetermined, however, whether they are present in amounts sufficient to cause a significant lowering of the temperature of bubble formation below that of boiling for pure water as is postulated in Thorkelsson's theory. The activity of Crater Hills Geyser appears attributable to the presence of abundant spring gases.

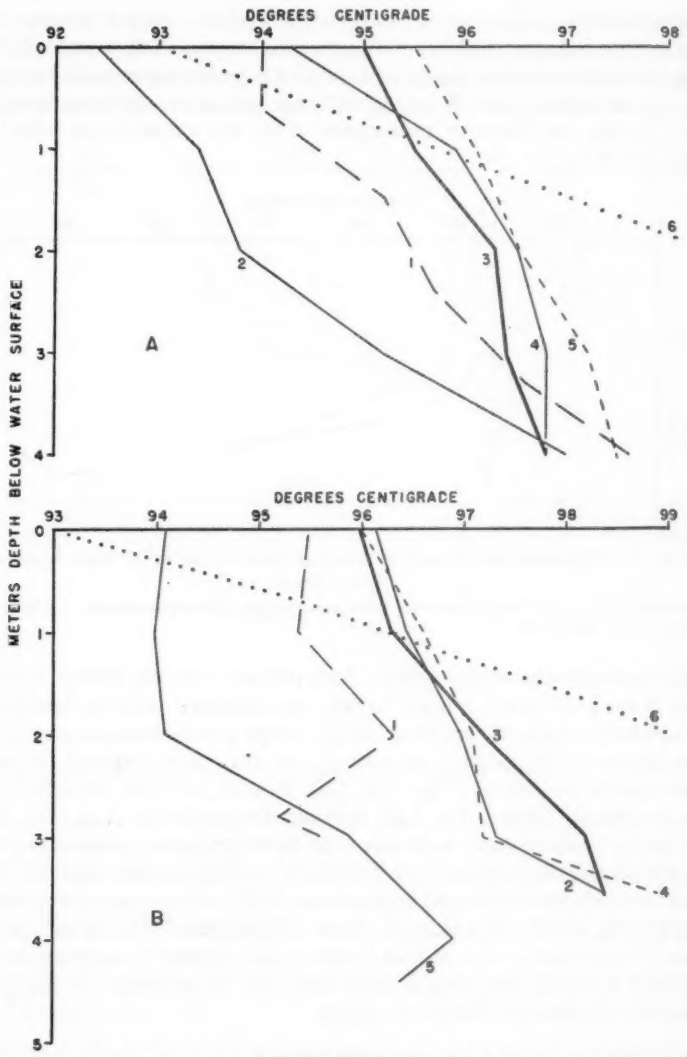

FIGURE 14.—*Temperature-depth curves of Lioness Geyser, of Scalloped Spring, and of its neighboring spring 50 feet south*

A.—Lioness, a dormant geyser. (1) From maximum thermometer data. (2), (3), (4), (5) From spot readings of resistance thermometer. (6) Boiling curve, August 6, 1947.

B.—(1) Temperature-depth curve for Scalloped Spring from average of temperatures during 15-minute immersion at each depth. (2), (3), (4) From spot readings of resistance thermometer. (5) Spot readings in spring 50 feet south of Scalloped Spring. (6) Boiling curve, August 5, 1947.

2. Subterranean connections between geysers are probably quite common; the rarities are probably those connections which are large enough and close enough to

the surface to ostensibly influence the actions of the interconnected geysers. Such a connection probably exists between Sawmill and Tardy. A more direct connection between Grand and Turban geysers certainly exists; its presence creates an interesting Bernoulli effect whereby eruptions of Turban cause water to be withdrawn from Grand's column and, if Grand's water is hot enough, initiates an eruption of Grand.

3. A regular increase of temperature along all depths in the water column, the cardinal point in Bunsen's theory, was seldom found in the geysers examined. Instead temperatures fluctuated greatly with time. In the accessible well of Jewel Geyser the temperatures were actually found to drop preceding some eruptions; in other words, during quiescence higher temperatures occurred than those which immediately preceded eruptions.

4. Since the time of Lang, the cause of termination of an eruption has usually been attributed to an influx of relatively cool water. This may indeed be the case for Spasm Geyser but is probably not so for Grotto and Castle geysers since an eruption of each is always followed by periods of steaming up to two hours long. A small geyser 80 feet west of Anemone Geyser indicated, however, that steaming could occur even after relatively cool water had entered the system.

5. In compiling temperature-depth curves, the use of a maximum thermometer gravely limits the accuracy of the profile. A defect of all thermometers (in varying degrees) is that their dimensions may confine the readings to those parts of the geyser tube which are probably only remotely, if at all, connected with the mechanism by which the geyser operates. The use of several remote-reading thermometers to simultaneously read temperatures at different depths is highly recommended. If only one such thermometer is available, a method of getting significant temperature depth curves for accessible portions of the tube was suggested in the section entitled "Improved methods of compilation" (of temperature-depth curves).

6. A comparison of temperature-depth curves for several geysers indicated that convection currents in geysers are important cooling devices. Where convection was inhibited, as in the lower portion of Chinaman Spring or along the entire length of Big Cub Geyser, the temperature-depth curve was noted to most closely approach the boiling curve for the various depths. Aside from these two instances in a non-erupting hot spring and a dormant geyser, boiling conditions were rarely encountered in the depths of any other geysers.

7. A layer of superheated water seldom extending down to the 1-meter depth commonly occurred at the surface of many of the geysers and springs. No satisfactory explanation was found for its persistence in the face of its metastable condition.

8. Although boiling conditions were rarely demonstrated in the depths of the geysers examined by the writers, the observations of others, particularly those by Fenner (1936), indicate that in the Yellowstone geyser areas, generally speaking, the temperature increase with depth in many places would almost follow the increase of the boiling point, suggesting that here an additional supply of thermal energy would be able to transform the geysers into steam vents. In Iceland, according to measurements by Barth (1949), the boiling point is approached only at the upper-most levels; whereas the deeper parts of the geyser areas exhibit temperatures far below the boiling point. Additional thermal energy in this case might stimulate geyser action.

This means either that the volcanic heat fed into the geyser basins in Iceland is relatively small or that the total volume of ground water underlying the geyser systems is relatively much larger in Iceland than in Yellowstone Park. Whatever the reason, such differences in the temperature relations may explain the fact pointed out by Barth (1947) that, in Iceland, less than 1 per cent of the hot springs show geyser action, whereas in the Yellowstone National Park about 10 per cent of all hot springs are geysers.

REFERENCES CITED

Allen, E. T., and Day, A. L. (1935) *Hot springs of the Yellowstone National Park*, Carnegie Inst. Washington, Pub. 466, p. 164–267.

Barth, Tom. F. W. (1947) *Geysers of Iceland*, Am. Geophys. Union, Tr., vol. 28, no. 6, p. 882–886.

Bunsen, R. (1847) *Physikalische Beobachtungen über die hauptsachlichsten Geisir Islands*, Annalen der Physik und Chemie, Bd LXXII. J. D. Poggendorf, Leipzig.

Fenner, C. N. (1936) *Bore-hole investigations in Yellowstone Park*, Jour. Geol. vol. 44, p. 225–315.

Thorkelsson, Thorkell (1940) *On thermal activity in Iceland and geyser action*, Isafoldarprentsmidja, Reykjavik, 139 p.

von Nidda, Krug (1837) *On the mineral springs of Iceland*, Edinburgh New Philos. Jour., vol. 22, p. 99–100.

University of Chicago, Chicago, Ill.; Mineralogisk Museum, Oslo 45, Norway.
Manuscript Received by the Secretary of the Society, June 23, 1948.
Project Grant 512/47.

BULLETIN OF THE GEOLOGICAL SOCIETY OF AMERICA
VOL 60, PP. 887-908 MAY 1949

STRATIGRAPHY AND ORIGIN OF BAUXITE DEPOSITS

BY E. C. HARDER

CONTENTS

	Page
Abstract	887
Stratigraphy	888
General statement	888
Paleozoic bauxite and high-alumina clay	888
Bauxite of the Mesozoic	889
Eocene bauxite horizons	891
Late Tertiary and Pleistocene bauxites	893
Origin	897
Mechanical and chemical sedimentation	897
Weathering *in situ*	899
Conclusions	904
References cited	905

ABSTRACT

Known bauxite deposits range in geologic age from Devonian to Recent. Those of principal commercial importance, however, are of Medial Cretaceous (Albian), Late Cretaceous (Senonian), Early Eocene, Miocene, Pleistocene, and Recent age. Bauxite deposits of the Albian occur in the Var district in southeastern France. Bauxite of the Senonian is found in the Herault district in southern France and in the south of Greece. Deposits of Early Eocene age occur in Hungary, Yugoslavia, and the United States. Miocene bauxite is found in Jamaica. Deposits of latest Tertiary, Pleistocene, and Recent age include the important tropical bauxites of the Guianas and Brazil in South America, those of French Guinea and Gold Coast in Africa, and those of India, Malaya, and Netherlands Indies in Asia and Australasia. The low-grade bauxite of Russia is Devonian and Carboniferous; that of China mostly Carboniferous and Permian. Bauxite deposits are significant stratigraphically because they mark long periods of emergence, quiescence, nondeposition, and subaerial weathering.

Bauxite and laterite may result from the weathering of any one of many types of rocks or their weathered derivatives. However, rocks of originally high or moderately high alumina content and with a relatively large percentage of soluble constituents lend themselves more readily to lateritization and bauxite formation. Important bauxite deposits are known to occur on limestone, such as those in central Europe and the Mediterranean region; on diorite, syenite, granite, and metamorphosed volcanics and sediments, as those in the Guianas, Malaya, and Netherlands Indies; on nepheline syenite and phonolite, as in Arkansas, U. S. A., Pocos de Caldas, Brazil and the Los Islands, French Guinea; on arkose, slate, and phyllite, as on the French Guinea mainland and in Gold Coast; on basalt, as in central India; and on sedimentary clays, as in southern Georgia and Alabama, U. S. A. Besides rock types, the composition of ground water, topographic relief, and climatic conditions such as temperature and rainfall, influence lateritization and bauxite formation to an important extent.

STRATIGRAPHY

GENERAL STATEMENT

The importance of bauxite and laterite deposits as geological horizon markers is perhaps not sufficiently appreciated by geologists. Bauxite or laterite represents nondepositional intervals. Some deposits may mark entire geologic eras, although probably the bauxite has formed during only a part of such a long interval and perhaps only late in the interval following profound erosion. Others occupy intervals measured in geologic periods or epochs. Still others represent only parts of a single epoch. The size or extent of a bauxite bed generally bears no relation to the length of the erosional on nondepositional interval it occupies; thick beds may represent relatively short geologic time breaks, and thin, discontinuous deposits may occupy long erosion intervals. This, of course, may be because suitable conditions for lateritization were not present, or were present only during small portions of the interval, or because the laterite or bauxite deposits formed may have been partially or entirely removed by subsequent erosion. Where important lateritization results are in evidence, it may be assumed the laterite originated late in the erosion interval that may be indicated. Thus, the Guiana bauxite deposits were probably formed in late Tertiary or Pleistocene time, even though they lie on a pre-Cambrian floor and represent the alteration of pre-Cambrian materials; Hungarian bauxite is very likely of Eocene age although it is underlain by Upper Triassic rocks.

PALEOZOIC BAUXITE AND HIGH-ALUMINA CLAY

The oldest known bauxite deposits are those of the northern and central Urals, north and northwest of Sverdlovsk, and those of the Tikhvin district near Leningrad (Moldavantsev, 1934; Gladkovsky, 1942; Karjavin, 1942; Nalivkin, 1942; Denisevich, 1942). The deposits of the northern Urals, mostly diasporic, were probably formed in Early Devonian time since they lie on Upper Silurian limestone and are overlain by Middle Devonian argillaceous shales. Those of the central Urals, on the other hand, occur at several stratigraphic horizons in the Middle Devonian, and some are found in the Lower Carboniferous. The Tikhvin deposits, the first to be exploited in the Soviet Union, lie on Upper Devonian micaceous sand and clay and are overlain by Lower Carboniferous sandstone, sand, and clay. Most of the Russian deposits consist of siliceous and ferruginous laterite and lateritic clay, but some contain workable pockets and lenses of bauxite.

The extensive high-alumina, diasporic, and boehmitic clay strata of Kweichow, Szechuan, and Yunnan provinces in southwestern China and the diasporic clays of the Poshan district of Shantung province in eastern China (Wang, 1932; Hsieh, 1935; Li and Hsieh, 1946) are also of Paleozoic age. The Kweichow diaspore deposits form a fairly persistent bed, averaging 8 meters thick, lying on Ordovician dolomitic limestone and overlain by Lower Carboniferous coal-bearing beds which in turn are overlain by Permian limestone. The Yunnan boehmite-bearing strata lie between the Devonian and Lower Carboniferous. The Szechuan high-alumina clays lie on the Loping coal series of Medial Permian age and are overlain by Yanghsin limestone, while the Poshan diasporic clays occur between Permo-Carboniferous rocks and the overlying Triassic, and may be of Early Mesozoic age.

Next in age after the Russian deposits and in an intermediate position between the earlier and later Chinese bauxite-bearing strata are the diaspore deposits of Clearfield County, western Pennsylvania, and those in east-central Missouri, both occurring in Pennsylvanian rocks. Both are associated with much more important deposits of flint clays and burly or nodule clays. The Clearfield County clay deposits (Foose, 1944) are in the Mercer beds of the Pottsville series (lowest Pennsylvanian). A bed of soft, plastic clay 5–25 feet thick occurs just below the Mercer coal bed on the eroded surface of the Connoquenessing sandstone or shale, the latter formation being at the base of the Pottsville series and unconformably above the Mississippian. The flint clays are found as lenses of varying thickness and irregular occurrence in the middle part of the Mercer plastic clays, and the nodule clays and associated diaspore occur in the central portions of the flint clay lenses. The nodule-bearing clay horizon is a very useful datum in the Pottsville series.

In Missouri, diasporic clay with associated diaspore (McQueen and Forbes, 1928; McQueen, 1943) forms irregular masses in pockets of flint clay enclosed in Cherokee (Pennsylvanian) sandstone. The sandstone, with included clay pockets, occurs in sinkhole-like depressions in the surface of the Jefferson City and Gasconde dolomites of Ordovician age. The flint clay pockets are numerous and average 75–100 feet in diameter and 50 feet in depth. Not all of them have associated diaspore and diasporic clay.

BAUXITE OF THE MESOZOIC

The oldest bauxite in the Mesozoic, except possibly that of Shantung, China, is the high-silica, ferruginous bauxite of the Velebit mountain region in Croatia which is in Upper Triassic rocks. It occurs as lenses in the Raibler limy, ferruginous sandstones which are overlain by Hauptdolomit (Upper Triassic) and underlain by the Wengener beds, also Upper Triassic, or by the Muschelkalk of the Middle Triassic. The nondepositional interval it represents is, therefore, relatively short.

Bauxite deposits of the Bihar Mountains in western Rumania are probably Early Cretaceous. They are hard, dense, and high in iron and occur as irregular sheets and lenses on the uneven surface of the Malm (Upper Jurassic) limestone. A thin bed of dark Lower Cretaceous limestone immediately overlies the bauxite and underlies later limestones or eruptive rocks. Locally, the dark limestone is absent.

Relatively unimportant bauxite deposits of the Department of Ariege in the northern part of the Pyrenees, France, are of approximately the same age as those of the Bihar Mountains. These deposits occur as beds and lenses along the contact of Jurassic dolomite and overlying limestones of the Urgonian or Aptian (Lower Cretaceous).

One of the world's most important bauxite zones is that at the base of the Middle Cretaceous, along which are found the extensive deposits of dark-red, ferruginous, boehmitic or monohydrate bauxites of southeastern France, central Italy, western Montenegro, Greece, and perhaps also those of western Hungary (De Lapparent, 1930; Harder, 1930).

The deposits of southeastern France extend discontinuously from the Department of Herault eastward through the Departments of Bouches du Rhone and Var to within 50 or 60 miles of the Italian border. Wherever their geologic relation is

evident, the deposits consist of beds or lenses usually lying on the eroded surface of Lower Cretaceous or Jurassic limestones (Pavlovski, 1925). In many places they lie on Urgonian (Lower Cretaceous) limestones, elsewhere on Neocomian rocks, and in still other places on rocks of the Malm (Upper Jurassic) or Lias (Lower Jurassic). The deposits are probably all older than Cenomanian (Middle Cretaceous), although Cenomanian limestones do not always form the capping rock, which may be Senonian or Danian (Upper Cretaceous) or even Eocene. Therefore, the bauxites of southeastern France were probably formed during a nondepositional interval in the Albian (earliest Medial Cretaceous) and are presumably residual products left by the decomposition of Albian, Aptian, and Urgonian limestones, and in some places where weathering was very active of Neocomian and even Jurassic rocks. There is some question, however, whether sediments were deposited in early Albian time or whether lateritization extended throughout the Albian period. Following Albian bauxitization, submersion occurred, and Cenomanian and younger limestones were deposited discordantly over the newly formed bauxite. That Cenomanian rocks are not universally present as capping rocks of the bauxite deposits is probably due in part to nondeposition and in part to removal during erosion periods after Cenomanian time.

Bauxites of the Apennine Mountains in central Italy occur east of Rome and north of Naples. They are in beds and lenses associated with Cenomanian and Turonian limestones.

Bauxite deposits in the region between Kotor and Niksic, western Montenegro, occur as lenses and irregular bodies between Lower Cretaceous and Middle Cretaceous limestones. Many of them are extensive horizontally and protrude downward as pockets into the underlying limestone.

The principal bauxite deposits of Greece are north of the Gulf of Corinth, but important deposits also occur near Athens and on Euboea and Amorgas islands in the Aegean Sea. They consist of layers and lenses underlain by Upper Jurassic limestone with nerinees and overlain by Upper Cretaceous rudistid limestone, occupying the time interval of the middle and early parts of the Cretaceous period. The Greek bauxite, although of the same dark-red, ferruginous type as that found elsewhere along the Mediterranean coast, is more indurated and thus resembles the Rumanian bauxite. The emery of Naxos, Samos and Turkey is believed to be the metamorphosed equivalent of Greek bauxite.

Some of the bauxite deposits of the central and southern Urals are reportedly associated with Cretaceous rocks, including certain better-grade ores of gibbsitic or boehmitic type now used in the Russian aluminum industry.

Hungarian bauxite deposits occur north of Lake Balaton along a northeast-southwest belt that extends almost to Budapest. They were formed between the deposition of the Dachsteinkalk or of the Hauptdolomit, both of the Upper Triassic, and that of the Eocene. They therefore occur in a hiatus that represents a very long period embracing both the Jurassic and Cretaceous, and it is not possible to say whether they are related in age to the French bauxite of the early Medial Cretaceous, or whether they should be referred to the Istrian and Dalmatian bauxitization period of the early Eocene.

EOCENE BAUXITE HORIZONS

Lower Eocene bedded bauxites the next important deposits upward in the time scale, are widespread and varied in physical and chemical characteristics (Harder, 1930). They comprise the bauxites of the Istrian peninsula, Dalmatia, Herzegovina, and southern Montenegro along the Adriatic Coast in Yugoslavia, those of the Barcelona region in northeastern Spain, the Jammu deposits of Kashmir in northwestern India, and the important belt of bedded bauxite deposits in the United States extending from central and southern Georgia through southeastern Alabama and northeastern Mississippi to central Arkansas.

Most of the Istrian bauxites are pocket deposits in solution cavities in the Upper Cretaceous rudistid limestone. Usually they are found at the surface or are covered by only a few meters of soil. In a few places, however, they are under several meters of Eocene beds, generally nummulitic limestone. Their occurrence at or near the surface is in most places due to the removal by erosion of nearly horizontal Eocene rocks leaving the bauxite exposed as lenses on the uneven surface of the underlying rudistid limestone and in solution pockets within it.

The principal bauxite deposits in Dalmatia and Herzegovina occur as lenses, usually underlain by Lower Eocene alveoline limestone and overlain by the "promina beds" of the Upper Eocene, consisting of thin-bedded limestones and limestone breccias. In many places the alveoline limestone is absent, and the bauxite lies on the rudistid limestone, the uppermost Cretaceous of this region. Although commonly the Yugoslavian deposits are interbedded lenses, in many places the upper surface of the underlying limestones has become uneven because of erosion and solution, and bauxite fills pockets, troughs, and other solution cavities in it.

Bauxite of southern Montenegro occurs in the region of Bar and Ulcinj as lenses and irregular bodies along the contact of the Upper Cretaceous rudistid limestone and the overlying Eocene miliolid limestone. There are also pocket deposits in the rudistid limestone.

Bauxite of the Barcelona district occurs as pockets and irregular lenses on the uneven erosion surface of Triassic and Lower Eocene limestones. Cretaceous and Jurassic rocks are absent in the bauxite areas. The deposits are veneered with soil, but no capping rocks are in evidence.

Diaspore deposits of the Jammu district, India (Fox, 1923; Middlemiss, 1928) are found at the base of the Eocene. They are overlain by the Sabathu coal beds (Eocene) and underlain by Jurassic limestone, from which they are generally separated by a layer of siliceous breccia.

In southeastern United States the belt of Eocene bauxite-bearing strata extends from central and southwestern Georgia through southern Alabama and northeastern Mississippi (Shearer, 1917; Morse, 1923; Burchard, 1925; Rettger, 1925; Cooke, 1926; Adams, 1927) to Pulaski and Saline counties, central Arkansas. The bauxite and associated sediments vary so that no single stratum can be readily followed throughout the belt, but the general bauxite zone persists.

In Wilkinson County, Georgia, at the eastern end of the belt, the bauxite deposits occur at the base of the Eocene. They overlie Lower Cretaceous clays and are overlain by Jackson sand and clay (Upper Eocene). To the southwest in Sumter

and Macon counties, Georgia, the bauxite beds occur at or near the top of the Midway (Paleocene), being overlain by the Wilcox (Lower Eocene) clay and sand. In southeastern Alabama, bauxite beds and lenses are associated with the Naheola formation, the uppermost member of the Midway group. The Naheola formation is overlain by Wilcox beds. In northeastern Mississippi the bauxite occurs at the top of the Porters Creek clay of the Midway group and at the base of the immediately overlying Ackerman formation of the Wilcox group.

The bauxites are mostly of the white, gray, or pink, low-iron, trihydrate type and occur usually as moderately thin sheets of considerable horizontal extent underlain and overlain by clay or as groups of pockets or lenses in clay. The contact with the overlying clay is in most places smooth and quite sharp, while that with the underlying clay is irregular and gradational. Frequently the underlying clay is bauxitic, compact or pisolitic. Pocket deposits occur in southwestern Georgia and southeastern Alabama, possibly indicating the former presence of limestones, commonly associated with the Midway clays underlying the bauxite horizon, that may by their solution have formed an uneven surface. Most of the bauxite deposits of Mississippi are of low grade, high in both silica and iron oxide.

In central Arkansas, the bauxite deposits, although of the same age and of a type similar to those in Georgia, Alabama, and Mississippi, present a new feature in that they are for the most part closely associated with large masses of intrusive nepheline syenite that were not covered by the Paleocene sedimentation (Branner, 1897; Hayes, 1901; Mead; 1915; Bramlette, 1936). When the Paleocene sea retreated and the Midway sediments, mostly limestone with an upper blue clay member, emerged, weathering began to attack the nepheline syenite hills, as well as the flat-lying Midway blue clay surrounding them. Because of its solubility and high-alumina content, the nepheline syenite yielded readily to bauxitization, and rich, heavy deposits up to 20 or 30 feet thick developed on the summits and flanks of the nepheline syenite hills and ridges, while relatively thin low-grade deposits formed over the Midway blue clay. A layer of variable thickness of residual clay derived from the nepheline syenite occurs as a gradational zone between the fresh rock and the bauxite. Locally, this zone may be quite thin. A granitic texture generally characterizes the bauxite overlying the syenite and in places persists through the intervening clay zone. The bauxite overlying the Midway clay is pisolitic in many places.

Toward the end of the period of bauxite formation and prior to resubmergence in Wilcox time, portions of the newly formed bauxite layers were broken up and deposited as boulders, pebbles, and sand on the lower slopes of the nepheline syenite hills and on adjacent portions of the surrounding Midway surface; they are the present conglomeratic phases.

Wilcox sediments, first clays and lignites and later sands, were deposited on the old bauxitized land surface. The present Wilcox sediments in the central Arkansas bauxite field range up to several hundred feet thick and exhibit considerable variability. Characteristic lenslike features occur in its clay, sand, and lignite beds, especially in the lower portion.

LATE TERTIARY AND PLEISTOCENE BAUXITES

Bauxite deposits of late Tertiary age, and probably in part of Pleistocene age, occur in many parts of the world. Some of them participate in a major way in the present world bauxite production, while others are of great potential importance. Among them are the deposits of British Guiana and Surinam (Dutch Guiana) in northern South America; those of Jamaica, Haiti, and Santo Domingo in the West Indies; the impure ferruginous bauxite and bauxitic clay strata associated with basaltic rocks in County Antrim in Northern Ireland; the ferruginous clays with bauxite fragments in the Vogelsberg Mountains, Germany; the recently discovered ferruginous, bauxitic laterite in northwestern Oregon; and the bauxite and laterite deposits occurring in various parts of India as alteration products of the post-Cretaceous Deccan basaltic flows.

The bauxite deposits of British Guiana occur within a very long otherwise unrecorded interval embracing most of Paleozoic, Mesozoic, and Cenozoic time (Harder, 1936; Bishopp, 1937; Bracewell, 1947; Hose, Bryn Davies, Grimes-Graeme 1937–1947). They lie on crystalline rocks (or on residual clays derived from them) of pre-Cambrian age, although certain associated intrusives and metamorphosed sediments and volcanics may be younger. The crystalline basement consists of gneisses and schists, both acid and basic, and the intrusive dikes and masses in it are granitic, syenitic, dioritic, and doleritic. Topographically, the basement is formed of low ridges with shallow intervening valleys representing an old land surface, and the bauxite deposits occur as decomposition blankets over the tops and along the flanks of the ridges. They are generally underlain by residual clays, white or varicolored, locally extending to a depth of 100 feet or more.

The bauxite beds range up to 40 feet or more in thickness. The upper part normally consists of a siliceous capping 1–6 feet thick of bauxite pebbles and larger masses in a bauxitic clay matrix, and projections of the latter extend downward into the bauxite. From the lower part of the bauxite bed, pipes and veins of bauxite project downward into the underlying residual clay. High-grade bauxite forms the main central portions of the beds.

Overlying the bauxite, or the residual clay where the bauxite is absent, are unconsolidated sands and clays of the White Sand Series (late Tertiary or possibly early Pleistocene). These sediments range up to 300 feet or more thick in the bauxite district and consist of interbedded plastic clays, sands, and locally lignite in the lower portion with a thick white sand formation dominating the upper portion.

Because of the wide time gap represented by the bauxite horizon, the exact time of bauxite formation is difficult to determine. If the overlying White Sand Series deposited after the submergence of the old land surface is Miocene or Pliocene, then bauxite formation must have ceased in Medial or Late Tertiary time. Perhaps it ceased earlier, since the siliceous capping may represent a considerable period of erosion characterized by deoxidization and silicification, possibly during the gradual lowering of the land surface and accompanied by a prevalence of lagoons, marshes, and swamps.

Bauxite deposits of Surinam are similar to those of British Guiana except that no

overlying sediments of the White Sand Series are in evidence in the principal bauxite districts; doubtless post-Tertiary erosion removed them. The bauxite deposits, therefore, occur at the surface with little or no overburden; many of them rise as hills above the generally low, flat, and often marshy surrounding country.

The bauxite-bearing area of the Guianas is a crescent-shaped belt, one end of which passes under the ocean in northwestern British Guiana while the other end leaves the mainland near the boundary of Surinam and French Guiana. Inside this embayment are the White Sand Series and later sediments; outside are mainly the crystalline, metamorphic, and intrusive rocks of the basement complex.

The highlands of north-central and west-central Jamaica are underlain by extensive yellow and white limestones ranging from Eocene through Oligocene according to foraminiferal evidence, but apparently with no pronounced break in sedimentation until the beginning of the Miocene (Hose, 1942–1946). The surface of these limestones shows the characteristic pinnacle and trough features common in pure limestones of karst topography, and the depressions in many places are occupied by red earth or by dark-red or yellow-brown earthy bauxite, having geological relations not unlike those of the bauxite of the Mediterranean region. As post-Oligocene deformation and differential erosion have brought limestones of different geological ages to the surface in different areas in the island, bauxite may lie on limestones of different age even in geographically adjacent districts.

Except for 1–2 feet of sod and soil, bauxite occurs at the surface and extends downward as much as 75 or 80 feet because of the unequal erosion of the underlying limestones. Horizontally individual deposits may continue for half a mile or more and may be connected by narrow bauxite-filled depressions with adjacent deposits, so that groups of deposits may extend over several square miles. No post-Oligocene formations have been found overlying bauxite in Jamaica, and neither has bauxite been found on Miocene, Pliocene, or younger formations. However, since bauxite occurs in contact with solid limestone on the floors and sides of the deposits, it is assumed that its formation has been more or less continuous since Medial Tertiary time. Absence of bauxite associated with rocks younger than Oligocene is perhaps explained by these rocks being chemically unfavorable to bauxite formation.

Bauxite deposits of Haiti and Santo Domingo are very similar to the deposits of Jamaica and are believed to be of approximately the same age.

The principal bauxite deposits of County Antrim (Cole, 1912), Northern Ireland, are found as irregular lenses or masses in the Interbasaltic zone, a formation of impure iron ore, bauxite, ferruginous clay, and lithomarge, interlayered between the Upper Basalt and Lower Basalt of late Eocene or Oligocene age. One or more thin layers of similar material also occur in the Lower Basalt. The bauxites are ferruginous and siliceous materials of low grade believed to be mainly the decomposition products of basalt formed in intervals between successive flows. There are also, however, pale siliceous bauxites, probably derived from the weathering of associated rhyolite flows.

Bauxite of the Vogelsberg Mountains (Harrassowitz, 1926) occurs in ferruginous clays derived from the weathering of Upper Miocene basalt flows. It consists mostly of nodules and fragments imbedded in terra rossa or variegated clays, chiefly red.

Brown iron ore in irregular segregations is abundantly associated with the bauxitic material.

Extensive deposits of ferruginous, bauxitic laterite and associated iron ore deposits, occurring as alterations of Miocene basaltic flows, have recently been found in Washington and Columbia counties, northwestern Oregon (Libbey, Lowry, and Mason, 1944). The basaltic flows, of which there is a succession, some of them separated by a considerable time interval, inundated the well-worn surface of Oligocene sediments, first filling the valleys and finally leveling the whole region in the late Miocene. This level basalt surface was then subjected to long and intensive weathering of the lateritic type which developed a deep soil blanket and resulted in the present topography. The ferruginous, bauxitic laterite is in horizontal beds and lenses in the residual mantle. Generally 1–2 feet of clay overlies a variable thickness, perhaps 100 feet or more, of oölitic, pisolitic, or pebbly laterite, some moderately hard, some soft and claylike, ranging in Al_2O_3 content from 25 to 40 per cent or higher, and rich in iron. Between the laterite and the underlying fresh basalt is a residual cushion of varicolored clays. In some localities silt deposits several feet thick overlie the residual mantle.

Bauxite and laterite deposits have a fairly wide distribution in the peninsula of India, but those of greatest potential importance occur along a broad east-west belt extending from the Central Provinces eastward through southern Rewa State along the southern boundary of Korea State and then on through Surguja State and a part of Jashpur State into western Bihar Province (Fox, 1947). Deposits of somewhat less interest are scattered along the Western Ghats from Bombay southward to Belgaum and beyond. A few occurrences are known in northern Bombay Presidency, in Madras Presidency, and on the central plateaus.

The deposits are of two principal types: (1) bauxite pockets or lenses in clay or limestone, and (2) cappings of laterite and bauxite on high, flat-topped plateaus, and table mountains. In the northeastern part of the Central Provinces in the region of Katni a group of bauxite pockets and lenses occurs in clays overlying Cambrian Vindyan limestone. Most of them are in valleys or on the lower slopes of ridges. Near Kapadvanj in northern Bombay Presidency a lens of bauxite lies on gray limestone of undetermined age and is overlain by several feet of clay, sandy clay, and a little limestone. Most of the laterite and bauxite cappings are probably related to Deccan trap flows of post-Cretaceous age, and in many places the basaltic flows underlie them, forming great cliffs on the sides of the table mountains. A varying thickness of residual clay (lithomarge) occurs between the laterite and the fresh basalt. Even where basalt is absent and the bauxite, laterite, and lithomarge lie on a floor of schists, gneisses, intrusives, and other rocks, basaltic flows may at one time have capped the hills now occupied by bauxite and laterite, and the latter may be their decomposition products. Little or no overburden covers the bauxite or laterite, and that which is present looks like disintegrated laterite or lateritic clay. In many places a hard iron-oxide crust a few inches to a foot or more thick, and often in part pisolitic, forms the surface of the laterite capping.

As it has no superimposed strata, the Indian bauxite is difficult to date. Since, however, the Deccan basalts are post-Cretaceous and since they, as well as the lat-

eritic cappings, were profoundly eroded subsequently, the latter were probably formed some time during the Medial or Late Tertiary.

The bauxite deposits of Malaya and Netherlands Indies occur as nodules and fragments in ferruginous clayey soil that forms a decomposition mantle overlying various rocks but appearing to be best developed over metamorphosed volcanics of the Pahang series mapped in part as late Paleozoic and in part as Triassic. The rocks composing the series are predominantly phyllites and schists, but shales, sandstones, and limestones do occur. No younger rocks overlie the bauxite, which is believed to be post-Tertiary. The bauxite is of the gibbsitic or trihydrate type similar to bauxites in many other parts of the tropics.

Deposits of bauxite similar to those in Malaya and Netherlands Indies are found in the Caroline Islands in the Pacific.

An intensive search for good-grade bauxite has recently been made in Australia, but only relatively low grade materials have been found, although small deposits of fairly good ore occur in Victoria and Queensland. The Victoria deposits (Raggatt, Owen, and Hills, 1945) are stated to be of Oligocene or Late Miocene age. They occur above the Older Basalt (Tertiary) and are overlain by the Yallourn formation of lignite, clay, and sand—the uppermost Tertiary of this region. Large low-grade surface deposits of the usual tropical ferruginous, lateritic type are found in New South Wales and Tasmania, and lateritization is also widespread in Western Australia.

Bauxite deposits of Africa practically all belong to the tropical lateritic type occurring at the surface and being underlain by residual clays in varying thickness separating the bauxite from the underlying rocks of different varieties (Bauer, 1898; Lacroix, 1913; Kitson, 1925; Dixey, 1925; Goloubinow, 1938). Probably all the bauxite deposits are of recent origin geologically, although differences in their topographic relationships suggest considerable differences in age between deposits. Thus, the laterite and bauxite in Gold Coast and in Nyasaland form cappings of high tablelands and plateaus 1000–2000 feet above the neighboring lowlands, while the deposits in French West Africa are in low, moderately hilly districts with relief of only a few hundred feet. Thus, while some deposits, presumably affected by crustal movements, may date back to the Tertiary, in other places bauxitization may be proceeding now.

Rocks of many different kinds and of widely different ages underlie the bauxite and laterite. In Gold Coast there are flat-lying shales and mudstones underlying the bauxite in the Mt. Ejuanema district and steeply dipping phyllites, graywackes, metamorphosed lavas, and intrusives below the bauxite capping in Ashanti; in the Boké district in French Guinea underlying rocks are metamorphosed arkosic and argillaceous sediments and doleritic intrusives; in the Los Islands, French Guinea, there is intrusive nepheline syenite; in the Seyschelles Islands north of Madagascar granite, diorite, and diabase are involved in the lateritization; and in Nyasaland orthoclase-hornblende syenite underlies the bauxite.

Of the African bauxite deposits, only those in Gold Coast have been developed into production, but others of great potential importance occur.

Most of the bauxite deposits of Brazil, like those of Africa, are of the tropical lateritic

type. They seem to be of fairly recent origin, and at least in one district (Pocos de Caldas in southwestern Minas Geraes) bauxite appears to be forming at the present time. The tableland forming type of laterite is less in evidence in Brazil than in India or parts of Africa, indicating greater quiescence and possibly more recent origin. The deposits occur in rolling to moderately hilly country on the upper slopes or flanks of hills.

The only bauxite area of present importance is that of Pocos de Caldas where blanket deposits mantle rolling, grassy hills consisting of phonolite, tinguaite, and foyaite (Santos, 1937; Pinto, 1938). Brown porous bauxite up to 25 feet thick lies on the fresh rock and grades upward near the surface into a dense, fragmental type of high-grade bauxite mixed with soil. A bauxite deposit at Mutuca Vargem near Bello Horizonte, Minas Geraes, has a characteristic layering. At the surface is a hard crust of dark-red iron laterite that grades downward into ferruginous earth, in all about 10 feet thick. Below this is a thin layer of pisolitic iron laterite underlain by pink and red bauxite about 5 feet thick with vertical iron-oxide pipes along the central part. At the base is a network of bauxite pipes in a matrix of clay. The underlying fresh rock is not in evidence. At Chapada da Agua Quente some miles north of Ouro Preto, Minas Geraes, in a region of deeply weathered pre-Cambrian schists there is a flat-lying surface deposit of low-grade ferruginous bauxitic laterite several square miles in extent underlain by varicolored residual clays. Numerous other laterite and bauxite occurrences, including the peculiar phosphatic bauxite knolls on the Maranhao Coast east of Rio Gurupy, are found in different parts of Brazil, but they do not present any noteworthy stratigraphic features.

ORIGIN[1]

MECHANICAL AND CHEMICAL SEDIMENTATION

Students of the geology of bauxite and laterite deposits agree that the processes involved in the formation of aluminum hydroxides during rock decay are chemical processes that are strongly influenced by special rock, soil, ground-water, biological, topographic, and climatic conditions such as temperature and rainfall. As regards the accumulation of such aluminum hydroxides into bauxite deposits, however, there is a considerable diversity of opinion, ranging from mechanical or chemical sedimentation to residual accumulation by leaching of more soluble constituents during weathering. It has been proposed that aluminum hydroxides might have been deposited by a mechanical process, involving the separation of impurities, the physical sorting of particles of aluminous materials, and their deposition more or less in the same manner as that of sandstones, shales, or other clastic sediments. More commonly the hypothesis has been advanced that aluminum hydroxides are carried in solution or colloidal suspension and are precipitated in quiet waters, possibly lagoons, much like limestones or other chemical sediments.

Mechanical accumulation of bauxite actually does occur locally by the disintegration by weathering of previously existent bauxite deposits and the reworking of the

[1]For a more comprehensive, although somewhat outdated discussion of the origin of bauxite, the reader is referred to Harder, (1930). The writer is indebted to McGraw-Hill Book Co., New York for permission to use some of this material.

resulting fragments and particles into detrital beds on the surface of the original deposit or perhaps more frequently at lower levels in the vicinity of the original deposits. Such detrital bauxites occur in British Guiana overlying and flanking original bauxite beds, in Arkansas adjacent to deposits formed earlier *in situ* from nepheline syenite, and in India as low-level laterites below the hill deposits. It seems unjustified to suppose, however, that extensive deposits of more or less pure bauxite could accumulate as clastic beds by the mechanical sorting during transporation and sedimentation of disseminated particles of aluminum hydrates formed by rock weathering and existing in a residual soil mantle.

The hypothesis of chemical sedimentation was advanced by early French and American geologists and is still largely adhered to by many Russian geologists who have devoted much time to the study of bauxite deposits in the Ural Mountains and elsewhere in the Soviet Union. Although the chemical sedimentation hypotheses vary in detail, in general they visualize the solution of aluminum along with iron and titanium in thermal waters highly charged with certain salts or acids and their subsequent deposition as hydroxides during cooling and by reaction with calcareous waters or waters containing carbon dioxide, organic acids, hydrogen sulfide, or certain salts.

Among early French geologists who suggested chemical sedimentation of bauxite were M. H. Coquand (1870), M. Auge (1888), and S. Meunier (1889). They visualized the French bauxite deposits as being formed by the action of thermal waters taking aluminum and iron salts into solution and issuing as hot springs in the floors of lakes or lagoons; there, becoming mixed with waters in which calcareous sediments were being deposited, they reacted with the calcium carbonate to deposit the aluminum and iron salts as hydroxides. C. W. Hayes (1902), an American geologist who studied the bauxite deposits of northern Georgia and Alabama and central Arkansas during their early development, suggested that surface waters penetrating to considerable depths became heated and then, coming into contact with pyrite-bearing shales, as in Georgia, or hot nepheline syenite, as in Arkansas, became charged with acids, acid salts, or alkalies and dissolved aluminum, iron, and other associated elements. These hot, charged solutions rising to the surface and coming into contact with limestones, as in Georgia, or cooled nepheline syenite, as in Arkansas, were believed to have precipitated the aluminum and iron as gelatinous hydroxides. H. K. Shearer (1917) believed that hydrogen sulphide played a part in the formation of the bauxite deposits of southern Georgia. The hydrogen sulphide solutions, it is claimed, found outlets in the beds of lakes or lagoons in which clay was being deposited, became oxidized and formed sulphuric acid which attacked the clay particles, producing aluminum sulphate, the latter being precipitated as aluminum hydroxide by excess hydrogen sulphide. W. A. Nelson (1923) explained the origin of the southern Appalachian bauxite deposits by the action of sulphuric-acid-bearing waters upon bentonite beds and the precipitation of the dissolved aluminum salts as aluminum hydroxide through the action of organic acids in swamp waters when the aluminum-bearing waters reached the surface. The same general hypothesis of origin was proposed by W. B. Jones (1929) for the various bauxite deposits of Alabama, with the variation that a more general source than bentonite is assumed for the aluminum-bearing compounds.

Of the geologists that advanced the hypothesis of normal marine or fresh water sedimentation for the Russian bauxite deposits, among the first were S. G. Malyavkin, (1926) and A. D. Arkhangelsky (1933), followed more recently by A. K. Gladkovsky (1942), N. A. Karjavin (1942), and others. They have suggested the solution of aluminum and iron compounds during the weathering of various rocks, their transportation and accumulation as alumino-ferric colloids during subsequent inundation and gradual submersion, and their later precipitation under littoral conditions in quiet lagoons or along shores protected by numerous islands. The inundations may have started with fresh water followed later by invasion of the sea. The conditions of precipitation are believed to have been strongly influenced by the hydrogen ion content of the waters; different types of bauxite are supposed to have been formed as these conditions and the oxygen content of the waters changed. Many deposits are reported as highly oxidized, dark red, and rich in aluminum and iron hydrates in their lower parts, becoming deoxidized and gray in their upper parts with contamination of pyrite and siderite, probably under the influence of organic matter. The main precipitating agent mentioned by the Soviet geologists is the calcium carbonate of the limestone floor that underlies the majority of the Russian bauxite deposits. Overlying the bauxite layers are later sediments, consisting in many places of bituminous limestones and shales; perhaps these rather than deoxidizing conditions during actual deposition are responsible for the upper deoxidized phases of the bauxite deposits (Harder, 1933).

Although the various reactions proposed in the chemical sedimentation hypotheses for the origin of bauxite deposits are chemically possible, the writer believes they involve unnecessary complications when compared to reactions concerned with the simple leaching of soluble constituents as proposed in the hypothesis of residual accumulation of bauxite by weathering.

WEATHERING IN SITU

Most geologists who are familiar with the occurrence of laterite and bauxite deposits maintain that they are residual, being formed *in situ* by the leaching of siliceous and other impurities through the action of chemical agencies and particularly under conditions that accompany surface weathering and erosion of aluminum-bearing rocks. Such a hypothesis seems to follow naturally from the fact that it is the least soluble constituents of the rocks that remain behind to form the bauxite and laterite deposits. By the same token, it makes it more difficult to agree with the Russian and other proponents of the chemical sedimentation hypothesis that requires the solution and transportation of these difficultly soluble substances.

In the decomposition of rocks by weathering, there is a gradual removal of the more soluble constituents with alkalies, lime, and magnesia going first, followed by combined silica, leaving the iron oxides, titania, and alumina—and free quartz, where present—as relatively insoluble residues. Thus, normal weathering processes are in the direction of laterite and bauxite formation. On the other hand, ordinarily these processes are not generally followed to completion, and intensification of weathering action, such as occurs in the tropics, is necessary to produce lateritization or bauxitization. The abundance of bauxite and laterite in tropical or semitropical regions and their scarcity or absence in colder regions is due to the fact that decom-

position of rocks is most intensive and most nearly complete in the former regions. In temperate and cold climates, disintegration becomes progressively more important and decomposition less so. However, even in tropical regions, climatic conditions vary widely from the arid climate in the desert regions to the humid conditions of the rain belts. These variations doubtless explain why bauxite and laterite deposits are localized rather than of general occurrence. Some observers claim that, not only is a general warm, moist climate necessary for lateritization, but there must be a regular and distinct alternation of wet and dry seasons.

Some differences of opinion exist as to the extent to which solution and redeposition of alumina, iron oxide, and other lateritic constituents take place during lateritization. Since veins of gibbsite frequently intersect a matrix of fine-grained aluminum hydrate, and iron-oxide infiltrations occur along cracks and fissure planes, and gibbsite crystals are common in vugs or small groups scattered through the bauxite, it would seem that at least locally even the difficultly soluble lateritic materials are subject to solution, redeposition, and replacement.

Bauer (1898) early showed the true nature of laterite. By microscopic examination of laterite specimens from the Seyschelles Islands north of Madagascar he determined that they were a mixture of aluminum hydrates and hydrated iron oxides with or without quartz. Moreover, he found that these constituents retained the original texture of the igneous rock, such as diabase, diorite, or granite, from which they were derived and the outlines of the original feldspars, amphiboles, or pyroxenes. Inside of the mineral outlines, however, were scaly aggregates of gibbsite and diaspore stained by hydrated iron oxides. In case of the lateritization of granite, original quartz grains remained unaltered.

Maclaren (1906) and Campbell (1909–1910) tried to formulate the conditions that appear most favorable to laterite and bauxite formation. Maclaren believed the necessary changes of solution and redeposition were accomplished largely by carbonate-bearing waters under the influence of successive saturation and desiccation due to the slow fluctuation of the water table resulting from regularly alternating wet and dry seasons. The movement in this surface zone of alternating wetness and dryness supposedly takes place mainly through capillary openings, and the walls of these same openings presumably serve as loci for solution and redeposition.

Campbell gave the conditions that favor lateritization as: (1) alternating wet and dry seasons, (2) a pronounced dry season, provided enough rain falls during the wet season for abundant vegetation, (3) tropical temperature giving luxuriant vegetation, (4) fluctuating water level not far from the surface, and (5) gently sloping surface of the ground.

Both Maclaren and Campbell believed that there is a certain amount of solution even of the more insoluble constituents of soil or rock but that the redeposition of these materials follows soon and enriches the main process of lateritization by the leaching of soluble impurities.

Lacroix (1913), after a comprehensive study of lateritization in French Guinea, divided the layer in which lateritic action is prevalent into two horizontal zones, the lower or zone of leaching and the upper or zone of concretion. The two zones grade into each other, the action begun in the lower being continued in the upper. However, the laterite in the two zones differs in appearance; that in the zone of

leaching essentially retains the original rock texture, while that in the zone of concretion gradually develops cellular, concretionary, pisolitic, and fragmental structures at the expense of the original rock texture. Moreover, there is believed to be upward migration of iron oxide to form a surface crust and a general tendency in the upper zone to segregate iron and aluminum hydrates.

According to Lacroix, rocks fall roughly into three classes as regards their amenability to lateritization: (1) gabbro, diabase, and nepheline syenite, which alter directly to gibbsitic laterite in the zone of leaching; (2) peridotite, which alters in the leaching zone to porous, ferruginous laterite; and (3) granite, gneiss, and schist, which change to clayey alteration products in the lower part of the zone of leaching with a gradual development of aluminum hydroxides in the upper part. In all cases segregation and reworking of the hydroxides take place in the zone of concretion.

Harrassowitz (1926) carefully reviewed the literature on rock decomposition and lateritization and did some original work on the Vogelsberg Mountains laterites in Germany. He developed a classification of the origin of laterite not unlike that of Lacroix and other previous investigators. He proposed three divisions of the mantle of residual, decomposed material formed during lateritization: (1) the zone of decomposition where the original aluminum-bearing silicates alter to siallite (hydrous aluminum silicates) but retain the original rock texture; (2) a mottled zone where allite (aluminum hydrate) forms and the original rock texture disappears; and (3) the upper cellular ferruginous crust where enrichment by alumina and silica gels and iron and aluminum hydrates takes place. The siallite zone may be missing locally, and the alteration may occur directly from fresh rock to allite; likewise, in places the upper iron crust may be absent.

Among geologists who favor the weathering *in situ* hypothesis for the origin of bauxite deposits there is still some difference of opinion as to the manner in which the changes from the original aluminum-bearing compounds in the parent rocks to the aluminum hydroxides of the bauxite deposits have progressed. Some believe that for the most part the alteration takes place directly from the aluminum silicates and other minerals of the parent rock, while others have stressed the importance of intermediate decomposition products such as clay minerals from which the bauxite is eventually formed. The latter suggest that such minerals as feldspars normally alter to kaolinite and that the kaolinite is changed to aluminum hydroxide by the solution and removal of silica. On the other hand, some geologists who believe in the direct alteration of original aluminum silicates to bauxite go so far as to say that aluminum hydrates do not form from kaolinite, that the latter is itself an end product.

Field evidence indicates that bauxite forms both by direct alteration of original aluminum silicates such as feldspar and nepheline and by alteration from kaolinite or other clay minerals. It is difficult to determine which is the more normal process, but this may perhaps be indicated by a study of the relative prevalence of each in nature. Of course, not all bauxite occurrences lend themselves to such a study; usually the relation of the bauxite to the parent rock is quite obscure. The main evidence available indicating that clay minerals such as kaolinite alter to aluminum hydroxides are:

(1) A clay zone of varying width is in many places found between the fresh

parent rock and the bauxite; the transitional character of this zone is indicated by the fact that in many cases the texture of the fresh rock persists through it into the bauxite or laterite. The classic example of such an occurrence is the alteration of the Arkansas nepheline syenite to kaolinite and the alteration of the latter to so-called granitic-textured bauxite (Mead, 1915). However, similar intermediate kaolinite or lithomarge zones have been described in connection with the lateritization of schists, gneisses, and granites in French Guinea, West Africa (Lacroix, 1913), of several types of rocks in the Sudan (Arsandaux, 1913), and of basalt in India.

Recently some geologists have questioned whether the kaolin cushion between the fresh rock and the bauxite is really a transition stage or whether it represents a resilicification of bauxite formed originally from the fresh rock (Goldman and Tracey, 1946). Also, the further suggestions may be advanced that: (1) bauxite may have formed directly from the fresh rock when climatic and ground-water conditions favored bauxitization and kaolinization followed when conditions changed; or (2) mineral composition of the original rock may have varied so that direct bauxitization occurred at one point and kaolinization at another.

(2) Many bauxite deposits are separated from the underlying fresh rock by 100 feet or more of residual clay, as in the Guianas, northern South America. If the bauxite originated by direct alteration of the fresh rock, it would be difficult to explain why such a heavy layer of residual clay should form underneath the bauxite bed and subsequent to the formation of the bauxite. It would be more natural to ascribe the origin of the bauxite to the alteration of the residual clay.

(3) In a number of widely separated bauxite fields with different geologic relations, such as those in the Guianas and in Brazil, pipes and veins of bauxite, many of which consist of high-grade gibbsite, extend downward from the base of the bauxite bed as a network into the underlying residual clay. In such zones, transitions occur between nearly pure bauxite and nearly pure kaolinite. After microscopic examination of a typical sample of residual clay taken underneath a Guiana bauxite deposit, Dr. C. S. Ross (Personal communication) says: "It is essentially kaolinite but has cloud-like areas of exceedingly fine-grained gibbsite disseminated in kaolinite."

(4) In many places deposits of bauxite in the form of beds or lenses are interlayered with or lie on top of sedimentary clay beds, and commonly have gradational lower contacts. No igneous rocks or other type of sedimentary rock to which the bauxite could possibly be related are in evidence in the neighborhood. Occurrences of this kind are common in Arkansas and in southeastern United States. Moreover, in many parts of the tropics, bauxite and laterite are formed by the alteration of shales, phyllites, and schists (Cooper, 1936), the prominent minerals in which are micas, clay minerals, and other hydrous aluminum silicates.

(5) Some mention is perhaps desirable of the probable origin of the so-called terra rossa type of bauxite common throughout the Mediterranean region of Europe and more recently found also in the Ural Mountains and in Jamaica and other West Indies islands. These deposits are commonly high in iron oxide and moderately low in silica, and they lie directly on the eroded surface of limestones, often very pure. It is generally believed that these deposits represent the residual end products

left by the solution and removal of the soluble constituents of the limestones and that probably they are mostly the altered accumulations of fine clay particles previously disseminated through the limestone. No other plausible explanation is apparent, although a tremendous amount of erosion would be necessary for the accumulation of bauxitic residual products from the very pure limestones from which they are derived.

The evidence for the direct alteration of nepheline, feldspar, and other primary aluminum silicates to bauxite and laterite is also mostly based on field observation:

(1) There are numerous examples of fresh rock altering directly to bauxite with practically knife-edge contacts between the fresh rock and the bauxite. Such occurrences are known in many parts of the tropics where lateritization is apparently taking place at present. In the Pocos de Caldas district, Minas Geraes, Brazil, porous bauxite containing less than 4 or 5 per cent silica is found in contact with fresh phonolite and nepheline syenite, and unaltered cores of these rocks are in many places surrounded by lateritized material. In the Los Islands in French Guinea, spongy, porous bauxite commonly lies directly against nepheline syenite and contains fragments of the fresh rock. Near Freetown, Sierra Leone, ferruginous laterite is in contact with peridotite. In the Guianas and elsewhere, dolerite, diabase, gabbro, and diorite have alteration rims of bauxite or ferruginous laterite directly in contact with the fresh rock. Although such contacts have been examined microscopically, there is no indication that clay minerals have formed even momentarily during the transition from original silicates to hydroxides. In fact, incipient gibbsite is found in partially altered feldspars, amphiboles, and other silicates.

(2) Evidence believed to indicate common and widespread secondary kaolinization or silicification of bauxite in Arkansas has been reported. Therefore, it is argued that the kaolinite cushion between the fresh nepheline syenite and the bauxite has probably resulted from the silicification of previously formed bauxite, although some of the kaolin may have been formed directly from nepheline syenite. Whatever the origin of the kaolin, however, the Arkansas bauxite is considered a direct alteration product of nepheline syenite (Goldman and Tracey, 1946). Moreover, considerable doubt is expressed as to whether kaolin will ever alter to bauxite, and it is suggested that kaolin itself is an end product. However, the writer wonders whether the kaolinization of bauxite may not be open to as much doubt as the bauxitization of kaolinite. At least in some cases, for example in British Guiana, the siliceous capping over many bauxite deposits appears to consist of a bauxite-clay conglomerate—bauxite pebbles in a clay matrix—rather than of kaolinized or resilicified bauxite.

The study of laterite and bauxite deposits in various parts of the world suggests that such deposits may form from almost any type of rock, except possibly the most siliceous, provided suitable climatic conditions prevail and suitable solutions are present to dissolve and leach the nonlateritic constituents. Rocks high in aluminum and iron and particularly rocks containing readily soluble minerals are, of course, much more easily altered and yield heavier and richer deposits of aluminum and iron hydroxides because of their resulting porosity than do dense materials such as clays which resist the passage of solutions. It is mainly rocks of the former type,

such as nepheline syenite, phonolite, dolerite, diabase, and gabbro, that exhibit direct alteration of original aluminum and iron silicates to aluminum and iron hydroxides. The direct alteration of granites, siliceous gneisses, and schists to laterite is probably rare, and at least in these rocks evidence favors preliminary alteration to clay minerals which are subsequently changed to bauxite or laterite. The alteration of clay minerals, such as kaolinite, to aluminum hydroxides under suitable conditions seems a well-established fact.

CONCLUSIONS

Bauxite and laterite deposits represent periods in the earth's history during which land surfaces, after denudation and approximate base leveling, remained quiescent and subject to chemical weathering for long periods. However, lateritization (or bauxitization) is not universal under the above conditions. It is governed to a considerable degree by temperature and rainfall; a warm, humid climate with alternating wet and dry seasons hastens the process and thus promotes localization of laterite and bauxite deposits in tropical or subtropical regions. A low relief of the land surface is essential so that the maximum proportion of rainfall may sink into the ground. The chemical composition of the ground water is also an important factor; the presence of appropriate solvents is required to hasten solution and chemical reaction. Rocks with a high percentage of soluble constituents are favorable to chemical weathering as the solution of these constituents results in high porosity which permits maximum action on insoluble residues. Rocks rich in lateritic constituents such as aluminum, iron, and manganese give rise to more extensive and purer deposits of these elements than rocks high in combined silica, quartz, and other nonlateritic constituents. The relative proportion of lateritic substances in the rock determines whether bauxite, iron ore, or manganese ore results.

The nondepositional intervals represented by bauxite or laterite are of different lengths. In places they constitute a hiatus that embraces several geologic eras, such as that represented by the Guiana bauxite deposits which lie on the pre-Cambrian and are overlain by unconsolidated sediments of late Tertiary or Pleistocene age; elsewhere the nondepositional interval may extend through one or more geologic periods, as in case of the bauxite horizon in central Hungary, bridging the gap from Triassic to Eocene; the diaspore strata of Kashmir, occurring between the Eocene and Jurassic; and those of Kweichow in southwestern China, occupying the position of missing Silurian and Devonian rocks. In still other places the time during which laterite or bauxite formation took place may be limited to a few geologic epochs, as in Russia, representing portions of the Devonian and Carboniferous; in southern France underlain by Jurassic or Lower Cretaceous and overlain by Lower, Middle, or Upper Cretaceous; in southeastern United States occupying the interval between Cretaceous or Paleocene below and Eocene above; in Rumania between the Jurassic and Lower Cretaceous; and in parts of Yugoslavia between the Cretaceous and Lower Eocene; or may even be more restricted as illustrated by certain intra-epochal bauxites in Lower Eocene rocks in Dalmatia. It should be understood, however, that the interval during which actual formation of bauxite took place was in most cases very much shorter than the depositional record indicates, particularly where

the interval involved represents eras or periods, in which case long and extensive erosion preceded lateritization.

Further study is required to determine the principal chemical compounds and reactions involved in the formation of bauxite and laterite. Aluminum and iron hydroxides can be produced from silicates and other compounds of these metals in a number of ways, but the chemical reactions that predominate in the formation of natural deposits of bauxite and laterite and the conditions under which they take place are still to be determined.

Twenty or thirty years ago it was generally believed that the common method of bauxitization involved an intermediate kaolin stage between the fresh rock and the bauxite. Later, abundant examples were found in the field of the direct alteration of primary aluminum silicates to aluminum hydroxides. Microscopic examination showed that minute scales of gibbsite develop in a disseminated form in primary aluminum silicates during their early weathering stages. As weathering proceeds, these become more abundant, and eventually gibbsite will replace entire former aluminum silicate crystals. Gradual slumping, due to external pressure and favored by porosity during the change from aluminum silicates to aluminum hydroxides, tends to obliterate the original crystal texture. Also, some solution and redisposition of aluminum hydroxide occurs and aids in reducing the porosity.

Recently it has been claimed by some geologists that all bauxite originates directly by the alteration of primary aluminum-bearing rocks and that kaolin or other clay minerals will not alter to bauxite. The occurrence of bauxitic clays and siliceous bauxites is explained by the resilicification of bauxite rather than by the alteration of clay to bauxite. In the writer's opinion, however, field evidence favors the view that, although silicification of bauxite is not ruled out, bauxitization of kaolin is common. Microscopic examination of bauxitic clay has provided further evidence for this view.

Another interesting phenomenon in the development of bauxite deposits meriting further study is that some of them consist mainly of the trihydrate, gibbsite, and others largely of the monohydrate, boehmite intermixed locally with diaspore. Boehmitic bauxite deposits are strikingly common in association with limestone, and this occurrence may be significant. General field evidence seem to indicate that first gibbsite forms during the lateritization of aluminum silicates and that aging, pressure, and possibly heat change the gibbsite to boehmite and eventually the latter to diaspore. All stages are found in bauxite deposits, and there is even evidence that a final stage in the metamorphism may be the development of emery and corundum.

REFERENCES CITED

Adams, G. I. (1927) *Bauxite deposits of the southern states*, Econ. Geol., Bull., vol. 22 p. 615–620.

Arkhangelsky, A. D. (1933) *Origin of the bauxites of USSR*, Soc. Nat. Moscou, Sec. Geol. 11, p. 434–436.

Arsandaux, H. M. (1913) *Contribution a l'etude de l'alteration des roches silicatees-alumineuses dans les regions inter-tropicales*, Soc. Franc. de Mineral., Bull., vol. 36, p. 70–110.

Auge, M. (1888) *Note sur la bauxite, son origine, son age et son importance geologique*, Soc. Géol. France, Bull., vol. 16, 3d ser., p. 345.

Bauer, M. (1898) *Beitrage zur Geologie der Seyschellen, insbesondere zur Kenntnis des Laterits*, Neues Jahrb., vol. 2, p. 163–219.

Bishopp, D. W. (1937) *Memorandum on the occurrence of bauxite in British Guiana*, Geol. Survey Br. Guiana, Bull. 8, 68 pages.

Bracewell, S. (1947) *Geology and mineral resources of British Guiana*, Imp. Inst. London, Bull., vol. 45, no. 1, p. 47–69.

Bramlette, M. N. (1936) *Geology of the Arkansas bauxite region*, Ark. Geol. Survey, Inf. Circ. 8, 68 pages.

Branner, J. C. (1897) *Bauxite deposits of Arkansas*, Jour. Geol., vol. 5, p. 263–289.

Burchard, E. F. (1925) *Bauxite in northeastern Mississippi*, U. S. Geol. Survey, Bull. 750-G, vol. 45, no. 1, p. 101–146.

Campbell, J. M. (1909–1910) *Origin of laterite*, Inst. Min. Metall., Tr., vol. 19, p. 432–443.

Cole, G. A. J. (1912) *The interbasaltic rocks (iron ores and bauxites) of northeast Ireland*, Geol. Survey Ireland, Mem.

Cooke, W. (1926) *Geology of Alabama; The Cenozoic formations*, Ala. Geol. Survey, Spec. Rept. 14, p. 251–297.

Cooper, W. G. G. (1936) *Bauxite deposits of the Gold Coast*, Gold Coast Geol. Survey, Bull. 7, 34 pages.

Coquand, M. H. (1870–1877) *Sur les bauxites de la chaine des Alpines (Bouches du Rhone) et leur age geologique*, Soc. Géol. France, Bull., 2d ser., vol. 28, p. 98–115.

Denisevich, A. A. (1942) *Concerning the shape and composition of bauxite ore deposits in the northern Urals*, Acad. Sci. USSR, Geol. Ser. no. 5–6, p. 102–114.

Dixey, F. (1925) *Bauxite deposits in Nyasaland*, Min. Mag. vol. 33 no. 4 p. 201–205.

Foose, R. M. (1944) *High-alumina clays of Pennsylvania*, Econ. Geol., vol. 39, p. 557–577.

Fox, C. S. (1923) *The bauxite and aluminous laterite occurrences of India*, Geol. Survey India, Mem., vol. 49, pt. 1, p. 102–104.

——— (1947) *Geology and mineral resources of Surguja State*, ESA, Indian Govt. Surguja.

Gladkovsky, A. K. (1942) *The Eifelian and Givetian bauxite occurrences in the Iss and southern Serov districts, the lower Ludlow productive series of the Iss District*, Acad. Sci. USSR, Bull., Geol. Ser., no. 4, p. 35–46.

Goldman, M. I., and Tracey, J. I. Jr. (1946) *Relations of bauxite and kaolin in the Arkansas bauxite deposits*, Econ. Geol., vol. 41, p. 567–575.

Goloubinow, R. (1938) *Les bauxites de Tougue, French West Africa*, Serv. Mines, Bull. 1, p. 75–80.

Harder, E. C. (1930) *Ores of aluminum, in* J. D. Edwards, F. C. Frary, Z. Jeffries: *The aluminum industry*, McGraw-Hill, New York.

——— (1933) *Origin of bauxite deposits*, Econ. Geol., vol. 28, p. 395–398.

——— (1936) *British Guiana and its bauxite resources*, Canad. Inst. Min. Metall., Bull. 295, pp. 739–758.

Harrassowitz, A. (1926) *Laterit, Material, und Versuch erdgeschichtlicher Auswertung*, Geb. Borntraeger, Berlin.

Hayes, C. W. (1901) *Arkansas bauxite deposits*, U. S. Geol. Survey, 21st Ann. Rept., pt. 3, p. 435–472.

——— (1902) *Description of the Rome quadrangle*, U. S. Geol. Survey, Geol. Atlas, Folio 78, 6 pages.

Hose, H. R., (1942–1948) Private reports to Jamaica Bauxites Ltd.

——— Bryn Davies, D. A., and Grimes-Graeme, R. (1937–1947) Private reports to Demerara Bauxite Co. Ltd.

Hsieh, C. Y. (1935) *A microscopical study of the bauxite deposits in the Tzechuan-Posham district, central Shantung*, Geol. Survey China, Bull. 25, p. 55–62.

Jones, W. B. (1929) *Summary report on the bauxite deposits of Alabama*, Ala. Geol. Survey, Circ. 7, 36 pages.

Karjavin, N. A. (1942) *Bauxite occurrence "Krasnaya Shapochka" in the Karpinsk District of Sverdlovsk*, Acad. Sci. USSR, Bull., Geol. Ser., no 4.

Kitson, A. E. (1925) *Outlines of the mineral and water power resources of the Gold Coast, British West Africa*, Gold Coast Geol. Survey, Bull. 1.

Lacroix, A. (1913) *Les laterites de la Guinee et les produits d'alteration*, Nouv. Arch. Mus., vol. 5.

de Lapparent, J. (1930) *Les bauxites de la France Meridionale, Mem. Expl. de la Carte* Geol. Detail. France, Minis. des Travaux Publiques.

Li, C. Y. and Hsieh, C. Y. (1946) *Potential sources of aluminum in southwestern China*, Am. Inst. Min. Metall. Eng., Tech. Paper 1938.

Libbey, F. W., Lowry, W. D., and Mason, R. S. (1944) *Preliminary report on high alumina iron ores in Washington County, Oregon*, Ore. Dept. Geol. Min. Indus., GMI Short Paper 12, 23 pages.

Maclaren, M. (1906) *On the origin of certain laterites*, Geol. Mag., Dec. 5, vol. 3, no. 12, p. 536–547.

Malyavkin, W. F., (1926) *Bauxite*, Acad. Sci. USSR, Bull., p. 145–178.

McQueen, H. S. (1943) *Geology of the fire clay districts of east central Missouri*, Mo. Geol. Survey, Water Res., 2d ser., vol. 28, 250 pages.

——— and Forbes, C. R. (1928) *Mining of diaspore and flint fire clays in Missouri*, Min. and Metall., vol. 9, p. 271–275.

Mead, W. J. (1915) *Occurrence and origin of the bauxite deposits of Arkansas*, Econ. Geol., vol. 10, p. 28–54.

Meunier, S. (1889) *Response a des observations de M. Auge et de M. A. de Grossouvre sur l'Histoire de la bauxite et des minerais siderolithigues*, Soc. Géol. France, Bull., 3d ser., vol. 17, p. 64.

Middlemiss, C. S. (1928) *Bauxite deposits of Jammu Province*, Jammu and Kashmir Govt., Min. Survey Rept.

Moldavantsev, E. (1934) *Bauxites of the northern Urals and the problems of their investigation*, Central Geol. Pros. Inst. of Russia, Tr., fasc. 24, 56 pages.

Morse, P. F. (1923) *Bauxite deposits of Mississippi*, Miss. St. Geol. Survey, Bull. 19, 208 pages.

Nalivkin, D. V. (1942) *Relating to Ural bauxites*, Acad. Sci. USSR, Bull., Geol. Ser., no. 4, p. 3–5.

Nelson, W. A. (1923) *Appalachian bauxite deposits*, Geol. Soc. Am., Bull., vol. 34, p. 525–540.

Pavlovski, A. (1925) *Les bauxites Francaises*, Jules Charles et A. Bruner, Paris.

Pinto, Mario da Silva (1938) *Bauxita em Poços de Caldas, Prospeccao nos Campos da Fazenda do "Recreio"*, Dept. Nac. da Produccao Mineral, Rep. dos Estados Unidos do Brasil, Bol. 22.

Raggatt, H. C., Owen, H. B., and Hills, E. S. (1945) *Bauxite deposits of the Boolarra-Mirboo north area, South Gippsland, Victoria*, Australia Min. Res. Survey, Bull. 14, 65 pages.

Rettger, R. E. (1925) *Bauxite deposits of southeastern Alabama*, Econ. Geol., vol. 20, p. 671–686.

Santos, Tharcisio de Souza (1937) *Contribuicao para o estudo da bauxita do planalto de Poços de Caldas, Contribuicoes ao Terceiro Congresso Sulamericano de Chimica*, Inst. de Pesquisas Tech. de Sao Paulo, Bol. 17, p. 109–134.

Shearer, H. K. (1917) *A report on the bauxite and Fuller's earth of the Coastal Plain of Georgia*, Ga. Geol. Survey, Bull. 31, p. 123–132.

Wang, C. C. (1932) *Bauxite deposits of Poshan and Tzechuan districts, Shantung*, Geol. Survey China, Bull. 18, p. 23–27.

Aluminium Secretariat Limited, 2100 Sun Life Building, Montreal, Quebec, Canada

Manuscript Received by the Secretary of the Society, July 2, 1948

V6
1
9
4
9
UM

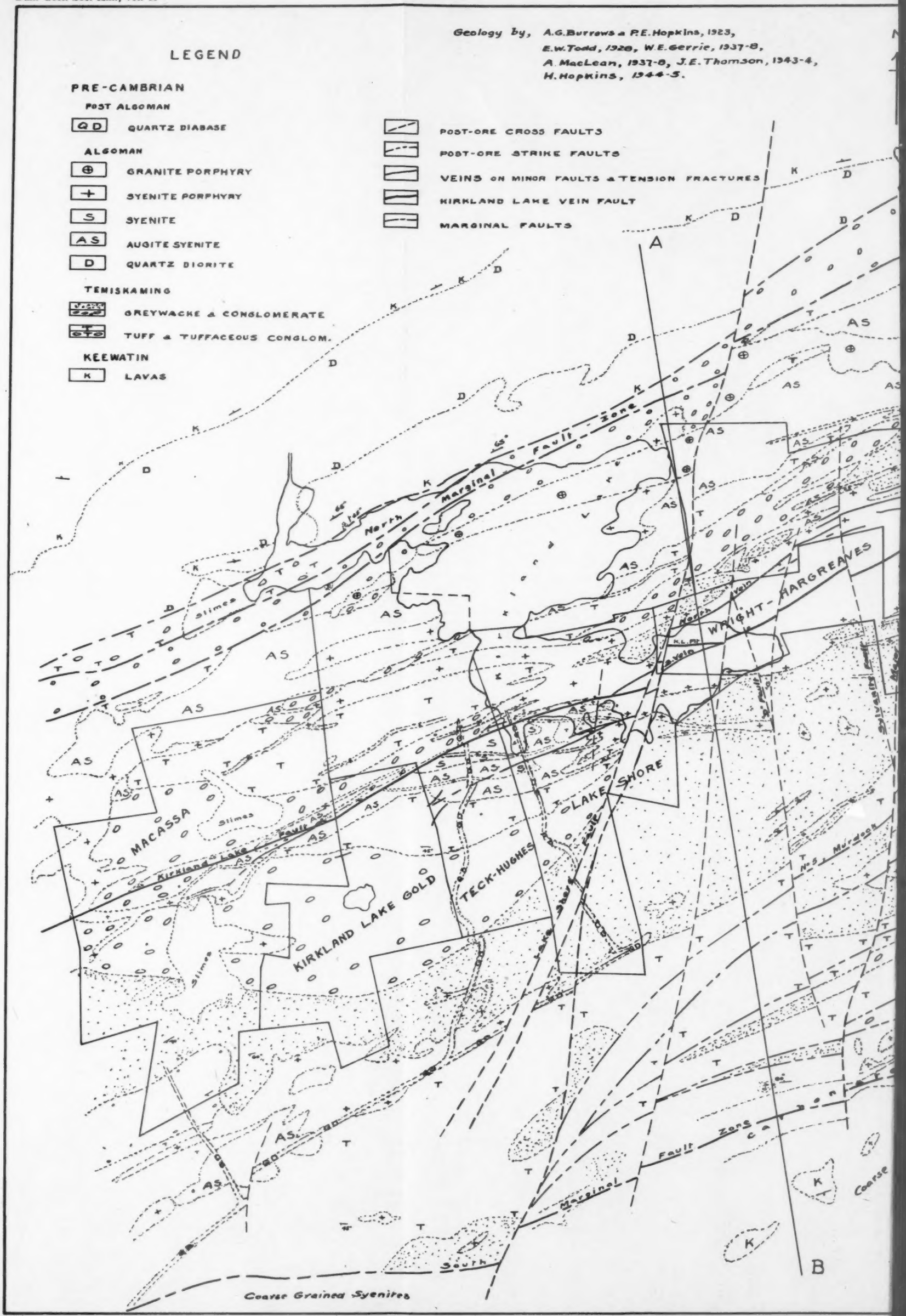

GEOLOGICAL PLAN, KIRKLAND LAKE, ONT

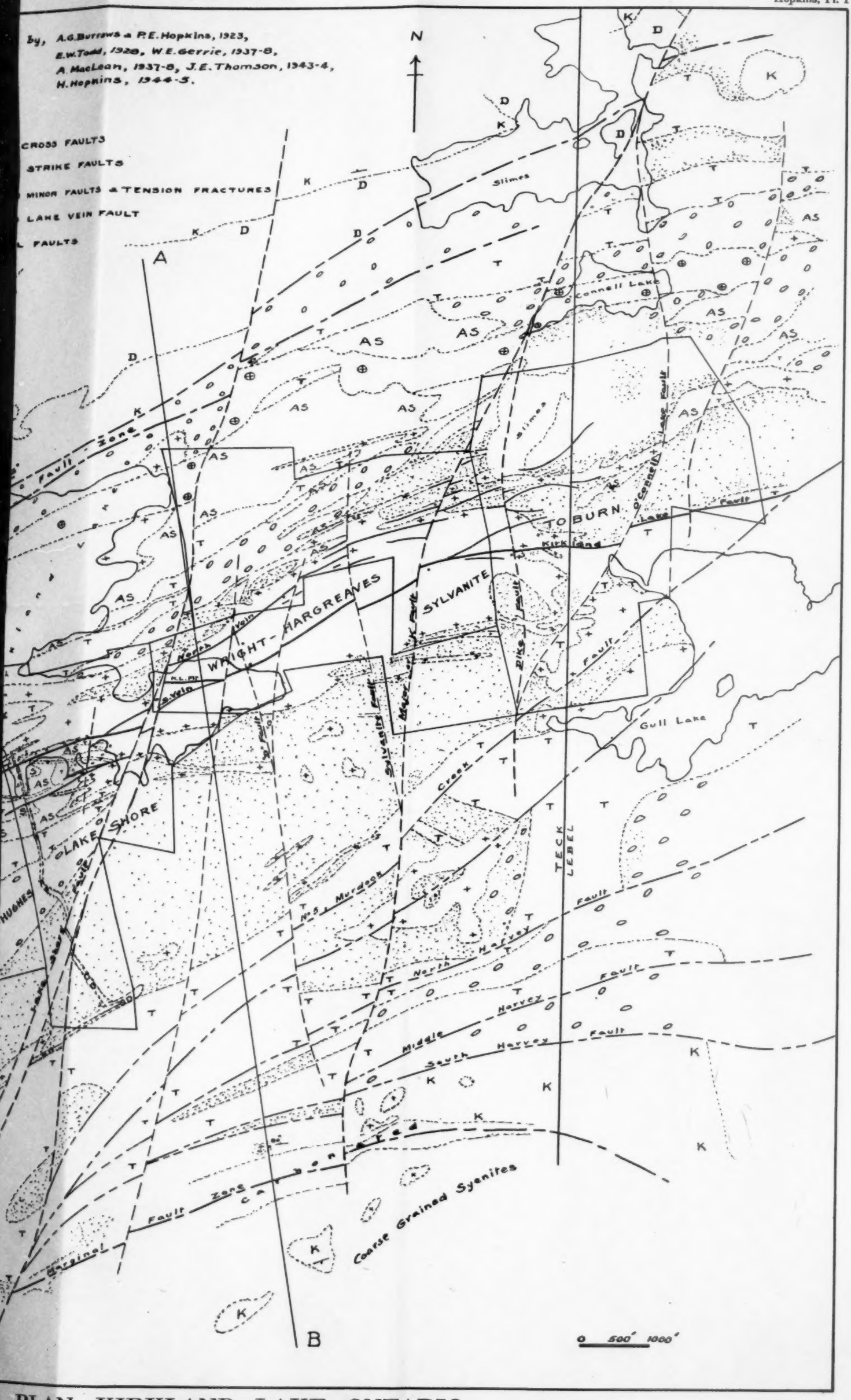

PLAN, KIRKLAND LAKE, ONTARIO

BULLETIN OF THE GEOLOGICAL SOCIETY OF AMERICA
VOL. 60, PP. 909-922, 1 PL., 10 FIGS. MAY 1949

STRUCTURE AT KIRKLAND LAKE, ONTARIO, CANADA

BY HAROLD HOPKINS

CONTENTS

	Page
Abstract	909
Introduction	910
Structural relationship to major gold belts	910
General geology	910
Kirkland Lake fault trough or graben	912
Kirkland Lake fault and subsidiary structures	914
Post-ore faulting	920
Summary	922
References cited	922

ILLUSTRATIONS

Figure	Page
1. Sketch showing relation between faults at Kirkland Lake and some major fault zones in Ontario and Quebec	911
2. Section along A-B of Plate 1	913
3. Plans showing relation of subsidiary vein faults and tension fractures to the Kirkland Lake fault	914
4. Composite plan showing attitude of the two major intrusives	915
5. Section 5200 feet west of A–B of Plate 1	916
6. Section 700 feet east of A–B of Plate 1	917
7. Section 6000 feet west of A–B of Plate 1	918
8. Section 5500 feet west of A–B of Plate 1	919
9. Section 400 feet west of A–B of Plate 1	920
10. Section 1700 feet east of A–B of Plate 1	921

Plate	Facing page
1. Geological plan, Kirkland Lake, Ontario	909

ABSTRACT

The structure at Kirkland Lake, Ontario, Canada, has been influenced by faults of several ages. Rocks present in the area are Keewatin lavas and agglomerates, Temiskaming sediments, and Algoman intrusives. The ores occur in the sediments and later intrusives and are cut by quartz diabase dikes.

The north and south margins of the 2-mile-wide sedimentary belt are found highly sheared by faulting, and this belt of younger rocks appears to be in a fault trough or graben, the older Keewatin rocks being found outside the marginal fault zones.

The several Algoman intrusive stocks have their larger axes roughly paralleling the strike of the sediments, have a general westerly plunge, and a divergence in dips of the north and south contacts causes a widening with depth.

The vein structures are thrust faults and associated tension fractures. The main vein fault, the Kirkland Lake fault, occurs slightly to the north of the center of the sedimentary belt, strikes N. 67° E., dips steeply south, and, cutting through the sedi-

ments and intrusives, has a thrust of 1400 feet. Vein faults of smaller movements branch off this fault on the footwall side in the east half of the camp and on the hanging wall side in the west half with the tension fractures showing the same relationship.

Post-ore faulting of several ages is evident, the earliest being a horizontal movement along the Kirkland Lake fault followed by strike faulting and rotatory cross faulting, each of two ages.

INTRODUCTION

Kirkland Lake, nearly 400 miles north of Toronto, is situated in Teck Township, District of Temiskaming, Province of Ontario, 48°9′ N. Lat. 80°3′ W. Long., at 1038 feet above sea level. Study of the structure of the area has been assisted by underground workings in seven contiguous gold mines extending over 3 miles laterally and 7200 feet vertically. From west to east the mines are Macassa, Kirkland Lake Gold, Teck-Hughes, Lake Shore, Wright-Hargreaves, Sylvanite, and Toburn (Pl. 1).

W. H. Wright first discovered gold in 1911, and further discoveries were made in 1912 by the Tough brothers and H. Oakes. Beginning in 1915, the seven mines have produced half a billion dollars from ore averaging a little better than .5 ounce per ton. The average fineness of the bullion is around 853, while that of the native gold is 941.

STRUCTURAL RELATIONSHIP TO MAJOR GOLD BELTS

Much progress has been made recently in correlating many different mining areas with major structural belts. W. G. Miller (Knight, 1924) pointed out that some deposition of gold in Ontario was related to belts of sediments, and in 1915 P. E. Hopkins (Knight, 1924) suggested that the sediments at the Croesus Mine (Fig. 1) were continuous with those of the Porcupine camp 50 miles west. C. W. Knight (1924) mapped two gold belts in northeast Ontario stretching 70 miles to the Quebec border. These two belts, roughly 30 miles apart, follow bands of Temiskaming sediments which Burrows and Hopkins mapped (1923). Many of the gold deposits were related to intrusive acid porphyries.

Most recent work has shown that most of the workable deposits are associated with belts of sediments and with long regional fault zones. Geologists of the Dominion and Provincial surveys have mapped these fault zones some 100 miles into the Province of Quebec. Wilson (1943), Norman (1943; 1944), and Ambrose (1944) have identified a south fault zone known as the Cadillac-Bouzan Lake fault; Thomson (1941) maps this through Larder Lake and Kirkland Lake, and it may ultimately be traced westward to Matachewan and Midlothian, following the south sedimentary belt. The Porcupine-Destor fault is associated with the north sedimentary belt (Fig. 1).

The association of the workable mineral deposits with these two fault zones is shown (Fig. 1) by the mines which have produced or are producing gold or base metals. Many of the mines are not directly on these major structures but are near by.

GENERAL GEOLOGY

The rocks in the Kirkland Lake area are pre-Cambrian, comprising Keewatin lavas and agglomerates and Temiskaming conglomerates, tuffaceous conglomerates,

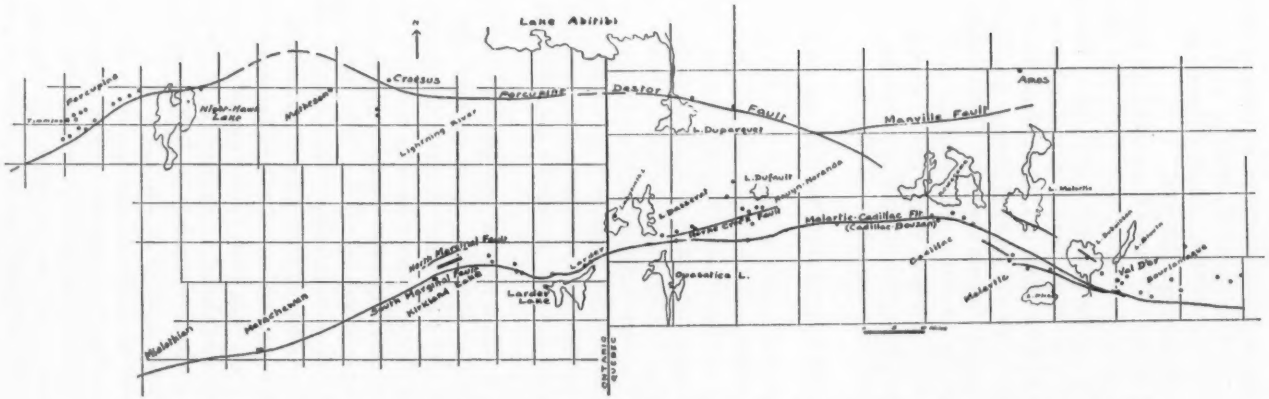

FIGURE 1.—*Sketch showing relation between faults at Kirkland Lake and some major fault zones in Ontario and Quebec*
Location of mines that have produced or are producing shown by circles

tuffs, and graywackes, and Algoman intrusives, in order of their intrusion: augite syenite, syenite, syenite porphyry, granite porphyry, quartz syenite, and granite, all premineral and closely related in time. Distinctly later, and after the deposition of the ores, quartz diabase dikes were intruded.

The surface geological plan (Pl. 1) shows Keewatin rocks south of the south marginal fault zone, which is usually aligned with the Larder Lake-Cadillac-Bouzan Lake fault zone, and north of a north marginal fault zone. Between these two fault zones, which are about 2 miles apart, lies the belt of sedmentary rocks with their intrusives. Slightly north of the center of the belt occurs the Kirkland Lake fault. The ores are along this structure and its subsidiaries. The sedimentary beds have the general attitude of the north limb of a syncline in which minor cross folds occur; their strike is within a few degrees of that of the marginal fault zones, and the longer of the horizontal axes of the intrusive stocks follows similar trends. The major intrusives are wedge-shaped in section, thickening with depth due to diverging contacts, and dip more steeply than the sediments (Fig. 4).

KIRKLAND LAKE FAULT TROUGH OR GRABEN

A section (Fig. 2) shows the major structure. The attitude of the south fault zone is not known from underground workings, but on surface the nearly vertical shearing in the tuffs over a width of some 300 feet indicates a steep-dipping fault. A carbonate zone, such as occurs irregularly along the major fault zones that traverse the country, is present on the south side of the fault. On the line of section, the Keewatin lavas south of the south marginal fault zone occur only as remnants in a coarse-grained syenite, but in larger areas near by the lavas dip and face south. Just north of the fault in a small outcrop of interbedded graywacke and conglomerate these beds dip steeply north and may represent a portion of the south side of the main sedimentary syncline.

The north marginal fault zone is better known from diamond drilling from surface and underground to a depth of 3000 feet. As on the south side, the sediments are almost vertically sheared over a few hundred feet, and scattered carbonate zones are encountered. Quartz diabase dikes are offset by the faults, indicating that some of the movement was post quartz diabase. North of the fault the massive-looking Keewatin lavas are well exposed and dip 65° N. Thus the general structure of the Keewatin here is that of an east-west anticline. While faults in this zone are actually seen on the surface, their presence could be inferred structurally. West of the section is a small outlier, a few yards square, of bedded Temiskaming graywackes lying in the Keewatin lavas. These beds strike N. and dip 25° E., indicating not only an unconformity with the lavas, which strike approximately N. 60° E. and dip 65° NW., but also a fault, because the sediments across the fault, a few feet south of the outlier, strike E., and dip steeply south or are vertical.

Thus the major structure at Kirkland Lake appears to be a graben, the folded Temiskaming sediments having been dropped between steep-dipping faults 2 miles apart and in the region of an anticlinal fold in the Keewatin. The throws on these faults, apparently thousands of feet, are not measurable at present; in the center of the trough, the Temiskaming sediments are still present at a depth of 7000 feet.

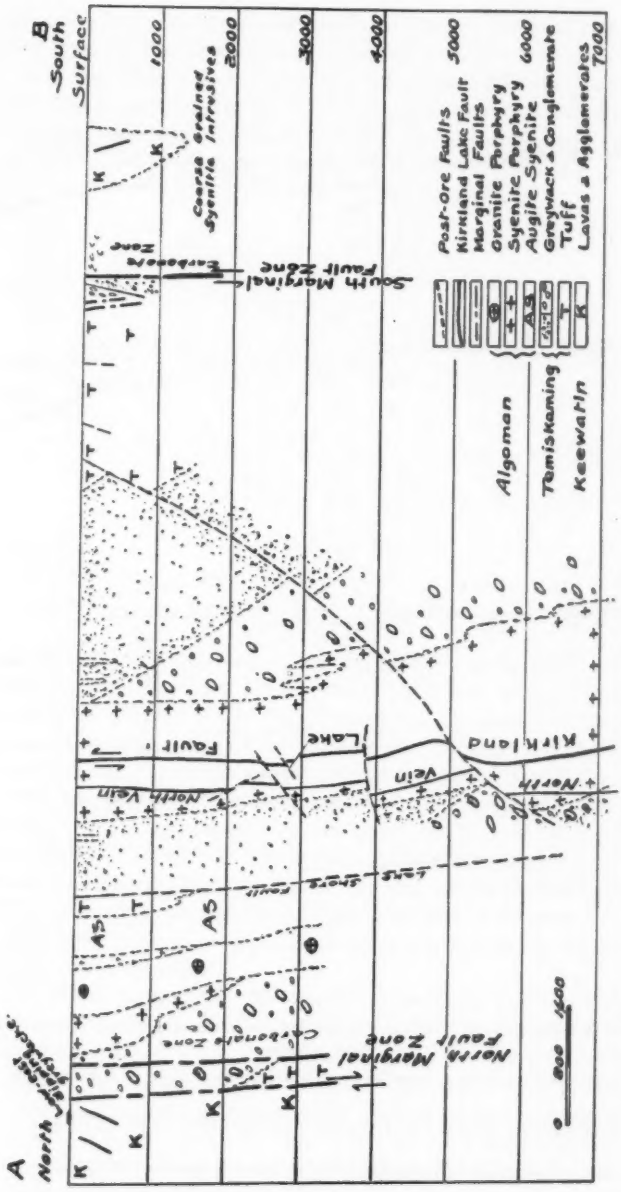

FIGURE 2.—*Section along A–B of Plate 1*
Showing Kirkland Lake fault trough or graben

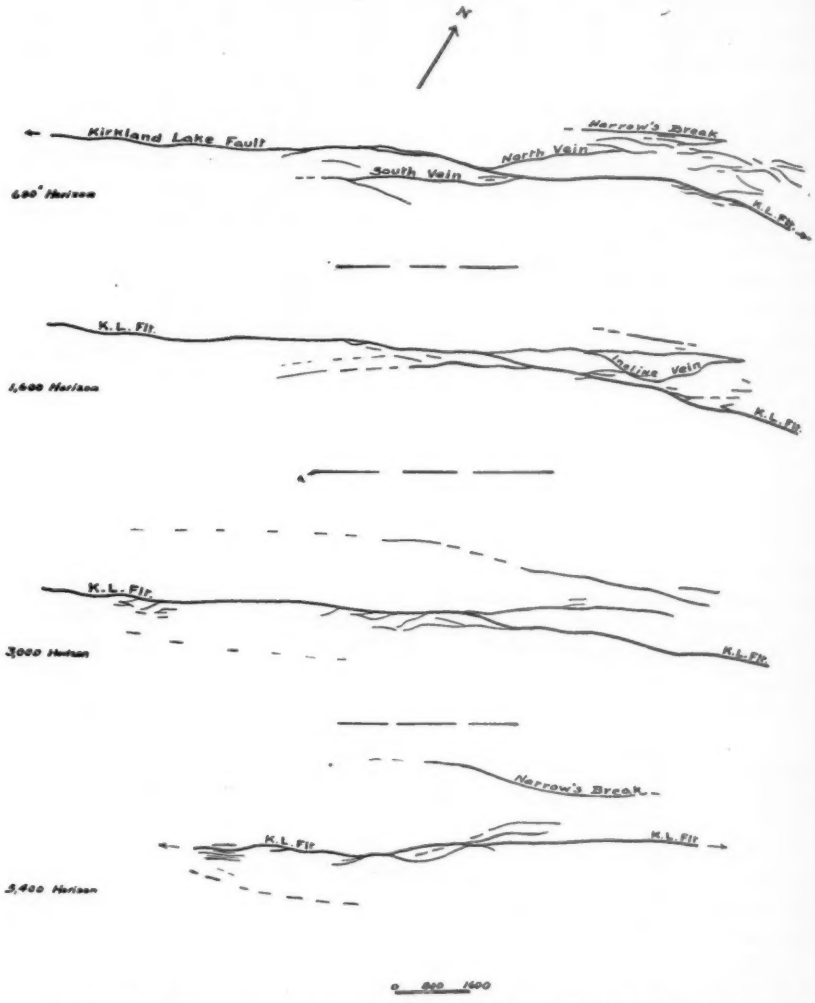

FIGURE. 3.—*Plans showing relation of subsidiary vein faults and tension fractures of the Kirkland Lake fault*

Different horizons are shown, as well as the relationship after adjusting for post-ore faults

KIRKLAND LAKE FAULT AND SUBSIDIARY STRUCTURES

Economically, the Kirkland Lake fault is the most important in the area. Located just north of the center of the trough (Pl. 1), it strikes N. 67° E., roughly parallel to the sedimentary belt, dips steeply south, and has been followed in mine workings to a depth of 7000 feet.

Tyrrell and Hore (1926) first described this fault in the west half of the camp. For many years the main structures in the mines were regarded as two parallel faults known as the north and south veins, but the original Kirkland Lake fault of the west half (known partly as the north vein) is apparently continuous with the south vein in the east half. In the center of the camp the structure is known as the diagonal vein (Robson, 1936) running between the north and south veins.

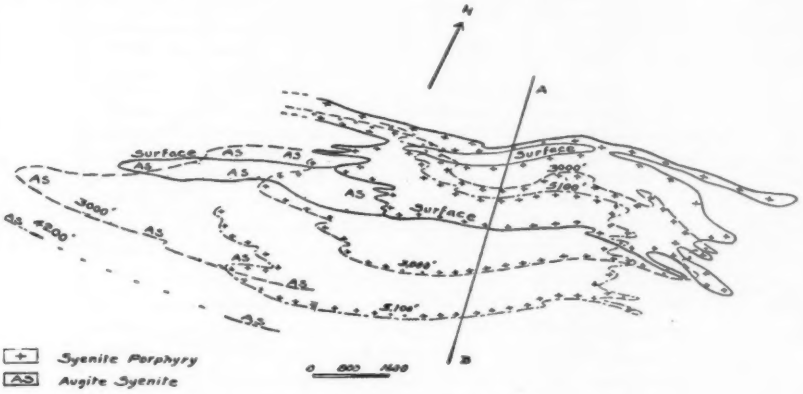

FIGURE 4.—*Composite plan showing attitude of the two major intrusives*

Geological sections on the footwall and hanging wall of the fault show correlation of the various rocks, and vertical movement of 1400 feet is apparent. Mylonite is present along the old fault plane, and the south side has moved relatively up. Post-ore horizontal movement along the fault is shown by offsetting of the quartz diabase dikes some 100 feet east on the south side, and the latest plane of movement is represented by gouge, chlorite, calcite, quartz, barite, and gypsum. The fault may be represented by a single plane or by two or three planes a few feet apart. In places the fault shows splits with planes that reach 100 feet apart, and these form bows in the structure, on plan and section (Figs. 3, 5), which may extend over several hundred feet. Where more than one plane is present, the ground between the faults is disturbed by cross-over faults; regions where these are plentiful in the bow structures provide the widest ore bodies.

Just east of the center of the camp two important vein faults, on which the north and south veins occur, branch off either side of the Kirkland Lake fault. The South vein fault, branching off the hanging wall, extends westerly and, while the dip on upper levels is very steep, on lower levels the fault appears to parallel the flatter south contact of the augite syenite (Fig. 4). The south side of the fault moved relatively up some 500 feet, and offsetting of the quartz diabase dikes indicates later horizontal movement similar to that on the Kirkland Lake fault. The North vein fault branches off the footwall of the Kirkland Lake fault and is traced to the east end of the camp where it dies out. This fault dips steeply south and roughly parallels the north contact of the main syenite porphyry stock (Figs. 2, 4; Pl. 1). In some

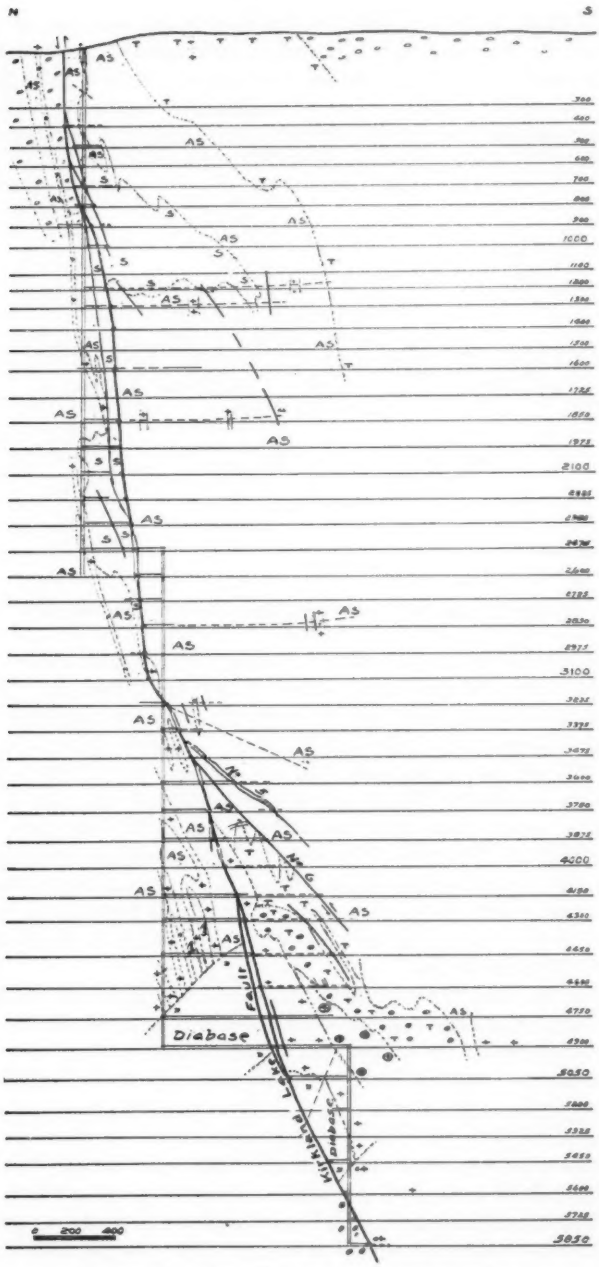

FIGURE 5.—*Section 5200 feet west of A–B of Plate 1*

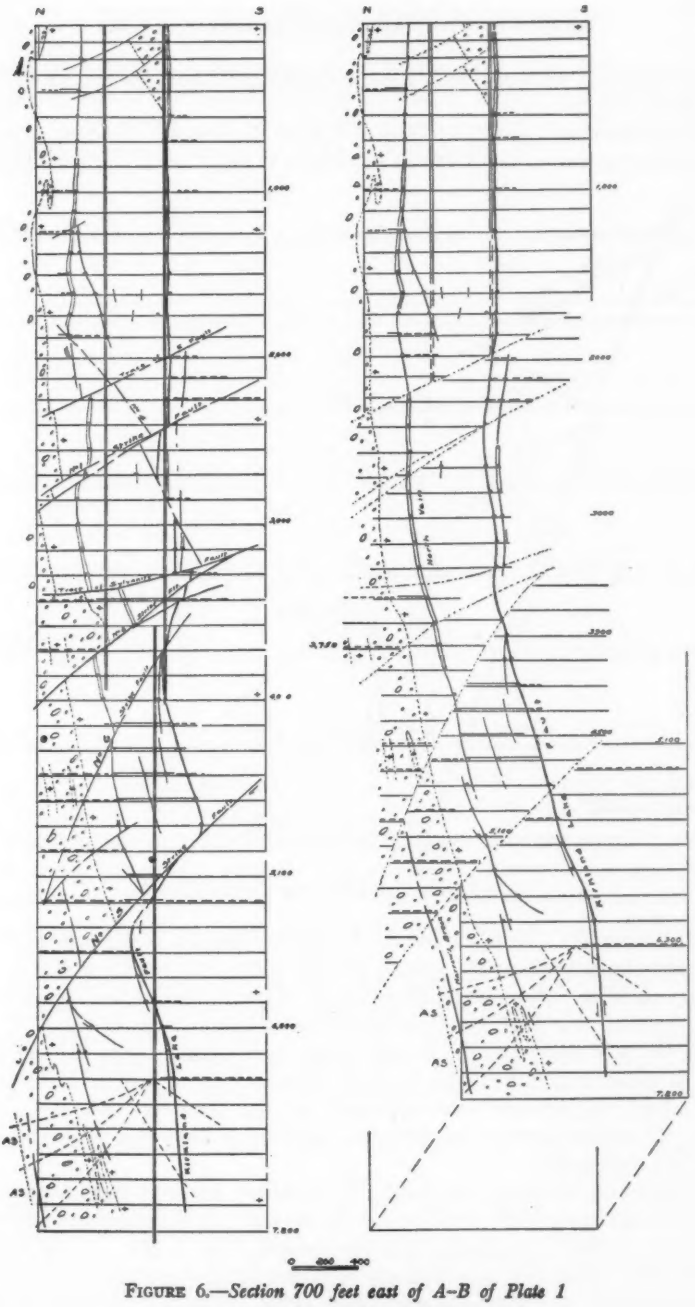

FIGURE 6.—*Section 700 feet east of A–B of Plate 1*
Drawing at right shows section with faults restored

regions, especially on upper levels, the trace of this fault is represented by en echelon structures (Fig. 10).

Another important fault, No. 6 (Figs. 5, 7, 8), in the west half of the camp branches off the hanging wall of the Kirkland Lake fault at lower levels and diverges to the

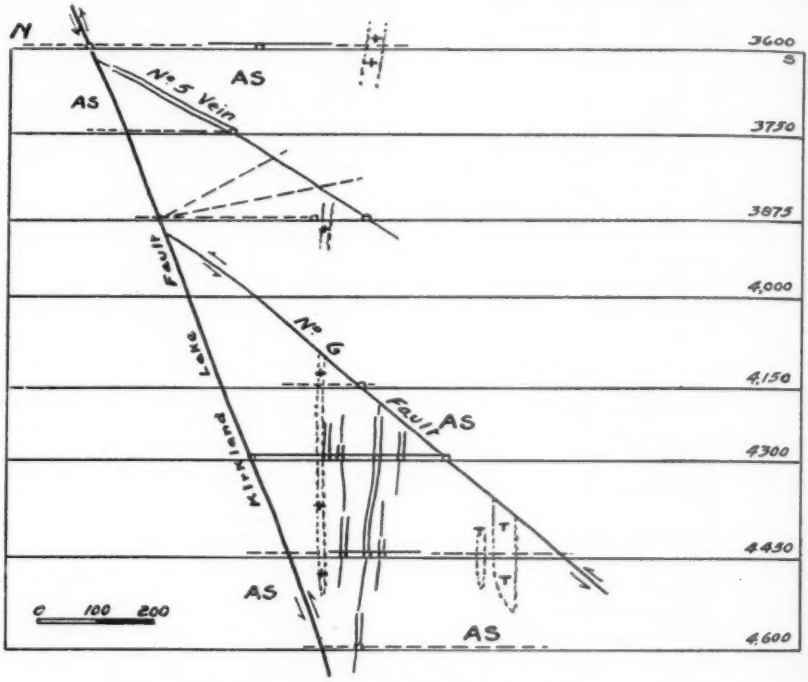

FIGURE 7.—*Section 6000 feet west of A–B of Plate 1*

east, at a low angle. It dips about 40° S., and the junction of the two faults shows a westerly plunge of about 25°, roughly parallel to the plunge of a remnant of a sedimentary anticline. More than 1000 feet north of the Kirkland Lake fault is another, nearly parallel, vein fault known as the Narrows Break (Figs. 3, 10).

Vein faults of lesser magnitude were formed coincidentally with the larger ones. Some of these parallel the major faults in strike and dip or perhaps in strike only, while others angle between these structures with dips from vertical to low, north or south. Favorable locations for these structures are in the wedge-shaped blocks between the main faults.

An interesting feature is the transfer of subsidiary vein structures from one side of the Kirkland Lake fault to the other. In the east half the structures extend over a width of 1500 feet, practically all in the footwall (Figs. 6, 10). In the west half, the subsidiary structures are practically negligible in the footwall but are present in the hanging wall, particularly in lower levels (Figs. 5, 7, 8). These features suggest

torsional strains during the formation of the vein faults. The relationship between the minor vein faults and the Kirkland Lake fault at different horizons is shown in Figure 3. Compensation has been made for post-ore faults so that the structures are those at the time of formation of the vein structures.

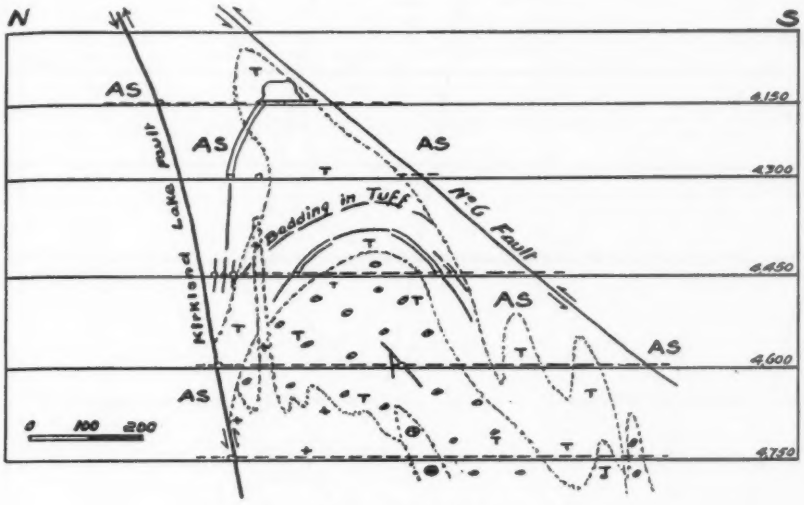

FIGURE 8.—*Section 5500 feet west of A–B of Plate 1*

Rock contacts are not favorable for formation of vein structures, but the latter often parallel such contacts (Figs. 6, 8). In Figure 8, a curving vein is seen in the tuff, paralleling the contact between that rock and tuffaceous conglomerate. Vertical tension fractures in a fault wedge formed between the Kirkland Lake and the low-dipping No. 6 faults are shown in Figure 7; and north-dipping tension fractures (often with low dips) are seen between the steep-dipping Kirkland Lake and South vein faults in Figure 9.

The ore deposits are found on the Kirkland Lake fault and subsidiary structures and are associated with all the Temiskaming and Algoman rocks. The principal gangue minerals, present in small proportions, are quartz and calcite. Minerals in very small amounts are albite, orthoclase, ankerite, barite, tourmaline, actinolite, and apatite. Secondary minerals are represented by sericite, carbonates, chlorite, and pyrite.

Gold, of late deposition, is associated with auriferous pyrite, the tellurides calaverite, petzite, altaite, coloradoite, and melonite, plus minor amounts of chalcopyrite, hematite, galena, sphalerite, molybdenite, and graphite.

The largest ore shoots are vertical and without apparent zoning.

A late filling of glassy quartz and calcite, along with some barite and gypsum along the vein structures, followed the late post-ore movements.

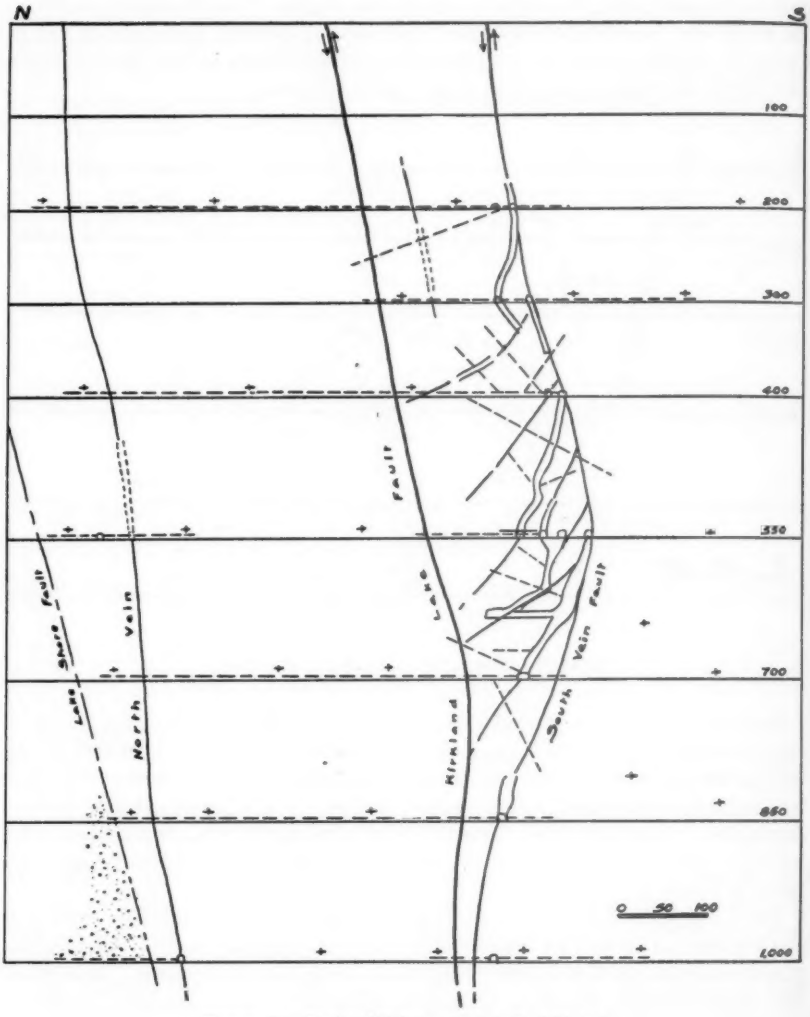

FIGURE 9.—*Section 400 feet west of A–B of Plate 1*

POST-ORE FAULTING

In addition to the horizontal post-ore movements on the Kirkland Lake fault and other vein structures, post-ore faulting of at least four ages has been described by the writer (1940; 1941). The faults occur mainly in the east half of the camp (Fig. 6; Pl. 1); they occur as strike faults and later cross faults. An earlier strike fault has a southerly dip, but the later and larger ones dip north. The largest of

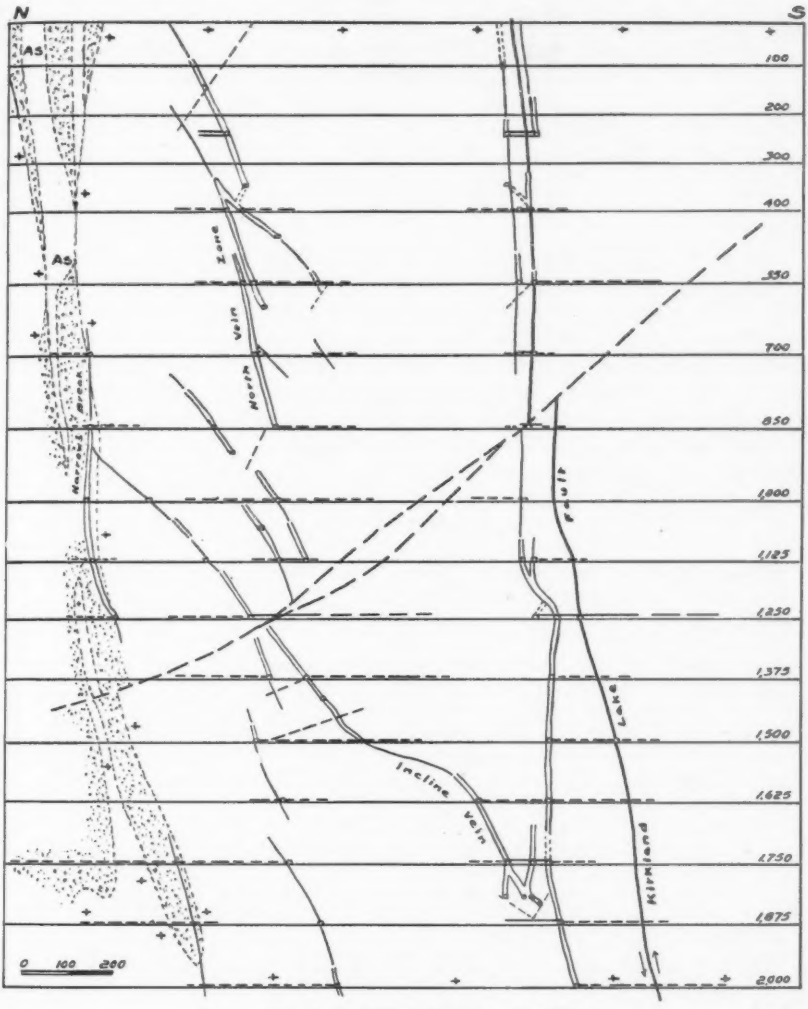

FIGURE 10.—*Section 1700 feet east of A–B of Plate 1*

all, No. 5, is a curving structure in dip and strike: 2 miles south of the ore zone this fault is more like a cross fault, striking north and south, but in the ore zone it strikes parallel to the ore bodies, N. 65° E., while the dip varies from 45° N. on upper horizons to 80° N. on the lower ones. The movement has been shown to be an underthrust (1940), and the displacement seen on this fault is approximately 700 feet. Though this strike fault cuts cleanly the rock contacts and subsidiary vein structures, it tends to drag the strongest structure, the Kirkland Lake fault (Fig. 6).

The cross faults, which displace the strike faults as well as the veins, are rotatory, the pivotal points being north of the ore zone to a maximum of 8000 feet. Some of these theoretical points are above the present surface, while in one case the point is 8600 feet deep. The movements on these faults are usually determined with the help of sections drawn on the hanging wall and footwall of each fault; these show the throws and heaves varying from 100 to 550 feet.

SUMMARY

The ore zone at Kirkland Lake is in an area showing evidence of much igneous activity and instability, reflected in faulting of various ages and under varying conditions. It is also associated with a regional fault zone which appears to form the southern margin of the Kirkland Lake fault trough. The ores are intimately connected with the Kirkland Lake fault system which cuts through the downfaulted and folded Temiskaming sediments and Algoman intrusives. The instability of the area following the deposition of the ores is shown by the alternate periods of tension and compression during which quartz diabase dikes are intruded, thrust faults are formed, and normal cross faults result.

REFERENCES CITED

Ambrose, J. W. (1944) *Preliminary map, Duparquet-Larder-Rouyn region, Ontario and Quebec*, Geological Survey Canada, Paper 44-29.

Burrows, A. G., and Hopkins, P. E. (1923) *Kirkland Lake gold area*, Ontario, Dept. Mines, vol. 32, Pt. 4, p. 1–52.

Hopkins, Harold (1940; 1941) *Faulting at the Wright-Hargreaves mines, with notes on ground movements*, Canad. Inst. Min. Metall., Tr., vol. 43, p. 685–707; Tr., vol. 50, p. 295–319 (1941).

Knight, C. W. (1924) *Lightning River gold area*, Ontario Dept. Mines, vol. 33, pt. 3, p. 41–49.

Norman, G. W. H. (1943) *Notes on the structure of the Cadillac-Bourlamaque area, Abitibi County, Quebec*, Geological Survey Canada, Paper 43-6 (1944). Preliminary map, Rouyn-Malartic-Destor region, Abitibi and Témiscamingue counties, Quebec, Geological Survey Canada, Paper 44-27.

Robson, W. T. (1936) *Lake shore geology*, Canad. Inst. Min. Metall., Tr., vol. 39, p. 99–141.

Thomson, J. E. (1941) *Geology of McGarry and McVittie townships, Larder Lake area*, Ontario Dept. Mines, vol. 50, pt. 7, 99 p.

Todd, E. W. (1928) *Kirkland Lake gold area*, Ontario Dept. Mines, vol. 37, pt. 2, 176 p.

Tyrrell, J. B., and Hore, R. E. (1926) *The Kirkland Lake fault*, Royal Society Canada, Pr. Tr., 3rd ser., vol. 20, sec. 4, p. 51–63.

Wilson, M. E. (1943) *Preliminary maps Rouyn-Beauchastel, Temiskamingue County, Quebec*, Geological Survey Canada, Paper 43-7.

Wright Hargreaves Mines, Kirkland Lake, Ontario

Manuscript Received by the Secretary of the Society, July 2, 1948

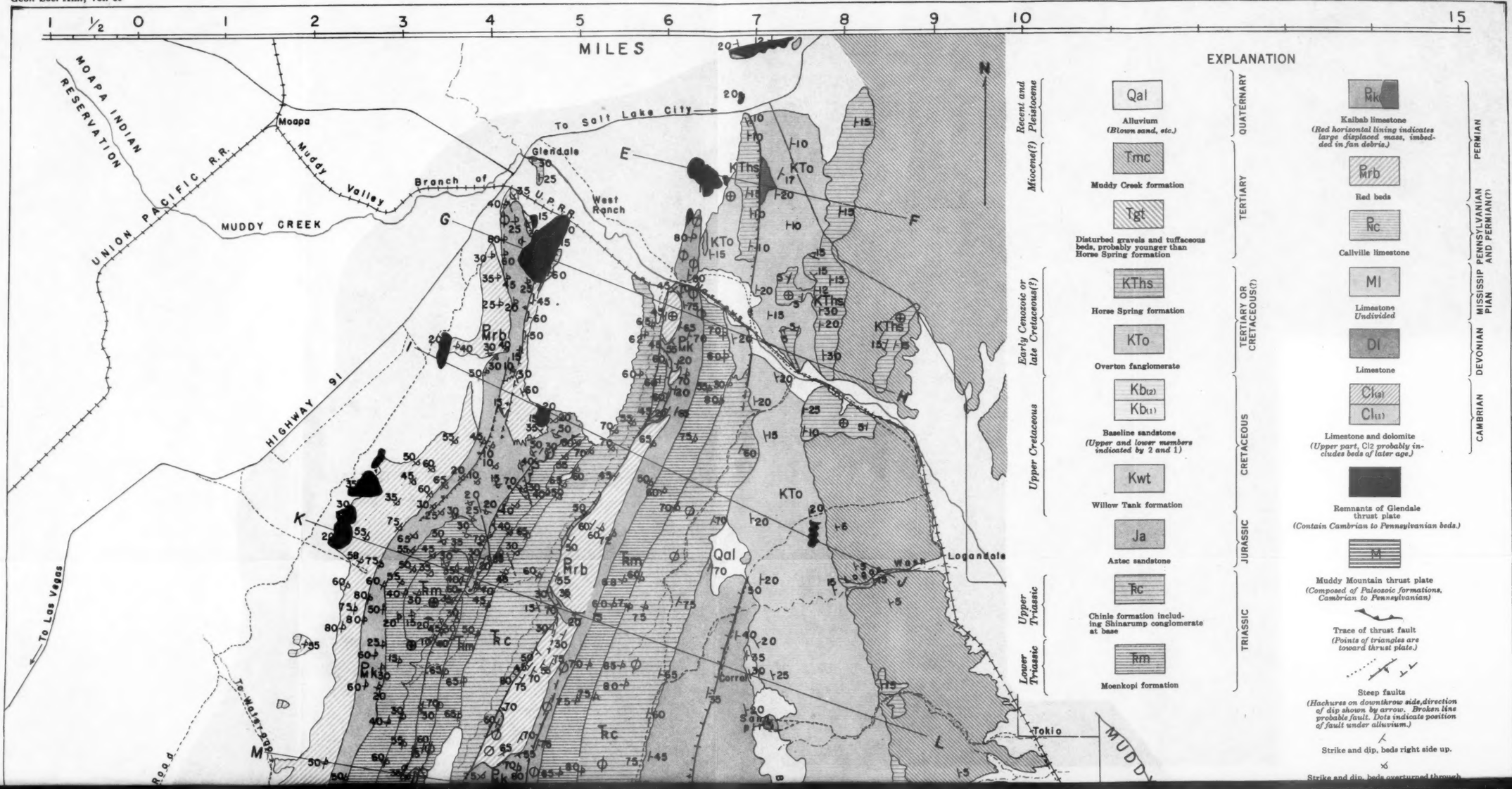

EXPLANATION

Recent and Pleistocene	Qal	Alluvium *(Blown sand, etc.)*	QUATERNARY
Miocene(?)	Tmc	Muddy Creek formation	TERTIARY
	Tgt	Disturbed gravels and tuffaceous beds, probably younger than Horse Spring formation	
Early Cenozoic or late Cretaceous(?)	KThs	Horse Spring formation	TERTIARY OR CRETACEOUS(?)
	KTo	Overton fanglomerate	
Upper Cretaceous	Kb(2) / Kb(1)	Baseline sandstone *(Upper and lower members indicated by 2 and 1)*	CRETACEOUS
	Kwt	Willow Tank formation	
	Ja	Aztec sandstone	JURASSIC
Upper Triassic	Tc	Chinle formation including Shinarump conglomerate at base	TRIASSIC
Lower Triassic	Trm	Moenkopi formation	
	Pmk	Kaibab limestone *(Red horizontal lining indicates large displaced mass, imbedded in fan debris.)*	PERMIAN
	Prb	Red beds	
	Pc	Callville limestone	PENNSYLVANIAN AND PERMIAN(?)
	Ml	Limestone *Undivided*	MISSISSIPPIAN
	Dl	Limestone	DEVONIAN
	Cl(2) / Cl(1)	Limestone and dolomite *(Upper part, Cl2 probably includes beds of later age.)*	CAMBRIAN
		Remnants of Glendale thrust plate *(Contain Cambrian to Pennsylvanian beds.)*	
	M	Muddy Mountain thrust plate *(Composed of Paleozoic formations, Cambrian to Pennsylvanian)*	

Trace of thrust fault *(Points of triangles are toward thrust plate.)*

Steep faults *(Hachures on downthrow side, direction of dip shown by arrow. Broken line probable fault. Dots indicate position of fault under alluvium.)*

Strike and dip, beds right side up.

Strike and dip, beds overturned through

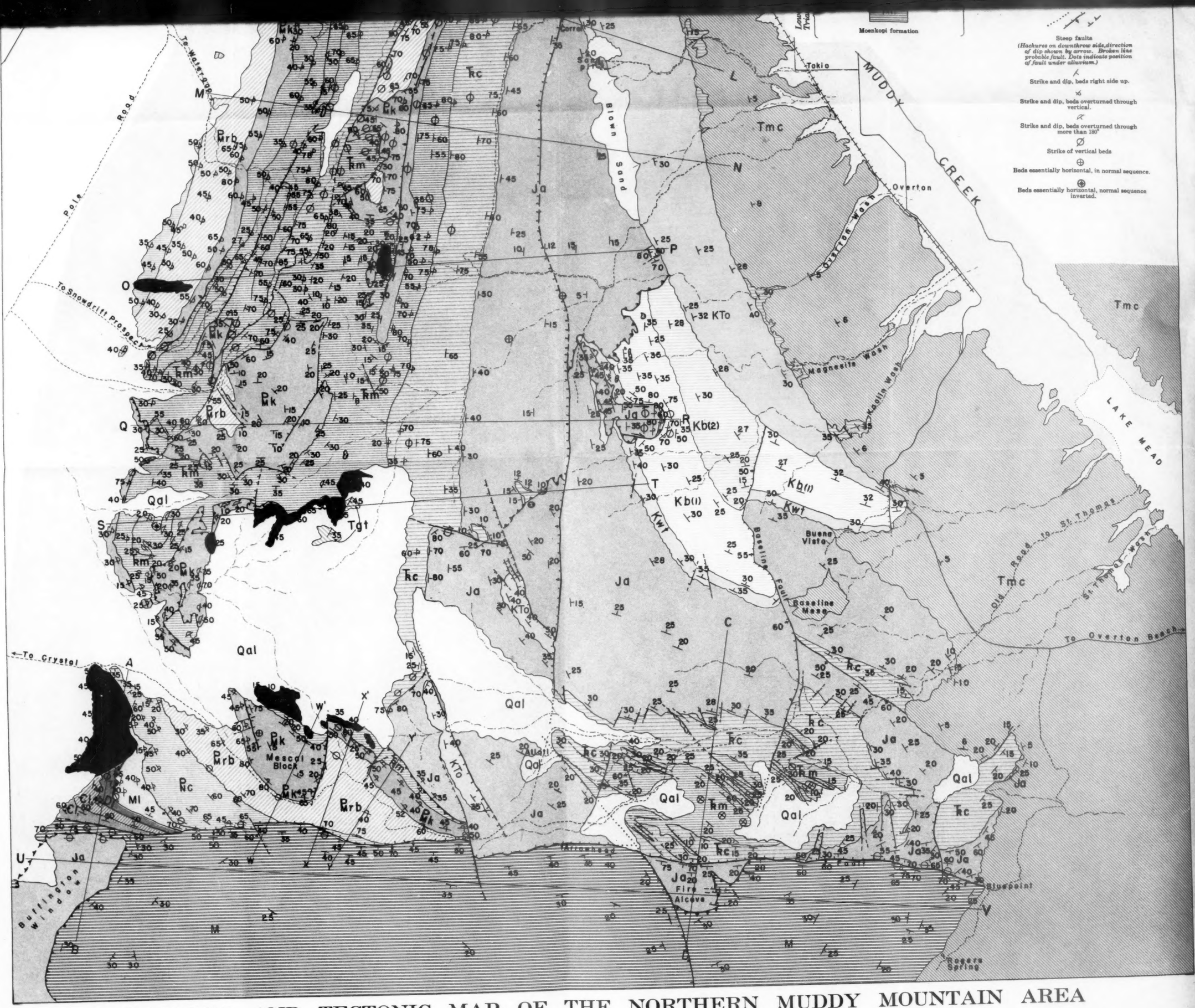

GEOLOGIC AND TECTONIC MAP OF THE NORTHERN MUDDY MOUNTAIN AREA

BULLETIN OF THE GEOLOGICAL SOCIETY OF AMERICA
VOL. 60, PP. 923-966, 14 FIGS, 11 PLS. MAY 1949

STRUCTURE OF THE NORTHERN MUDDY MOUNTAIN AREA, NEVADA

BY CHESTER R. LONGWELL

CONTENTS

	Page
Abstract	924
Introduction	925
Acknowledgments; field work	925
Regional setting; topography	926
Stratigraphy	926
Paleozoic formations	926
Mesozoic formations	931
Triassic and Jurassic	931
Cretaceous	931
Undated formations—Cretaceous or Cenozoic	933
Cenozoic formations	936
Structure	937
General statement	937
Muddy Mountain thrust and Arrowhead fault	937
Glendale thrust and related features	938
General discussion	938
Weiser syncline	941
Narrows anticline	944
Faults within the belt of thrusting	945
Remnants of the Glendale plate	946
Masses dragged and pushed by the thrust plate	949
Willow Tank thrust	950
Transverse faults	952
Summit thrust	953
Valley-of-Fire anticline	955
Normal faults	955
Interpretation of the evidence	959
Relation between Muddy Mountain and Glendale thrusts	959
Arrowhead fault and Valley-of-Fire anticline	960
Possible development of the Glendale thrust	963
Normal faults	964
Geologic dates of structural events	965
References cited	966

ILLUSTRATIONS

Figure	Page
1. Index map	927
2. Topographic map of northern part of Muddy Mountains and surrounding area	928
3. Geologic map of principal areas underlain by Cretaceous formations	934
4. Section through the Muddy Mountain thrust plate	939
5. Hypothetical restoration of the Muddy Mountain thrust	940

Figure Page
6. Section showing relation between Glendale and Muddy Mountain thrusts 940
7. Section through Valley-of-Fire anticline and Arrowhead fault 940
8. Simplified restoration of the recumbent Weiser syncline 942
9. Block diagram to explain outcrops in southern part of the Weiser syncline 944
10. Generalized section through the Glendale thrust zone before final deformation and erosion 948
11. Sections showing structure within the Mescal and Summit blocks 953
12. Sections through Valley and Waterpocket faults, to show probable evolution of structure .. 958
13. Diagram showing Arrowhead fault trace in relation to average trend within Glendale thrust belt 962
14. Sections showing possible stages in development of Glendale thrust 964

Plate Facing page
1. Geologic and tectonic map of the northern Muddy Mountain area 923
2. Aerial view southwest across Muddy Mountains 938
3. Aerial view northeast along Buffington anticline and window 939
4. Map outlining principal structural features of the area 940
5. West-east structure sections through Glendale thrust zone 942
6. Vertical view at west end of Arrowhead fault 944
7. Vertical view of Weiser syncline (right) and Narrows anticline 945
8. Fragment of Kaibab limestone piercing limb of recumbent syncline 946
9. Oblique aerial view eastward along Arrowhead fault and Valley-of-Fire anticline 947
10. Views showing fracture sets and faults cutting Jurassic and Cretaceous beds 956
11. Vertical view showing features near east end of Arrowhead fault 957

ABSTRACT

Instead of a single large thrust in the Muddy Mountain area, Nevada, as reported from earlier field study, the writer distinguishes two superposed thrusts which may represent distinct orogenic episodes separated by a considerable time interval. Both thrusts "root" to the west. The structurally lower thrust (for which the name Muddy Mountain thrust is retained) is the more extensive; as reported previously, it has brought Paleozoic carbonate formations over Jurassic sandstone, with the heave-component of slip at least 15 miles. The higher thrust (here called the Glendale thrust) has heave-displacement of at least 5 miles. Together with associated smaller thrusts, it involves formations of early Upper Cretaceous age, as well as thick piedmont deposits that may be considerably younger. "Orogenic deposits" several thousand feet thick were laid down in front of the Glendale thrust as it advanced. Accurate dating of these strata would give an exceptional record of structural events.

Conglomerate at the base of the Upper Cretaceous section, containing boulders and cobbles derived from resistant units in older systems as low as the Permian, indicates earlier strong deformation not far west of the Muddy Mountain area. This earlier orogenic episode may have included development of the Muddy Mountain and other large thrusts in the region which are not known to involve formations younger than Jurassic. Therefore the earlier orogeny can now be dated merely as post-Jurassic and pre-Upper Cretaceous.

Overturned and faulted folds associated with the Glendale thrust rival in complexity some structural features of the Swiss Alps. Important transverse faults with large strike-slip component pose problems of origin; the largest of these displaces the Muddy Mountain thrust plate as much as 2 miles vertically and may be genetically related to the Glendale thrust. Numerous normal faults, variously oriented, bear witness to movements ranging in date from the Glendale thrusting episode to late Cenozoic time.

INTRODUCTION

In 1919 the writer studied the Muddy Mountains as part of a larger area in southern Nevada and western Arizona. Since the field area was far too large for detailed mapping in one season, much of the work was necessarily of reconnaissance nature. Stratigraphic and structural features revealed by the study were of such interest that more detailed investigation of critical units in the area was planned. Unfortunately the summer climate in this low-altitude portion of southern Nevada almost prohibits effective mapping, and therefore continuation of the project could not be fitted into a full-time University schedule. After several years the results of the initial study were published without benefit of thorough field revision (1928).

In 1941 the writer secured leave in the winter and spring months, in order to resume field studies in this area. Although more than 20 years had elapsed since the first attempt, several intervening seasons had been spent in higher ranges southwest of the Muddy Mountains, and the early months of 1934 were devoted to study along the Colorado River above the Hoover Dam (1936). Thus later study was based on considerable acquaintance with the regional geology and was begun with definite objectives.

ACKNOWLEDGMENTS; FIELD WORK

The Geological Society of America granted funds to cover expenses of the field work, and the United States Geological Survey furnished a truck and other field equipment. Yale University granted the writer leave of absence during the part of the year most favorable for field work in the Nevada desert. All of this generous aid is gratefully acknowledged. Richard Merriam and Jacob Emery were capable field assistants.

Intensive work was restricted to the northern part of the Muddy Mountains, comprising about 150 square miles. The chief goals were an accurate geologic map of this area, delineation of the structural features, and securing of evidence for dating structural events.

The only serviceable base map is one of the topographic sheets prepared by engineers of the Metropolitan Water District (California) during preliminary stages of the Hoover Dam project. This map has a scale of about 2 miles per inch and contour interval 100 feet. Relief in most of the area is moderate, and therefore representation of the topography is much generalized, although the major features are recognizable qualitatively. Since this base has little value for accurate representation of the geology, the mapping was done on plane-table sheets, with an explorer's telescopic alidade, to the scale 1.5 inches per mile. A triangulation net was established, instrument stations were located by resection, and stadia rod was used to plot points on formation boundaries and other features. Some 2000 instrumental points were established in this way, to provide dependable horizontal control. Intermediate details were drawn in from vertical airplane photographs furnished near the close of the field season by the U. S. Soil Conservation Service. The enlarged prints, measuring 9 by 11 inches, have a scale of about 4 inches per mile and depict the surface geology with exceptional clarity.

REGIONAL SETTING; TOPOGRAPHY

The Muddy Mountains lie directly west of the lower Virgin River and almost directly north of the "great bend" that changes the general course of the Colorado River from west to south (Fig. 1). The high part of the range, including Muddy Peak, is clearly visible from the vicinity of the Hoover Dam. North of the mountain unit is a wide lowland bordering Muddy Creek, and on the west is the depression occupied by California Wash. Thirty-five to 40 miles airline from the east side of the range, the Grand Wash Cliffs form the abrupt western boundary of the Colorado Plateau (Pl. 9), in which the stratified formations are little disturbed. Thus the Muddy Mountains are separated from the eastern edge of the Basin and Range province by the Virgin Mountain blocks and their bordering structural depressions.

Topographically the Muddy Mountains are separated into two distinct major units by an abrupt north-facing scarp (Fig. 2; Pl. 2). This division reflects important structural differences. South of the scarp is a rugged, irregular mass consisting chiefly of Paleozoic limestones and dolomites in a wide thrust plate. North of the scarp altitudes are comparatively low; bedrock, consisting largely of much-deformed Mesozoic and late Paleozoic formations, is generally weak, though abrupt ridges of moderate height reflect the more resistant stratigraphic units. The present report deals chiefly with the northern division, although the map and sections include a belt south of the dividing scarp to show the major structural relationships.

STRATIGRAPHY

GENERAL STATEMENT

Since most of the rock formations of the area are described elsewhere (Longwell, 1928), and since structural features are the primary concern of the present study, only a brief outline of the stratigraphy will be given here, supplemented by new data that affect descriptions or interpretations of certain formations. Sedimentary deposits related to important tectonic events deserve particular attention.

PALEOZOIC FORMATIONS

As shown in Table 1, Paleozoic strata of Cambrian, Devonian, Mississippian, Pennsylvanian, and Permian age have been recognized in the area. Ordovician and Silurian strata have not been identified, though they may be present. Thick Ordovician and probable Silurian sections are present a short distance west of the Muddy Mountains in the Arrow Canyon range (Fig. 1). In the Muddy Mountain thrust plate about 100 feet of dark-gray limestone, mottled with yellow, strongly resembles part of the Pogonip limestone, which is widespread in southern and central Nevada. The distinctive Eureka quartzite, conspicuous in the Arrow Canyon Range, is not present in the Muddy Mountains. Rapid changes in thickness and character of strata occur northwestward in this belt, toward the axis of the Cordilleran geosyncline. These changes appear all the more abrupt because of foreshortening by large-scale thrusting.

In the Muddy Mountain thrust plate are exhibited the formations ranging from Cambrian to Pennsylvanian; erosion has removed all younger strata. The plate con-

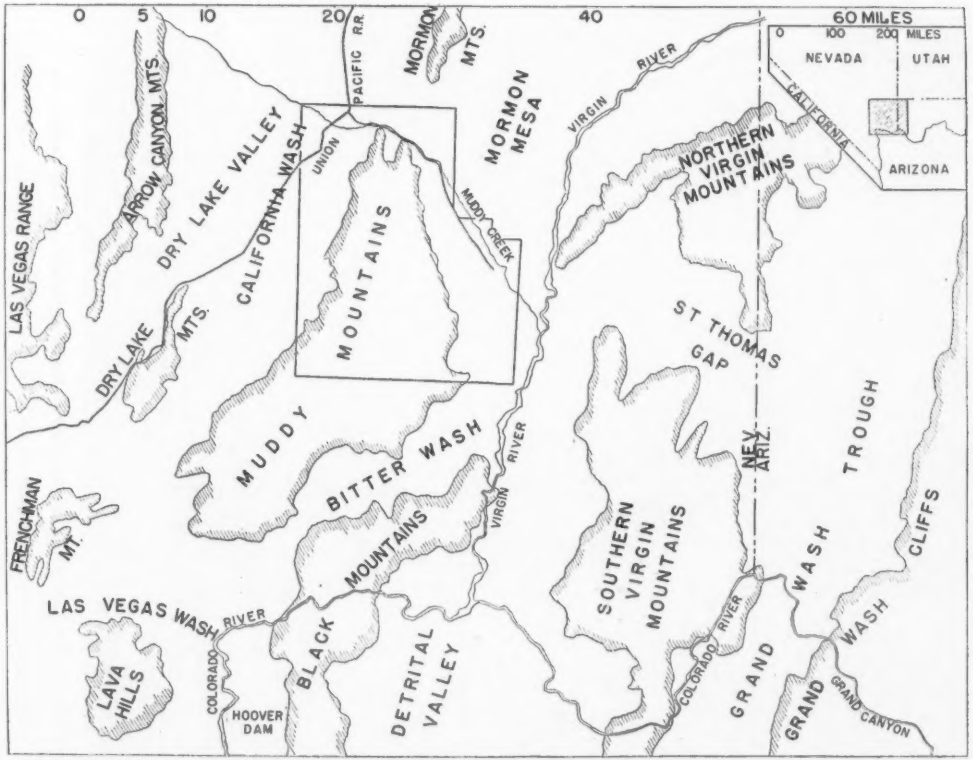

FIGURE 1.—*Index map*

Showing Muddy Mountains in relation to neighboring topographic units. Area mapped in this report is outlined. Inset shows location of entire index map in larger regional setting.

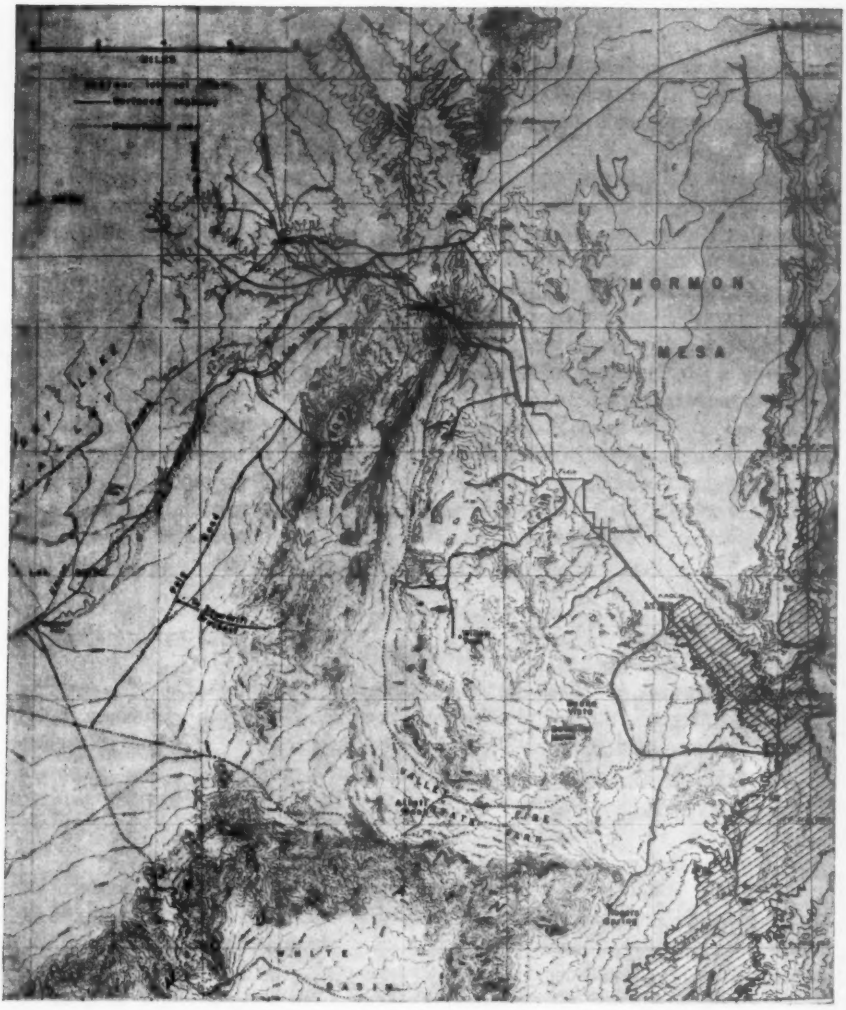

FIGURE 2.—*Topographic map of northern part of Muddy Mountains and surrounding area*

Diagonal lining in southeastern part covers arm of Lake Mead, in Virgin and Muddy valleys

sists almost exclusively of limestones and dolomites, the latter in large part of secondary origin. The plate is represented as a tectonic unit, undivided (Pl. 1). However the formations are differentiated in the belt directly to the north, where they are overridden by the Glendale thrust.

In the initial study of the area no fossils were found older than Devonian, and all lower strata were tentatively included in that system. Later work has led to

TABLE 1.—*Formations of the Muddy Mountain area, Nevada*

Age classification	Formation name	Thickness (Feet)	Characteristics
Recent	Alluvium (Not named)	Variable	Silt and sand on valley floors; coarser debris on slopes.
Recent or Pleistocene	Terrace gravels (Not named)	Variable	Stream-laid unconsolidated gravels; on terrace remnants above present channels.
Pleistocene	Correlative with Chemehuevis fm.?	0 to hundreds of feet.	Clay, silt, sand, and gravel, in isolated remnants above present streams.
	Unconformity		
Miocene?	Muddy Creek formation	0–2000	Clay, silt, sand in basins, grading laterally into coarser slope deposits. Gypsum, salt, and other salines included.
	Angular unconformity		
Early Cenozoic or Late Cretaceous	Horse Spring* formation	1000–2700	Limestone, dolomite, magnesite, clay, silt, volcanic ash, sandstone, conglomerate, etc.
	Overton fanglomerate	20–3000	Extremely coarse fan debris, with some interbedded lenses of silt.
	Angular unconformity		
Upper Cretaceous	Baseline sandstone	3500±	Friable sandstone, gray, reddish, and variegated. Contains many lenticular beds of conglomerate, some very coarse, especially in upper part.
	Willow Tank formation	300±	Coarse conglomerate at base, overlain by gray and buff clays, interbedded with tuffaceous sandstones.
	Angular unconformity		
Jurassic	Aztec sandstone	2500±	Thick-bedded sandstone, normally brick red, strongly cross-bedded.
Triassic	Chinle formation (Shinarump conglomerate at base)	1500–3500	Variegated shales and sandstones, with conglomerate and conglomeratic sandstone at base. Contains silicified logs.
	Moenkopi formation	1500±	Upper continental member of shale, largely chocolate-brown, in part gypseous, with interbedded sandstone; lower marine member of interbedded limestone, shale, sandstone, and gypsum.

* Gravels and tuffaceous beds, highly tilted locally and in scattered outcrops, may be part of the Horse Spring formation or younger.

TABLE 1.—*Continued*

Age classification	Formation name	Thickness (Feet)	Characteristics
	Unconformity		
Permian	Kaibab limestone	600–800	Upper and lower limestone members, separated by middle member, chiefly gypsum.
	Red beds (not named)	2000±	Brick-red and mottled sandstone, with subordinate sandy shale.
Permian(?) and Pennsylvanian	Callville limestone	2000±	Gray limestone, largely thin-bedded. Considerable interbedded sandstone in upper part.
Mississippian	Bluepoint limestone	500±	Chiefly dark-gray limestone.
	Rogers Spring limestone	600±	Chiefly gray crystalline limestone, with some cherty zones.
Devonian	Muddy Peak limestone	600±	Gray limestone, with thin beds of sandstone in upper part.
Cambrian (and younger?)	Not named	1800±	Gray limestone and dolomite. Thin beds about 800 feet above base contain Franconia fauna. Lower part resembles Muav limestone of Grand Canyon district.
	Base of thrust sheet		

recognition, in the basal part of the thrust plate, of dolomitized limestones with the peculiar mottled patterns that characterize the Muav limestone, of Middle Cambrian date, in the Colorado Plateau and also in Frenchman Mountain, 25 miles southwest of the Muddy Mountains (Fig. 1). Although no fossils have been found in the thoroughly dolomitized and much-crushed beds, there is no reasonable doubt that these strata correspond in part to the Muav horizon. Higher in the section, thin-bedded limestones contain abundant trilobites and some brachiopods, which C. E. Resser identified as elements of the Upper Cambrian Franconia fauna. Between this zone and the fossiliferous Devonian lies about 1000 feet of limestone and dolomite beds of uncertain age. Probably some Ordovician is included, in view of the thick section representing that system only 20 miles to the west. The base of the Devonian has not been certainly determined. A thick, massive unit of coarse-grained gray limestone is the most distinctive member of the Mississippian section. The Callville limestone, originally classified as Pennsylvanian, probably includes some Permian also.

The Permian red beds are fully 2000 feet thick. This section was earlier correlated

with the Supai formation of the Colorado Plateau, which it closely resembles; however, McKee (1939) has questioned the equivalence. The Kaibab limestone consists of two distinctive limestone members separated by a gypseous unit about 100 feet thick. An additional upper member—the Harrisburg member of Reeside and Bassler (1922)—made up of white limestone and gypsum is present locally, but in much of the area it was removed by pre-Triassic erosion. Probably the lower limestone unit and the overlying gypseous beds correspond to McKee's (1938) Toroweap formation in the plateau. However, it seems best for purposes of the present paper to follow the older usage of including the entire assemblage of members under the name of Kaibab limestone.

MESOZOIC FORMATIONS

Triassic and Jurassic.—The Moenkopi formation (Lower Triassic) consists of two distinct units: a basal marine member made up of thin-bedded limestone and gypsum, with subordinate sandstone and shale; and an upper nonmarine member, largely red and chocolate-brown shale and sandstone, with considerable gypsum. The distinctive Shinarump conglomerate, disconformable on the Moenkopi, grades upward into the bright-colored Upper Triassic Chinle shales and sandstones. The Chinle appears to be as thick as 3500 feet in the long belt extending south from Muddy Creek; however, it is uncertain to what extent the original thickness of the weak beds may have been altered by strong deformation in this belt. The overlying thick-bedded and strongly cross-bedded Jurassic sandstone is fully 2500 feet thick at a maximum. Normally it is brick red; but over large areas the original color has been altered, by some kind of chemical action, to lavender, yellow, cream, and even pure white. It is the equivalent of Hewett's Aztec sandstone of the Goodsprings district, and this name is extended to the Muddy Mountain area.

Cretaceous.—Deposits now dated as Cretaceous were initially included in the Overton fanglomerate, of uncertain age (Longwell, 1928). Two Cretaceous units are sufficiently distinctive, throughout the belt of outcrop, to merit names as formations. The lower unit, here called the Willow Tank formation,[1] has at the base a coarse conglomerate, ranging in thickness from a few feet to a maximum of 30 feet, which lies with sight angular unconformity on the Jurassic sandstone. Pebbles and boulders in the conglomerate represent resistant members of all of the older Mesozoic formations, and some of the Paleozoic units as well. Many of the boulders measure 10 to 12 inches in largest dimension; and, although they are pretty well rounded, their size and stratigraphic range suggest derivation from an area of localized deformation not many miles distant. The conglomerate is succeeded rather abruptly by about 300 feet of fine-grained deposits, largely gray and buff clays interspersed with layers of tuffaceous sandstone. At several horizons the clays are distinctly bentonitic; fresh pieces have a soapy feel, and wetting causes swelling into sticky, slippery masses, which crack with drying.

The clays contain fragments of silicified wood, including some that have been

[1] New name. The section as described here was measured near Willow Tank, about 5 miles southwest of Overton (Figs. 2, 3; Pl. 5).

identified as a species of the fern *Tempskya*, as reported by Rubey and Callaghan (Hewett *et al.*, 1936). This species is otherwise known only from the lower part of the Upper Cretaceous in Wyoming and Idaho. Other fossils collected by the writer are in general agreement with this age assignment. Shells of *Unio* and other freshwater forms from localities south of Overton were studied by John B. Reeside, Jr. who identified the following:

Unio aff. *U. hamili* McLearn and *U. vetustus* Meek
Unio sp., fragments of a large oval form
Diplodon? n. sp.
Musculiopsis? sp.
Viviparus cf. *V. montanensis* Stanton
Lioplax? cf. *L.? endlichi* (White) and *Goniobasis ortmanni* Stanton
Melampus? cf. *M. caurinus* McLearn
Physa cf. *P. usitata* White
Lymnaea (*Pleurolimnaea*) n. sp.
Planorbis (*Gyraulus*) cf. *P. praecursoris* White
Helix? sp.
Cyprid ostracodes, several species
Fish teeth and bones
Fruits of *Chara* or a related plant

Reeside states,

"The most significant specimens are two beak fragments of a corrugated *Unio* that belongs to a type we have not had above the Bear River, i.e., early Upper Cretaceous. . . . My best judgment of the age of the beds, based on the fauna alone, is that they are not younger than early Upper Cretaceous and might be as old as the Lower Cretaceous beds at Eureka, Nevada. However, the *Tempskya* argues strongly for early Upper Cretaceous. The assemblage, incidentally, is that of a quiet pond."

Fruits of *Chara* and related plants, found at one locality, were identified by R. E. Peck, who concludes that the horizon

"is pretty close to Bear River in age. My conclusion is based on the occurrence of *Aclistochara mundula* Peck—range, Upper and Lower Cretaceous, abundant throughout the Gannett group, upper part of the Kootenai, and Bear River, especially characteristic of the Bear River; *Chara* cf. *C. stantoni* Knowlton —*C. stantoni* is known only from the Bear River; numerous specimens of a species of *Metacypris* that are also found in the Gannett group and Bear River."

Above the Willow Tank formation is a thick succession of sandstones, characteristically white to gray through several hundred feet from the base, but with tones of red and brown, irregularly distributed, in the upper part. The name Baseline sandstone[2] is here applied to the formation, which is more than 3000 feet thick in the section along Baseline Wash, west of the Baseline fault. Clearly the formation is made up largely of reworked sand from the Jurassic Aztec sandstone. The lower whitish sandstones are fine- to medium-grained, and some masses are so free from iron that they are exploited as glass sand. In some sections there are lenses of conglomerate, and locally even the lower part of the section is considerably colored with ferric oxide and contains many concretionary nodules of limonite. Somewhat above the middle of the section a thick layer of coarse conglomerate appears abruptly, containing boulders up to 2 or 3 feet in diameter, made of Jurassic sandstone and of older limestones. Layers of similar conglomerate recur at higher horizons; and this change in textural character, together with the average higher coloration in the upper part of the section, is the basis for dividing the formation into two members. The maximum

[2] New name. Type section measured in and near Baseline Wash (Fig. 3).

thickness of the lower member is about 2000 feet; of the upper, about 1500 feet. The upper member is restricted to a belt west of a large normal fault known as the Baseline fault (Pl. 1); this member, with part of the lower member as well, was eroded from the eastern (upthrown) fault block before younger deposits were laid down.

The only significant fossils reported from the Baseline sandstone are specimens of *Microtaenia paucifolia* found by Rubey and Callaghan in a siltstone layer several hundred feet above the base of the lower member, in a glass-sand pit east of the Baseline fault. This plant indicates a horizon below the middle of the Upper Cretaceous. Although the upper member has yielded no fossils, probably it represents the same epoch, since there is general conformity and similarity of sedimentation throughout the formation.

UNDATED FORMATIONS—CRETACEOUS OR CENOZOIC

A conspicuous unconformity separates the Baseline sandstone from younger coarse fan deposits to which the name Overton fanglomerate is here restricted. In the vicinity of Overton Wash a dissected thrust plate of Jurassic sandstone lies on the Cretaceous formations, and north of the wash these formations disappear beneath this plate (Fig. 3). The Overton fan lies on the eroded plate, and south of the wash the younger deposits appear to be generally conformable with the Baseline sandstone. However, this appearance of conformity is illusory. As indicated by the map (Fig. 3; Pl. 1), a large part of the Baseline section was eroded east of the Baseline fault before the Overton fan was formed. Evidently the Cretaceous formations remained essentially horizontal during the development of the thrust and of the normal fault. The later deposits were then spread out nearly parallel to the eroded Baseline strata, and later all the beds were strongly tilted.

Present exposures of the formation bear witness to an original great sheet of debris spread out along the east front of a growing highland that had its long axis trending somewhat east of north, essentially parallel to the present outcrops of deformed Permian and Triassic formations (Pl. 1). Because of later deformation and erosion, the main belt of outcrop of the fan deposit now trends northwest, thus revealing a section crossing the great fan obliquely, the debris grading from extremely coarse rubble near the highland source, through alternating layers of coarse- and finer-grained material, to sandstone and siltstone almost devoid of coarse conglomerates. This arrangement is shown, somewhat diagrammatically, in figure 3, which also brings out the unconformable relation of the fan deposit to older formations. The uppermost member of the deposit, however, is a thick sheet of coarse fanglomerate which extends to the southern limit of the outcrop belt, though it thins and grows less coarse-textured toward the south. This upper member is firmly cemented with calcium carbonate, and because of superior resistance it forms a high hogback ridge extending several miles southward from the vicinity of Overton Wash. This wash, and two others south of it, have superposed courses that cross the high ridge through narrow V-shaped gaps. West of the ridge these washes and their tributaries have dissected into badlands the lower weak portion of the fan deposit and the Baseline sandstone beneath. Within the wide badland tract some of the coarse-textured members in the fan make more or less continuous, though comparatively low, strike ridges.

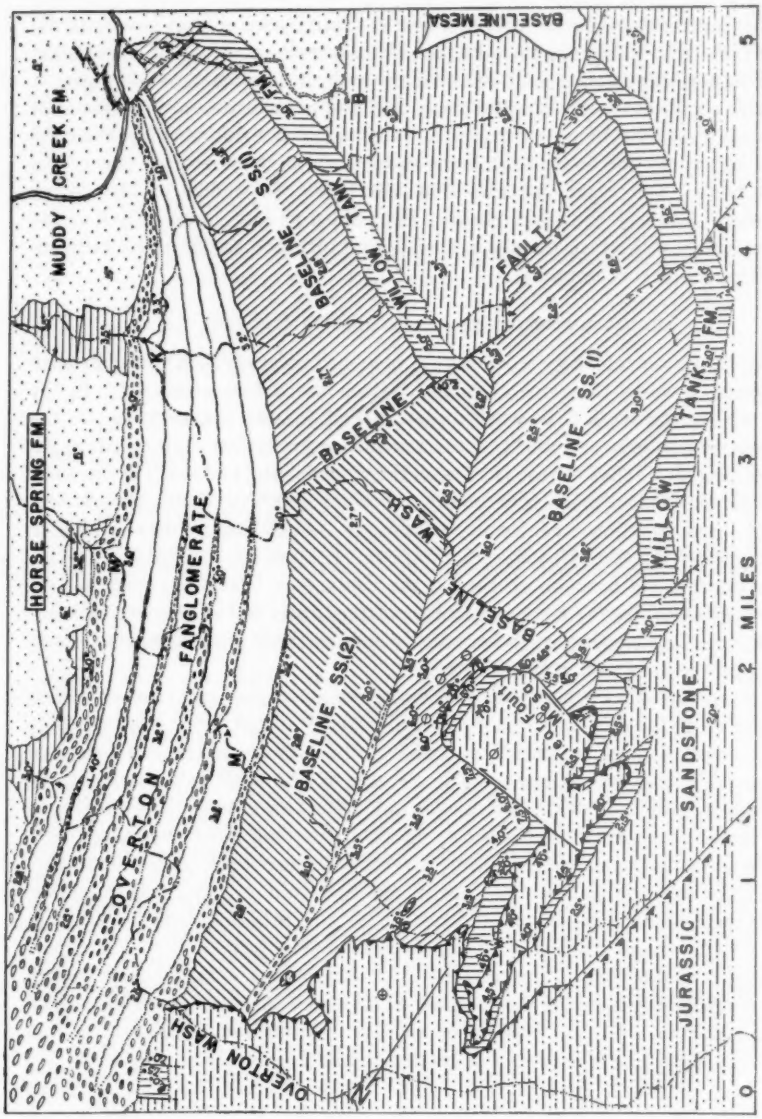

FIGURE 3.—*Geologic map of principal area underlain by Cretaceous formations (Willow Tank and Baseline)*

(1) and (2) designate lower and upper members of Baseline sandstone. Trace of Willow Tank thrust shown by black triangles (these are disconnected where plate is downfaulted). Compare Plates 1 and 5. W. T., Willow Tank.

North of Overton Wash, where these coarse members thicken and coalesce, the fanglomerate through the entire width of its outcrop forms a broad ridge, across which Muddy Creek and several of its tributaries farther south have cut deep valleys.

The coarsest debris in the fan appears near Muddy Creek, where blocks of limestone 20 feet or more in greatest dimension are not uncommon. Two blocks of phenomenal size are included. About 2 miles north of Muddy Creek a mass of Kaibab limestone, much contorted and fractured but still intact, is at least half a mile long. This mass, clearly a component of the Overton fan, lies more than half a mile east of the nearest possible bedrock source. Presumably this huge fragment was detached from a ridge of Kaibab limestone and pushed more than half a mile to its present position by the advancing Glendale thrust sheet (Pl. 5, section E–F). Nearly 2 miles south of Muddy Creek a great slab of Paleozoic limestone and dolomite, exposed continuously through a distance of 1800 feet along the strike, is included in the fanglomerate, which there dips eastward 20°. The maximum thickness of the slab as exposed is about 300 feet. Bedding is dintinct and in general little-disturbed, although the entire mass has been minutely shattered and recemented, as is characteristic of all remnants of the Glendale thrust sheet. The presence of this mass within the fan deposit indicates that the thrust plate was pushed far out on the piedmont slope and that part of it was buried under later erosional debris (Pl. 5, section I–J). Tilting was followed by bevelling to the present topographic surface, and only the one large fragment of the buried plate has survived.

Some unidentifiable fragments of bone in a local bed of siltstone are the only fossils found thus far in the Overton fanglomerate. Fine-grained sediments that form a considerable part of the formation in the southern part of the outcrop belt may eventually yield diagnostic fossils. Dating of the fanglomerate is particularly desirable, since the formation provides a clear record of an important episode in orogeny.

The Horse Spring formation, largely lacustrine, succeeds the Overton fanglomerate conformably. Large quantities of magnesite, soft dolomite, borate minerals, travertine, and volcanic ash indicate unusual conditions of deposition (Longwell, 1928). These deposits have yielded no fossils except possible casts of tree roots and some fragments of leaves and coniferous wood that give no definite information on the age (Hewett *et al.*, 1936). The area of this report has limited outcrops of the Horse Spring strata; more extensive exposures in the southern part of the range afford the best displays of the formation in its varied aspects.

Some valleys deeply incised into extensive deposits of unconsolidated gravels, notably in the southwestern part of the map area, expose older beds of conglomerate, tuffaceous sandstone, and white volcanic tuff, all steeply tilted. A few large outcrops of these beds are indicated on the geologic map as "Tertiary (?) gravel and tuff"; numerous small exposures of similar strata could be represented only on a map of much larger scale. Wide distribution of the scattered outcrops suggests an extensive deposit, laid down during a time of active eruptions from a reservoir of siliceous magma. Possibly the beds represent part of the Horse Spring interval, during which this type of volcanic activity was widespread. However, none of the types of chemical deposits peculiar to the Horse Spring formation were found associated with the beds, and in the absence of any evidence for dating either group it is assumed that

the tuffaceous beds are the younger. The chief reason for this assumption is the lack of any deposits resembling the Overton fanglomerate between the tuffaceous beds and the older formations.

CENOZOIC FORMATIONS

Deposits known to be of Cenozoic age are distributed widely in the intermont basins. In the marginal parts of the range these deposits overlie various older formations, with which they are generally in conspicuous unconformity. Over wide areas these younger strata have essentially the attitude in which they were deposited; locally they have been folded or sharply tilted adjacent to faults.

The Muddy Creek formation is the most widely distributed of these known Cenozoic units. It is a typical interior-basin deposit, coarse-grained near mountain borders, fine-grained in the wide lowlands, and containing abundant salines that indicate aridity at the time of deposition. The Virgin River and Muddy Creek have cut deeply into the formation, which is dissected into extensive badlands on both sides of each stream. Silt, fine sand, and clay, yellowish and cream-colored, form the bulk of the formation. These materials are in regular layers, thin or moderately thick, commonly arranged in rhythmic alternation. Probably the deposits are in large part lacustrine, though the lake waters may have been shallow and fluctuating, with some of the deposition on playa flats. Layers of gypsum and gypseous clay are abundant, and a thick bed of glauberite was exposed west of the Virgin River before the area of outcrop was covered by Lake Mead. Thick masses of rock salt also were almost entirely concealed by the lake. This salt may belong in the lower part of the Muddy Creek formation; but, since it was exposed in large plugs which had domed and in many places cut across the typical Muddy Creek strata, the salt may be somewhat older.

Layers of basaltic lava, which flowed northward from the vicinity of the Colorado River, are intercalated with the Muddy Creek deposits. One of the flows is exposed a short distance south of the Muddy Valley.

Few fossils have been found in the formation. Stock (1921) has reported bones of mammals which suggest Miocene age, though the evidence is not wholly satisfactory. Earlier listing of the formation as of questionable Pliocene age had no paleontological basis.

Deposits younger than the Muddy Creek formation, in apparent order of decreasing age, are the following: (1) Cemented gravels and associated caliche, capping mesas and buttes that stand several hundred feet above their surroundings. (2) Light-colored silts and clays that rest unconformably on eroded Muddy Creek beds, near present stream levels and extending to considerably higher altitudes. These silts and clays, which contain bones of Pleistocene mammals and shells of small mollusks, seem to correlate with extensive remnants of fine-grained deposits along the Colorado River, which record filling of the valley to a depth of several hundred feet, followed by re-excavation (Longwell, 1936). (3) Unconsolidated gravels at various elevations, which record stages in downcutting of the drainage. (4) Alluvium in the present stream valleys.

The capping of cemented gravels (1), rich in caliche, once overlay a wide intermont surface that sloped toward and with the larger stream valleys of present time. This capping must have been destroyed rapidly as soon as the streams began dissecting

the weak underlying Muddy Creek deposits. Existing remnants of the capping are on more resistant bedrock near the margins of the larger valleys, except for the large remnant forming Mormon Mesa, which protects the Muddy Creek formation in the wide angle between the Virgin River and Muddy Creek.

STRUCTURE

GENERAL STATEMENT

The major tectonic features of the area are two large thrust faults. In the earlier study the evidence for large-scale thrusting was recognized, but was interpreted as indicating a single thrust sheet, of which the northern part had been relatively uplifted and almost destroyed by erosion (Longwell, 1922; 1928). Close field examination shows clearly that the northern remnants represent a thrust sheet structurally much higher than the more extensive Muddy Mountain thrust. Exposures of the latter are restricted to one side of a transverse fault (the Arrowhead fault), south of which the wide plate has been greatly elevated, and locally cut through by erosion. Presumably this thrust underlies the northern part of the area also, far beneath the present land surface (Fig. 7).

The northern part of the Muddy Mountain area is of critical interest to the structural geologist because: (1) erosion has barely stripped away most of the higher (Glendale) thrust sheet, thus revealing exceptionally complex deformation in the strata directly beneath; (2) a thick section of "orogenic sediments" that accumulated directly east of the severely deformed belt has been tilted and well exposed. These sediments supplement the structural features in recording the orogeny and offer a possible means of dating the important episodes with some exactness.

MUDDY MOUNTAIN THRUST AND ARROWHEAD FAULT

The Muddy Mountain thrust and related features have been described in earlier papers (Longwell, 1921; 1922; 1928), and a brief outline of salient facts, supplemented by pertinent new information, will suffice here. The exposed portion of the thrust plate, made of resistant Paleozoic dolomite and limestone, forms a rugged highland with an abrupt front facing northward. Contact of the plate with the underlying Jurassic sandstone is best displayed near the western border of this highland, along the crest of a large anticline trending 20°E. The anticlinal axis plunges both northeastward and southwestward, and erosion has removed the thrust plate from a wide area extending about 8 miles along the axial trace of the fold. Within this area the Jurassic sandstone, its normally brick-red color locally bleached to yellow and white, contrasts strongly with the adjacent dark carbonate rocks of the thrust plate (Pl. 3). Breccia at the thrust contact is locally as much as 10 feet thick, and the beds of dolomite are severely shattered through a thickness of 200 to 300 feet, or even more. Liesegang patterns are prominent in the jointed sandstone beneath the thrust, and irregular leaching which has removed or altered the red color of the sandstone over large areas indicates chemical action related in some way to the zone of movement. In general the thrust surface nearly parallels the bedding both above and beneath, though locally the beds were deformed and transected.

East of the large window the formations in the thrust plate have been folded and faulted, although in a belt directly south of the Arrowhead fault the beds have rather

simple structure, with southward dips. About 8 miles east of the window the base of the plate is exposed in the eroded footwall block of a large normal fault (Pl. 1). There also the Jurassic sandstone lies beneath, and the thrust surface is generally parallel to bedding, although the strata in the plate are considerably crumpled locally. This consistent structural relationship is the basis of the section shown in Figure 4. Further evidence in the southern part of the range suggests that the Jurassic sandstone underlies the thrust plate in most of its known extent.

The Paleozoic rocks of the plate rode up on the younger formations somewhere west of the western border of the range, in the area now covered by alluvium. From comparative study of large thrusts in the Las Vegas region, it is inferred that the Muddy Mountain thrust had the general form shown in Figure 5 before it was modified by folding, normal faulting, and erosion (Longwell, 1945a). Since the forward part of the plate was faulted down and concealed under later deposits in the Virgin River basin, the original width of the plate and the full displacement cannot be determined.

Wherever the fault surface has been seen, the Arrowhead fault dips 50°–80°S. Dips as low as 50° seem to be restricted to a short stretch about 2 miles from the western end of the fault; steeper angles are more characteristic. The best exposures, less than a mile west of Bluepoint, reveal dips ranging from near vertical to 70°S. Genetic relationship of this fault to the Muddy Mountain and Glendale thrusts is an important matter on which some of the evidence is not clear. There was a strike-slip component of movement, eastward on the south side, as indicated by strong drag effects directly north of the fault. In the earlier study the fault was interpreted as a large "tear" that existed while movement on the Muddy Mountain thrust was in progress, permitting differential displacement of the plate on the two sides. This interpretation assumed (1) that the Glendale thrust, now known to be a distinct fault at a higher structural level, was part of the Muddy Mountain thrust, and (2) that dip displacement on the Arrowhead fault was normal—down on the south—whereas it is now known to be reverse—up on the south. An essential key to interpretation of the structure appears near the west border of the range, where the fault passes into a sharp monoclinal fold on which the thrust plate and the Jurassic sandstone beneath are bent down to the north (Fig. 6; Pl. 6). From this point eastward for several miles, displacement on the transverse fault steadily increases, as indicated by the appearance of successively younger formations along the north side of the fault (Pl. 1). On the supposition that the Jurassic sandstone lies beneath the Muddy Mountain thrust plate throughout its known width, as represented in Figure 4, throw on the Arrowhead fault near its easternmost exposure is more than 2 miles (Fig. 7). It is strongly indicated, therefore, that the thrust plate is present deep beneath the northern part of the area, and that displacement on the Arrowhead fault occurred after the thrusting. Possible contemporaneity of the transverse fault with the Glendale thrust is discussed on a later page.

GLENDALE THRUST AND RELATED FEATURES

General discussion.—As shown on the map (Pl. 1), in the structure section (Fig. 6), and in the aerial photograph (Pl. 6), near the west end of the Arrowhead fault the

AERIAL VIEW, SOUTHWEST ACROSS MUDDY MOUNTAINS

From high altitude. Irrigated Muddy Valley in foreground. The dark formation beyond is the Overton fanglomerate. At right, severely folded belt that was overriden by the Glendale thrust. Dark highland in upper middle ground is formed of Muddy Mountain thrust plate.

AERIAL VIEW NORTHEAST ALONG BUFFINGTON ANTICLINE AND WINDOW

Light-colored Jurassic sandstone overlain by Paleozoic dolomite and limestone in Muddy Mountain thrust plate. Large block of Horse Spring beds faulted down across anticline, upper right middle. Plunging nose of anticline, about 8 miles distant from observer, is near southwest corner of Plate 1. (Copyright by R. C. Frampton)

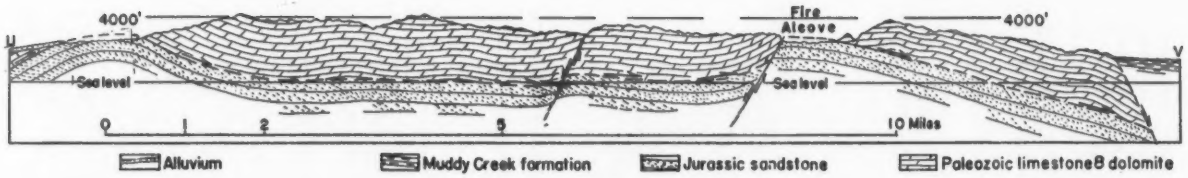

FIGURE 4.—*Section through the Muddy Mountain thrust plate*

Along line U-V on Plate 1

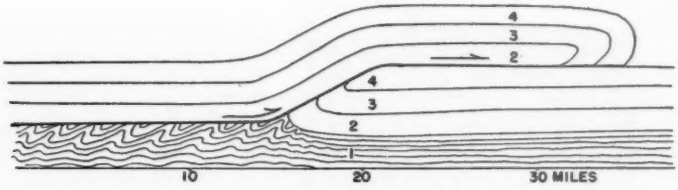

FIGURE 5.—*Hypothetical restoration of the Muddy Mountain thrust*

Based on a study of several large thrusts in southern Nevada, exposed at different levels. The visible part of the Muddy Mountain plate corresponds to the forward portion, above the incline, shown in the figure; the folded "prow" has been either downfaulted and concealed, or eroded before fragmentation of the plate by faulting. Diagram represents only part of known displacement

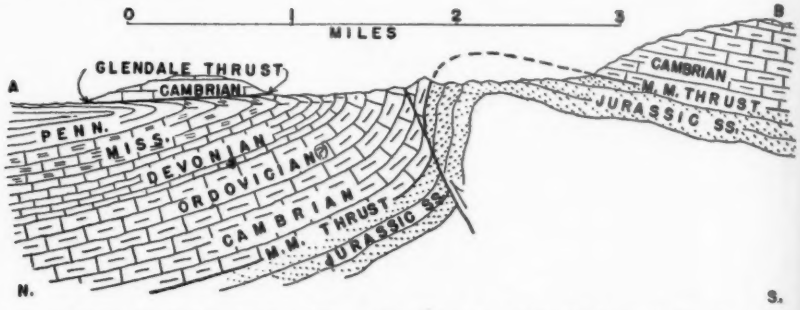

FIGURE 6.—*Section showing relation between Glendale and Muddy Mountain thrusts*

Along the line A-B of Plate 1. Overturning of beds beneath the Glendale remnant actually is toward the east—not toward the north as the diagram may suggest.

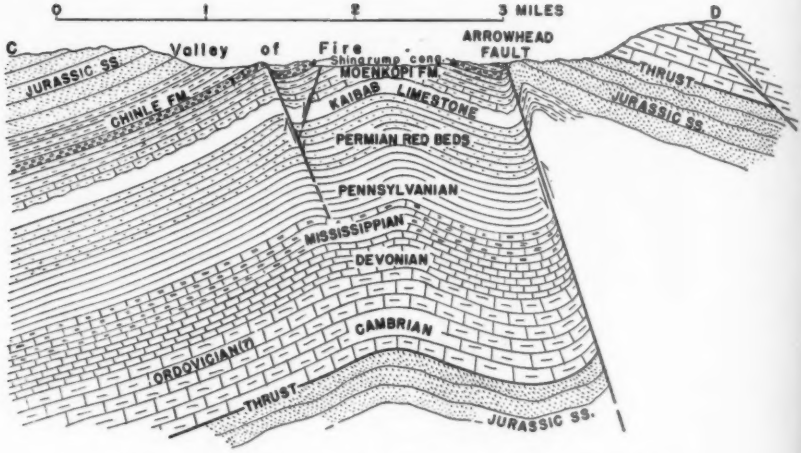

FIGURE 7.—*Section through Valley-of-Fire anticline and Arrowhead fault*

Along line C-D of Plate 1

UNIVERSITY OF CALIFORNIA

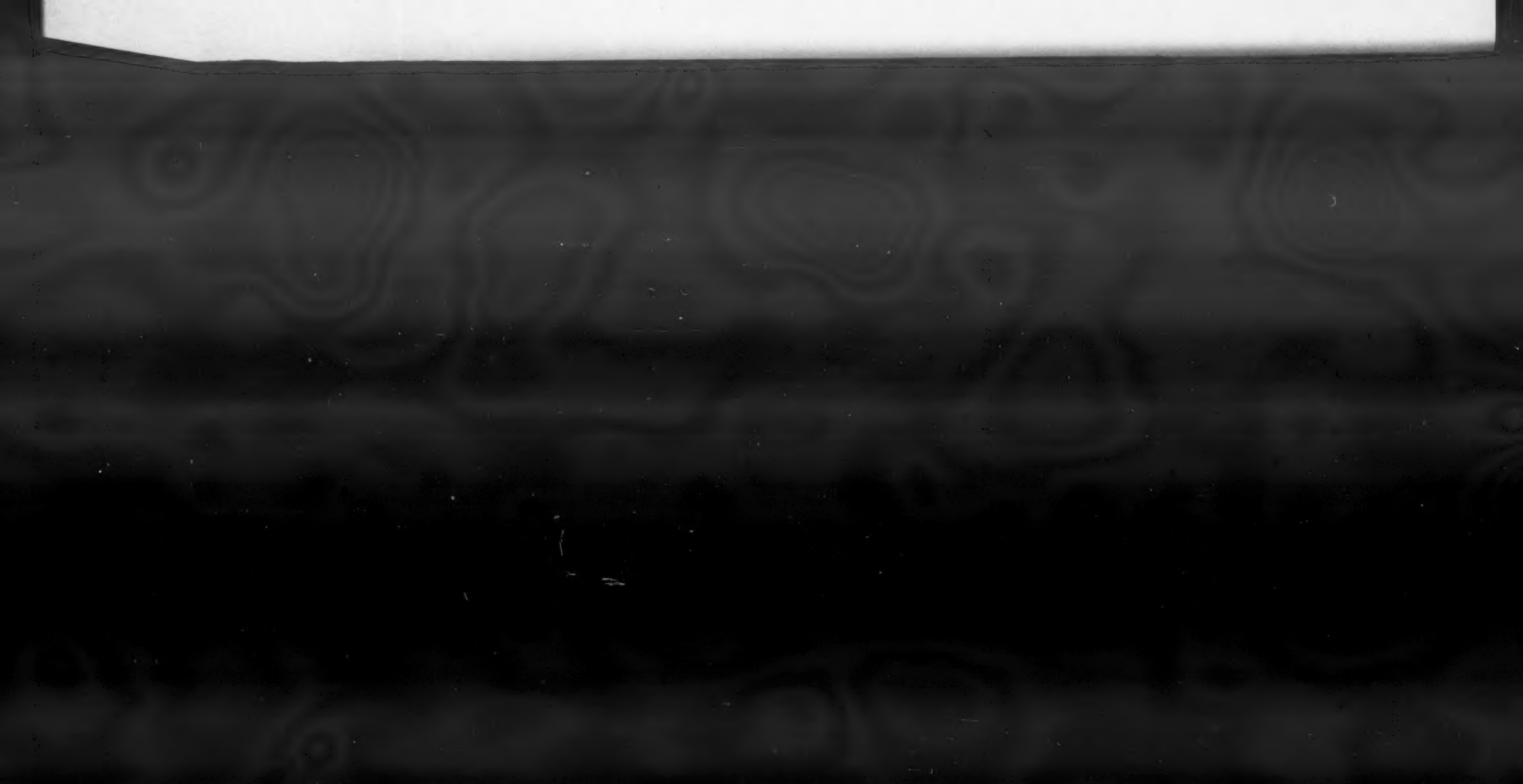

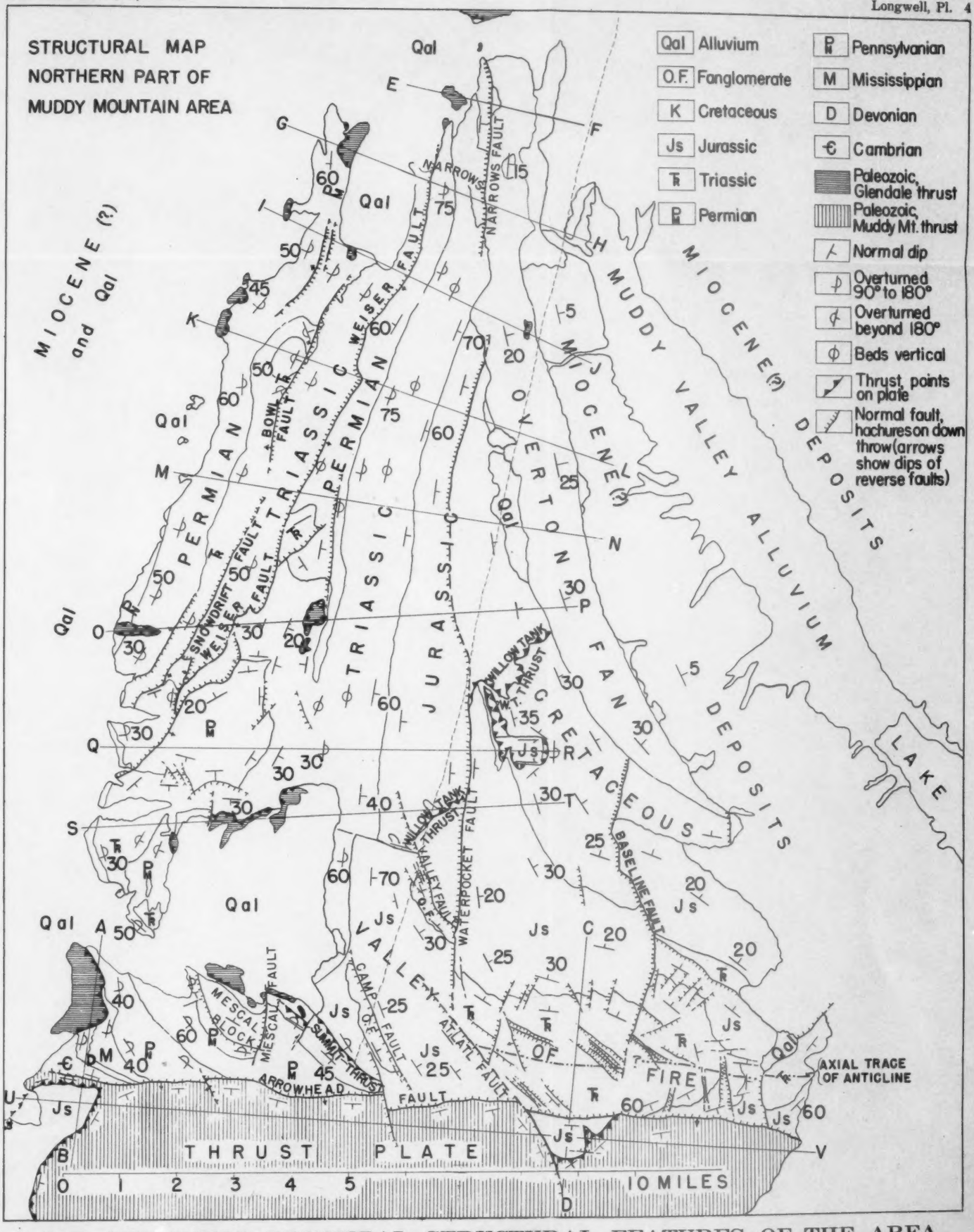

MAP OUTLINING PRINCIPAL STRUCTURAL FEATURES OF THE AREA

The larger outcrop belts of formations are indicated. Glendale thrust plate reached eastward approximately to the broken red line.

W.T., position of Willow Tank.

formations in the Muddy Mountain thrust plate bend down sharply to the north. In the zone of bending the strike of formations is nearly west; but a short distance farther north the strike turns abruptly to north, and the formations are overturned to the east beneath a thrust plate containing Cambrian strata that dip westward, under the piedmont alluvium. No inference is required in this interpretation; though the entire section is of carbonate rocks, each formation, from Cambrian to Pennsylvanian, is quite distinctive and can be followed through the changing attitude in continuous outcrop. Thus the Muddy Mountain thrust plate was in turn overridden by another plate, which is represented by 20 mappable remnants distributed in a belt extending northward across Muddy Creek near Glendale (Pl. 1). Apparently the thrust extends still farther north, into the southern part of the Mormon Mountains.

In contrast with the exposed part of the Muddy Mountain thrust, the Glendale thrust surface does not have a simple relation to bedding above and beneath it. Formations beneath are overturned, thrown into complex folds, and cut by steep faults. At some localities the Paleozoic beds in the thrust plate are flat lying or gently tilted; but in many places they dip steeply into the thrust surface. Complexity of the structure, in plan and in section, is evident from study of the geologic map (Pl. 1), the structural map (Pl. 4), and the structure sections (Pl. 5). The following features merit special description and explanation.

Weiser syncline.—In the deformed belt that lay directly beneath the Glendale thrust plate, the major structural features are the overturned Narrows anticline and the recumbent Weiser syncline. These large folds, much complicated by faulting and crumpling, are most evident in the structure sections G-H, I-J, K-L, and M-N. The upper limb of the recumbent syncline is best displayed in the western parts of Sections K-L and S-T, where the inverted strata have been secondarily domed and erosion has exposed them to considerable depth. In these and several other localities in the belt, strata in the upper synclinal limb have been rotated eastward through more than 180°; the resulting attitude is indicated on the geologic and structural maps by a special symbol.

Section K-L passes through a particularly clear exposure of the Weiser syncline. Over a considerable area the inverted upper limb has been bulged upward to form an elongate dome, erosion of which has resulted in the great natural amphitheater here called the Bowl (Pls. 2, 7). This unusual topographic feature is floored with the weak shales and thin sandstones in the upper member of the Moenkopi formation. The steep walls, 400 to 500 feet in height, display the inverted lower member of the Moenkopi, with the Kaibab limestone, more or less eroded, at the top. The east side of the depression, nearly straight, reflects in its form a steep reverse fault on which the strata in the floor have been lifted in relation to older strata in the east wall. Farther east the upper limb of the syncline resumes the westward dip, and part of the lower limb is revealed, also dipping westward from the abrupt fault contact with Permian beds in the overturned Narrows anticline. These relations, with a generalized restoration of the major syncline and anticline, are represented in Figure 8. As indicated on that diagram, the steep fault west of the anticlinal axis has vertical displacement, on the line of Section K-L (Pl. 5), of about 1600 feet. The fault

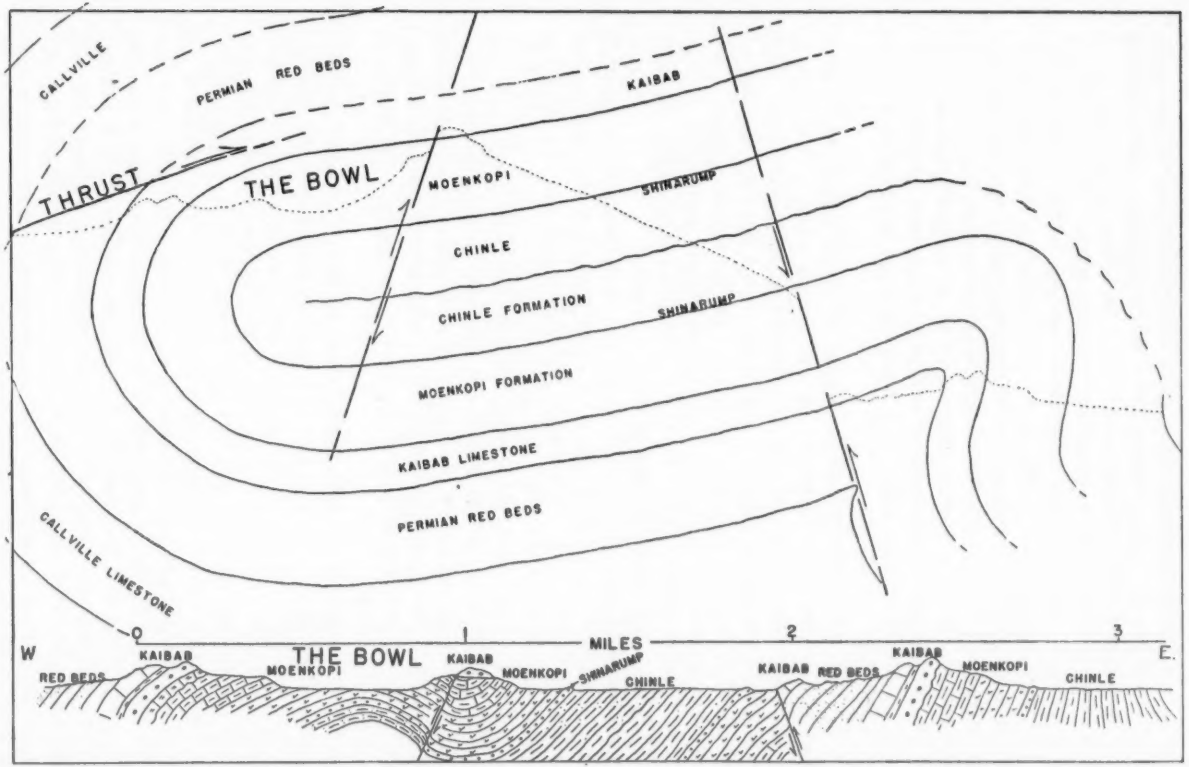

FIGURE 8.—*Simplified restoration of the recumbent Weiser syncline*

Syncline actually much deformed, as shown by outcrops in and east of the Bowl. Above, restoration of the syncline and the Narrows anticline, omitting deformation by folding and faulting shown in actual west-east section below. Dashed line in upper diagram shows approximate position of present surface.

folding and faulting shown in actual west-east section below. Dashed line in upper diagram shows approximate

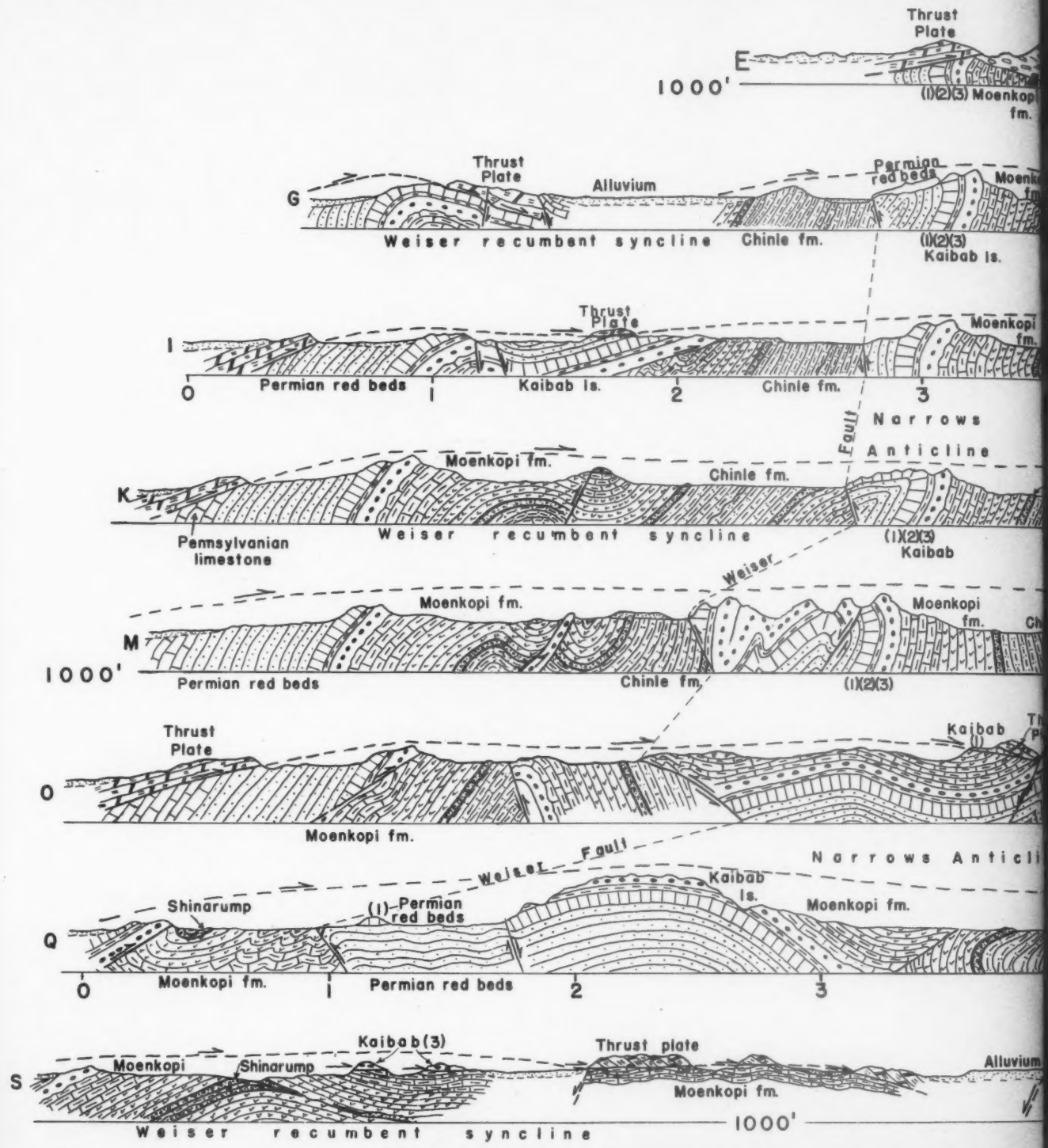

WEST-EAST STRUCTURE SECTIONS T

Sections on lines indi

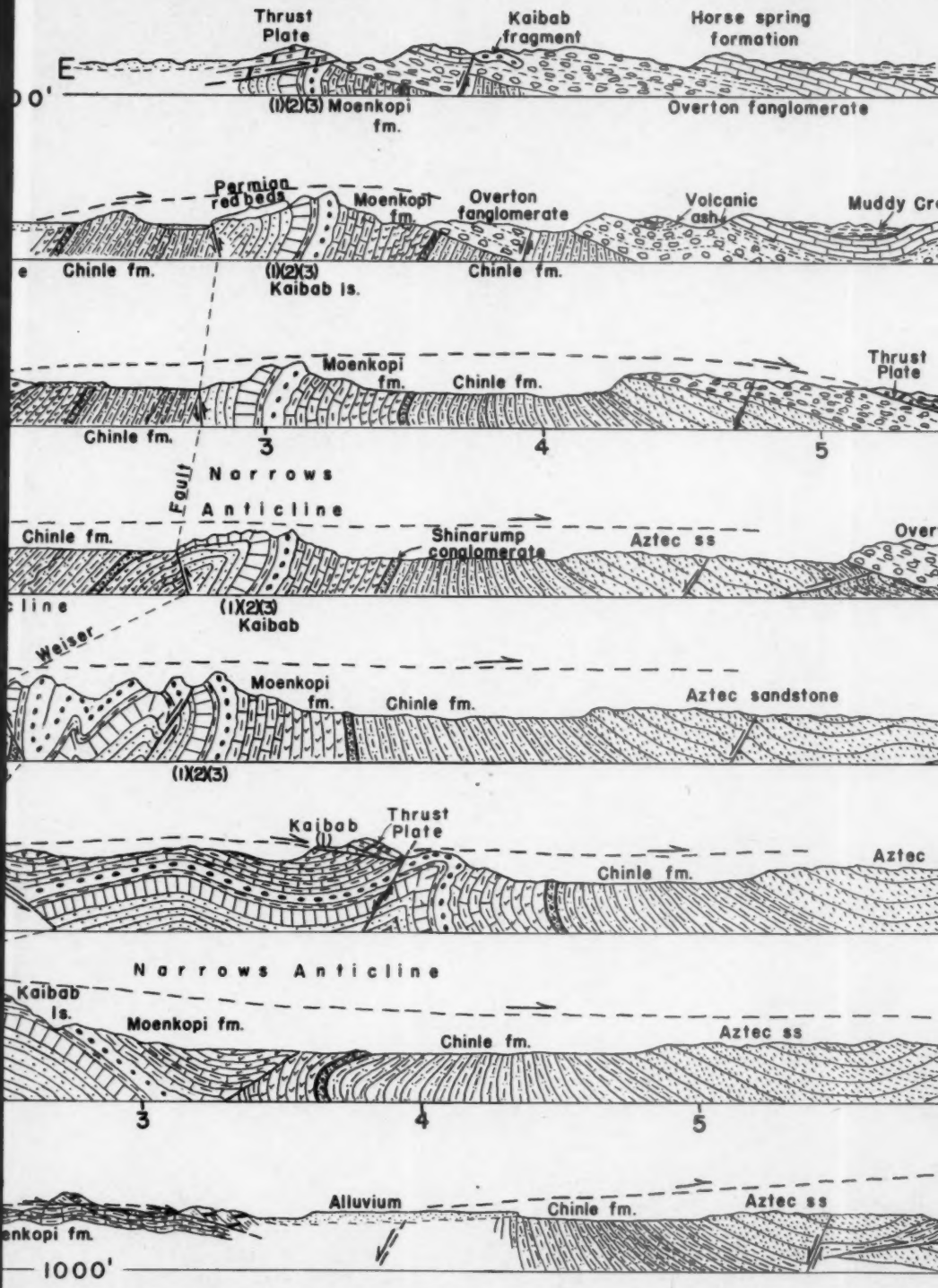

CTURE SECTIONS THROUGH GLENDALE THR

Sections on lines indicated in Plates 1 and 4

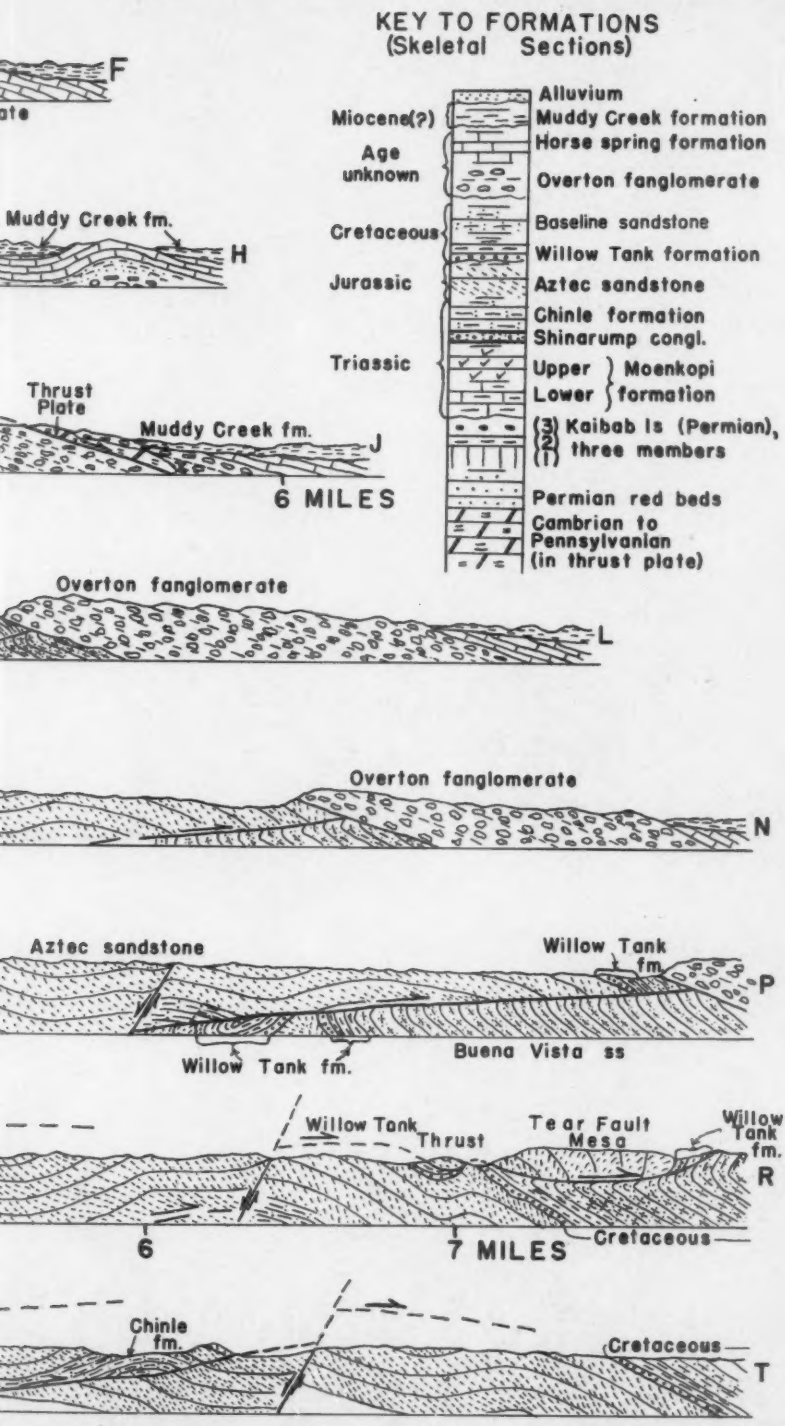
KEY TO FORMATIONS
(Skeletal Sections)
Alluvium
Miocene(?)
Muddy Creek formation
Horse spring formation
Age unknown
Overton fanglomerate
Cretaceous
Baseline sandstone
Willow Tank formation
Jurassic
Aztec sandstone
Chinle formation
Shinarump congl.
Triassic
Upper } Moenkopi
Lower } formation
(3) Kaibab ls (Permian),
(2) three members
(1)
Permian red beds
Cambrian to Pennsylvanian (in thrust plate)
F
Muddy Creek fm.
H
Thrust Plate
Muddy Creek fm.
J
6 MILES
Overton fanglomerate
L
Overton fanglomerate
N
Aztec sandstone
Willow Tank fm.
P
Willow Tank fm.
Buena Vista ss
Willow Tank Thrust
Tear Fault Mesa
Willow Tank fm.
R
6
7 MILES
Cretaceous
Chinle fm.
Cretaceous
T

THRUST ZONE

at the east side of the Bowl has much smaller throw. Limbs of the syncline were much deformed by secondary folding as well as by faulting.

Variations in the expression of the Weiser syncline, as shown in the cross sections, emphasize the extreme deformation that occurred directly beneath the Glendale thrust. Thus at the west end of Section G–H, the bend of the fold is clearly revealed; but a short distance farther east, faulting has carried the limb of the fold, together with the overlying remnant of the thrust plate, below the level now occupied by recent alluvium. Section I–J crosses the only remnant of Permian red beds preserved on the recumbent upper limb. In this section, moreover, the Kaibab limestone has moved over and deformed the Moenkopi beds beneath. This type of movement occurred commonly, on such a scale that the contact between Kaibab and Moenkopi is represented in several parts of the map as a thrust surface (Pl. 1). Gypseous beds at the base of the Moenkopi facilitated the movement of the strong Kaibab, which was carried along by frictional drag under the overriding thrust plate of older Paleozoic formations. Large masses of the Kaibab were torn loose and dragged considerable distances eastward from their normal positions in the limb of the syncline. Some of these masses are given particular mention on a later page.

Sections M–N and O–P show remarkable effects of deformation. In M–N the upper limb of the syncline is thrown into sharp folds, and one of the small anticlines is pierced by a large fragment of Kaibab limestone. This mass protrudes to form a prominent butte, about 500 feet in length and up to 150 feet wide. On each side of the butte is a prominent shear zone, marked by extensive brecciation and by slickensided surfaces dipping 60° W. The Moenkopi beds are turned up sharply in section and bend around the intruded mass in plan (Pl. 8). Whether the Kaibab mass is continuous downward as shown in the section is of course problematic. The mass must have been forced upward a long distance; by any logical reconstruction of the fold, the Kaibab in the lower limb at this location is fully 2000 feet, and possibly much more, below the present surface.

In Section O–P the recumbent syncline is unrecognizable, because of faulting and erosion. Movement on the Snowdrift fault, a steep reverse fault of large throw, has brought to the present surface and tilted steeply eastward the Moenkopi and Chinle beds that belong in the lower limb of the syncline; east of this fault the upper limb has been entirely eroded, unless some part of it may be preserved below the hanging wall of the Weiser fault, which in this vicinity has unusually low dip. Southward from this location there has been more pronounced uplift, as shown in Section Q–R, where erosion has effectively destroyed evidence of the recumbent syncline. Steep dip of formations southward from the area of uplift again brings the higher structural elements below the level reached by erosion, and the upper limb of the recumbent syncline, overlain by remnants of the Glendale thrust plate, is particularly well displayed in Section S–T.

Distribution of formations in the outcrops near the west end of Section S–T is puzzling until it is realized that in that part of the area the recumbent syncline plunges southward, with the axis of the uplift shown in Q–R. The relation between outcrops and structure is represented in Figure 9. On the line of Section S–T, and farther south, the formations are clearly in inverted order; they are in the upper

limb of the recumbent syncline. As seen in cross section, the geometric form is that of a broad anticline, since the inverted formations are domed along an axis trending generally north. Toward the north the axis rises, and erosion has cut progressively deeper into the inverted section. North of an alluvial-filled valley the

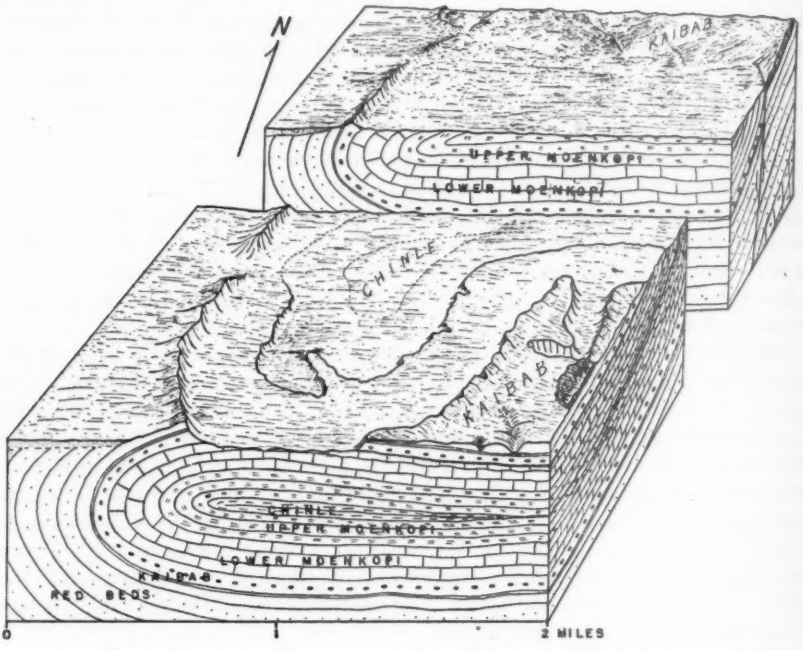

FIGURE 9.—*Block diagram to explain outcrops in southern part of the Weiser syncline*

Structure near west end of line S-T, Plates 1 and 5. The recumbent Weiser syncline plunges southward

formations are in normal stratigraphic order, since they are in the lower limb of the syncline—the upper limb is there wholly eroded. The Chinle is the youngest formation involved in the fold, and only the lower part of the upper Triassic section appears, in discontinuous outcrops. Evidently a great thickness of strata had been eroded from this part of the area before the recumbent syncline was developed. The significance of this erosion is discussed on a later page.

Narrows anticline.—In the cliff on the north side of the Narrows of Muddy Creek, beds of the Kaibab limestone mark the summit of an anticline sharply overturned to the east. The axis of this fold rises steeply southward, and on the line of Section G–H the Kaibab has been eroded to expose the Permian red beds. From this location southward a fault cuts the western limit of the anticline, bringing the older formations in this limb upward against Chinle beds to the west. The distance of this fault from the crest of the anticline varies, as shown in the several sections. Between Sections G–H and I–J, both the Kaibab and Moenkopi limestones are preserved east of the

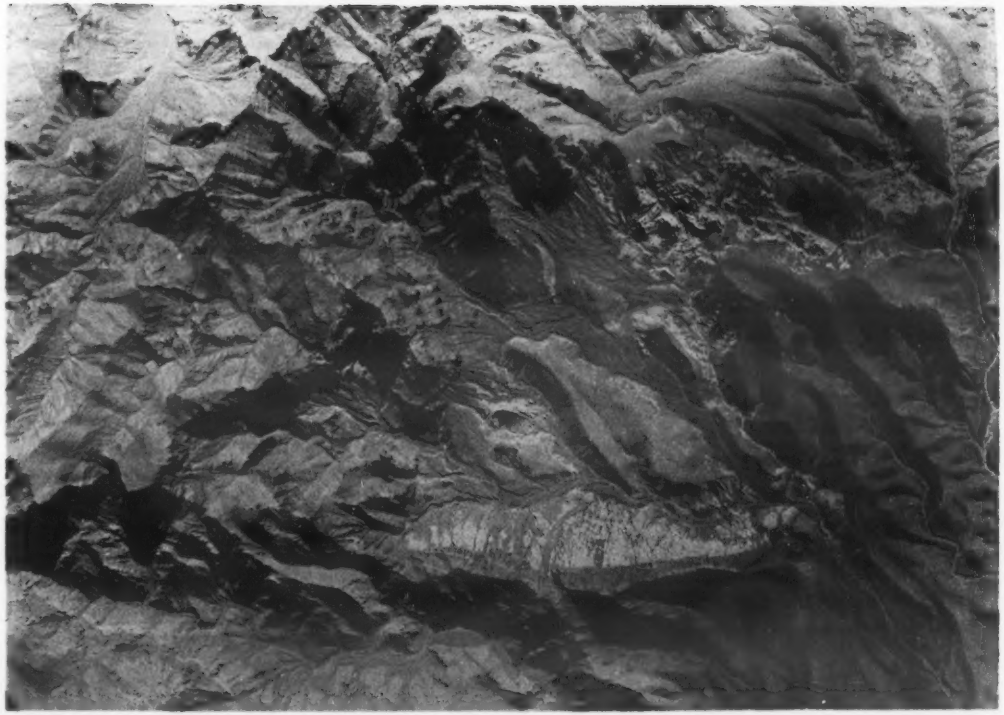

VERTICAL VIEW AT WEST END OF ARROWHEAD FAULT

Looking down at north end of Buffington window (south at top of view). Light-colored Jurassic sandstone at core of anticline. Note that beds in thrust plate dip steeply left on east side of fold, but in left foreground some beds are seen to turn sharply into nearly east-west strike and vertical dip. This is the sharp monocline at west end of Arrowhead fault.

VERTICAL VIEW OF WEISER SYNCLINE (RIGHT) AND NARROWS ANTICLINE
Permian red beds at core of anticline, lower left. Note small remnant of Kaibab in upper limb. North-south length of Bowl (upper right) about 1 mile. (*See* Plate 5, section K-L; also Figure 8.)

fault. For several miles farther south the red beds form a continuous outcrop, except for a narrow band of Kaibab limestone that has escaped erosion in the western limb of the fold, as shown in Section K–L and in Plate 7. Two additional large remnants of Kaibab form prominent buttes adjacent to the fault.

From the vicinity of Section M–N southward, structure connected with the anticline is more complex. Sharp buckling oblique to the main axis has turned the Kaibab up in local cross folds with vertical limbs. An embayment floored with steeply dipping Moenkopi beds is involved in this oblique buckling, which is modified by a northeast-trending fault that lowers the Moenkopi against Kaibab and the underlying red beds in a sharply localized dome. A steep fault trending north cuts the east limb of the main anticline, causing duplication of Kaibab members in the outcrop. The anticline divides, and an eastern branch—which appears to be the continuation of the main anticline—extends southward about 3 miles to a plunging termination. This branch of the fold is strongly overturned directly east of a thrust plate remnant, as shown in Section O–P. A western branch of the anticline bears southwestward, with broad crest and moderately inclined limbs. Moenkopi beds carry over the crest in a broad depression of the axis. Farther south the Kaibab emerges in a wide area, marking a culmination of the anticlinal axis (Section Q–R). This branch of the fold in its swing southwestward becomes involved with the recumbent Weiser syncline. Its broad, open form throughout its course contrasts with the steeply overturned form of the Narrows anticline proper, as shown in Sections O–P and Q–R.

Relations between the Weiser syncline and the Narrows anticline merit further discussion, particularly in the light of evidence revealed near the west end of Section S–T. In a belt along the line of that section, the inverted Kaibab and Moenkopi strata are exposed through an east-west distance of more than 3 miles. These inverted strata that form the upper limb of the recumbent syncline have been eroded farther north (Fig. 9), where the structural elements have been brought higher in relation to the present topographic surface. Study of all structure sections, from S–T northward, suggests that the upper limb of the syncline, with the Glendale thrust plate above it, once extended eastward beyond the crest of the Narrows anticline. However, such a simple reconstruction of the fold is subject to important modifications. A remnant of the thrust plate shown in Section O–P lies directly on the west limb of the Narrows anticline; hence the upper limb of the recumbent syncline, if it once existed at that location, was removed before the plate was finally thrust into this position.

Abundant additional evidence, some of which is cited and explained hereafter, shows that major structural features within the thrust zone were developed either before or concurrently with final emplacement of the thrust plate. Extensive erosion during early stages of the deformation is indicated by absence of the Jurassic Aztec sandstone from the stratigraphic section involved in the recumbent Weiser syncline. The Chinle formation also was partly eroded before the syncline was closed, and within a belt near Section S–T this early erosion reached below the Shinarump conglomerate. Significance of this evidence is discussed in connection with the orogenic history.

Faults within the belt of thrusting.—The Weiser fault, which can be traced through

a distance of 12 miles along the west side of the Narrows anticline, is one of the most conspicuous features associated with the Glendale thrust. Continuity of the fault and some variations in its attitude are shown on Plate 5, Sections G–H to Q–R. In general, it is a steep reverse fault with eastward dip. However, through a mile or more on either side of Section O–P the dip is so low that the trace has a sinuous outcrop (Pl. 1). Farther north the dip at a few localities appears to be nearly vertical, and in one limited outcrop the dip is steep to the west, suggesting normal movement. Displacement is large throughout the exposed length of the fault. From Section K–L northward the throw, measured stratigraphically, appears to increase from about 1600 feet to 2000 feet or more. Toward the southwest the measure of throw decreases. South of Section Q–R, where the fault disappears beneath alluvium, Moenkopi limestone in the hanging wall has been brought up against Kaibab limestone, the two formations there having inverted order in the upper limb of the Weiser recumbent syncline. Between Sections O–P and Q–R the fault divides through a distance of about 2 miles, the two branches bounding a block fully 2000 feet in maximum width (Pl. 1).

The Weiser fault and the shorter Snowdrift fault dip eastward and thus had their upthrow opposite that of the Glendale thrust. On the other hand the Bowl fault, which strikes parallel with the Weiser and Snowdrift faults, had its upthrow on the west, in agreement with the Glendale thrust. Varied movements on faults, as well as highly irregular doming and other bizarre structural features in this belt, indicate that the zone in front of and beneath the thrust was subjected to intensive stresses leading to localized failure which may be described as bursting. The slab of Kaibab limestone driven upward through inverted younger strata has been described (Section M–N, Pl. 5). About 3 miles southwest of this unusual feature, and generally on strike with it, a much larger block of Kaibab limestone has been forced up between bounding faults. The west side of this block is in the hanging wall of the Snowdrift reverse fault. An irregular fracture, with sharply angular turns, extends along the north and east sides of the block, and the western branch of the Weiser fault forms the southeastern boundary. The block has been squeezed into synclinal form and tilted sharply southeastward. Maximum uplift of this squeezed-up horst was about 1000 feet.

Several reverse faults of limited extent appear to represent localized yielding to shearing stress beneath or in front of the thrust plate. Examples are the fault cutting the overturned Kaibab west of the Snowdrift fault, Section O–P; and another at the west end of Section Q–R, on which overturned Kaibab was forced upward over Shinarump conglomerate.

Remnants of the Glendale plate.—On Plates 1 and 5 remnants of the Glendale thrust plate are not differentiated into formations, for two reasons: (1) Showing the remnants by one distinctive convention helps the reader to visualize the major structural relations. (2) In some remnants the formations cannot be certainly identified, because extreme shattering and secondary dolomitization of the dominantly carbonate rocks have obscured the fossil evidence and many of the distinctive physical characteristics. Nevertheless, enough evidence remains for confident identification of Cambrian, Devonian, Mississippian, and Pennsylvanian strata in the group of

FRAGMENT OF KAIBAB LIMESTONE PIERCING LIMB OF RECUMBENT SYNCLINE

Piercement block of Kaibab appears as dark elongate oval, near left of view. Surrounding Moenkopi beds are inverted. South at top of view. (*See* section M-N of Plate 5.)

OBLIQUE AERIAL VIEW EASTWARD ALONG ARROWHEAD FAULT AND VALLEY-OF-FIRE ANTICLINE

Note offsetting faults. Valley-of-Fire anticline in middle distance. Arm of Lake Mead in Virgin Valley; southern Virgin Mountain block beyond; Grand Wash Cliffs on distant sky line. (Copyright by R. C. Frampton)

remnants. The Lower Mississippian crystalline limestone has kept its identity particularly well and is recognized in several of the more easterly units of the group. Cambrian strata with the mottling characteristic of the Muav limestone make an important part of the largest remnant, in the southwestern part of the area. The east-dipping section of the plate shown in Section S–T includes Devonian strata, with Mississippian and Pennsylvanian beds following in normal stratigraphic order toward the east. Several other remnants contain beds recognized as belonging to one or more of the four systems.

Details of structure within the several remnants are varied. In general, strata in the westernmost outcrops of the plate dip westward, nearly parallel to the thrust surface itself, as represented in Sections I–J, K–L, and O–P. In the large remnant near the southwestern corner of the area, however, the general westward dip is complicated by sharp folding; locally the beds are vertical or have highly irregular dips. Along the line of Section S–T dips within the plate are uniformly eastward, at a steep angle. Since the beds there are in normal stratigraphic order, evidence suggests that the thrust developed by shearing rupture of a large anticline, with riding forward of the upper limb (Fig. 5). This suggestion has some support in the structure of the remnant that rests on the Narrows anticline about 4 miles farther north, shown in Section O–P.

All remnants in the northern part of the belt have generally simple structure, with bedding nearly parallel to the thrust surface (Sections E–F, G–H, I–J). Although the remnants are too scattered for confident reconstruction of the plate in all details, the inference seems warranted that the plate had structure generally similar to that shown in Figure 10, with acute deformation locally due to irregularity of the overridden surface. This interpretation is developed further in a later section.

The remnant at the west end of Section O–P is exceptionally crushed and broken. In fact most of the mass consists of megabreccia, with jumbled blocks embedded in a well-cemented matrix of finer tectonic debris. Some blocks of the underlying red beds are mixed with fragments of the older strata. The elongate form of the remnant reflects sharp downbending along an east-west axis, with some faulting along the margins; this lowering of the block structurally is responsible for its preservation with much greater east-west than north-south dimension. No similar large-scale brecciation is found in any other remnant of the thrust plate. In fact, the beds are remarkably intact in most of the remnants, although close examination reveals that the rock was shattered minutely and later recemented. Secondary dolomitization of the limestones has been thorough in most of the remnants, except for the Lower Mississippian crystalline limestone, which for some reason resisted this kind of alteration.

The remnant of the plate embedded in the Overton fan (represented near the east end of Section I–J) is of particular interest. Fan debris adjacent to this remnant is very coarse, and bedding is crude. In an overall view along the strike, however, no divergence can be detected between stratification in the fan and in the thrust plate; the carbonate beds that make up the remnant, traceable along the strike through more than a third of a mile, appear to be an integral part of the fan deposit. Presumably this part of the plate, as it was pushed eastward, moved over the fan surface and therefore essentially parallel to the crude bedding beneath. No doubt the

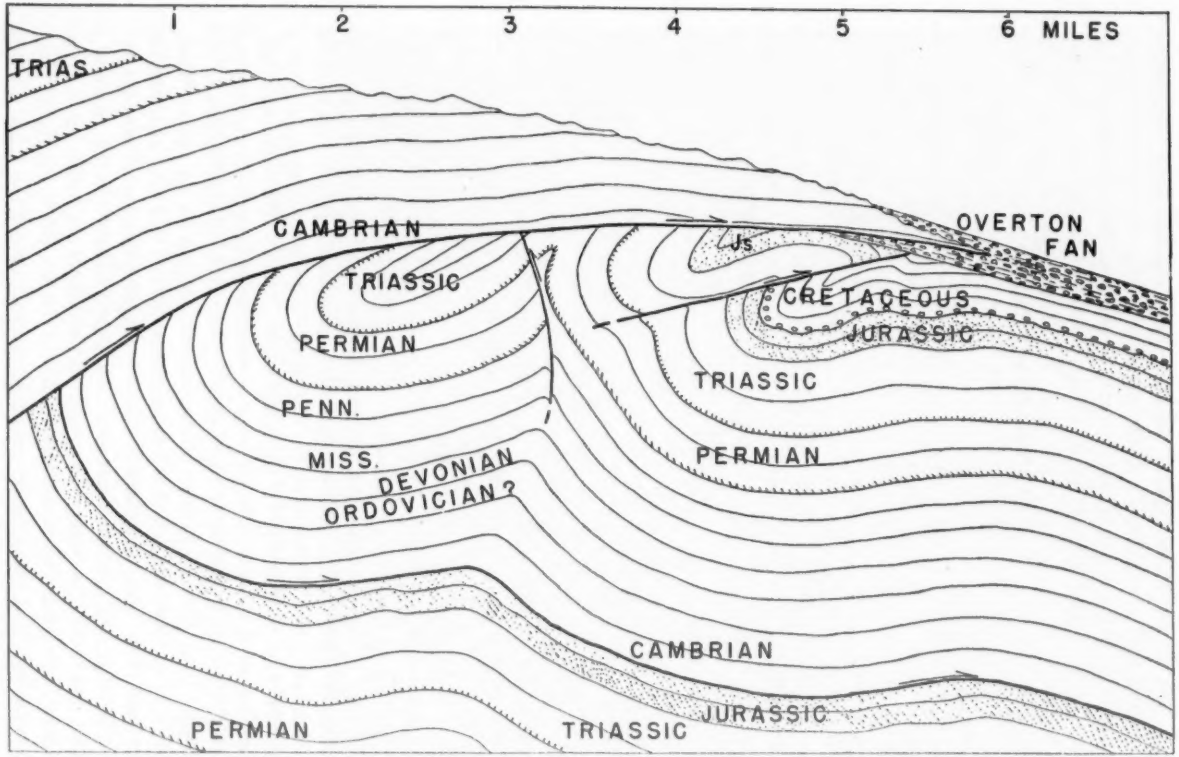

FIGURE 10.—*Generalized section through the Glendale thrust zone before final deformation and erosion*

Representing the thrust plate while it was active, with the eroded "prow" buried in fan debris. The related Willow Tank thrust is shown; also the Muddy Mountain thrust, at depth. Many details of deformation are omitted.

plate in this location was initially much thicker than the remnant now exposed; erosion removed the plate over much of the area and left only a thin remnant to be buried under later fan deposit. Doubtless a considerable part of the plate was eroded, together with the inclosing fanglomerate, after the beds were tilted to their present attitude.

The rock composing the remnant shows minute shattering and thorough dolomitization. The beds are essentially parallel to the thrust surface; thus their attitude does not suggest proximity to the original front of the thrust plate, in accord with the concept of the plate represented in Figure 5. Possibly, of course, the original "prow" of the plate, with its structure of downcurved beds, was destroyed by erosion before any part of the plate progressed as far eastward as the remnant inclosed in the Overton fan.

Masses dragged and pushed by the thrust plate.—In several parts of the area blocks that have thrust relation to the rocks beneath them were not parts of the thrust plate itself; they were caught beneath the plate and dragged varying distances to their present locations. These blocks, most of which consist of Kaibab limestone, range from small fragments a few tens of feet across to massive slabs a mile or more in greatest dimension. All have been sheared and mashed; some are best described as mangled. The largest masses were derived from the upper limb of the recumbent Weiser syncline, where the plate of older rocks was in contact with inverted Kaibab beds. Gypsum in the lower part of the Moenkopi and within the Kaibab section itself acted as a lubricant on which the stiff limestone members of the Kaibab slid in response to frictional drag. Commonly the gypseous middle member of the Kaibab, about 100 feet thick, was eliminated by squeezing and shearing, so that the lower limestone member now rests directly on the upper cherty member. Where sliding occurred on the basal Moenkopi, the thin beds of that formation were much contorted and brecciated.

One of the largest masses of dragged Kaibab lies along and south of Section S–T. Although the Kaibab beds in that area are generally in their correct position in the recumbent syncline, they have been so dragged and deformed that they are mapped (Pl. 1) as a thrust plate. Locally the Kaibab strata are imbricated and dip steeply into the contact with the Moenkopi, along which there is severe brecciation and distortion. Near the southern end of this exposure, two windows eroded through the Kaibab mass reveal at the base a coarse breccia made of Kaibab blocks, resting on sharply overturned drag folds in the thin-bedded Moenkopi. A similar extensive mass of dragged and sheared Kaibab lies between Sections I–J and K–L. Smaller masses which were moved through considerable distances lie on the Narrows anticline, along and south of Section O–P. Unlike the extensive sheets of Kaibab discussed above, which were pushed along in essentially their proper (though inverted) stratigraphic horizons, the masses on the Narrows anticline lie on Moenkopi strata that are in normal stratigraphic order. The nearest possible source of the dragged masses was west of the Weiser fault, and probably west of the Snowdrift fault, fully 2 miles from their present positions. Perhaps the two blocks were transported as a unit; they are now separated by a narrow valley cut below their level into the Moenkopi. The southern block is extremely contorted and shattered and has been crushed

into the weaker Moenkopi beds beneath it. Part of the northern block is covered by older rocks in a remnant of the Glendale plate.

Many huge blocks of Kaibab and of Moenkopi limestone in the western part of the Overton fan must have been pushed forward at the prow of the thrust sheet. The outstanding example is the gigantic mass of Kaibab limestone along the line of Section E–F. Other similar blocks that range in length up to 400 or 500 feet lie at the base of the fan south of Muddy Creek. Since these masses were torn from bedrock and pushed or dragged forward by the advancing thrust plate, we may speak of tectonic erosion and deposition.

Willow Tank thrust.—The thrust exposed in the vicinity of Willow Tank is minor in scale, as compared with the Muddy Mountain and Glendale thrusts; but it has particular interest, because it involves formations much younger than the larger thrusts and therefore bears more directly on the problem of dating some part of the deformation. Moreover, several special features connected with the Willow Tank thrust are unusual and remarkably well displayed.

As now exposed the thrust can be followed along the strike less than 5 miles. Possibly it is much more extensive, since the measurable displacement appears to be at a maximum near the point where the thrust disappears to the north beneath the Overton fan deposits. The thrust plate is broken by a large normal fault, east of which a large part of the plate has been removed by erosion. The southern termination of the thrust as now exposed is a tear fault, essentially vertical, striking slightly north of west. Farther south the thrust has no outcrop, because a large normal fault —the Valley fault (Pl. 4)—has dropped the thrust plate below the present surface (Fig. 12). Whether the tear fault continues farther east than the outcrop of the thrust could not be determined, since mantle conceals the bedrock at the critical locality. If the tear extends downward only to the base of the thrust plate—as appears probable—it would not extend eastward beyond the Valley fault, where the plate is eroded. Extension of the tear westward beyond the outcrop area of Aztec sandstone cannot be traced with assurance, since exposures of the weak Chinle shales are poor.

Chinle beds below the Aztec sandstone are exposed in two small anticlines that bulge the Willow Tank thrust plate upward near its southern margin. East of the large normal fault, the exposed part of the plate consists of Aztec sandstone and a few remnants of the Willow Tank formation. One of these remnants, about 1½ miles southeast of Willow Tank, is strategically situated to give a minimum measure of displacement on the thrust in that part of the area.

East and northeast of Willow Tank the eroded edge of the nearly horizontal thrust plate is extremely ragged. Three small klippes of the red Aztec sandstone are conspicuous on the lighter-colored Cretaceous beds. Of greater interest and importance structurally is the large klippe that extends north and south from Willow Tank (Fig. 3; Pls. 1, 4). The narrow north-south portion of this remnant, about 1½ miles in length, owes its preservation to a sharp synclinal fold which has brought the thrust plate below the general level. Attached to the synclinal remnant is a remarkable block bounded by two east-west tear faults. This block literally "ploughed" across the thick section of Cretaceous beds, which are strongly upturned along

the sides and front of the block. In the eastern half of the block itself the beds are isoclinally folded, with vertical dips in the mid-portion passing into strong overturning near the east end (Fig. 3; Pl. 5, Section Q–R). East of the block the "invaded" Cretaceous strata are overturned or have abnormally steep dips in a belt several hundred feet wide, within which the strike bends strongly eastward in an arc conforming to the prow of the invading block.

The folded Jurassic beds between the tear faults, more resistant than the surrounding Cretaceous rocks, hold on their bevelled edges a large remnant of an old land surface, 200 to 300 feet higher than the present adjacent surface. This remnant appears on the map (Fig. 3) as Tear Fault Mesa. Along its cliffy southern margin are several good exposures of the tear fault, marked by polished surfaces with prominent striae. The fault has a steep northward to nearly vertical dip, up to its junction with the thrust bounding the east end of the block. Striae on the steep surface of the tear fault pitch consistently 20°–30° E. Since the entire section, including the Overton fanglomerate, has been tilted eastward 30° or more after the thrusting occurred, the striae pitched westward at a low angle when they were formed.

Along the sides of the tear-fault block the Cretaceous beds are turned up sharply, and their strike is turned strongly eastward (Fig. 3). The effect of drag is especially conspicuous along the north side, although the tear fault on that side is less well exposed than the fault on the south. Near the southeast corner of the tear-fault block a small remnant of Aztec sandstone, with basal Cretaceous conglomerate on its eastern edge, lies south of the tear fault. This smaller block is in thrust relation to Cretaceous beds beneath it and presumably is a remnant of the main thrust plate. The base of the Willow Tank formation in this block lies about a third of a mile west of the corresponding horizon near the front of the large tear-fault block, and presumably this distance is a measure of differential displacement between the two blocks. The minimum displacement of the tear-fault block is readily determined as about a mile, since the Aztec sandstone forming most of the block must have been moved from a position beyond the Jurassic-Cretaceous contact that lies west of the klippe.

Other questions arise on the structural relations of the tear-fault block. How far westward into the thrust plate did the two tear faults extend? Surely the fault at the southern margin of the block had considerable length, to permit the large adjustment indicated by differential displacement of a third of a mile between adjacent blocks. No direct evidence of the fault is to be seen in the synclinal remnant of the plate at the west side of the klippe. However, the trace of the fault is not straight, and a slight curvature would carry it along the south end of the synclinal remnant. The northern fault, on the other hand, can be traced continuously to the west edge of the klippe, except for a short stretch concealed by alluvium. Presumably this fault also permitted differential displacement within the thrust plate; but the wide gap between the tear-fault block and remnants farther north prevents a reliable quantitative estimate. Available evidence does suggest strongly that the tear-fault block was displaced considerably less than the part of the plate north of it. North of Overton Wash, and directly under the Overton fan deposit, the Willow Tank formation resting on Aztec sandstone in the thrust plate has escaped erosion in a small block depressed

between faults (Fig. 3). Comparison with the same horizon beneath the plate near Willow Tank gives minimum displacement on the thrust of 1½ miles. The increase by half a mile, as compared with displacement of the tear-fault block, may of course be considerably more than the measure of strike-slip on the northern tear fault, since the Overton Wash section is nearly 2 miles away. However, the evidence indicates clearly a progressive increase of displacement on the Willow Tank thrust as it is followed northward, with at least partial adjustment to the differential movement accounted for by slipping along tear faults.

Nearly 5 miles north of Willow Tank the lower part of the Cretaceous section is exposed through a distance of half a mile along the strike. Presumably the thrust lies beneath, as shown in Section K–L (Pl. 5), since the outcrop of Aztec sandstone extends unbroken southward to the vicinity of Willow Tank (Pl. 1). Possibly the westward recession of the Aztec-Willow Tank contact in Section K–L, as compared with its position in Section O–P, indicates a decrease in displacement on the thrust north of the latter section. This supposition rests largely on assumption that the general strike of the thrust parallels the strike of the Glendale thrust and associated folds.

Except for localized anticlinal and synclinal buckles, the thrust surface in the vicinity of Willow Tank and Overton Wash is almost horizontal. That this was not the original attitude is indicated clearly by structural evidence. The Overton fan, deposited across the eroded edge of the thrust plate, was later tilted northeastward almost uniformly with the underlying Cretaceous section, which is transected by the thrust. Presumably the fan deposits had an original dip of a few degrees in a direction somewhat south of east—essentially at right angles to the front of the highland created by the Glendale orogeny. If the combined sedimentary section, post- and pre-thrust in age, were tilted back to its original attitude, the Willow Tank thrust plate would dip westward at somewhat less than 30°. As already noted, restoration of the original attitude would give the eastward-pitching striae on the surface at Tear Fault Mesa a westward pitch considerably less than the average dip of the thrust. This relation accords with evidence that the tear fault block "ploughed" more deeply into the Cretaceous section than did adjacent parts of the thrust plate.

TRANSVERSE FAULTS

Four prominent transverse faults that have been described separately have some features in common that suggest a group relationship. They are the two tear faults bounding the block at Tear Fault Mesa, the tear fault that intersects the Valley fault, and the Arrowhead fault. The Arrowhead is of course in a class by itself in the matter of scale; moreover, it has a large vertical component of slip which the three smaller faults lack. However, the Arrowhead fault has an important strike-slip component also, and in the direction of its trace it is remarkably like the smaller transverse faults.

It is of interest to examine the transverse faults in relation to the structural trends of the Glendale thrust zone. These trends have an average direction about N. 20° E. The faults at Tear Fault Mesa strike E.–W. to S. 85° E. Average strike of the Arrowhead fault—discounting offsets due to cross-faulting—is about S. 87° E. Thus these three faults intersect the average Glendale trends at 70° to 75°. The tear fault at the

southernmost exposure of the Willow Tank thrust strikes about S. 72° E. and therefore is almost exactly at right angles to the Glendale trend.

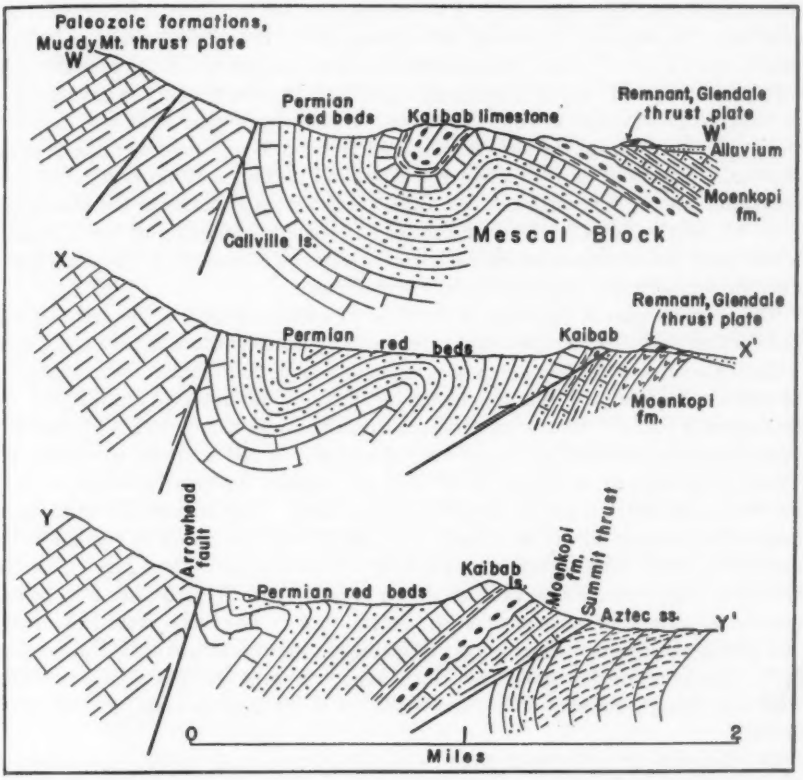

FIGURE 11.—*Sections showing structure within the Mescal and Summit blocks*

Along lines W-W', X-X', and Y-Y' of Plate 1

The three smaller transverse faults seem clearly related to the Glendale orogeny. Possible relation of the Arrowhead fault to the same episode of deformation is discussed in a later section.

SUMMIT THRUST

One of the most puzzling structural features of the area is a comparatively small thrust block that lies a short distance north of the Arrowhead fault and west of the Valley of Fire (Fig. 11; Pl. 1). The name Summit thrust is chosen for the fault, because of its location near a point on the Valley-of-Fire road long known to local inhabitants as Summit (Pl. 4). With a visible length of nearly 2 miles, the thrust strikes northwesterly and dips southwest at a maximum observed angle of 35°.

The lower marine member of the Moenkopi formation, strongly overturned, has been thrust northeastward over Aztec sandstone, the beds of which are also overturned (Fig. 11, Section Y–Y′). Toward the southeast the thrust can be traced to an abrupt ending against a large normal fault; if it continues beyond this fault, it is concealed by alluvium. In the other direction, the outcrop of the thrust disappears under fan debris, but the thrust block of overturned Moenkopi and Kaibab strata runs through with consistent structure to a northeast-trending fault that appears to have an important strike-slip component. Northwest of this transverse fault the Summit thrust, if it continues at the same stratigraphic horizon, is concealed by thick alluvial deposits. The block of overturned Moenkopi and Kaibab is abruptly offset at the cross fault, and farther northwest the Kaibab is thrust somewhat over the Moenkopi (Fig. 11, Section X–X′). Older Paleozoic limestone in remnants of the Glendale thrust plate lies across the bevelled edges of overturned Moenkopi and Kaibab beds, near the southern edge of a wide gravel-covered area.

The southern part of the Summit thrust block consists largely of the Permian red beds, which underlie a wedge-shaped area tapering eastward to a narrow strip, and widening westward to a maximum of considerably more than a mile. In a large part of this area the weak red beds are masked by alluvium; but outcrops are sufficient to demonstrate that the formation underlies the entire area as mapped, and that the beds are much deformed, with near-vertical and overturned attitudes predominant. The structure shown in Section X–X′ (Fig. 11) explains the great width of red-bed outcrop in the western part of the wedge-shaped area. Farther east the Arrowhead fault cuts obliquely across the thrust block, modifying it as shown in Section Y–Y′ and finally almost eliminating the red-bed section at the point of the wedge. Abrupt change in the structure westward, as shown in Section W–W′, probably is to be explained by strike-slip movement on the Mescal fault. The block east of this fault was folded, and the Kaibab limestone, lifted high in the overturned anticline (Section X–X′), has been largely removed by later erosion. West of the Mescal fault the folds were less strongly developed (Section W–W′), and the Kaibab beds have survived erosion.

Development of the Summit thrust, with the abrupt change in structure between this thrust block and the Mescal block, presents an interesting problem. The latter block has in its western part a nearly north-south structural trend that seems related to the Glendale belt of folding and thrusting. Pronounced eastward curving of this trend along the south side of the block suggests the influence of stresses related to movement on the Arrowhead fault. This influence is seen also in the Summit thrust and in the overturned fold south of it (Sections X–X′, Y–Y′). The Mescal fault, and the conspicuous structural differences in the blocks adjoining it, may be explained by the northward bend in the Arrowhead fault at this locality. Since upward movement of the Arrowhead hanging wall had an eastward component, resistance to the movement because of the bend must have set up differential compression directly to the north. This detail in the mechanics of the deformation, and also the relation of Glendale thrust-plate remnants to the Summit and Mescal blocks, are discussed in the section on the probable sequence of tectonic events.

VALLEY-OF-FIRE ANTICLINE

Through more than 6 miles in the eastern part of its course, the Arrowhead fault is nearly parallel with and about a mile south of the axial trace of a large anticline (Pls. 1, 4, 9). Although this fold is cut by numerous faults, and considerable areas underlain by the weak formations involved are mantled with alluvium, the essential structure is clearly recognizable. Moenkopi strata, including a considerable thickness of the lower marine member, are exposed in the areas of greatest structural height. Chinle and Aztec beds dip northward and southward from the crest and swing continuously around the east end of the fold, thus reflecting an eastward plunge which is clearly evident also in the pronounced dips. Toward the west the fold grows indistinct, partly because of complicating faults and partly because alluvium is widespread in critical areas. Moreover, the strong north-south deformation associated with the Glendale thrust would in itself mask the expression of the less intensive east-west fold. Since the most conspicuous part of the anticline is displayed in the area known as the Valley of Fire, this major structural feature is appropriately called the Valley-of-Fire anticline.

The maps (Pls. 1, 4) indicate that pronounced dips north and northeast from the crest of the anticline affect a belt several miles wide. Moreover, on the south flank of the fold the southward dips extend beyond the Arrowhead fault into a wide area of the Muddy Mountain thrust plate. The symmetry of structure in the two blocks separated by the Arrowhead fault is well shown in Section C–D (Fig. 7). Indeed, this symmetry is deceptive until a careful field study is made, since the Jurassic Aztec sandstone below the thrust north of *D* appears to match the same formation near *C*, and it might be inferred, therefore, that the thrust plate once extended northward across the anticline.

Of the numerous faults that cut the anticline, three have especially modified its form. Near the east end of the fold a fault with irregular north to northeast trend has brought up the Chinle formation in a wide area where the plunge of the axis would normally carry this formation to considerable depth. The Baseline fault causes a large offset of formation boundaries on the north flank of the fold and possibly some offset also of the axial trace, although precise locating of the trace, except near the plunging east end, is difficult because of alluvial cover and disturbance on northwesterly faults. The important Atlatl fault seems to be in part responsible for the abrupt obscuring of the anticlinal structure as the fold is followed westward in the Valley of Fire. The consistently northeastward dips in both the hanging wall and the footwall of this fault are strong enough to conceal the gentle arching of the broad anticlinal crest if this antedated faulting and attendant deformation.

NORMAL FAULTS

Within the belt that was covered by the Glendale thrust plate, most of the large faults are reverse, with steep dips. These faults strike generally northeast, in harmony with the structural grain of the belt. Farther east most of the faults are normal and strike from northeasterly through north to northwest. Some faults in

the eastern belt have fairly uniform trend throughout their known extent. Others shift trend abruptly; in particular, the north and northwest trends are combined in some major faults. All the larger faults have downthrow on the west side.

The largest normal faults are the Baseline, Narrows, Waterpocket, Valley, Atlatl, and Camp (Pl. 4). The Baseline fault has particular interest because of its irregular strike, its large displacement, and the clear evidence of its early development. The zigzag trend of the fault trace reflects a system of fractures that appear in the Jurassic and Cretaceous rocks as sets of master joints (Pl. 10). One set strikes somewhat east of north, and another strikes northwestward. The fault alternates in strike between these two general directions. Its surface, coated with iron oxide and dipping about 50° W., is well exposed at many points. Offset of the distinctive conglomerate at the base of the Willow Tank formation is more than 8000 feet, measured along the fault trace which is strongly oblique to the strike of the strata. Measured at right angles to the strike, the offset is about 7400 feet; since the average dip of the beds is 30°, the vertical component of displacement is about 3700 feet.

Toward the south the fault divides. One branch, essentially parallel to the strike of beds, causes duplication of Chinle and Aztec strata; the other branch cuts across the north limb of the Valley-of-Fire anticline, causing strong stratigraphic offset. Northward the fault is clearly traceable as it crosses the Baseline sandstones, but it disappears abruptly at or near the base of the Overton fan deposits. Possibly the lowermost Overton beds are cut by the fault also, since at this locality the Overton and Baseline deposits are so similar that a precise contact cannot be drawn between them. However, most of the Overton section is unaffected by the faulting.

The Narrows fault is traceable for about 3 miles, with a strike almost exactly north. In the north half of its visible course the fault has dropped a thick section of Horse Spring limestone against Overton fanglomerate. The large block of Kaibab limestone in the fan deposit, already described, evidently has been cut by the Narrows fault, which forms the straight western side of the block as now exposed. Throw of the fault in this part of its course, as estimated from the structure of the Horse Spring limestone, is 700–800 feet. Farther south the fault is concealed by Muddy Valley alluvium although it is clearly visible in the valley where the road crosses an outcrop of Chinle beds. The fault reappears south of the valley, with considerably decreased throw, and finally becomes untraceable in the belt underlain by nearly vertical beds of weak Chinle shale.

The Waterpocket fault is most clearly displayed in the stretch west of Tear Fault Mesa and Willow Tank. There the fault displaces the Willow Tank thrust plate, which has been eroded from the footwall block except for remnants that are favorably located. Some outcrops reveal the fault surface, dipping 55°–60° W. The thick-bedded Aztec sandstone forms both hanging wall and footwall; since this formation contains no distinctive horizons, it is not possible to estimate with any confidence the measure of displacement. However, relations of the Willow Tank thrust plate on opposite sides of the fault suggest displacement of at least several hundred feet.

Although the fault cuts only the monotonous Aztec sandstone, the location of the trace throughout the 2-mile stretch discussed above is rather clearly marked by a

FIGURE 1. FRACTURE SETS IN AZTEC SANDSTONE
Some small faults make obvious offsets in contact with Chinle, near top of view (south). Conglomerate at base of Cretaceous section, dipping 30° northeast, ends abruptly at Baseline fault, left of *C*.

FIGURE 2. VIEW CONTINUED NORTHWARD FROM FIGURE 1, ABOVE
Point *C* is on basal beds of Cretaceous. Baseline fault, just to right of *C*, takes zigzag course to upper left of view.

VIEWS SHOWING FRACTURE SETS AND FAULTS CUTTING JURASSIC AND CRETACEOUS BEDS

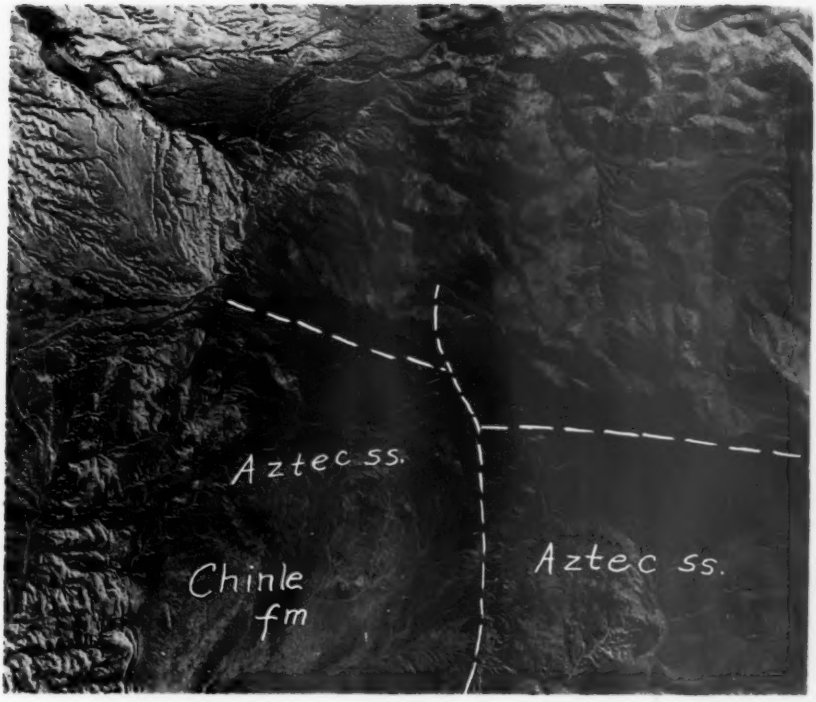

VERTICAL VIEW SHOWING FEATURES NEAR EAST END OF ARROWHEAD FAULT
South at top. This fault, at base of scarp, is offset by a north-south fault, as shown. The light-colored formation at left is the Muddy Creek formation, the beds dipping 20° to 50° eastward.

change in color of the rock. In the hanging wall the sandstone is the deep brick red characteristic of the formation; on the footwall side, color tones range through lavender, yellow, and gray to pure white. Bleaching has affected the sandstone in a zone of considerable but irregular thickness both above and below the thrust. This bleached zone has not yet been eroded from the footwall of the normal fault, although only remnants of the plate remain. On the hanging-wall side the plate is downthrown sufficiently to conceal the bleached zone. Farther south, where erosion has cut deeper, the bleached zone appears both above and below the thrust, as it is exposed west of the Waterpocket fault.

Northwest of Willow Tank the fault cannot be traced continuously, because of local alluvial cover and the uniform appearance of the Aztec sandstone. Farther north there is a conspicuous zone of fracture marked by a topographic trench in which blown sand hides all details of structure. Although alluvium conceals the Overton fanglomerate along the northward prolongation of the fault trace, the fault probably breaks the fanglomerate (Pl. 5, Section I–J). Conceivably the Waterpocket and Narrows faults are one and the same; a slight change in strike would bring them together somewhere in the area of poor outcrops between the faults as mapped. On the other hand they may be separate fractures, arranged en echelon and genetically related.

Toward the south the Waterpocket fault is traceable continuously to the broad apron of alluvium north of the point known as Atlatl Rock (a pictograph exhibit) on the Valley-of-Fire road. In this southern part of its visible course the fault has large displacement, as indicated by the abrupt ending against it, on the west, of a thick fanglomerate section. This section, many hundreds of feet thick, is in a tilted block; the beds dip steeply into the northwest-striking Valley fault, which coalesces with the Waterpocket fault. Near the junction the dip of the Valley fault beneath the fanglomerate is no more than 20°, as indicated by the westward bend of the trace in crossing a valley. Since the beds of fanglomerate there dip 50° into the fault, suggestion is strong that the block has been rotated on a curved fault surface, concave upward (Longwell, 1945b). Similar response of the Valley fault trace to topography farther northwest indicates that low dip of the fault surface is persistent. Beyond the northwest limit of the fanglomerate outcrop, alluvium mantles much of the surface, and the exact position and form of the fault trace are uncertain. The approximate average course of the trace, as inferred from effects on the Willow Tank thrust plate, is mapped. Possibly the fault continues farther than mapped, but structural features are obscure in the massive Aztec sandstone.

Inspection of the map (Pl. 1) may arouse some question whether the fanglomerate in the blocks bounded by the Valley and Camp faults is correctly referred to the Overton fan. A few miles northeast of these blocks, the Overton fan deposits rest on a Cretaceous section more than 3000 feet thick, whereas in the Valley and Camp blocks the fanglomerate lies on the Aztec sandstone. There is no reasonable doubt, however, that identification of the rock in the two blocks as Overton fanglomerate is correct; coarse fragments—the chief constituents—apparently were derived from the Glendale thrust plate, and the degree of induration is closely similar to that in the coarser part of the Overton fan. Absence of Cretaceous deposits in the Valley and

Camp blocks is explained by folding, thrusting, and erosion before the Overton deposition, as represented in Figure 12, B. The large displacement on the Valley and Waterpocket faults, to account for the present distribution of the fanglomerate, is shown by Figure 12, A.

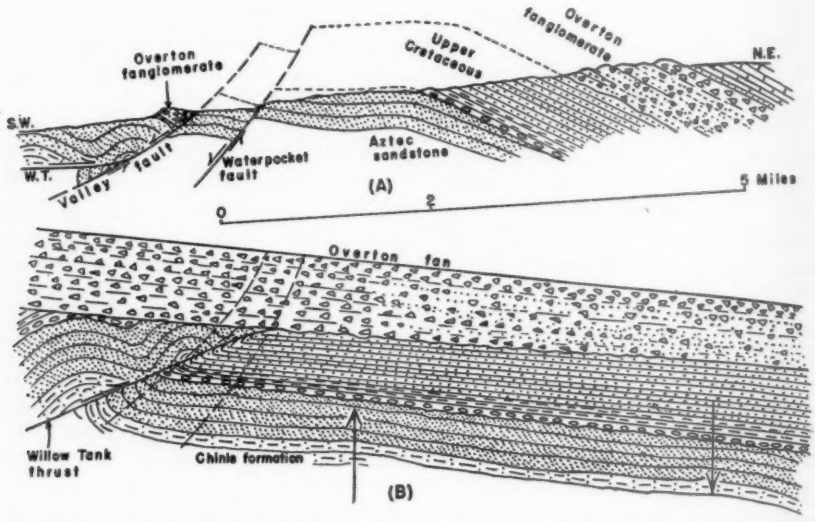

FIGURE 12.—*Sections through Valley and Waterpocket faults, to show probable evolution of structure*

A, section to show present relation of the Valley fault block to main outcrop of Overton fanglomerate. *B*, idealized section as it was before movement on Valley and Waterpocket faults. Large arrows suggest deformation by bending, perhaps contemporaneous with the faulting.

Throw on the Atlatl fault also is large, since beds high in the Aztec sandstone are brought in contact with the upper member of the Moenkopi formation. If the Chinle formation in this part of the area is 2000 feet thick, and if only half the thickness of the Aztec is involved, the stratigraphic throw on the fault is more than 3500 feet. Although much of the fault trace is concealed by alluvium, it is projected with assurance southeastward to the prominent break on the west side of Fire Alcove, where the Muddy Mountain thrust plate is displaced with large throw (Fig. 4). Toward the northwest the fault disappears under a wide apron of alluvium; probably it continues in that direction for a considerable distance, between the Valley and Camp faults.

In the Camp fault block the steeply tilted beds of fanglomerate, several hundreds of feet thick, give a minimum measure of displacement on the fault. Presumably large displacement was required to lower the fanglomerate so far in relation to the Valley fault block. Much of this displacement, however, probably was accomplished by movement on the intervening Atlatl fault. Alluvium conceals the trace of the Camp fault both northwest and southeast of the ridge formed by the fanglomerate. There is no indication that the fault breaks the Muddy Mountain thrust plate.

The fault that terminates the Summit thrust block on the east offsets the trace of the Arrowhead fault fully a quarter of a mile. This fault has not been studied farther south, and evidence is lacking on the nature of the displacement. Considerable strike-slip movement is suggested, since the dip of the Arrowhead fault is steep in that vicinity. Toward the north the fault trace disappears under alluvium.

Numerous other faults cut the Valley-of-Fire anticline; six that trend nearly north are in three pairs, each bounding a narrow graben block. These faults appear to have small or moderate throw. Some of the northwesterly faults have displacement measured in hundreds of feet, with strong tilting of blocks to make strike ridges wherever the beds are resistant. The Shinarump conglomerate plays a prominent role in revealing these faults. Doubtless many others escape detection because weak Chinle and Moenkopi beds affected are covered with alluvium. Of all the faults thus far recognized on the anticline only one, half a mile east of the Atlatl fault, has reverse displacement.

Numerous faults cutting the base of the Aztec sandstone, along the north flank and east end of the plunging anticline, conspicuously offset the formational boundary. Trends of these faults range between wide limits (Pl. 1). Doubtless the displacements represent adjustments to stresses during growth of the anticline, and most of the faults extend only short distances down the flank of the fold (Pl. 10, fig. 1).

The large north-south fault that drops Aztec sandstone against Chinle shales near the east end of the Valley-of-Fire anticline has a throw of 1000 feet or more. Since the trace disappears northward under a wide alluvial cover, it is not possible to determine whether it is the same fault that emerges from this cover and extends northeastward; but this interpretation is favored by continuous outcrop of the Chinle formation on the southeast. Considerable displacement of the Muddy Creek beds along the northeastern extension of the fault indicates a late date for at least part of the movement, though initiation of the fault early in the history of the anticline is probable. An appreciable offset of the escarpment in line with the fault trace at the south indicates that the fault extends into the thrust plate. The trace of the fault can be followed for some distance southward on top of the plate, but absence of any scarp on the resistant carbonate rocks suggests that the fault in that part of its course has been long inactive (Pl. 11).

North of Bluepoint, strong eastward dips (20°–50°) in the Muddy Creek beds suggest late faulting, possibly along the northward extension of the major fault that bounds the Muddy Mountain thrust plate on the east. No evidence of recent movement on this fault was seen south of Bluepoint, where alluvium masks the fault trace (Pl. 11).

INTERPRETATION OF THE EVIDENCE

RELATION BETWEEN MUDDY MOUNTAIN AND GLENDALE THRUSTS

Several considerations suggest that the Muddy Mountain thrust antedates the Glendale thrust. One aspect of the evidence is negative: The Muddy Mountain thrust, so far as known, involved no formation younger than Jurassic, whereas the Glendale thrust affected a thick section including Upper Cretaceous strata and also

deposits that possibly are post-Cretaceous. Perhaps it is merely fortuitous that no strata younger than Jurassic have been found associated with the larger thrust, but the wide remnant of the plate now exposed seems to represent the forward part of a thrust like that shown in Figure 5, and therefore it probably moved for many miles along the pre-thrusting surface of the land. If the thick Cretaceous formations now exposed only a few miles north of the Arrowhead fault existed when the Muddy Mountain plate rode forward, it is hardly conceivable that all parts of these formations could have escaped overriding, whereas the next older formation—the Aztec sandstone—was everywhere caught beneath the wide plate. Moreover, in other parts of the region similar large thrust plates overrode the Aztec sandstone (Longwell, 1926; Hewett, 1931). At least one of these plates moved over gravels derived from formations in the plate and deposited in front of the moving mass (Longwell, 1926, p. 570). Thus it is strongly suggested that the region experienced major orogeny when no considerable deposits younger than Jurassic were present, and that the Muddy Mountain thrust is a product of this orogeny.

A more potent argument for later dating of the Glendale thrust is found in study of the anticlinal fold, here called the Buffington anticline, which is responsible for the large window near the west border of the Muddy Mountain plate. This fold trends N. 20° E., which is the average strike of folds in the Glendale thrust belt. In fact, the large plunging anticline is logically considered a southward prolongation of the Glendale belt of folding. Folds in this belt, the overturned Narrows anticline and the recumbent Weiser syncline, were overridden by the Glendale thrust and patently were developed in an orogenic pulse of which the thrusting was the culminating event. Since the Buffington anticline involves the Muddy Mountain thrust plate, presumably this plate was in its present position before the Glendale folding and thrusting.

The Arrowhead fault, which clearly is younger than the Muddy Mountain thrust, provides independent evidence. On the other hand there is strong suggestion that movement on the Arrowhead fault was in progress before emplacement of the Glendale thrust plate was completed. The Summit thrust, its relation to the Mescal block, and the form of the latter block are best explained as incidental effects of movement on the Arrowhead fault. However, remnants of the Glendale thrust plate lie across the upturned edges of Kaibab and Moenkopi strata on both sides of the Mescal fault (Pl. 1). Surely this must mean that the Summit and Mescal blocks had acquired essentially their present attitudes before the Glendale plate overrode them. Planing of the sharply tilted blocks may have been accomplished by erosion before the thrust plate advanced, or at least in part by shearing abrasion as the massive plate was pushed forward. Whatever the mechanical details the Glendale thrust appears to represent an orogenic episode appreciably later than the development of the Muddy Mountain thrust.

ARROWHEAD FAULT AND VALLEY-OF-FIRE ANTICLINE

The Valley-of-Fire anticline, with its axial trace closely parallel to the Arrowhead fault, appears to be genetically related to this fault. However, some aspects of the fold-fault combination are puzzling. Since the Arrowhead fault is a steep reverse fault, it may seem reasonable to relate both the fault and the anticline to north-

south compression, and to ascribe the steep dip of the fault to rotation with steepening of the south limb of the fold. But the steep southward dips in the strata of the thrust plate are not the simple expression of an anticlinal limb. These dips are most pronounced between the Atlatl fault and the Buffington window—that is, west of the area in which the Valley-of-Fire anticline is recognizable. Moreover, the dips in the plate are generally steepest near the Arrowhead fault and become gentler southward. At several localities, the Paleozoic beds in the hanging wall are overturned to an attitude essentially parallel with the fault. Therefore the southward dips in the northern part of the plate seem to be related genetically to the fault; they fit into the pattern of the Valley-of-Fire anticline only incidentally.

Displacement on the Arrowhead fault attests a force with an important east-west as well as a north-south component. The east-west component is indicated not by direct evidence of strike-slip displacement, but chiefly by pronounced eastward bending of trend lines north of the fault. The full measure of this bending is revealed by the westernmost outcrop band of the Kaibab limestone in the Glendale thrust belt. This band, marking the inflection of the Weiser recumbent syncline, extends southwestward from the vicinity of the Bowl, with minor interruptions and deviations, to a point about 4 miles north from the west end of the Arrowhead fault. There the band of Kaibab turns toward the southeast and can be projected confidently, across short gaps concealed by alluvium, to the southeast corner of the Mescal block (Fig. 13). From that vicinity the outcrop belts of the Permian red beds and successively older formations also can be projected to the northwest, to their logical positions beneath alluvium in the northeast-trending belt beneath the Glendale thrust plate (Pls. 1,4). Thus all these units swing eastward as they approach the Arrowhead fault, and at the south side of the Mescal block the beds strike essentially parallel to the fault. Although the Mescal fault complicates the structural picture, the eastward "hook" in the trends of Kaibab limestone and Permian red beds carries to the east end of the Summit thrust block. It is more than 6 miles (Fig. 13) from that point westward to a line in projection with the normal Glendale trend. This of course is not to be taken as a measure of eastward displacement by bending. The curvature of trend lines has resulted in part from uptilting of the section northward as well as eastward.

Thus the sharp eastward bending of the trend lines north of the fault indicates not only an eastward component in the Arrowhead zone of movement, but also strong north-south compression. Several other features reflect the north-south compression: (1) reverse displacement on the Arrowhead fault, the block south of the fault having moved obliquely upward to the north; (2) the Summit thrust and the related Mescal tear fault; (3) the sharp buckle in the Aztec-Chinle contact directly north of the Summit block; (4) the Valley-of-Fire anticline. This assemblage of impressive structural units, in their relation to the fault, suggest that the block south of the fault was shoved somewhat north of east, with a lifting component. If movement on the fault accompanied development of the Glendale thrust, as some evidence suggests, the thrusting force acted differentially to cause failure under shearing stress in a zone transverse to the orogenic belt. Figure 13 represents schematically the relations of the principal structural elements. The trace of the Arrowhead fault makes an angle of about 18° with a line normal to the average trend in the Glendale belt of

thrusting. The axial trace of the Buffington anticline is conspicuously parallel to the average trend of the Glendale belt and presumably represents the same episode of deformation.

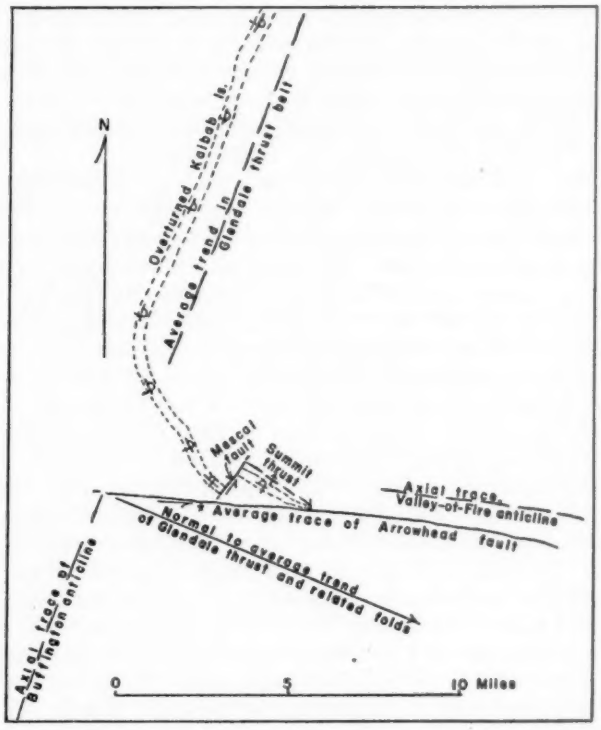

FIGURE 13.—*Diagram showing Arrowhead fault trace in relation to average trend within Glendale thrust belt*

The outcrop belt of overturned Kaibab limestone gives measure of curvature as the belt approaches the Arrowhead fault.

One structural element may suggest that the Valley-of-Fire anticline is younger than the Glendale thrusting. In the north flank of the fold pronounced northward dips continue through a belt several miles wide, involving the Cretaceous section and the eastern part of the Overton fanglomerate as well. However, strikes in the Cretaceous and Overton beds curve from nearly east-west through northwest to nearly north, and presumably the steep eastward component of dip in the fanglomerate reflects a late pulse of compression in the Glendale belt. Perhaps this pulse was accompanied by renewed movement on the Arrowhead fault and further growth of the Valley-of-Fire anticline. Thus the fault may be correlated with late stages of the orogeny, whereas the thrust remnants on the Summit and Mescal blocks indicate

an earlier correlation also. Therefore the Arrowhead fault is plausibly interpreted as an incidental effect of the Glendale orogeny.

POSSIBLE DEVELOPMENT OF THE GLENDALE THRUST

The thick Baseline sandstone, consisting largely of reworked sand from the Aztec sandstone but containing much material from older formations also, had its source to the west. This deposit of coarse-grained material, containing many beds of conglomerate, testifies to fairly rapid uplift of the source area. Earlier low relief and ponded drainage are indicated by the Willow Tank clays, which however were formed at a time of volcanic activity as indicated by included pyroclastic material. Coarse conglomerate at the base of the clays testifies to still earlier uplift and deep erosion. The large boulders suggest a near-by source.

It is assumed, therefore, that folding began in the Glendale thrust zone before the start of the Upper Cretaceous epoch (Fig. 14, A). Erosion reduced the belt of uplift to low relief, and all except the coarsest debris was swept outside the area of present Cretaceous outcrops. The drainage became ponded, perhaps through volcanic activity, and lacustrine clays accumulated. Renewed folding and uplift, in the present Glendale belt and probably extending farther west, gave rise to a thick accumulation of sand and gravel. Erosion cut deeply into the stratigraphic section; conglomerate layers in the Baseline sandstone contain pebbles of white quartzite that probably were derived from the Ordovician Eureka quartzite which, though it is not recognized in the Muddy Mountains, is prominent in the Arrow Canyon Mountains, 20 miles to the west (Fig. 1).

More intense orogeny followed, with development of the overturned Weiser and Narrows folds, the Glendale thrust, and the subsidiary Willow Tank thrust. Some aspects of this structural development are suggested schematically in Figure 14, B, C. Although the Weiser syncline and the Narrows anticline doubtless took form at the same time, Figure 14, B is focused particularly on the recumbent syncline. As shown in some of the structure sections (Pl. 5) the syncline has in both its limbs an incomplete section of the weak Triassic beds. Growth of such a large fold to the closed, recumbent stage, in such a way as to protect these weak strata from destruction by erosion, presents a difficult mechanical problem. It is suggested that after most of the Jurassic strata were removed (Fig. 14, A) the anticline west of the syncline was rolled forward, the axis of the syncline shifting steadily eastward as the crest of the recumbent anticline advanced. Probably the anticline broke to initiate the Glendale thrust before the stage represented in *B* was attained. Another adjustment occurred, however, before the thrust plate moved forward—the Narrows anticline became tightly compressed and was moved upward on the steep Weiser fault (*F*) (Fig. 14, C). Other faults and secondary folds developed, as shown in Plate 5. No doubt this secondary deformation produced large irregularities in the path of the moving thrust block. However, the massive plate sheared off the protruding obstacles, and the resulting rubble, including mangled blocks up to half a mile long, was pushed forward to become the coarsest part of the fan debris. At some stage in the deformation the Narrows anticline became strongly overturned, and the Willow Tank thrust was produced. The Glendale plate finally overrode part of the fan, and the

latest effect of compression was steep tilting of the fan itself and of the strata beneath it.

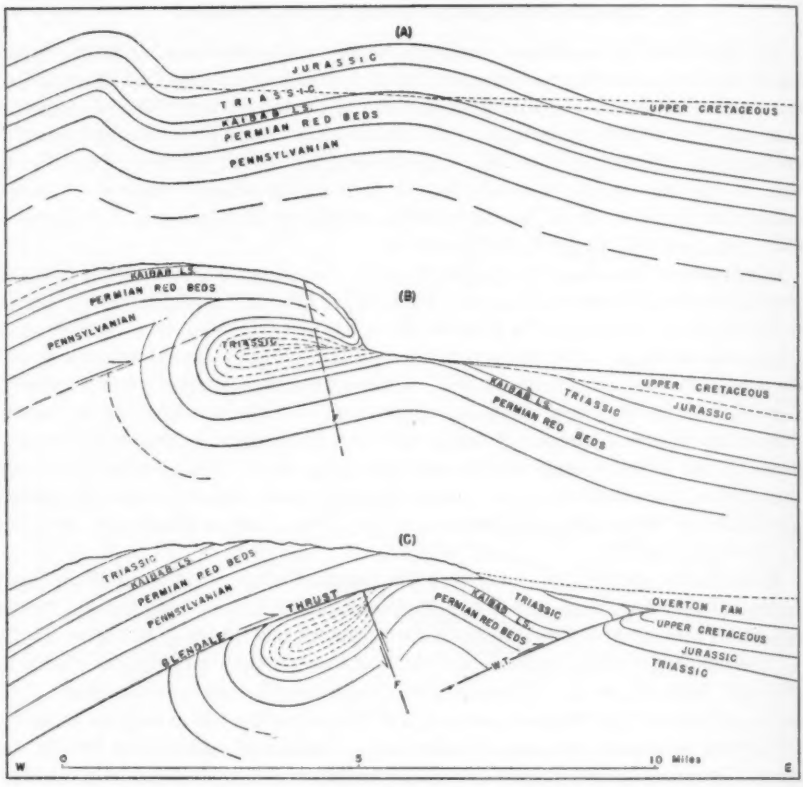

FIGURE 14.—*Sections showing possible stages in development of Glendale thrust*

In *A* it is assumed that rudimentary folding in the belt began before deposition of Cretaceous sediments. Completion of recumbent syncline shown in *B* probably did not occur until thrust was initiated and the Narrows anticline was compressed more than indicated. This anticline probably was overturned at the stage of thrusting represented in *C* W. T., Willow Tank thrust.

NORMAL FAULTS

Since the large north-south faults are downthrown to the west, probably some of them represent failure under the load of the advancing Glendale plate. This explanation is favored particularly for the Baseline fault, since it is older than much of the fan deposit. If the Narrows fault originated at the same time, there was recurrent movement after the Overton and Horse Spring deposits were formed. All the northwest-trending faults are in or near the Valley-of-Fire anticline and probably represent adjustments to stresses during or shortly after movement on the Arrowhead

fault. They cannot be ascribed to tensile stress set up by the strike-slip component of displacement, since fractures so developed should trend northeastward.

The large fault transverse to the east end of the Summit block probably has a large strike-slip component; there appears to be no other logical explanation for the large offset of the steep Arrowhead fault and for the abrupt termination of the Summit thrust block. Possibly movement on this north-south fault occurred late in the structural development, after strike-slip movement on the Arrowhead fault had ceased. However, the north-south fracture must have been present when the Summit thrust moved, since the thrust has large stratigraphic throw—at least 3000 feet—where it intersects the cross fault. Probably the latter fault continues farther south than mapped.

GEOLOGIC DATES OF STRUCTURAL EVENTS

Stratigraphic evidence now available makes the probable time limits of the Muddy Mountain thrust post-Aztec and pre-Willow Tank. Presumably the Aztec sandstone is generally equivalent to the Navajo sandstone of southwestern Utah, which lies below Upper Jurassic strata. Present facts, therefore, suggest that the Muddy Mountain thrust may represent orogeny either late in the Jurassic or during the Cretaceous before Bear River time. Spieker has found in central Utah evidence of an orogenic movement between the Upper Jurassic and the Upper Cretaceous; he refers to this movement as the mid-Cretaceous orogeny (1946). Possibly the Muddy Mountain thrust will eventually be correlated with that movement. However, accumulating evidence indicates several orogenic episodes during Mesozoic time between the Pacific Coast and the Rocky Mountains. Therefore, long-distance correlation between southern Nevada and central Utah awaits close dating of structural features.

The basal conglomerate of the Willow Tank formation indicates uplift and deep erosion in southern Nevada before deposits correlated with the Bear River formation were laid down. The movement suggested by this evidence may well agree in date with the mid-Cretaceous orogeny recognized by Spieker. Was the Muddy Mountain thrust developed at that time, or earlier? Conceivably this thrust, and others in the region that involve no known formations younger than Jurassic, are effects of the deformation to which the Willow Tank basal conglomerate bears witness; if so, the mid-Cretaceous orogeny was of formidable proportions. On the other hand, if the thrusts now dated merely as post-Aztec should eventually be dated as late Jurassic or early Cretaceous, at least two orogenic episodes before Bear River time would be indicated. Until additional evidence for definite dating can be found, it is unprofitable to discuss the matter further, except to emphasize that the Willow Tank conglomerate suggests orogenic movement not long before Willow Tank deposition began.

The Glendale thrusting involves the Willow Tank and Baseline formations, and so far as present evidence goes the movement may have occurred either in the late Cretaceous or in Tertiary time. However, the Upper Cretaceous section itself gives an impressive record of repeated uplift not far west of the depositional area. The thick Baseline sandstone may be interpreted as an orogenic deposit, since beds of conglomerate become more closely spaced and coarser toward the top of the section.

Therefore violent disturbance of this section by an overriding thrust plate, followed by deposition of the coarse Overton debris, may signify merely the climactic stage of movement in an orogenic belt that widened progressively eastward. Moreover, successive movements indicated by coarsening debris in the Baseline sandstone and by the later Glendale thrusting may represent merely recurrent pulses in one major orogeny, the initial stage in which is recorded in the Willow Tank basal conglomerate.

Therefore, although there is good evidence indicating that the Glendale thrust developed later than the Muddy Mountain thrust, we do not yet have a valid basis for naming and dating distinct orogenic episodes in southern Nevada. As Spieker has stated (1946), the term Laramide has been used loosely to include a wide range of orogenic events, extending from early Cenozoic back to an unspecified date in the Cretaceous. The term can survive as a useful designation only if we find, on continued study, that it can be applied to a definite series of orogenic pulses, covering a moderate time interval and distinctly separable from earlier episodes of deformation. The orogenic history of southern Nevada is still too obscure to permit such a clean-cut division.

There is good possibility that fossil evidence will be found to date the Overton fanglomerate, which is the most critical stratigraphic unit in the Muddy Mountain area. Continued study in the general region may supply evidence also for dating the Muddy Mountain thrust and other seemingly related thrusts. This region, in which careful geologic mapping has only begun, may hold keys not only to important chapters in the structural history of the Basin-and-Range province, but also to some fundamental problems in tectonic theory.

REFERENCES CITED

Hewett, D. F. (1931) *Geology and ore deposits of the Goodsprings quadrangle, Nevada*, U. S. Geol. Survey, Prof. Paper 162.

———, Callaghan, E., Moore, B. N., Nolan, T. B., Rubey, W. W., and Schaller, W. T. (1936) *Mineral resources of the region around Boulder Dam*, U. S. Geol. Survey, Bull. 871, p. 121–122,

Longwell, Chester R. (1921) *Geology of the Muddy Mountains, Nevada*, Am. Jour. Sci., 5th ser., vol. 1, p. 39-62.

——— (1922) *The Muddy Mountain thrust in southeastern Nevada*, Jour. Geol., vol. 30, p. 63–72.

——— (1925) *The pre-Triassic unconformity in southern Nevada*, Am. Jour. Sci., 5th ser., vol. 10, p. 93–106.

——— (1926) *Structural studies in southern Nevada and western Arizona*, Geol. Soc. Am., Bull., vol. 37, p. 551–584.

——— (1928) *Geology of the Muddy Mountains, Nevada, with a section through the Virgin Range to the Grand Wash Cliffs, Arizona*, U. S. Geol. Survey, Bull. 798, 152 pages.

——— (1936) *Geology of the Boulder Reservoir floor*, Geol. Soc. Am., Bull., vol. 47, p. 1393–1476.

——— (1945a) *The mechanics of orogeny*, Am. Jour. Sci., vol. 243-A, p. 421.

——— (1945b) *Low-angle normal faults in the Basin-and-Range province*, Am. Geophys. Union, Tr., vol. 26, p. 107–118.

McKee, Edwin D. (1938) *The environment and history of the Toroweap and Kaibab formations of northern Arizona and southern Utah*, Carnegie Inst. Washington, Pub. 492, 268 pages.

——— (1939) *Studies on the history of Grand Canyon Paleozoic formations*, Carnegie Inst. Washington, Year Book, no. 38, p. 313–314.

Reeside, John B., Jr., and Bassler, Harvey (1922) *Stratigraphic section in southwestern Utah and northwestern Arizona*, U. S. Geol. Survey, Prof. Paper 129, p. 53–77.

Spieker, Edmund M. (1946) *Late Mesozoic and early Cenozoic history of central Utah*, U. S. Geol. Survey, Prof. Paper 205-D, p. 117–160.

Stock, Chester (1921) *Later Cenozoic mammalian remains from the Meadow Valley region, southeastern Nevada*, Am. Jour. Sci., 5th ser., vol. 2, p. 250–264.

YALE UNIVERSITY, NEW HAVEN, CONN.

MANUSCRIPT RECEIVED BY THE SECRETARY OF THE SOCIETY, MARCH 17, 1948.
PROJECT GRANT 351-40.